ABLATIVE PYROLYSIS OF BIOMASS

GEORGE VERNON CORDNER PEACOCKE

Doctor of Philosophy

THE UNIVERSITY OF ASTON IN BIRMINGHAM

October 1994

The University of Aston in Birmingham

ABLATIVE PYROLYSIS OF BIOMASS

GEORGE VERNON CORDNER PEACOCKE

Doctor of Philosophy
1994

SUMMARY

The primary objectives of this work were to design, construct, test and operate a novel ablative pyrolysis reactor and product recovery system. Other key objectives included the development of an ablative pyrolysis reactor design methodology, mathematical modelling of the ablation process and measurement of empirical ablation rate data at 500°C. The constructed reactor utilised a rotating blade approach to achieve particle ablation in a 258 mm internal diameter reactor. By fulfilling the key requirements of high relative motion and high contact pressure, pine wood particles of maximum size 6.35 mm were successfully ablated.

Sixteen experiments were carried out: five initial commissioning experiments were used to test the rotating blade concept and to solve char separation problems. Mass balances were obtained for the other eleven experiments with good closures. Based on ablatively pyrolysed dry wood, a maximum organic liquid yield of 65.9 wt% was achieved with corresponding yields of 12.4 wt% char, 11.5 wt% water and 9.2 wt% non-condensable gas. Reactor throughputs of 2 kg/h dry ablated wood were achieved at 600°C. The theoretical ablative pyrolysis reactor design methodology was simplified and improved based upon empirical data derived from wood rod ablation experiments. Yields of chemicals were qualitatively similar to those of other fast pyrolysis processes.

The product recovery system, comprising hot char removal, liquids collection in two ice-cooled condensers followed by gas filtration and drying, gave good mass balance closures. The most significant problem was char separation and removal from the reactor. This was solved by using a nitrogen blow line. In general, the reactor and product collection systems performed well.

Future development of the reactor would involve modification of the reactor feed tube to allow the reactor residence time to be reduced and testing of the rotating blade approach with different blade angles, configurations and numbers of blades.

Key words: biomass; reactor design; modelling; liquids; ablative fast pyrolysis

Acknowledgements

I would like to thank Prof. B.J. Tighe and Dr. E.L. Smith [Departmental Heads] and the Department of Chemical Engineering and Applied Chemistry for providing most of the facilities for this project and the Commission of the European Communities JOULE program for the financial funding.

I would also like to thank the following:

Ian Murkitt for his great attention to detail and fabricating the reactor and associated equipment: Maurice Santoro for the welding and the support frame, Dave Walton and Paul Tack for the GC analyses, Mike Lea and Dave Bleby for the electrical work and Steve Ludlow, Neville Roberts [retired] and Lynn Wright for the administration of orders, purchases and general equipment.

My friends at the University of Waterloo, Dr. Don Scott [retired], Dr. Desmond Radlein, Mr. Jan Piskorz and Mr Peter Majerski for the liquids analyses [GC-MS and HPLC] and their perpetual enthusiasm, optimism and advice.

Dr. Eric Smith for his help and discussions on the heat transfer modelling.

My colleagues in the Energy Research Group, in particular Robert Hague, Colin Dick and Louise Cooke for their assistance with the wood rod ablation experiments.

My parents, Jimmy and Georgina Peacocke for all their help and support in many ways.

Miss Kaisa Tiippana for her support and for making sure that I stayed well fed.

My special thanks goes to my supervisor, Dr. Tony Bridgwater for his considerate advice, patience and constructive comments during the course of the work.

Contents Page

List of Figures

Chapter 2

Chapter 3

Chapter 4

Chapter 5

Chapter 6

Chapter 7

Chapter 8

Chapter 9

Appendix IA

Appendix IB

Appendix II

Appendix III

Appendix IV

Appendix V

List of Tables

Chapter 2

Chapter 3

Chapter 4

Chapter 5

Chapter 6

Chapter 7

Chapter 8

Chapter 9

Appendix IA

Appendix IB

Appendix II

Appendix IV

Appendix V

Chapter 1. Introduction

1.1 Background

1.1.1 Agricultural policy

With the recent changes in overall agriculture strategies for Europe, most notably the Common Agricultural Policy [CAP], food production in Europe will be reduced with the land being "set aside" for other uses. About 20 million hectares of land will be made available with an additional 10-20 million hectares of marginal land becoming available by the year 2000. One of the consequences of the reduction in land usage is the possible abandonment of the land with demographic changes and deleterious environmental effects if the land is not maintained. The recent completion of the GATT agreement requires the removal of the protection for European agriculture and a transition to undistorted markets. With these changes in agricultural policay and practice, the utilisation of this available land for energy and industrial products from biomass is a very attractive alternative.

1.1.2 Environmental factors

Renewable energy technologies are seen as having environmental advantages since the use of biomass for energy and industry allows a significant quantity of renewables to be consumed without any overall contribution to the Greenhouse Effect. The neutral effect of biomass on CO_2 emissions was highlighted at the first "Earth summit" held in Rio de Janeiro in 1992. Carbon dioxide emitted during combustion is absorbed by new growing vegetation, i.e. a neutral effect on the CO_2 content of the atmosphere. Liquid fuels produced from biomass contain low quantities of sulphur which are low enough to be of minimal impact, in terms of SO_2 emissions, during conversion. NO_x emissions can be reduced by using lower combustion temperatures and by applying modern pollution control processes. Recent EC policies have forecast an increased development of integrating biomass production and conversion with improved management of the environment.

1.1.3 Energy policy

The total energy consumption for Europe in 1990 was 752.8 x 10^6 tonnes of oil equivalent [TOE] (1). At present, biomass supplies over 2.5% of the European Union's primary energy needs from a total 6% contribution by renewable energies, mainly in the form of direct combustion, equivalent to 27 x 10^6 TOE/year (2). In 1992 approximately 460 Mt of dry biomass resources were available of which 250 Mt were agricultural waste (1). Utilisation of

these wastes for energy purposes is attractive since it reduces demands on landfilling of wastes and on fossil fuels.

1.1.4 Economic aspects

The use of biomass has two areas for impact: a reduction in imports of raw materials for industries such as the pulping, paper and fibres industry. Local resources frequently cannot fulfil demand for fibres for use as building materials and paper and as a result, low added value imports with long transport distances are required, increasing trade deficits after depletion of local resources. The use of biomass to provide a range of products in the form of energy, materials and/or chemicals is a viable alternative.

1.1.5 Social aspects

With the utilisation of land released from food production, diversification of industry into biomass for energy, environmental and industrial applications will help to stabilise the potential depopulation of rural areas and secure jobs in more diverse, directly and indirectly related activities.

1.1.6 Biomass conversion

There are two main routes for converting biomass into liquid fuels; biological conversion and thermochemical conversion. The first route is by biological conversion. The fermentation of sugars derived from agricultural crops to produce alcohols followed by distillation is well established and commercially available. In the EC, the costs of sucrose from sugar beet or glucose production by the hydrolysis of starch makes potential processes uneconomic unless there are financial incentives such as tax allowances or low cost feedstocks. Only the carbohydrate derived part of the biomass can be converted. Numerous acid hydrolysis plants have been built, but only a limited number have proved effective and economically viable. The use of enzymes for biological conversion has been extensively studied and problems such as catalyst suitability, stability and product yield have been identified.

The second route is thermochemical conversion by heat and chemical reaction. Thermochemical conversion processes do not have the same restrictions as biological processing and therefore, it is potentially the most promising route for producing liquids from biomass. Pyrolysis is the main thermochemical conversion process being developed to directly convert biomass into liquids for use as fuel or as a source of chemicals. Other processes include direct liquefaction at high pressure and indirect liquefaction via gasification which have

also received considerable attention. Pyrolysis is an irreversible, thermal degradation process that occurs either in a non-oxidising environment or with such a limited supply of oxidising agent that partial gasification occurs to provide reaction heat. Three products are usually produced: a solid char residue, a gas and a complex, oxygenated, hydrocarbon liquid product. The relative yields and compositions of these products are dependent on the process variables. The liquid product has a heating value of approximately half that of conventional fuel oil, but it can be stored, transported and handled in analogous applications such as boilers, turbines and engines.

The pyrolysis of biomass, in particular of wood, is an ancient process estimated to be at least 10000 years old with its most common application being the production of charcoal. Ancient Egyptians used the pyrolysis liquid for embalming purposes while the Greeks and the Romans used it for filling seams and joints in wooden ships (3). Prior to the development of the petrochemical industry earlier this century, wood pyrolysis was the major source of chemicals such as acetone, acetic acid and methanol (4).

1.2 Purpose of the work

The EC JOULE [Joint Opportunities for Unconventional or Long-term Energy] programme is subdivided into five key areas, one of which is the Energy from Biomass Programme with a total budget of 11.5 million ECU's [1989-1991] (5). The Energy from Biomass Programme has five divisions covering the following areas:

- biomass resources,
- biological conversion,
- thermal conversion,
- integrated projects,
- systems.

The thermal conversion program is the largest sector with a total award of 7.5 million ECU. This work was carried out as one of the contracts in the thermal conversion division in conjunction with five other contracts on thermochemical conversion technologies. The rest of the thermal conversion division was concerned with: upgrading and characterisation, testing, slurries and environment, liquefaction, techno-economics and modelling.

This work was sponsored by the European Commission Directorate General XII JOULE programme to carry out fundamental research on the ablative fast pyrolysis of biomass in order to develop a new reactor technology and obtain detailed information on the operation of a 3-5 kg/h proto-type reactor. Ablative fast pyrolysis was selected for development over the range of fast pyrolysis technologies because it offers several advantages over more conventional fast pyrolysis technologies including high reactor specific throughputs, good temperature control

and more compact reactor design. The residence time of the vapours can also be decoupled from the solids and can be controlled by the use of an inert gas in the reactor.

1.3 Structure of the thesis

This project involved the design, construction and operation of a novel ablative fast pyrolysis reactor for the production of organic liquids, including the construction of a product separation and recovery system. A reactor design methodology was also developed and assessed. This thesis has the following structure:

Chapter 2 details the chemical and physical structure of biomass and its three principal components of cellulose, lignin and hemicellulose. The phenomenon of pyrolysis is defined and the process parameters which influence the formation of organic liquids reviewed and summarised. The effect of the process parameters on the yields of chemicals is also summarised.

Chapter 3 reviews the kinetics of biomass pyrolysis with a particular emphasis on fast pyrolysis models and reaction pathways for cellulose and whole wood. The secondary vapour phase reactions of primary pyrolysis products are also summarised.

Chapter 4 reviews current and recent ablative fast pyrolysis activities with a detailed description of the equipment, mass balances and operation where possible. Fundamental work on heat transfer and modelling of ablation is also reviewed and its contribution to the field discussed.

Chapter 5 details a theoretical ablative pyrolysis reactor design procedure for the specification of biomass throughputs, required heat transfer area and biomass contact area for a range of process parameters. A design sensitivity analysis of the process parameters with regard to the biomass throughput is also discussed.

Chapter 6 describes in detail the designed reactor and immediate associated equipment. The novel rotating blade concept used in the work is described and its associated advantages over other approaches to ablation summarised. The operation of the reactor is also summarised.

Chapter 7 describes the reactor and product collection systems used during the course of the experiments for which detailed mass balances were obtained. Operational results are also included and modifications to improve operability and recovery of products are described. Problems encountered during commissioning are also described with their solution.

Chapter 8 details the mass balances for the experimental runs with char, liquids and gas analyses. These results are compared with those of other fast and ablative fast pyrolysis research where possible and conclusions about the reactor performance made. In particular, focus is made on the liquid yields and analyses.

Chapter 9 describes the evaluation of the ablative pyrolysis reactor. The results of simple heat transfer experiments are described and modifications to the theoretical ablative pyrolysis reactor design methodology presented in Chapter 5 are described. The performance of the rotating blade approach is discussed. A new simplified procedure for the reactor design is presented and discussed.

Chapter 10 gives the conclusions from the work carried out.

Chapter 11 gives recommendations for the continuing development of the ablative pyrolysis reactor and work started during the course of this thesis.

Chapter 2. Biomass and Pyrolysis Fundamentals

2.1 Introduction

The objectives of this chapter are:

- define biomass and its constituents in chemical and structural terms [Section 2.2]
- define pyrolysis and its different regimes [Section 2.3]
- review the influence of biomass related parameters on product yields [Section 2.4]
- review the effects of the reactor parameters on product yields [Section 2.5]
- review the influence of process parameters on chemical yields [Section 2.6]
- summarise the key requirements of fast pyrolysis for liquids as fuels and as a source of selected speciality chemicals [Section 2.7]

2.2 Biomass and its components

Biomass may be defined as a renewable source of fixed carbon in the short term (6). This includes wood, grasses and agricultural crops. Biomass typically has three main constituents: cellulose, hemicellulose and lignin with minor constituents including resins, ash and extractives. Some typical constituent analyses for different biomass types are given in Table 2.01 below. Wood physical structure is not reviewed here, but a summary may be found in the literature (e.g. 7).

Table 2.01
Typical reported analyses of different biomass [wt% dry ash free] (8)

Biomass	Ash	Solvent soluble	Water soluble	Lignin	Hemicellulose	Cellulose
Bagasse	1.6	0.3	--	20.2	38.5	38.1
Beechwood	0.5	0.9	1.3	23.2	26.8	40.1
Hardwood	0.3	3.1	--	19.5	35.0	39.0
Rice straw	16.1	4.6	13.3	11.9	24.5	30.2
Softwood	0.4	2.0	--	27.8	24.0	41.0
Wheat straw	6.6	3.7	7.4	16.7	28.2	39.9

Biomass is elementally composed of carbon, hydrogen and oxygen with traces of sulphur and nitrogen. Some typical ultimate analyses for a range of biomass types are given below in Table 2.02 and show that biomass tends to have a high oxygen content, low sulphur and low ash compared to coal, with the notable exception of rice hulls which have a very high silica content of up to almost 70% of the ash (9). The high proportion of volatiles in biomass makes it a suitable material for thermochemical conversion [greater than 87 wt% for wood compared to 5.4 wt% for anthracite] (8).

Table 2.02

Analysis of biomass materials: comparison with coal and wastes [wt%, dry basis]

	C	H	O	N	S	Ash	Ref.
Beech	51.6	6.3	41.5	--	--	0.6	10
Maple	50.6	6.0	41.7	0.3	--	1.4	10
Oak waste	49.2	5.7	41.3	0.2	--	3.3	10
Rice hulls	38.3	4.4	35.5	0.8	0.1	21.0	8
Wheat straw	48.6	5.2	45.4	0.7	0.1	8.4	11
Sweet sorghum bagasse	49.9	5.4	33.8	1.4	0.1	10.5	12
MSW	33.5	4.6	22.4	0.7	0.4	38.4	13
Anthracite	79.7	2.9	6.1	0.9	0.8	9.6	8
Lignite	40.6	6.9	45.1	0.6	0.9	5.9	8
Yorkshire bituminous	87.5	3.3	3.5	--	0.7	5.0	14
No. 6 fuel oil	87.2	10.7	2.1	--	1.47	0.02	15

Of the range of available literature on biomass and coals, extensive analyses have been compiled for example by Hayn et al. (16) and Odgers and Kretschmer (15). Woody biomass has a lower higher heating value, typically 19.8-21.0 MJ/kg compared to coal [15.6-36.6 MJ/kg] (15, 17) and medium fuel oil [40.6 MJ/kg] (15). The three main constituents of biomass [cellulose, hemicellulose and lignin] are discussed below in terms of elemental, chemical composition and properties in order to show that each influences the yields and properties of the liquid products. Their influences on product yield and quality are discussed later and in Chapter 3 with respect to their decomposition kinetics and reaction pathways.

2.2.1 Cellulose

Cellulose is a polymer of anhydroglucose [β-1, 4 D-glucopyranose] and comprises approximately 40 wt% of dry wood as shown in Table 2.01 (18, 19). It is the primary component of the cell wall. Cellulose is a linear polymer with units linked together by glycosidic bonds and may be represented by the formula $(C_6H_{10}O_5)n$, as depicted below in Figure 2.01 (20). It should be noted that the functional groups on the cellulose molecule have a significant effect on the chemical and physical properties of the biomass (20). The degree of polymerisation may be 7000-10000 units in wood, increasing to 15000 for cottonwood (21). Cellulose chemistry is not discussed here but extensive reviews may be found in the literature (e.g. 20, 22, 23). As a result of hydrogen bonding, cellulose chains tend to aggregate to form microfibrils.

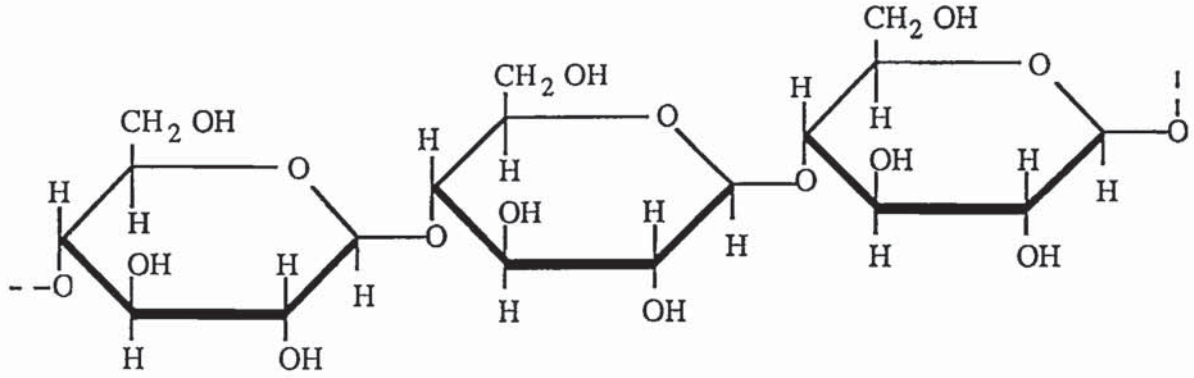

Figure 2.01. The Cellulose Polymer

2.2.2 Hemicellulose

Hemicelluloses are closely associated with cellulose in the cell wall as well as to lignin in the middle lamella and may be classified as non-cellulosic polysaccharides and related substances (18, 20). They are amorphous polysaccharides which are usually based upon hexoses [C_6 sugars] in softwoods, and pentoses [C_5 sugars] in hardwoods with 1, 4 β- linkages between the sugar monomers (20). It is a complex polymer with a variable chemical structure based upon a variety of sugars such as d-glucose, d-xylose, d-galactose and l-arabinose. Unlike cellulose, hemicelluloses exhibit a branched rather than a linear structure which decreases the number of inter-molecular hydrogen bonds and hence the degree of polymerisation to typically 100 to 200 units. Hemicelluloses can be differentiated from cellulose by their solubility in weak alkaline solutions and they are readily hydrolysed by acids to their component monomers. Xylan [acetyl-4-O-methylglucuronoxylan], a polymer of d-xylose $(C_5H_{10}O_5)$, forms the main hemicellulose of hardwoods and is illustrated in Figure 2.02 while

mannan, which is a polymer of d-mannose ($C_6H_{12}O_6$) forms the principal hemicellulose of softwoods and is depicted in Figure 2.03 (3, 18).

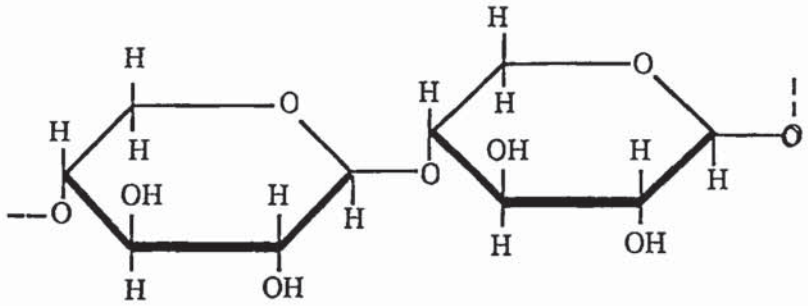

Figure 2.02. Xylan hemicellulose structure

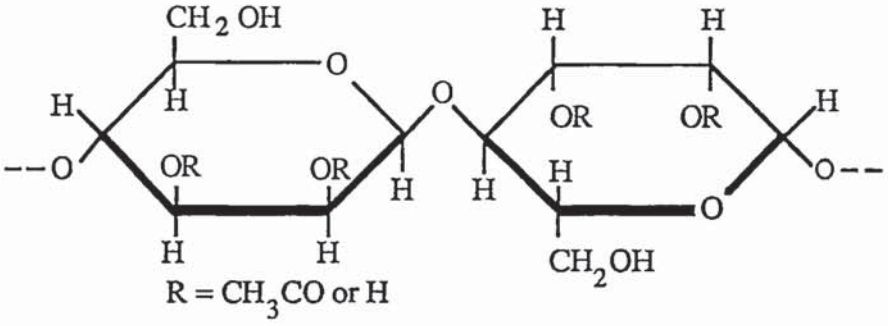

Figure 2.03. Mannan hemicellulose structure

2.2.3 Lignin

Unlike cellulose and hemicelluloses which are polysaccharides, lignin is composed of phenolic polymers composed of C_3-C_6 phenyl propane units. Lignin is the amorphous material that surrounds cellulose fibres in the middle lamella and cements them together; in addition, it serves as a reinforcement agent within the fibres (21, 24, 25). Lignin is a random, three dimensional polymer made up of phenyl propane units where the unit may either be a guaiacyl, syringyl or hydroxyl. Figure 2.04 below illustrates the lignin units.

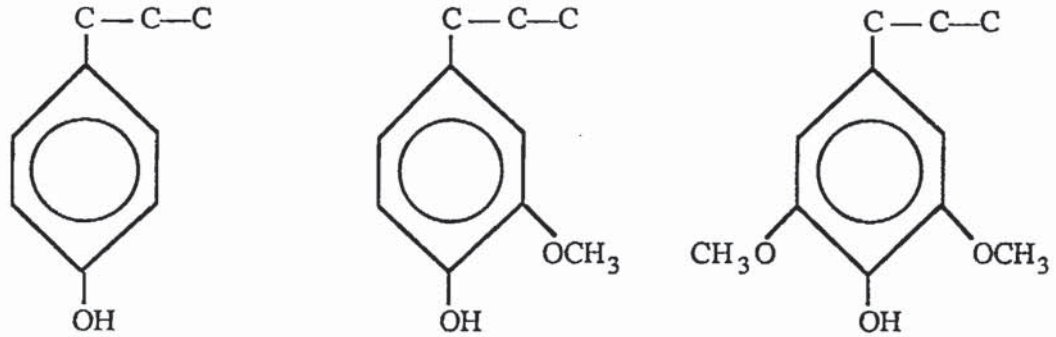

p-Hydroxylphenylpropane Guaiacylpropane Syringylpropane

Figure 2.04. Lignin monomers

These units are bonded together in several ways, the most common of which are α- or β-ether linkages [54-68%] as depicted in Figure 2.05 and the least common is carbon-carbon linkages which are less stable (26, 27). Guaiacyl units are exclusive to softwood lignins (28).

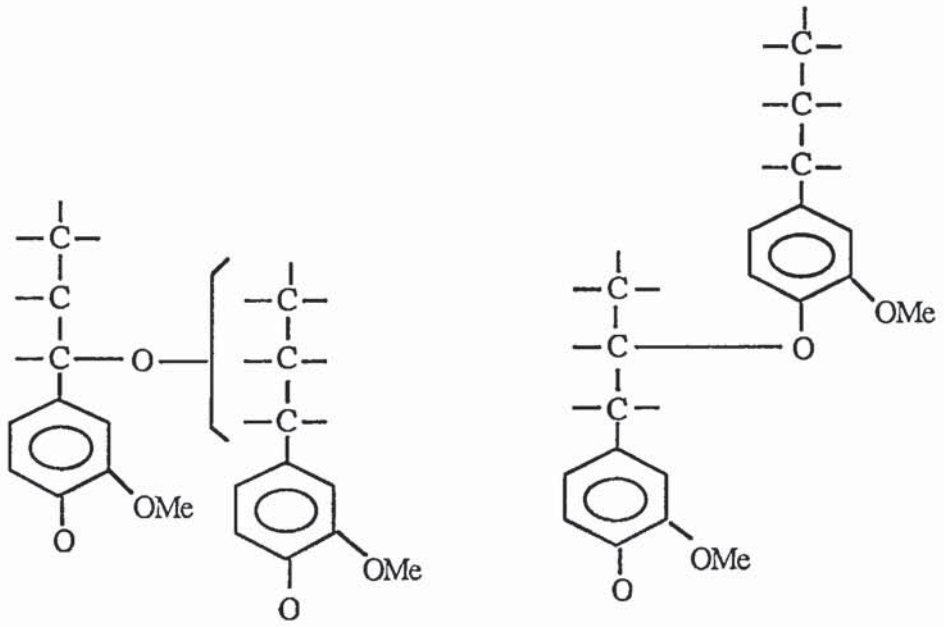

α - Alkylether bonding

β - 4' Ether bonding

Figure 2.05. Ether bonds in lignin (28)

The exact physical chemical structure of lignin is not known and the elemental analyses therefore tend to vary, e.g., one proposal by Shafizadeh (29) suggests an approximate elemental analysis of ($CH_{1.1}O_{0.4}$); another proposal by Wright (26) gives an empirical formula of ($CH_{1.7}O_{0.7}$). An abbreviated skeletal schematic of the lignin structure found in conifers is shown in Figure 2.06 (e.g. 25). Lignin has a relatively high energy content 26.7 MJ/kg, compared to 17.5 MJ/kg for cellulose and 15.7 MJ/kg for hemicellulose due to its lower oxygen content and its aromatic nature (25). Like hemicellulose, softwood and hardwood lignins differ in the balance of their constituent units (3, 24).

2.2.4 Other biomass components

Apart from the three primary components of biomass described above [Sections 2.2.1-2.2.3] other minor components may be termed collectively as extractives as they can be removed by their solubility in either water or polar organic solvents. They include resins, starches, waxes, lipids, hydrocarbons and a variety of phenolic compounds such as tannin; however, the relative amounts vary from biomass to biomass and also the part of the plant (7, 30). They play a minor role in the formation of wood pyrolysis products as their amounts typically found in wood varies from 1-5% on a dry wood basis [see Table 2.01, (16)]. The other

notable minor component of biomass is ash. Typically wood contains about 0.3 wt% to 1.0 wt% ash which is composed by: CaO 50%, K_2O 20% and lesser amounts of Na_2O, MgO, SiO_2, Fe_2O_3, and P_2O_5. Despite its low concentration in most biomass materials, ash can have a significant influence on the pyrolysis process as discussed later.

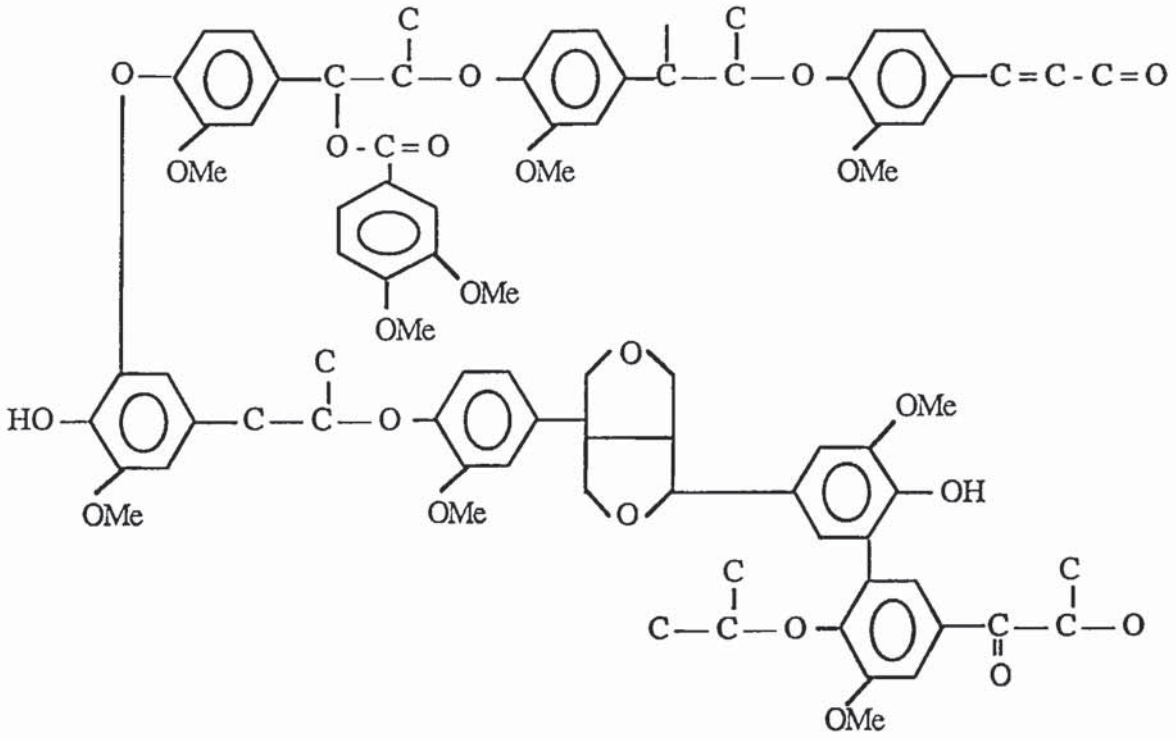

Figure 2.06. Abbreviated depiction of conifer lignin

In summary, there is considerable variation in the elemental and chemical composition of biomass which can have an influence on the final products of pyrolysis as discussed in the following sections. Cellulose is the major component of most biomass and since it can be easily recovered and purified, most attention has focused on this component.

2.3 Pyrolysis

2.3.1 Introduction

Pyrolysis may be defined as the thermal degradation of biomass in the absence of oxygen; however, this may include partial gasification (6). Commonly accepted definitions for slow, conventional, flash, fast and ablative pyrolysis are given based on the process parameters of reactor temperature, gas/vapour product residence time [as defined in Section 2.5.2] and temperature, biomass heating rate, reactor pressure and the rate of thermal quenching of the products. The significance of these key process parameters and related ones are described and discussed below. Three products are always produced: a solid char residue, a gas and a

complex, oxygenated hydrocarbon liquid product containing water; the relative yields and compositions of these products are dependent on the process parameters.

2.3.2 Slow pyrolysis

Slow pyrolysis has been used for centuries to produce charcoal, tars, alcohols such as ethanol and methanol and other solvents. This is usually carried out in batch processes using kilns or retort furnaces (e.g. 31, 32, 33). Slow pyrolysis is characterised by:

- long solids and volatiles residence times [typically greater than 5 s for volatiles; solids residence times can be minutes, hours or days],
- relatively low reactor temperatures [< 400°C],
- atmospheric pressure,
- very low heating rates ranging from 0.01°C/s to up to 2°C/s,
- very low rate of thermal quenching of the products [minutes to hours].

Char, viscous tarry liquid and gases are formed in approximately equal mass proportions due to the slow degradation of the biomass and extensive secondary intraparticle and gas/vapour phase reactions.

2.3.3 Conventional pyrolysis

Conventional pyrolysis is similarly characterised by:

- long solids and volatiles residence times [typically less than 5 s for volatiles; solids residence times can be longer] up to one minute,
- relatively low reactor temperatures [< 450°C],
- slow heating rates of about 2-10°C/s,
- atmospheric pressure,
- low rate of thermal quenching of the products (34, 35).

Yields of organic liquids products from conventional pyrolysis are typically low, e.g. 20 % with char yields of typically 20-25 wt%, 20 wt% water and the balance non-condensible gases comprised mainly of carbon dioxide (36).

2.3.4 Flash and fast pyrolysis

Graham et al. reviewed the literature up to 1984 on flash and fast pyrolysis and made a distinction between fast and flash pyrolysis in terms of heating rates, reactor temperatures and residence time (37). Flash pyrolysis was characterised by:

- moderate pyrolysis temperatures [400-600°C],
- atmospheric pressure,
- high heating rates [10-1000°C/s],
- gas/vapour product residence times less than 2 s to maximise liquid yields at gas/vapour product temperatures less than 500°C.

Fast pyrolysis was characterised similarly by:

- higher heating rates than flash pyrolysis [$>10^5$°C/s],
- higher reactor temperatures [> 600°C] to give primarily a gaseous product at the expense of liquids and char,
- shorter gas/vapour product residence times of less than 0.5 s (38),
- rapid thermal quenching of the products [100-1000°C/s].

Fast pyrolysis therefore gives higher reaction rates due to the higher temperatures. Over the past five years, the distinction between flash and fast pyrolysis has largely disappeared and now the term "flash" has largely disappeared and is gradually being replaced by a more generalised definition for fast pyrolysis of:

- high heating rates [> 1000°C/s],
- reactor temperatures greater than 450°C,
- short vapour product residence times [< 2 s for liquid fuels, < 1 s for speciality chemicals],
- rapid product quenching [< 40 ms] (39).

2.3.5 Ablative fast pyrolysis

Ablative fast pyrolysis is characterised by the dominant mode of heat transfer which is by conduction to the biomass under conditions of high relative motion [> 1.2 m/s] and high contact pressure between the biomass and the solid heat transfer surface. The combined effects of the applied pressure and the relative velocity are that the reaction products are rapidly removed from the reaction interface to expose fresh biomass for pyrolysis, maximising heat transfer rates and hence ablation rates.

Some ablative heat transfer can be assumed to occur in fluidized beds, particularly circulating fluidized beds or transported beds, where rapid mixing of the biomass with the solid heat carrier can occur and the product char layer may be mechanically abraded from the biomass. One example is the Ultrapyrolysis reactor where hot solids are blasted against the biomass to maximise heat transfer (38, 40, 41, 42). The other effect of using mutual destruction of the entrained biomass and heat transfer solids was to also rapidly abrade off the product char. Ablative pyrolysis research is reviewed in Chapter 4.

By manipulating the process parameters, the yield of a desired product may be optimised. The particular focus of this chapter is assessing the parameters which can be manipulated to maximise the yields of organic liquids. The liquid product is valuable as apart from its use as a fuel, it can also be used as a source of speciality chemicals [see Section 2.6]. The liquids can also upgraded to a substitute gasoline-like fuel and/or high octane enhancers by high pressure catalytic hydrotreatment (e.g. 43, 44, 45). The raw product vapours can also be upgraded or chemically changed using catalysts (e.g. 46, 47, 48). The process parameters can be divided into three categories:

- those related to the feedstock,
- operation of the pyrolysis reactor,
- recovery of the liquid products.

The process parameters described below are considered by most researchers to significantly affect both the yields and composition of the pyrolysis products. It is not possible to isolate the effect of any single parameter as there are significant interactions between products as the reactions develop. The process parameters which are examined are:

Biomass related [controllable to a more limited extent]

- biomass pretreatment [additives/ash content, moisture, chemical composition,
- biomass density,
- biomass particle size,
- biomass particle shape,
- biomass properties [specific heat capacity, thermal conductivity, permeability],
- intrinsic properties of the biomass.

Reactor operation [substantially controllable]

- reactor temperature [temperature at which pyrolysis occurs],
- gas/vapour product reactor residence time,
- gas/vapour product temperature,
- biomass heating rate and heat transfer,
- biomass decomposition temperature,
- pressure [hydrostatic and mechanical],
- gaseous [reactor] environment.

Recovery of the liquid products [substantially controllable]

- rate of thermal quenching of the products;
- time/temperature profile of the cooling products.

2.4 Biomass related process parameters

2.4.1 Introduction

Biomass is a heterogeneous material and highly anisotropic and as discussed earlier has a complex chemical composition [see Section 2.2]. The properties of grain structure, biomass thermal conductivity, permeability, moisture content and particle size influences on liquid yields are reviewed. Some typical values for wood physical and thermal properties are summarised in Table 2.03 below demonstrating the wide range of values.

Table 2.03
Some typical physical properties of wood (49, 50, 51, 52, 53)

Property	Typical	Literature Values	Units
wood heat capacity	1500	1100-2800	[J/kg K]
density	500	340-1100	[kg/m^3]
thermal diffusivity	8×10^{-8}	10^{-6}-10^{-8}	[m^2/s]
thermal conductivity	0.1	0.1-0.3	[W/mK]
permeability		0.005-5	[darcy]
wood char thermal conductivity	0.1	0.04-0.15	[W/mK]

Biomass is a very good thermal insulator which makes heat transfer into the biomass difficult and imposes certain restrictions on the size and shape of particles for fast pyrolysis in particular reactor configurations. Biomass can be modified by chemical treatment, but to modify its thermal and physical properties [i.e. by densification] is much more difficult and energy intensive.

2.4.2 Biomass pretreatment

Biomass pretreatment involves either the physical [drying, comminution, sizing] or chemical [ash/additives content, elemental composition] modification of the feedstock. This section will look at the influence on pyrolysis liquid yields of ash, additives, moisture content, particle size and shape and physical and thermal properties.

2.4.2.1 Ash content

The ash composition of biomass varies from approximately 0.5 wt% for most woods to over 20 wt% for materials like rice hulls. Ash composition and concentration influences the yields and chemical composition of the liquids by catalytic action and this has been studied by several researchers. Gray et al. investigated the effects of moisture, calcium ion exchange and ash on product yields for reactor temperatures from 340 to 460°C (54, 55). Using Woodex [formed from wood wastes by compression and extrusion], the feedstock was modified in two ways. To remove ash, Woodex samples were acid washed by soaking for 7 h at 25°C in 0.5 N HCl [acid:woodex 50 ml/g] and then water washing to neutrality with demineralised water. Samples were also calcium-exchanged by soaking the samples in 1 N calcium acetate for 24 h at 25°C to 0.62 mequiv/g.

Ash free, dry Woodex had increasing liquid yields from 24 wt% at 340°C to 37 wt% at 460°C, but Woodex containing 16.7 wt% water had a low increase in yields from 26 wt% to 27 wt% for similar temperatures. The char yields also decreased from 32 to 27 wt%. For the calcium exchanged and the untreated Woodex, the addition of water had little influence on yields with the calcium exchanged Woodex showing similar results to the untreated Woodex. Gray proposed that the ash catalyses the dehydration and fragmentation of the biomass, whereas water modulates the extent of fragmentation by hydrating active sites and thereby reducing catalytic activity. For the ash free material, the water was interfering with reactions in a non-selective manner.

Shafizadeh et al. also carried out an extensive series of experiments assessing the effects of ash composition and concentration on the yields of liquids and chemicals from cellulose during pyrolysis under vacuum (56). Using a range of celluloses, they found that even small concentrations of ash [0.015 %] could reduce the liquid yield from 69 to 59 wt%. They also investigated various feed pretreatments to assess the effects on the yields of liquids and chemicals, in particular levoglucosan. The results are shown in Table 2.04 overleaf.

Work carried out by Scott et al. on a range of feedstocks has similarly shown that the ash concentration in biomass has a detrimental influence on organic liquid yields (57). A range of feedstocks were studied including peat, corn stover, hybrid poplar aspen, bagasse and eastern red maple. Organic liquid yields dropped from 65 wt% [moisture free feed] at 0.6 wt% ash in the wood feedstocks to 27.3 wt% at 11.0 wt% ash in corn stover for similar reactor parameters. The results are similar to those obtained by Gray where the ash is believed to catalyse the degradation of the primary vapours to char, water and gases with sodium, present in the ash [approximately 13 wt%], thought to act as a gasification catalyst at fast pyrolysis temperatures. Therefore for high organic liquid yields, the ash content of the feedstock

should be low [< 0.5 wt%] with low concentrations of potassium and sodium. The further influence of ash on chemicals yields is discussed in Section 2.6.

2.4.2.2 Washing and chemical treatment of the biomass

To change the elemental and chemical composition of the biomass, several pretreatment methods can be used with different effects. Different washing procedures have been used on biomass: distilled water washing-to remove a significant quantity of the ash, and acid washing-in varying degrees to remove ash and hydrolyse the hemicellulose component of the biomass [see Table 2.04].

Water washing can be used to remove a high proportion of the ash in the biomass. Acid washing can be used in two ways: the first is the partial removal of the ash and some hemicellulosics [mild acid hydrolysis] with some residual acid ions [e.g. SO_4^{2-} ions if sulphuric acid is used] remaining in the biomass matrix. The second is a more severe acid washing [total ash removal and hemicellulose hydrolysis] followed by water washing with distilled de-ionised water to remove residual acid and hemicellulosics. Shafizadeh et al. compared water washing and acid pretreatment to study the influences on the yields of chemicals such as levoglucosan [LG] and its furanose isomer, 1,6-anhydro-β-D-glucofuranose [LGF], as shown in Table 2.04 (56). Water washing alone has a significant effect on the product yields, with an increase in the organic liquid yields from 58 to 70 wt% and a reduction in the char yield from 9 to 5 wt%; however, the degree of ash removal was not reported. Acid washing had a more significant influence on yields as shown in Table 2.04.

Table 2.04

Effects of water and mild acid washing on product yields from cellulose and cotton fabric

Substrate	Pretreatment	Char	Liquid	Levoglucosan	LGF
Whatman CF11	none [0.015 wt% ash]	7	58	29	3
	water wash [97°C]	4	70	33	3
	1% H_2SO_4	5	79	48	7
Cotton fabric	none	10	46	14	1
	water wash #	9	59	28	2
	1% H_2SO_4 [20°C]	5	73	42	4
	5% H_2SO_4 [20°C]	3	76	50	6

washed with boiling absolute ethanol, then water at 97°C

There is little work on the pyrolysis of pretreated feedstocks under fast pyrolysis conditions. The most consistent work is that of Scott et al. who have investigated various degrees of biomass acid washing followed by fast pyrolysis in a small 100g/h shallow fluid bed reactor (58, 59). Scott et al. performed a mild acid wash where the wood was heated in 5% H_2SO_4 for 2-6 hours at 80-100°C followed by washing with de-ionised water to a wash pH of 6.3. The results are presented in Table 2.05 below for two feedstocks (59). Organic liquid yields were increased with reductions in gas and char yields. The original wood sample contained 1700 ppm K, 1200 ppm Ca and 50 ppm Na, almost all of which were removed by acid washing and are known to catalyse the degradation of liquids to char and gases. Other methods of acid treatment were also investigated to assess their effects on product yields: different acid strengths were used and the results are summarised in Table 2.06 overleaf.

Table 2.05

Effects of mild acid washing on product yields and liquid composition [yields, wt% dry feed]

Feedstock	Poplar		Stake Cellulose	
	Untreated	Treated	Untreated	Treated
Reactor temperature [°C]	497	501	500	500
Residence time [s]	0.46	0.45	0.5	0.5
Water content [wt%]	3.3	16.5	24.1	3.1
Cellulose content [wt%]	49.1	62.8	94.0	95.0
Ash, [% dry basis]	0.46	0.04	2.5	0.32
Organic Liquid	65.8	79.6	58.2	65.3
Water	12.2	9.0	9.0	7.0
Char	7.7	6.7	15.4	19.0 *
Gas	10.8	6.4	15.3	0.9

* includes water soluble hydrolyzable oligosaccharides

Use of low concentrations of HCl even for short contact times, as show in Table 2.06, has a very significant influence on the liquid yield compared to the use of sulphuric acid. It is interesting to note that the water originally contained in the feedstock for method 2 was consumed during pyrolysis, although the gas yields are slightly higher. One point which is not usually remarked upon is the final fate of the added acid ions after pyrolysis, whether they are found in the char, liquid or gas products. The more profound effect of HCl compared to that of H_2SO_4 has not yet been explained.

Table 2.06

Effects of differing acid pretreatment on pyrolysis yields from poplar wood, 475-490°C, 0.5 s gas/vapour product residence time [yields, % dry feed basis]

Method number	1	2	3	4
Pretreatment	5% H_2SO_4, 100°C, 2 h	3.7% HCl 100°C, 2 h	0.5% HCl 165°C, 6 min	3, then as 1 100°C, 2 h
Ash, [% d.b.]	0.04	0.05	0.85	0.30
Moisture [wt% d.b.]	6.0	15.9	25.4	16.9
Cellulose content	67.0	67.8	65.4	69.2
Organic liquid	73.6	85.4	78.4	75.0
Water	6.3	--	2.9	5.2
Char	6.3	5.5	10.1	10.5
Gas	6.4	8.7	7.6	6.4

2.4.2.3 Effects of additives on biomass pyrolysis product yields

Early work on the effects of additives have looked at the suppression of volatiles formation and the promotion of char forming reactions for the development of flame retardation as extensively reviewed for example by Shafizadeh (60). Experiments were conducted by Shafizadeh et al. on the effects of temperature and additives on chemicals and liquids yields; selected results shown in Table 2.07 (29). The most significant reduction in organic liquid yields was with ammonium hydrophosphate.

Table 2.07

Pyrolysis products from cellulose and treated cellulose at 550°C [wt%]

Additive	none	+ 5% H_3PO_4	+ 5% $(NH_4)_2HPO_4$	+5% $ZnCl_2$
Organic liquids	66	16	7	31
Water	11	21	26	23
Char	5	24	35	31

Shafizadeh et al. from their work and a review of the literature concluded that the presence of Lewis acids, e.g. $ZnCl_2$, increased char and water yields at the expense of organic liquids with NaOH having a similar but lesser effect than $ZnCl_2$.

Work by Scott et al. also assessed the effects of acid washing and additives on the product yields and composition of liquids produced from hardwood and softwood following fast pyrolysis as summarised in Table 2.08 (61, 62, 63). De-ionising was performed by acid washing of the biomass with 0.1 % H_2SO_4 followed by washing with distilled de-ionised water. Addition of additives involved impregnation using an aqueous solution of additive. Yields of organic liquids from acid hydrolysed wood were increased by 15.1 wt% with the depolymerisation of cellulose forming 30 wt% levoglucosan. Deionising had a slight effect on the product composition with increased water yields.

Table 2.08

Effects of additives and pretreatment on IEA poplar product yields [wt% dry basis]

Pretreatment	untreated	acid hydrolysed	deionised	deionised + $(NH_4)_2SO_4$	deionised + H_2SO_4
Run no.	A-2	DT-10	S#3	S#4	S#7
Cellulose Content	49.1	65.5	--	--	--
Ash	0.46	0.02	--	--	--
Water content, [wt %]	3.3	16.5	0.0	3.0	7.0
Temperature	497	480	~530	~530	495
Organic liquids	65.8	80.9	60.5	66.1	66.1
Water	12.2	2.2	18.3	16.2	~17.0
Char	7.7	8.2	2.5	4.4	6.1
Gas	10.8	6.9	14.1	7.4	3.2
Levoglucosan	3.0	30.0	9.3	18.7	15.5
Hydroxyacetaldehyde	6.1	13.2	11.7	10.7	9.5

Scott proposed that during hydrolysis, sulphuric acid condensed with cellulosic hydroxyl groups to form sulphate esters [R-O-SO_2-OH] which are retained in the substrate and hence become available for catalysis during pyrolysis. They also proposed that $(NH_4)_2SO_4$ decomposed at 235°C to free H_2SO_4 gas and volatile NH_3 gas. Sulphuric acid was proposed to have the catalytic effect of promoting water formation and inhibiting degradation of

levoglucosan to hydroxyacetaldehyde [HAA]. This original hypothesis that levoglucosan decomposed to hydroxyacetaldehyde has since been rejected as it was later determined that the formation of levoglucosan and hydroxyacetaldehyde was by a competing pathway which was influenced by the ash content, in particular the sodium and potassium content [see Section 2.6.1]. As a further development of their work, Scott et al. assessed the effects of K_2CO_3 concentration on hydroxyacetaldehyde and levoglucosan yields. This confirmed that low concentrations of K catalysed the formation of hydroxyacetaldehyde over that of levoglucosan from cellulose decomposition and led to the development of a cellulose reaction pathway described in Chapter 3 (64).

A similar range of experiments has been carried out by Richards et al. on the influence of metal salts and acid washing on cellulose pyrolysis products with results shown in Table 2.09 (65). They demonstrated that the presence of transition metals [e.g. iron and copper] increased char yields at the expense of liquids but with high increases in LG and LGF yields.

Table 2.09

Vacuum pyrolysis of cottonwood sorbed with various salts [yields, wt% dry feed basis]

Sample	Additive [wt%]	Char yield	LG	LGF
Original Wood		15	0.4	--
acid washed [AW]		19	5.4	--
AW + $CuAc_2$	[0.45 % Cu]	29	11.2	--
$CuAc_2$	[0.43 % Cu]	15	5.9	--
AW + $CuCl_2$	[0.46 % Cu]	27	13.2	--
$FeAc_2$	[3.18 % Fe]	28	5.2	--
$FeCl_2$	[1.21 % Fe]	27	7.2	--
AW + $FeSO_4$	[1.69 % Fe]	38	6.1	3
$FeSO_4$	[1.69 % Fe]	36	7.5	2.3
Cellulose + $FeSO_4$	[1.1 % Fe]	37	2.8	2.4
AW + $FeSO_4$ [1 bar pressure]		47	1.4	4.9
newsprint + $FeSO_4$	[0.77 % Fe]	20	16.6	4.2

Ac: acetate salt

One other pretreatment of the biomass which has received very little attention is preheating of the biomass. This has the effect of lowering the degree of polymerisation of the biomass and also the crystallinity, both of which are known to influence the yields and composition of

products by favouring the depolymerisation pathway. A simpler feedstock pretreatment is that of hot [80-90°C] water washing of the feedstock.

To maximise the yields of organic liquids from the biomass, some degree of pretreatment should be used to reduce the ash content of the wood. The presence of specific ions can also have a dramatic effect on the yields of organic liquids and chemicals. This is an area requiring further investigation.

2.4.2.4 Biomass moisture content

Fresh wood typically contains between 66-150% water on a dry basis (66, 67). Water is important as it will influence the physical properties of the recovered pyrolysis liquids and the liquid heating value. In most laboratory experimental and commercial processes, the feed is normally dried to a uniform moisture content of less than 10% on a wet basis which can usually be achieved by air drying.

The effects of wood moisture content have been investigated primarily with respect to its influence on product yields. Beaumont and Schwob assessed the effects of moisture, reactor temperature and particle size on product yields and liquids composition at 350°C (19). Increasing the moisture content from zero to 26.2 wt% moisture free wood decreased organic liquid yields from 64.1 to 60.3 % with increasing char yields from 24.0 to 27.7 wt%. The organic liquid decrease was proposed to be due to the effect of water lowering the heating rate of the biomass and promoting secondary reactions. The differences may also be due to experimental error.

A study carried out by Kelbon considered the effects of moisture content, heat flux and particle size on pyrolysis yields. She studied three different moisture contents: 10, 60 and 110% [dry basis]. Kelbon found that increasing moisture content affected the thermal history of the pellet by delaying the onset of pyrolysis by as much as 150 s, thus lowering the initial rate of temperature rise within the pellet. This limited the fraction of the pellet which reacted during a fixed time period by as much as 20% because heating of the particle was hindered by the heat requirement for moisture vaporisation (68). Kelbon also found that liquid yields were greater for the intermediate moisture content [60%], a particle size of 1 cm and moderate heat fluxes [16 W/cm^2]. Evans and Milne also noticed a similar delay in pyrolysis [75 s] when investigating the effect of moisture on biomass pyrolysis with a smooth sequence of evolution of the pyrolysis products (69). Gray et al also evaluated the effects of moisture on the pyrolysis yields from Woodex (54). They found that for ash free feed, a water content of 16.7 wt% increased the char yields by 5 wt% at 460°C from 31 to 36 wt%. The high water content material also had relatively constant organic liquid yields which increased slightly from 26 to

28 wt% for an increase in reactor temperature from 340 to 460°C. The high moisture content had the effect of moderating the heating rate of the material and hence the yields were only slightly influenced by the reactor temperature as observed by Beaumont and Schwob (19).

Maniatis and Buekens studied the effect of moisture by pyrolysing a dry particle and a particle with 10 wt% [dry basis] moisture (70). The pyrolysis of the moist particle resulted in about 10% more water in the product. They concluded that the water produced by the dry sample was due to the pyrolysis process. Therefore, an optimum moisture content, that will enhance liquid production should be used so that proper temperature control of the reactor can be maintained and also to avoid the associated problem of disposing of the aqueous phase. This optimum will be dependent on the particle size and the heating rate of the system.

A general rule of thumb for fast pyrolysis conditions is that the water yields on a dry feed basis is 12 wt% with a 1 wt% increase in the feed moisture content contributing 1 wt% to the final water yield (71). This may be influenced by the gas/vapour product temperature as discussed in Section 2.5.8 and in Chapter 8.

2.4.3 Biomass particle size

As shown in Table 2.03, biomass has a low thermal conductivity. The size of the biomass particles will therefore influence the rate at which they can be heated. As the particle size increases, the rate at which heat is conducted into the biomass interior will be reduced. Slow heating tends to produce more char, which has a similar if not lower thermal conductivity to wood, and consequently a limit of approximately 2 mm has been suggested for fast pyrolysis fluid bed technologies (71). This limitation is removed in case of circulating fluid bed technologies and ablative systems where product char is continually abraded off the particle surface exposing fresh biomass for reaction and increasing heat transfer rates [see Chapter 4].

Experiments on particle size effects were made by Beaumont and Schwob and showed a small reduction in the yields of organics [67 wt% to 65 wt% at 450°C] with increasing particle size from 125-250μm to 250-500μm size particles (19). Other studies have evaluated the effects of particle size on the final product distributions. Scott et al. investigated the influence of particle size [44-105 μm, 105-250 μm and 250-500μm] on organic liquid yields (72). They found using aspen poplar that the char yields were ambiguous as finer particles were entrained out of the reactor before complete reaction with the maximum organic yield occurring with the middle size range of 250-500 μm [57 wt% organics compared to 53 wt% for 250-500 μm and 51 wt% organics for 44-105 μm at 500°C].

Maniatis and Buekens carried out experiments in a Pyroprobe [800°C, holding time of 20 s] to assess the effects of particle size on product yields [1.5 to 2.5 mm] (70). They found that there was a slight increase in char yield from 18 to 20 wt%, an increase in the organic liquid yield from 40 to 46 wt% and a decrease in gas yields from 39 to 32 wt %. They suggested that the temperature gradient and history changed as particle size increased. Pyrolysis at the inner core thus occurred at a lower temperature and resulted in increased tar formation. The slight increase in the char yield was attributed to enhanced thermal cracking of tar on the hot surface of the particle.

Kelbon et al. in their study of the interaction between moisture content, heat flux and particle thickness found that for dry particles, the thickest particle [15 mm] gave the highest liquid yield [65 wt%] at the lowest heating rate of 8.2 W/cm^2 which decreased to 23 wt% at 24.5 W/cm^2 (68). The reason for this was that the pyrolysis front into the particle was more "smooth" and extensive cracking of the volatiles only occurred at the highest heating rate. The yield for the smallest particle [5 mm] at the highest heating rate was 40 wt% organics.

2.4.4 Biomass particle shape

The shape of the biomass particles will influence heat transfer, heating rates and the escape of volatile products from the solid matrix. Saastamoinen has used spherical, cylindrical and flat particles, all with the same volume/surface area ratio in his experiments (73). He found that the mass loss was greater for flat particles and slowest for the spheres, in line with expectations. A similar study by Maniatis and Buekens assessed particle geometrical effects using a square [1.4 x 1.4 mm], a cylinder [diameter 1.4 mm] and a rectangle [0.5 x 1.4 mm] (70). Using temperatures of 600-900°C they found that the highest organic liquid yields were obtained with the cylindrical particles and the lowest with the rectangular particles. The possible reasons for this are that the volatiles efflux from the cylinder was lower and cracking of the vapour product was reduced due to lower heating rates and hence tar formation was optimised. A study by Roy et al. in a vacuum pyrolysis reactor [10 kPa absolute, 450°C] used particles ranging from wood flour to 1 cm chips (74). The maximum organic liquid yield was obtained from the wood flour as volatiles rapidly escaped from the wood flour due to the high surface area/volume ratio [60.8 wt% organics for wood flour compared to 50.7 wt% for 10 mm chips]. Work has also been carried out by Gulyurtlu et al. who confirms that small particles, less than 2 mm, are required for high liquid yields (75).

The problem of limitations on the particle size are removed in ablative pyrolysis systems where heat transfer is by direct conduction with a heated surface. Under conditions of rapid heat transfer, the thermal front advances only marginally in front of the pyrolysis front into the particle. Ablative pyrolysis research is reviewed in Chapter 4.

2.4.5 Biomass physical and thermal properties

The biomass properties of density, permeability, conductivity, specific heat capacity and grain structure have an influence on reactor design and product yields. The effects of each are discussed briefly below.

2.4.5.1 Biomass permeability and grain structure

It has been determined that the longitudinal permeability may be as high as 1000 times that across the grain for some species [and can vary by over a factor of 100 if various wood types are considered] (76, 77). The escape of the volatile products is expected to occur primarily parallel to the grain in fluid bed environments. In ablative reactors, the grain orientation is significant from heat transfer considerations. Parallel grain thermal conductivity is 2-2.5 times higher than that across the grain; therefore, heat transfer along the grain leads to higher heat transfer rates and hence increased ablation rates. In practice, the influence of grain orientation has not been experimentally studied and in a fast pyrolysis reactor, control of the grain orientation is generally not possible, except in specially controlled experiments [see Section 4.2]. Low permeabilities can affect the yield of organic liquids by increasing the residence time of the products within the particle, in turn this increases the probability of secondary reactions due the high pressures within the particle and reaction with the hot product char (24).

A study has been conducted by Lee et al. on grain structure and permeability using a 250 watt CO_2-laser radiation source to study wood pyrolysis at heat fluxes of 4.2-12.6 W/cm^2 (78). They measured a maximum pressure gradient of 220 kPa/cm with a maximum internal gas pressure of 30 kPa gauge across the grain while the pressure gradient measured parallel to the grain was 100 Pa/cm with a maximum internal gas pressure of 300 Pa gauge. This large difference in internal gas pressure, they suggested, was reflective of the low permeability across the grain of the volatile products during wood decomposition. Lee et al. also observed that more cracks were formed during heating along the grain. These cracks could be a consequence of the release of volatiles from within the particle to the surface, due either to the internal pressure build-up or char layer shrinkage.

Chan et al. also investigated the effects of parallel and perpendicular heating relative to wood grain direction (79). At heat fluxes of 8 W/cm^2 the effect of the grain direction on volatiles release rate was small. For heat fluxes of 6 W/cm^2, perpendicular heating resulted in an increased resistance to volatiles efflux. Other studies carried out by Chan et al. confirmed that the maximum rate of mass flux of volatiles occurred with heat fluxes of 25.1 W/cm^2 and parallel grain heating with increased CH_4 and C_2H_4 yields (80). Initially the volatiles release

rate rose faster and the time at which maximum mass flux of volatiles occurred was lower with respect to parallel heating, because of the lower interior temperature resulting from heating perpendicular to the grain. There was also about 20% shrinkage of the char layer. This shrinkage was due to the char becoming more friable, resulting in a more rapid transfer of heat to the interior and therefore the subsequent volatiles surge.

2.4.5.2 Biomass density

Biomass density varies widely for a given range of feedstocks. The density will influence reactor design and it is especially important for ablative pyrolysis reactor design as the reactor throughput depends upon the volume of biomass pyrolysed per second [see Chapter 5]. One way to increase an ablative pyrolysis reactor throughput, provided heat transfer requirements can be met is by densification. This is however energy intensive and expensive and typically the feedstock density is not modified. One exception is the use of refuse derived fuel [RDF] and municipal solids wastes [MSW] which are usually pelletised. Therefore significant changes in the feedstock density will influence the reactor specific throughput, defined in kg/m^2h. The biomass density will also affect fluidization behaviour in conventional fluidised beds with low density material being entrained out of the bed before reaction is complete.

2.4.5.3 Biomass thermal conductivity

Fast pyrolysis requires rapid heating of the biomass to avoid low temperature, low heating rate reactions where water, CO_2 and char are the main products. If the product char is not physically removed from the surface of the pyrolysing solid, it can have two effects: reduce heating rates with promotion of slow pyrolysis reactions and react with the product vapours to form secondary char. If the char layer is continuously removed during reaction, high heat transfer rates can be obtained and the criteria for fast pyrolysis fulfilled. This occurs in ablative reactors as reviewed in Chapter 4. The biomass thermal conductivity is significant in ablative pyrolysis reactor design as noted in Section 2.4.5.1. However, there is no information on thermal conductivity values above 200°C: this is required for detailed analytical models which account for the variation of the biomass properties during reaction.

2.4.5.4 Biomass specific heat capacity

The specific heat capacity is required in basic reactor design for the evaluation of energy requirements for pyrolysis. As with biomass thermal conductivity, there is little information on its variation with temperature and it is generally assumed to be constant under fast pyrolysis conditions up to the point at which the biomass decomposes.

2.4.6 Intrinsic nature of the feedstock on pyrolysis products

The intrinsic influences of a feedstock on the product yields and compositions are due to variations in biomass composition, its physical and thermal properties, ash content and composition. Results from the work of Piskorz et al. have shown slight product yield and compositional differences under similar conditions as shown in Table 2.10 (81).

Table 2.10

Effects of feedstock on liquid yields and composition [wt% dry feed], 0.5 s residence time

Feedstock	Brockville Poplar	White Spruce	Red Maple	IEA Poplar
Reactor temperature [°C]	504	500	508	504
Organic liquid yield	62.9	61.5	67.9	69.9
Cellobiosan	1.11	2.49	1.62	1.3
Glucose	0.55	0.99	0.64	0.41
Fructose	1.34	2.27	1.51	1.32
Glyoxal	1.42	2.47	1.75	2.18
Methylglyoxal/Levoglucosan	2.52	3.96	2.84	3.69
1,6 anhydroglucofuranose	--	--	--	2.43
Hydroxyacetaldehyde	6.47	7.67	7.55	10.03
Formic acid	5.4	7.15	6.35	3.09
Formaldehyde	--	--	--	1.16
Acetic acid	6.3	3.86	5.81	5.43
Diacetyl *	0.87	0.89	0.63	1.05
Acetol	1.70	1.24	1.15	1.40
Pyrolytic lignin	24.8	20.6	20.9	16.2

* originally believed to be ethylene glycol

Analytical work carried out by Elliot using GC-MS on pyrolysis and gasification liquids has shown that softwood derived pyrolysis liquids are different from hard wood derived liquids as the lignin structure in softwoods contain no dimethoxyphenol compounds [see Figure 2.06] (82). Hardwood derived lignin contains a significant proportion of dimethoxyphenols.

To summarise, because of the anisotropic nature of wood, the physical and chemical structure, product yields and distribution can be controlled to a limited extent by pretreatment involving water washing acid washing and additives. The physical and thermal properties are not easily modified without using an energy intensive process, i.e. densification. Particle size, shape and water content are more readily controllable.

2.5 Reactor system process parameters

2.5.1 Reactor temperature

Reactor temperatures normally quoted in the literature refer to the temperature of the heat transfer surface in ablative pyrolysis reactors or the bed temperature in fluid bed reactors where pyrolysis is occurring. The reactor temperature has five key influences:

- product yields,
- composition of the liquids,
- enthalpy of pyrolysis,
- the chemical kinetics of biomass decomposition,
- biomass decomposition temperature.

2.5.1.1 Reactor temperature effects on product yields

The phenomenon of fluid bed biomass fast pyrolysis was "re-discovered" by Scott and Piskorz in 1982 when they demonstrated that high organic liquid yields could be obtained at reactor temperatures of 500-525°C and short product residence times [< 1 s] using a small fluidised bed (72). Typical results are depicted in Figure 2.07 (83). During the following review, reference is frequently made to the work of the researchers at the University of Waterloo as they have published the most consistent data for fast pyrolysis over the last 14 years. Their work has consistently demonstrated that there is a distinct maximum in organic liquid yields around 500°C, with variation of the optimum due to the intrinsic nature of the feedstock, e.g. for cellulose, 85 wt% liquids have been obtained at 450°C (84) while Nunn et al. have shown that for sweet gum hardwood 55 wt% organics are obtained at 627°C (85). This general trend of maximum liquid yields at similar values to those given in Figure 2.07 is supported widely [e.g. 86, 84, 87, 88].

The exact reason for this maximum in organic liquids yield at 500°C has not been fully explained, although it is probable that at 500°C the energy supplied to the biomass is sufficient to heat the biomass to its decomposition temperature, provide the energy required for the endothermal heat of pyrolysis and vaporise the organic liquids without any additional energy being available for secondary reactions.

Scott et al. carried out an assessment of the influence of temperature on the yields of products for fast pyrolysis with cellulose and eastern maple as the feedstock in two different reactor configurations in collaboration with the University of Western Ontario (84). Their view was that if the particle temperature reached 450°C before more than 10% of the wood had reacted, then excessive char production would be avoided and liquid decomposition would be minimised by the rapid volatilisation and removal of the liquid components.

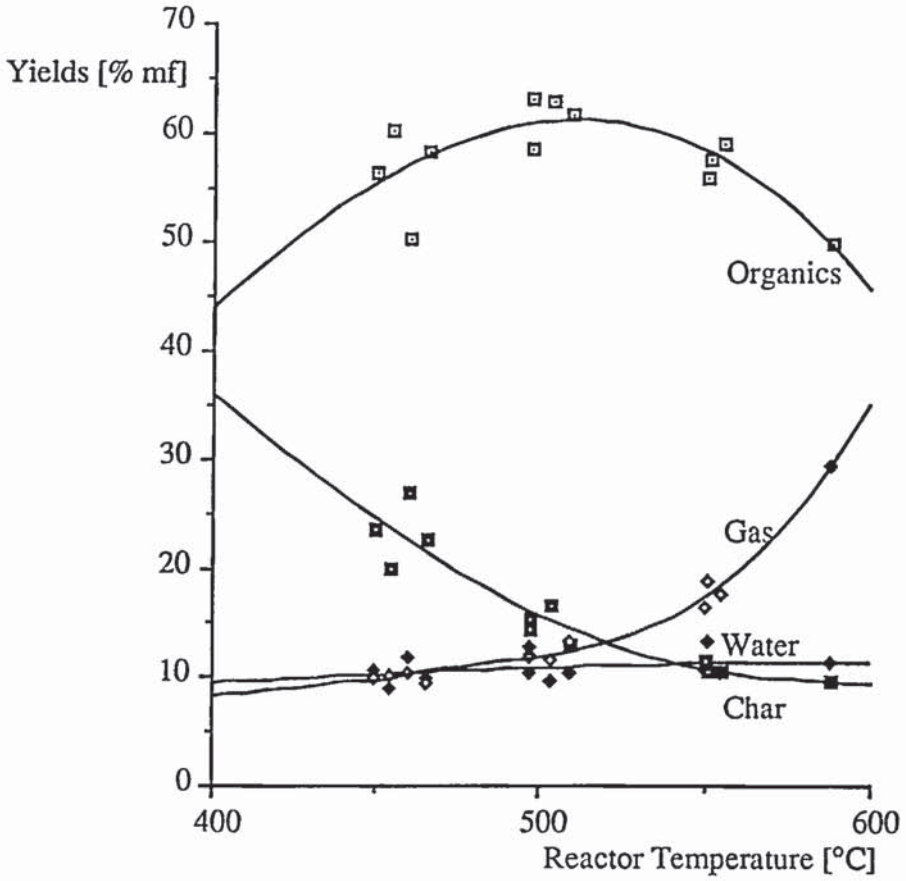

Figure 2.07. Variation of product yields with reactor temperature

From the kinetic and heat transfer modelling work of Lidén (83) and based upon the kinetic values of Thurner and Mann (89), Scott calculated that for 2 mm hardwood particles in a fluidized bed at 500°C, the above criterion would be satisfied. Under these conditions, the product distribution from any reactor, for the same gas phase residence times, would be expected to be a function of the reactor temperature only. The final product distribution and composition would then depend upon the history of the vapour phase and the secondary vapour phase kinetics [see Chapter 3]. Typically for the production of organic liquids in high yields, reactor temperatures of 450-600°C are used (90).

2.5.1.2 Chemical [and elemental] composition of the liquids

The chemical composition of pyrolysis liquids is also influenced by the reactor temperature. Work carried out and summarised by Elliot (91, 92) [see Figure 2.08] and Evans and Milne (93) [see Figure 2.09] has shown that as the pyrolysis temperature increases, the hydrogen/carbon and oxygen/carbon ratios decrease due to the formation of more stable aromatic ring structures with the loss of water. Evans and Milne proposed a change in the chemical product spectra from mixed oxygenates at 400°C to polyaromatic hydrocarbons [PAH] at 800 and 900°C as shown in Figure 2.09 (93).

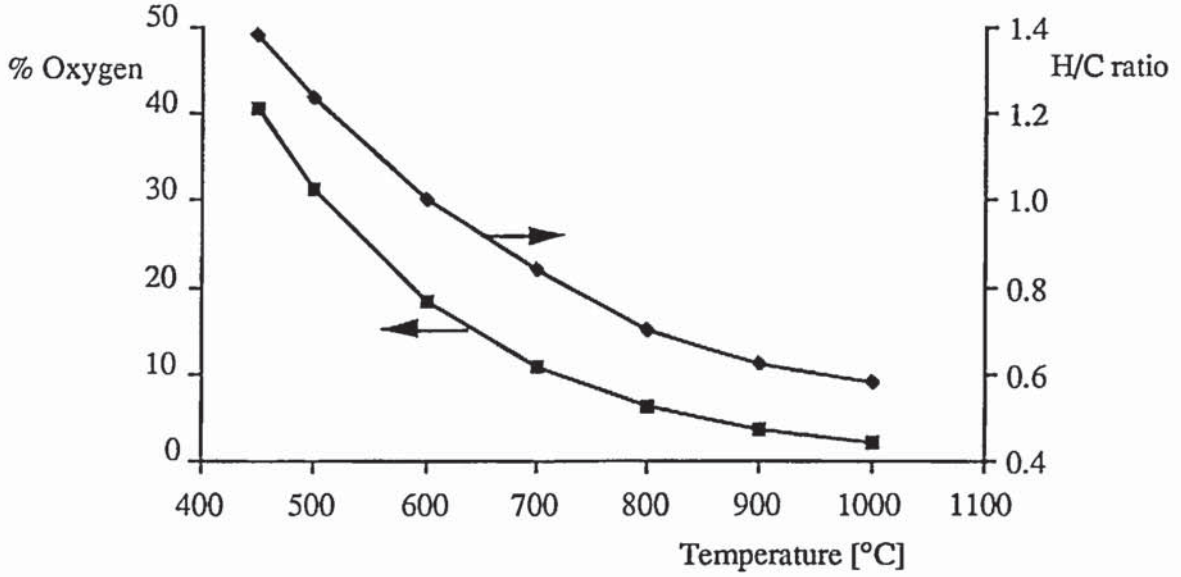

Figure 2.08. Variation of oxygen content and hydrogen/carbon ratio with temperature

400°C Mixed oxygenates → 500°C Phenolic ethers → 600°C Alkyl phenolics → 700°C Heterocyclic ethers → 800°C PAH → 900°C Larger PAH

Figure 2.09. Change in chemical composition with temperature

This is due to "thermal" treatment of the primary product vapours to secondary liquids. Similar changes in the chemical structure of the recovered liquids have also been studied by Vassilatos which confirms these findings (94). In high temperature pyrolysis experiments [700-900°C], he observed that the naphthalene yield increased with reactor temperature even though the overall liquid yield decreased. The time-temperature history of the product vapours will have a large influence on their final composition as discussed in Section 2.5.8.

Scott et al. have also looked at the effects of reactor temperature on liquid product yields (95). Some results are shown in Figure 2.10 below for Avicel cellulose pyrolysis. It can be seen that sugar derived compounds such as levoglucosan are favoured at lower reactor

temperatures with increasing temperature favouring fragmentation reactions. This formed the basis for the Waterloo cellulose pyrolysis pathway which is discussed in Chapter 3. The reader is also referred to the extensive results compiled by Halling using the data of the University of Waterloo (96).

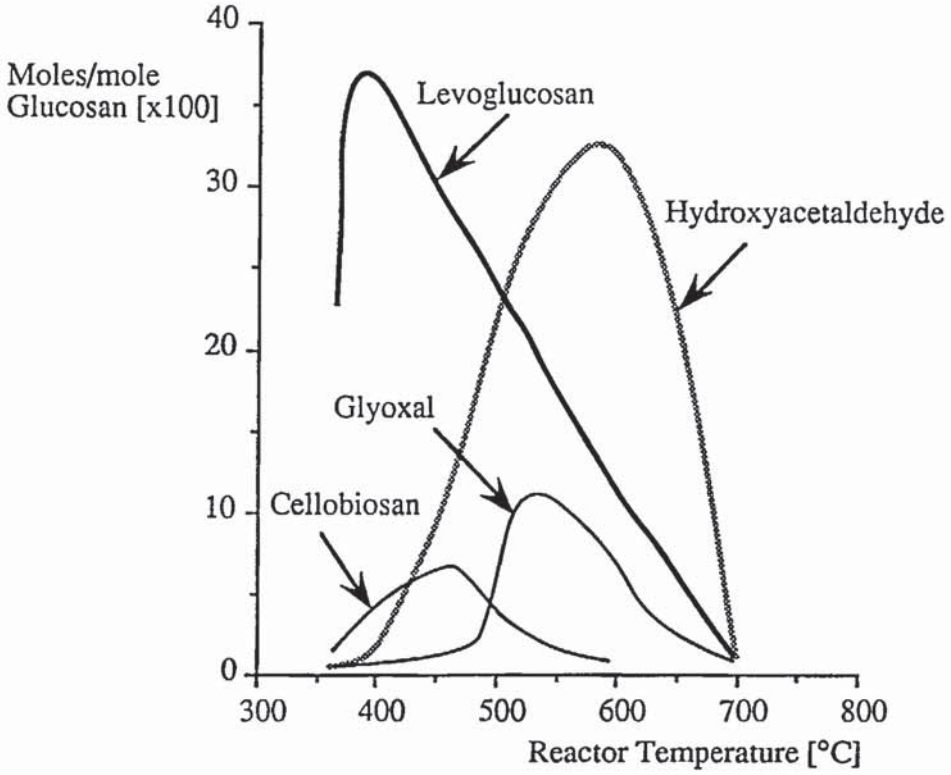

Figure 2.10. Variation of chemical yields with temperature for Avicel cellulose

2.5.1.3 Enthalpy of pyrolysis

The enthalpy of pyrolysis is the energy released or consumed during the primary decomposition of biomass to form char, liquid and gas products. There is a wide range of values quoted for the enthalpy of pyrolysis for slow and conventional pyrolysis conditions of low heating rates and low reactor temperatures for varying moisture contents, temperatures and wood types (e.g. 49, 97, 98, 99, 100). As an example, values range from 125 kJ/kg (101) to 500 kJ/kg for Douglas fir at a reactor temperature of 500°C (3). Shafizadeh was one of the first to show the changes in the enthalpy of pyrolysis with temperature by the use of Differential Thermal Analysis [DTA] (29). Figure 2.11 shows typical results and these highlight the problem of selecting a suitable value bearing in mind the variations in cellulose, hemi-cellulose, lignin and ash in different biomass sources. The enthalpy of pyrolysis is also influenced by particle size, heating rate and moisture content of the biomass, and therefore the selection of a suitable value is specific to the experimental conditions.

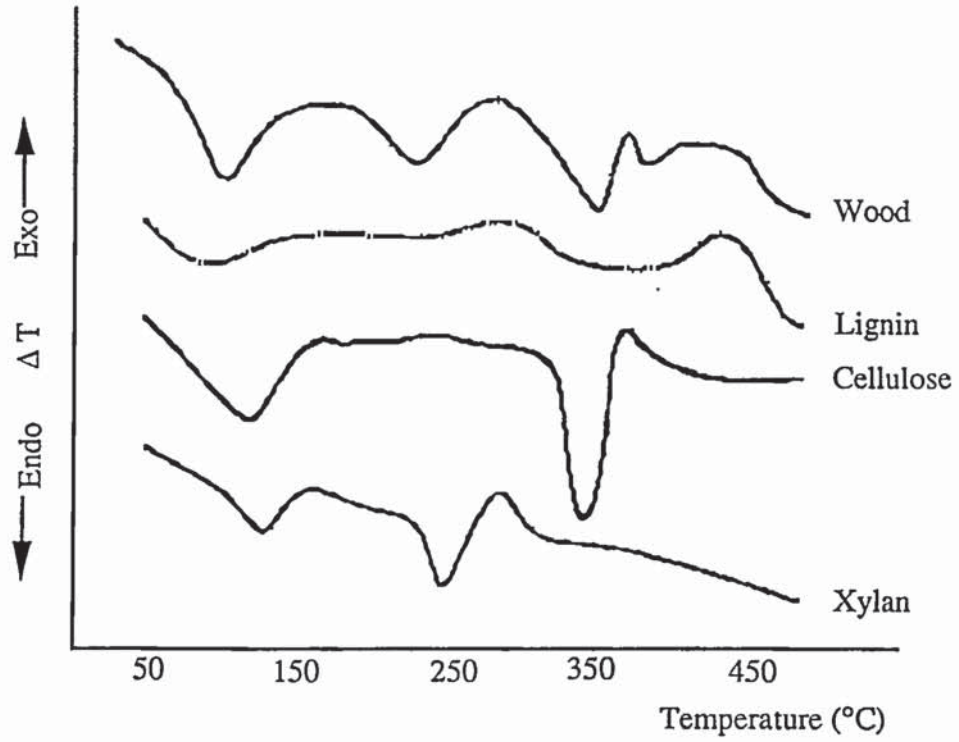

Figure 2.11. Differential Thermal Analysis of hardwood and its components

Roberts concluded that the enthalpy of pyrolysis was dependent on the particle size and heating rate due to the migration of volatiles through a particle causing convective cooling and internal convection coupled with heat conduction (77). This was also confirmed by Antal who has noted the effects of heating rate and particle size on the enthalpy of pyrolysis (102). The selection of a suitable value for wood pyrolysis under fast pyrolysis conditions is therefore difficult. Reed has proposed a value of 40 J/g, which appears to be the most commonly accepted value in the fast pyrolysis literature and is the value used in this work (49).

2.5.1.5 Reactor temperature and biomass temperature profiles

Depending on the reactor parameters and the feedstock size and shape, the temperature of the feedstock will differ from that of the reactor due to chemical reaction, heat conduction into the particle and convective cooling and/or heating of the product vapours as they exit the pyrolysing particle (29). Figure 2.12 illustrates possible temperature profiles during heat transfer in different regimes: fluid bed, turbulent mixed bed, entrained flow and ablative during conversion. The extent of vapour product migration from the particle therefore depends upon the thickness of the char layer on the particle surface. For entrained flow reactors where there is no turbulent mixing of the biomass with a solid heat carrier, the product vapours have to migrate through a relatively thick hot char layer, leading to secondary

reaction and product cracking. In ablation, the products are rapidly removed from the reaction interface with no char build up.

The work of Lédé has looked at the effects of reactor temperature, heat transfer rates, biomass thermal and physical properties and kinetics on the decomposition of cellulose in the chemical and ablation regimes. Lédé has shown that the reactor or medium temperature has little influence on the pyrolysis temperature of biomass whether it is in the chemical regime, i.e. the pyrolysis rate is limited by chemical reactions or in the ablation regime, i.e. rate of pyrolysis is heat transfer limited. He demonstrated for cellulose pyrolysis that for an increase of reactor temperature from 627°C to 1227°C the biomass "fusion" or pyrolysis temperature increased gradually from about 407-483°C for an assumed heat transfer coefficient of 10000 W/m^2K (103). Lédé et al. from fundamental experiments on wood rod ablation estimated that the wood decomposition temperature was 466°C ± 30°C for 600-900°C for estimated heat transfer coefficients ranging from 1000-20000 W/m^2K [see Section 4.2] (51).

Views that the fast pyrolysis of biomass occurs at a constant temperature, slightly influenced by the reactor temperature have been proposed by Reed (49), Kothari and Antal (104) Désrosiers and Lin (98) and Diebold (105). Studies by Diebold on the thermal "sawing" of wood with a hot Nichrome wire showed that upon cooling at the cut interface, a thin clear layer of depolymerised solid was left. Reed has proposed that under fast pyrolysis conditions, the wood is rapidly heated to 500°C without any significant decomposition.

2.5.2 Gas/vapour product residence time

Gas/vapour product residence time is defined as the ratio of net empty reactor volume [m^3] to the pyrolysis vapour/gas product formation rate plus the carrier gas/diluting gas volume flowrate [m^3/s], at the reactor gas/vapour phase temperature. Its significance is that secondary gas/vapour phase reactions can lead to reduced yields of organic liquids and certain oxygenated chemicals for temperatures greater than 500°C and for long residence times [> 2 s]. Evidence has been obtained during the course of the author's work that secondary condensation reactions occur at long residence times and gas/vapour product temperatures below 400°C, as discussed in Chapter 8 and 9. Secondary gas/vapour phase decomposition kinetics are reviewed in Chapter 3. Control of the gas/vapour residence time is therefore seen as being an essential parameter in fast pyrolysis, but equally important is the gas/vapour phase temperature.

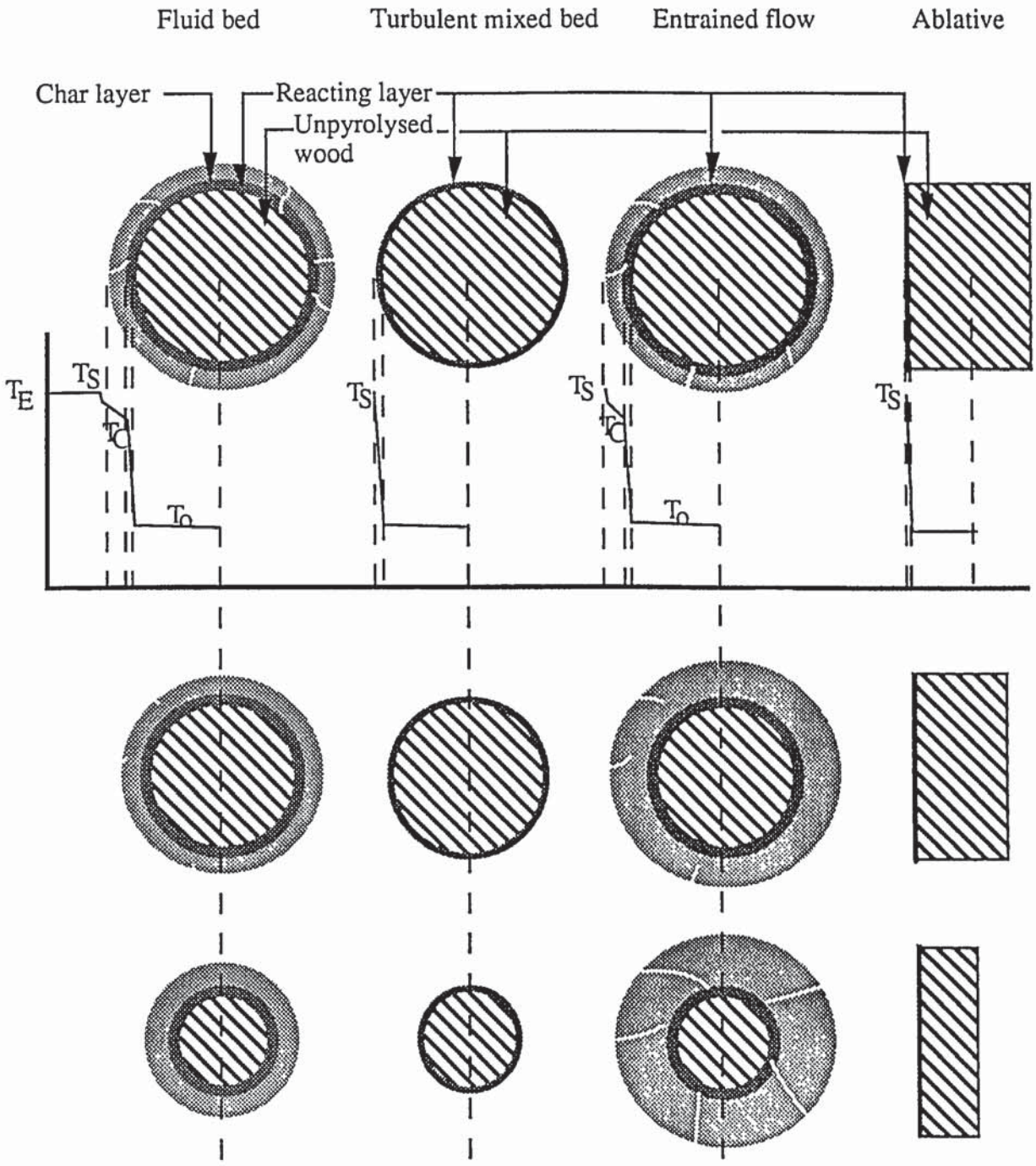

where:

T_E:	environment temperature	T_S:	surface temperature
T_C:	char temperature	T_o:	biomass temperature

Figure 2.12. Biomass temperature profiles in four different reactor configurations with increasing time

The effects of the gas/vapour product residence time on the yields of products were studied by Scott and Piskorz who showed that the liquid yield rapidly decreased with increasing residence time as shown in Table 2.11 (106). From these results, Scott and Piskorz specified residence times of the order of 0.5 s for optimal liquids production at 500°C, in conjunction with small particles [size -595 μm] for a liquid yield of 76.1 wt% on a dry wood basis (106). Scott et al. adopted a value of 0.5 s as their "standard" for optimal liquids production.

Table 2.11
Variation of organic liquid yield [wt%] with residence time, reactor temperature 500°C

Residence time [s]	0.38	0.44	0.54	0.54	0.68	1.07
Organic liquid yield	57.5	57.5	53.3	51.7	50	45.2

The reduction of residence time and consequently secondary gas phase reactions by using an inert gas as a temperature moderator and a diluent has been explored by Reed [see Section 4.3] (107). He showed that the liquid yields from a small scale laboratory ablative pyrolysis reactor were increased from 33 wt% to 48 wt% on increasing the volumetric flow of nitrogen by a factor of 6 through the reactor, although no estimates of the reduction in the apparent residence time were quoted.

The residence time of the vapours and also the gas/vapour temperature will also affect the chemical composition of the liquid product. A short residence time for the vapour products within the reactor will minimise the extent of secondary reactions [see Section 2.4.1.2] (84). Graham et al. have studied product yield variation with residence time for a reactor temperature of 650°C (108). They showed that the liquid yield reached an asymptotic value at about 0.5 s, as shown in Figure 2.13 overleaf. The asymptotic yield of 55 wt% organics at long residence times is not widely supported, although these results can be accounted for by the thermal quenching of the gas/vapour products with a cold solid. It is commonly believed that the liquid yields will continue to decrease with increasing residence times, as predicted by several kinetic models [see Chapter 3]. It is more likely that despite long residence times, the products will form more thermally stable compounds as gas/vapour phase reactions are limited. Therefore, an asymptotic value will be reached at gas temperatures of 400-500°C.

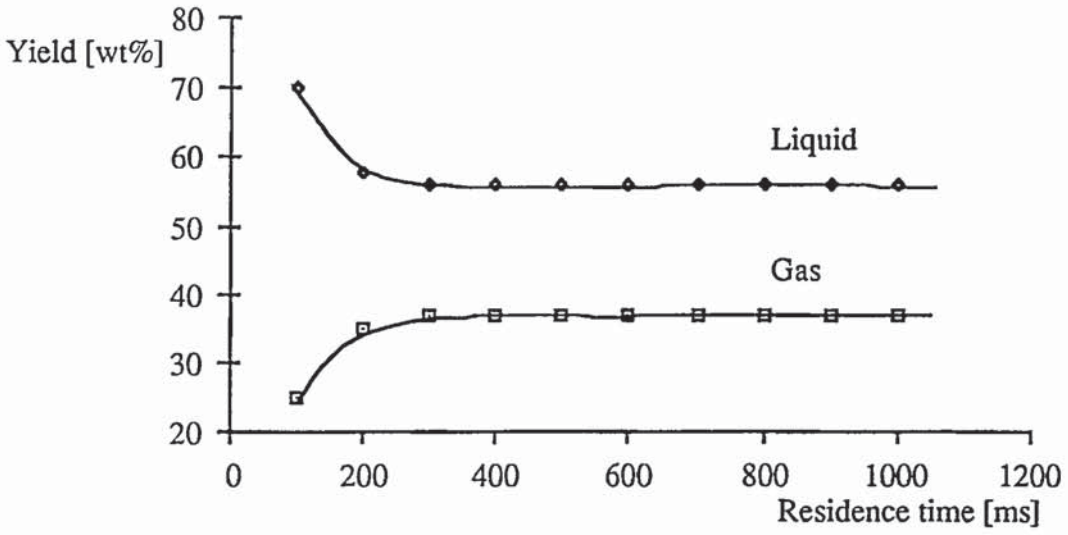

Figure 2.13. Variation of gas and liquid yields with residence time

2.5.3 Gas/vapour product temperature

The gas/vapour product temperature is the temperature of the gas/vapour products after formation at the surface of the biomass particle. The gas/vapour product residence time should not be discussed without including the gas/vapour product temperature. If the temperature of the products is above 500°C, the vapours will continue to react to form gases and soot with reduced organic liquid yields. Much of the work which has been carried out on the effects of temperature on the yields and composition of the liquids have focused on temperatures above 500°C, in particular on secondary vapour phase reactions, as discussed in Chapter 3. There is no available information on the effects of temperatures below 400°C, it would appear that below 400°C, condensation reactions occur with the formation of water.

Vapours from the vortex reactor of NREL [see Section 4.6] have been subjected to various degrees of "thermal treatment" to examine the effect on the liquid composition as shown in Table 2.12 (109), although the exact details of the thermal treatment were not specified. The continual exposure of the vapours to high temperatures will therefore influence the liquid composition. In ablative pyrolysis systems where no particle transport or carrier gas is used, the temperature of the vapour products may be moderated by the addition of a diluting and cooling gas such as recycled non-condensible gas products or an inert gas such as nitrogen.

Table 2.12
Thermal treatment of pyrolysis vapours from the NREL vortex reactor

Degree of thermal treatment	low	med	med-high
Composition [wt%]			
carbon	55.6	54.8	71.6
hydrogen	5.0	4.5	5.9
oxygen	39.2	40.6	22.3
nitrogen	0.1	0.1	0.2
Proximate analysis			
ash	0.05	0.05	0.05
water	16.9	24.8	23.6
fixed carbon	14.1	16.0	10.1
Density [g/cm^3]	1.23	1.19	1.13
Viscosity [@ 45°C, cP]	77	22	10

2.5.4 Heat transfer and heating rate

2.5.4.1 Heat transfer

The rate of heat transfer into the pyrolysing biomass will influence the yield of products and the design of a reactor. In this section two methods of heat transfer are discussed: gas-solid [convective] and solid-solid [conductive] heat transfer. Heat transfer in molten baths is beyond the scope of this thesis. In fluid bed systems [entrained flow, conventional fluid bed and circulating fluid bed], heat transfer is effected primarily by convective heat transfer from the hot fluidising gas to the biomass particle. Heat is also transferred to a lesser extent by abrasion of the fluidised bed solid and radiation from the reactor walls if externally heated.

Reed et al. carried out an assessment of the heat transfer requirements for fast pyrolysis (49). They specified that to achieve fast pyrolysis, heat fluxes of 50 W/cm^2 would be required at a temperature of 500°C. A study carried out by van den Aarsen et al. estimated that the heat transfer coefficient to a 1 mm diameter beech particle was approximately 50-250W/m^{2}K at temperatures of 700-900°C and that the particle would be reacted in less than 2 s with heating rates of approximately 500°C/s (110). Scott and Lidén have attempted to define some criteria for fast pyrolysis in terms of particle heating rate. One criterion was to assume that if the particle temperature reached 450°C before more than 10% of the wood had decomposed [as determined from a rate of weight loss kinetic equation], then excessive char production would

be avoided and the optimal production of organic liquids would be obtained. From the kinetic data of Thurner and Mann, they estimated that for gas-solid heat transfer environments, particles less than 2 mm are required for conventional shallow fluid beds for fast pyrolysis criteria to be fulfilled at a reactor temperature of 500°C (95).

A study by Graham and Bergougnou estimated particle size limitations from isochrones derived from heat transfer relationships. They concluded that fluid beds required small particles to obtain high heat transfer rates, typically 0.1-1 mm particles for heating rates up to 1000°C/s (37, 111). The other conclusion was that the average particle size to achieve fast pyrolysis at 500°C would have to be 0.5 mm in a convective heat transfer environment, 25% of the particle diameter suggested by Scott and Lidén. Simmons and Gentry also estimated the regimes under which particle fast pyrolysis would be kinetically or heat transfer limited (112). They determined that for a cellulose particle to reach the reactor temperature assuming only 10% decomposition at 500°C, the particle should be 70μm: for a particle size greater than this, the particle pyrolysis rate would be heat transfer limited, i.e. the ablation regime and the upper limit on the particle size was 200 μm at a reactor temperature of 500°C. Convective heat transfer correlations have been reviewed by in considerable detail by Prins (113) for fluid bed heat transfer and also by Maschio et al. (114).

Heat transfer in ablative conditions has been modelled primarily by Lédé (51, 115) and in collaboration with Diebold and Power (116). Lédé et al. have modelled in detail ablative heat transfer using a simple piece of apparatus comprised of ablatively pyrolysing wooden rods on a rotating heated disk. Heat fluxes of up to 2000 W/cm^2 were estimated for applied particle pressures of 3.5 x 10^6 Pa and a disk temperature of 1173K with observed ablation rates up to 3 cm/s. A further detailed description of his correlations can be found in Section 4.2 (103).

2.5.4.2 Biomass heating rate

Recent studies have shown that by increasing the heating rate, the reaction pathways can be optimised to maximise liquid products. High heating rates have been recognised as being a key feature by many researchers to minimise the formation of char (e.g. 117, 118, 50, 110, 119, 120). Maniatis and Buekens showed that heating rate had little effect on the yield of products above 100 K/s (70). Scott et al have estimated the heating rates in their fluid bed reactors to be 10^4-10^5 K/s (84), similar to those reported by Diebold [4.5 x 10^5 K/s] (121) and Lédé [> 1 x 10^6 K/s] (51). A detailed study by Gulyurtlu investigated the effects of heating rate, particle size and temperature on product yields. He measured the internal temperature of wood particles, size, 0.5, 2, 5 and 10 mm for two heating rates of 10 and 250°C/s, temperature 900°C. He concluded that it would take up to 2 s for the centre of a 2 mm particle to reach the reactor temperature and that particles less than 2 mm should be used to achieve high

heating rates [> 250 K/s] (75). The heating rate usually refers to the rate at which the whole solid particle is being heated. Due to the very good insulating properties of wood [thermal conductivity 0.1-0.2 W/mK] and wood char [0.15 W/mK at 500°C (53)] under fast pyrolysis conditions, the heating rate can only refer to the high temperature gradients at the thin reaction layer or for very small particles [< 100 μm].

2.5.5 Pressure

There are two way of applying pressure to the solid phase: hydrostatic [in the reactor gaseous environment] and mechanical [applied]. Firstly, the effects of reactor pressure on liquid and chemical yields are summarised and then the effects of mechanical pressure in ablative pyrolysis are discussed. Pressure also affects secondary pyrolysis reactions according to whether pyrolysis is carried out under vacuum or in a high pressure environment.

2.5.5.1 Low pressure [< 1 bar]

One of the primary examples of low pressure pyrolysis is that of Roy et al. (122). Wood chips were processed in a vacuum pyrolysis reactor at 200-450°C, reactor pressure 1.3-10.7 kPa. Roy found that increasing pressure reduced organic liquids yields with increasing gas yields. However, the estimated gas/vapour products residence times in the reactor were about 40s and therefore, secondary [condensation] reactions could have occurred, especially at low gas/vapour product temperatures. The results are shown in Table 2.13 overleaf. Heat transfer in the multiple hearth reactor is low, estimated at 25 W/m^2 and therefore, volatiles residence time in the particle may be long [particle dimensions typically 6.35-12.7 mm].

Shafizadeh et al. have also carried out work on the vacuum pyrolysis of cellulose. At temperatures greater than 250°C, vacuum pyrolysis of cellulose yields a volatile liquid which contains mainly levoglucosan [1,6-anhydro-β-D-glucopyranose] (60). Liquid yields of up to 63 % were obtained from cotton hydrocellulose. Purity and physical properties [ash content and degree of crystallinity] of the cellulose were found to have a profound influence on the yields of levoglucosan with low crystallinity and low ash [<0.05 wt%] enhancing levoglucosan yields. Some results are summarised in Table 2.14 for cellulose pyrolysis under different pressures (29, 56).

Table 2.13

Pressure effects on product yields from a multiple hearth reactor, temperature 450°C, [yields, wt% moisture ash free feed basis]

Pressure [kPa absolute]	Char	Organics	Water	Gas
1.3	23.0	50.0	15.6	11.4
1.6	21.3	50.9	16.5	11.3
3.3	25.6	45.8	17.0	11.6
4.0	25.5	47.4	16.9	10.2

Table 2.14

Effects of pressure on cellulose pyrolysis, 300°C [yields, wt% basis]

Conditions	1 atmosphere	202 Pa	202 Pa + 5 wt% $SbCl_3$
Char	34.2	17.8	25.8
Organic liquids	19.1	55.8	32.5
Levoglucosan	3.57	28.1	6.68
1,6- anhydro-β-d-glucofuranose	0.38	5.6	0.91
D-glucose	trace	trace	2.68
Hydrolyzable materials	6.08	20.9	11.8

This suggests that reduced pressure can increase yields of anhydrosugars, such as levoglucosan, by promoting rapid devolatilisation of products from the reaction zone (56). Work carried out by Scott et al. in a shallow fluid bed at 21 kPa absolute showed that the char and gas yields increased at the expense of organic liquid yields relative to the results obtained at atmospheric pressure (63). Possible reasons for the lower yields were postulated to be due to reduced heat transfer in the more dilute gas phase and lower heating rates. The use of a reduced pressure in an ablative pyrolysis system may be beneficial as an aid to reduce the reactor residence time where mechanical methods are used to generate the contact pressure between the biomass and the heated surface.

At 340°C, Agrawal and McCluskey demonstrated similar influences on product yields when they examined the effects of pressure on the pyrolysis of newsprint (123). With an increase in

pressure from 1 torr [133 Pa] to 700 torr [93300 Pa], and for a sample residence time of 1 hour in the pyrolysis zone, the organic liquid yield decreased from 61 wt% to 25 wt% with a corresponding increase in the char yield from 19 wt% to 25 wt%.

2.5.5.2 High pressure [> 1 bar]

The effects of high pressure on biomass pyrolysis in terms of product yields has been reviewed by Mok and Antal (124). Their general conclusion was that increasing pressure increases char formation as is expected with a decrease in volatiles formation. They also observed that an increase in pressure favours CO_2 and H_2 formation while the yields of CO, CH_4, C_2H_4, C_2H_6 and C_3H_6 are reduced. Mok and Antal also carried out experiments to study the effect of residence time on product yield. The experimental conditions used were a pressure of 5.05 bar and residence times of 1 and 10 seconds. They observed that long residence times encouraged the formation of C_2H_6, char and CO_2 at the expense of CO and C_3's. This work has also recently been continued to assess the effects of pressure on char yields in a TGA reactor, confirming that increasing the pressure increased char yields up to 41 wt% at 100 bar, a final temperature 800°C and a heating rate of 10°C/min (125).

Work has been carried out by Güell et al. on the effects of pressure on liquid structures in a wire-mesh reactor with a hydrogen atmosphere (126). Liquid yields rapidly dropped from 54 wt% organics to a relatively constant value of 42 wt% for an increase of pressure from 1 bar to 10 bar, a heating rate of 1000°C/s, and a peak temperature of 700°C. Analysis of the liquid fractions for the experiments indicated that in the presence of hydrogen and increasing pressure the mass average molecular mass tended to decrease until the molecules reached a point at which they could vaporise. The liquids are less polar due to the presence of hydrogen replacing some carbonyl groups and forming water. These results were quantitatively similar to those of Hajaligol et al. obtained in similar equipment, however in their work, the maximum liquid yield occurred at a higher peak temperature of 700°C (127). As part of a collaborative study on the comparison of results from a wire-mesh and the ablative pyrolysis reactor used in the author's work, liquid yields were found to decrease from 62.1 wt% to 48.7 wt% for a pressure increase from 1 to 10 bar [see Appendix IB].

The work of Steinberg et al. mainly involved the investigation of the fast pyrolysis of wood in an entrained flow reactor with reactive and non-reactive gases at different pressures, temperatures of 800-1000°C were used and consequently high gas yields were obtained (128, 129, 130). Using H_2 pressures of 345 kPa, 1380 kPa and 3450 kPa, they observed that the yields of hydrocarbons [CH_4, C_2H_6 and C_2H_4] and CO were significantly affected by the pressure employed and also by the residence time. In their studies the effect of temperature, pressure and residence time on gas yields were determined simultaneously. Using pressures

of 3450 kPa, they found that the main product accounting for the highest total carbon conversion was CH_4 whereas at the lower pressures of 345 kPa and 1380 kPa, it was CO, when a vapour residence time of 1 second was used. They also observed that the pressure at which methanation occurred, decreased with increasing temperature, i.e. at 800, 900 and 1000°C, they observed methanation pressures of 2414, 2069 and 1724 kPa respectively. In addition, they found that at all the pressures studied, the yields of CO_2, C_2H_4, benzene, toluene and xylene [BTX] decreased with increasing temperature due to secondary reactions.

Increasing the methane pressure from 138 kPa to 1380 kPa at 1000°C, Steinberg et al. found that the major product was CO which reached a maximum of about 55% at 100 psi (130). In addition, the ethylene yield increased with decreasing pressure, reaching a maximum of 22% at 345 kPa. The BTX yield remained almost constant at about 10 to 12%. At all helium pressures studied, CO was also the major product.

Limited higher pressure effects have also been studied by Samolada et al. in a fluid bed reactor. They qualitatively stated that increasing the pressure in the reactor suppressed the formation of methane and ethene [1-1.5 bar increase in pressure] (88). A detailed range of experiments have been conducted by Guanxing et al. on the effects of steam and dolomite on high temperature pyrolysis of biomass at 650°C and 500 kPa pressure (131). The char yield was reduced from 10.5 wt% to 7.2 wt% with a gradual increase in the proportion of steam due to low temperature gasification. Dolomite increased the char yield from 10.5 wt % to 31.5 wt% for a mass ratio of 1 dolomite:wood at a temperature of 650°C and pressure of 480 kPa.

Work has also been carried out on the fast pyrolysis of peat under high pressure, high heating rates and in reactive atmospheres by Eklund and Wanzl using the Curie-point technique (132). Pressures ranged from 5-20 MPa and temperatures from 800-1000°C, again higher than those used for optimal organic liquids production. They confirmed that the increase of pressure from 5-20 MPa increased the char yield from 17-23 wt%. The effects of two heating rates were also studied at 10 MPa and a temperature of 800°C. For heating rates of 500 K/s and 10000 K/s, the char yield deceased from 24 wt% to 19 wt% and the liquids yield remained relatively constant with only a slight drop from 50 to 49 wt%. High pressures promote secondary and tertiary reactions and depending on the reactor temperature and gas/vapour product residence times used, char formation and/or gas production is enhanced. For fast pyrolysis, atmospheric pressures should be used for ease of reactor operation and equipment specification.

Therefore, for the production of liquids in high yields, atmospheric pressure should be used. One penalty of operating at lower pressures is increasing safety problems as air ingress to the reactor could be a potential fire hazard.

2.5.5.3 Mechanical [contact] pressure

Contact pressure is used in ablation reactors where the biomass is brought into direct contact with a solid heated surface to effect conductive heat transfer to the biomass. By increasing the applied pressure, the rate of linear regression [ablation] of the biomass is increased. The most detailed work has been that of Lédé who has studied the ablation of wood rods, diameter 2-10 mm for a range of applied pressures and heated surface temperatures under conditions of relative motion. The measured ablation rate was increased from 3 mm/s at an applied pressure of 370 kPa to 9.5 mm/s at 1390 kPa for a heated surface temperature of 900°C, a rod diameter of 5 mm and a relative velocity greater than 1.2 m/s (51). Related work on ablative pyrolysis is reviewed in Chapter 4.

2.5.6 Reactor gaseous environment

The reactor gaseous environment is the gas/vapour phase in the reactor into which the pyrolysis products are released after volatilisation/release from the biomass. The gaseous environment in a reactor can have four functions:

- moderate the temperature of the gas/vapour products to minimise secondary reactions and "freeze" thermally sensitive chemicals,
- remove the volatile products from the hot reaction zone,
- act as a heat transfer medium to the biomass particles [radiative and convective heat transfer],
- react with the gas/vapour products or the hot pyrolysing solid directly.

The gas may be N_2, steam, H_2, helium, product gases [mainly CO, H_2O, CO_2 and CH_4] or CH_4. For the first case of moderating the temperature of the gas/vapour products, an inert gas such as nitrogen, helium or argon could be used. Use of gas to moderate the gas/vapour temperature has been studied by Reed who showed that a 6 fold increase in inert gas flow through their reactor increased the yield of liquids significantly from 33.5 wt% liquid to 48.6 wt% liquid for a heated disk temperature of 550°C [see Section 2.5.2 and 4.3] (107). Work carried out in wire-mesh reactors typically uses nitrogen or helium as a carrier gas to remove the volatile products from the hot wire-mesh to minimise secondary reactions (e.g. 126, 127, 133). The examples of the use of gases as the heat transfer medium are numerous in the literature, typically in conventional fluid bed reactors or entrained flow and circulating fluid bed reactors. The pyrolysis gases may also be combusted and be used as the heat transfer gas, e.g. Trebbi (134) and Maniatis et al. (135).

A study by Shankaranarayanan et al. looked at the effects of different gaseous environments on the pyrolysis of coffee wastes (136). The aim of the study was to investigate the influence

of N_2, H_2 and CH_4 as carrier gases on the product yields for catalysed and normal samples of waste of two different moisture contents [0 and 50%] in a batch reactor with a continuous stream of the hot gas through the solid. For the dry samples, and the different gases, the char yield remained relatively constant at 19 wt%, however when using methane, the gas yield rose to 62.9 wt% compared to 52 wt% for nitrogen and 50 wt% for hydrogen atmospheres. The organic liquid yield decreased with all gases to about 14 wt% at 800°C. For the wet normal sample at 800°C, they found that when using hydrogen as the gas, 56.8 wt% of hydrocarbons and olefins were formed. The addition of potassium carbonate had the effect of catalysing the degradation of the organic liquids to gases.

Work carried out by Scott et al. on the use of recycled product gas showed only slight differences in the overall liquid yields and considered the effects of reactive gases to be slight below 600°C (106). They also carried out fast pyrolysis experiments using methane in order to determine its influence on product yields: there was no significant difference in the products obtained using methane compared to nitrogen, e.g. total liquid yield at 500°C was 77 wt% wood fed for methane while in a nitrogen environment it was 75 wt% (72). Scott et al. suggested that light organics such as acetic acid, aldehydes and methanol were about 25% higher in the methane atmosphere and similar to the results observed by Steinberg et al as discussed below. Char yields were lower in methane than in nitrogen with a maximum difference in yield of 4 wt% [16 wt% in N_2 compared to 12 wt% in CH_4] at a reactor temperature of 450°C. Below 550°C, gas yields were higher in methane than in nitrogen with a maximum difference in yield of 5 wt% [12 wt% in CH_4, 7 wt% in N_2 at 475°C]. There was little difference between gas yields above 550°C.

Steinberg et al. reported studies of the effect of flash pyrolysis of biomass in hydrogen, nitrogen, argon, helium and methane atmospheres [see section 2.5.5.2] (128). Pyrolysis in hydrogen resulted in CH_4 being the major product whereas with methane, nitrogen, helium and argon, the major gaseous product was CO. However, with methane, the yields of C_2H_4 and BTX were found to be greater than those where an inert gas was used. For example, it was found that pine wood pyrolysed at 1000°C and 345 kPa yielded eight times as much C_2H_4 with methane than with helium. Yields of C_2H_4 and C_6H_6 greater than 50% based on wood carbon conversion were obtained at methane-to-wood ratios of six or more (130). Two mechanisms were proposed by Steinberg et al. to explain the increase in yields of benzene and ethylene (130). The first proposal was that the wood surface acted as a catalyst to thermally decompose methane. The second proposal, which Steinberg et al. thought was more likely, was that free radicals were formed during the pyrolysis of wood which subsequently reacted with methane forming methyl radicals; these radicals then combined to form ethane which, in turn, cracked to form ethylene.

Evans and Milne also carried out experiments in the presence of methane as well as in helium (69). Similar to Scott et al. they found that primary pyrolysis is not significantly influenced by the reactor gaseous environment. However, for secondary and tertiary reactions, they observed that the gaseous environment does affect the products formed. Like Steinberg et al., they observed an increase in olefins when methane was used as the gaseous environment. Furthermore, they also postulated that olefins enhancement in methane was probably due to the chemical interactions of the biomass-derived vapours with methane.

Steam is sometimes used as a carrier gas because it can be readily separated from the volatiles by condensation. At temperatures greater than 650°C, there is the possibility of steam reforming reactions taking place resulting in the formation of CO_2 and H_2 or reacting with the char to form H_2 and CO as noted by Guanxing et al. (131).

The general conclusion is that the gaseous environment does not affect primary pyrolysis as much as secondary gas phase reactions for temperatures below 600°C unless there is a catalyst present (69, 74, 129, 130).

2.5.7 Rate of thermal quenching of the gas/vapour products

One other area which has received less attention is the recovery of the liquid products. Graham has specified rapid cooling of the vapour products [< 40 ms] to preserve speciality chemicals (39). The rate of cooling will depend upon the recovery system used and will also affect the collection of the liquids and the rate of secondary gas/vapour phase reactions. The use of indirect heat exchange can give low temperature gradients and fractionate the larger molecular weight components which collect first and form a very viscous liquid which does not flow readily. This is an area requiring further work with respect to the design of liquids recovery systems.

2.5.8 Time-temperature profile of the gas/vapour products

Most work on this area has focused on the secondary degradation of the gas/vapour products with time and temperature [see Section 3.4], however there is no work on the time-temperature cooling history of the gas/vapour products. Low gas/vapour product temperatures favour condensation reactions which can lead to reduced organic liquid yields and higher water yields. This will depend upon the liquid recovery system used with rapid quenching of the product minimising secondary reactions. It may be considered that the liquid quality may be controlled by altering the cooling profile of the liquid. If a low viscosity liquid is required, by lowering the gas/vapour phase temperature, condensation reactions are promoted and the water content of the final liquid will be increased. By

maintaining a relatively constant temperature of 400-500°C, it is possible that the lignin derived macromolecules will undergo secondary reactions to produce lower molecular monomers such as polyphenols and other C_6 ring compounds. This is an area requiring further work.

2.6 Biomass pyrolysis for chemicals

Although the focus of this work is on the production of liquids for primary use as a fuel, the importance of the production of liquids for chemicals cannot be overlooked. This section therefore summarises the important influences on the production of selected chemicals.

2.6.1 Effects of ash on chemicals

The catalytic effects of ash on the yields of liquids have been reviewed in Section 2.4. Ash, in particular sodium and potassium salts, has very significant effects on the chemical composition as show in Table 2.15 from the work of Radlein et al. (137).

The yield of levoglucosan [LG], has increased by a factor of 10 and the hydroxyacetaldehyde [HAA] yield is drastically reduced by a factor of 27. Also the amounts of low molecular weight species are reduced. The original wood sample contained 1700 ppm K, 1200 ppm Ca and 50 ppm Na, almost all of which were removed by acid washing. These elements were originally thought to catalyse the degradation of levoglucosan to low molecular weight liquids such as hydroxyacetaldehyde. However, it has been shown that the formation of compounds such as levoglucosan and hydroxyacetaldehyde occur by competing parallel reactions, as further discussed in Chapter 3.

Other degrees of acid treatment were also investigated to assess their effects on product yields. Different acid strengths were used and the results summarised in Table 2.16 below. HCl appears to be more effective in removing hemi-celluloses, but it does not increase the yields of sugars and levoglucosan as much as the sulphuric acid wash does. Hydroxyacetaldehyde was prevalent in high concentration after HCl washing. Originally Scott et al. thought that the formation of HAA was as a degradation compound of levoglucosan. However, Richards proposed that it was a primary ring fragmentation compound of the cellulose itself. A further discussion of the possible mechanisms of levoglucosan and hydroxyacetaldehyde formation may be found in their paper (57). Radlein et al. have obtained hydroxyacetaldehyde yields of 17 wt% at 500°C from Avicel PH-102 cellulose with pretreatment of 0.01 wt% K_2CO_3 (64).

Table 2.15

Effects of mild acid washing on product yields and liquid composition [yield wt% dry feed]

Feedstock	Poplar		Stake Cellulose	
	Untreated	Treated	Untreated	Treated
Reactor temperature [°C]	497	501	500	500
Gas/vapour product res. time [s]	0.46	0.45	0.5	0.5
Moisture content [wt%]	3.3	16.5	24.1	3.1
Cellulose content [wt%]	49.1	62.8	93.9	91.3
Ash, [% d.b.]	0.46	0.04	2.5	0.32
Organic liquid	65.8	79.6	58.2	65.3
Water	12.2	9.0	9.0	7.0
Char	7.7	6.7	15.4	19.0 *
Gas	10.8	6.4	15.3	0.9
Oligosaccharides	0.7	1.19	--	**
Cellobiosan	1.30	5.68	--	3.10
Glucose	0.40	1.89	--	1.70
Fructose	1.31	3.89	--	2.00
Glyoxal	2.18	0.11	--	2.50
Methylglyoxal	0.65	0.38	3.30	--
1,6 anhydroglucofuranose	2.43	4.50	--	5.50
Levoglucosan [LG]	3.04	30.42	--	27.30
Hydroxyacetaldehyde [HAA]	10.03	0.37	17.10	0.40
Formic acid	3.09	1.42	7.40	0.10
Formaldehyde	1.16	0.80	--	1.00
Acetic acid	5.43	0.17	8.50	0.10
Diacetyl	1.05	--	--	--
Acetol	1.40	0.06	5.40	--
Aromatics [lignin]	16.2	19.0	--	--

* water soluble hydrolyzable oligosaccharides ** reported as char

Table 2.16

Effects of differing acid pretreatments on pyrolysis yields from poplar wood, 475-490°C, 0.5 s gas/vapour product residence time [yields, dry feed basis]

Pretreatment	1 5% H_2SO_4, 100°C, 2 h	2 3.7% HCl 100°C, 2 h	3 0.5% HCl 165°C, 6 min	4 3, then as 1 100°C, 2 h
Ash, [% d.b.]	0.04	0.05	0.85	0.30
Moisture	6.0	15.9	25.4	16.9
Cellulose	67.0	67.8	65.4	69.2
Levoglucosan	28.7	17.5	4.5	30.1
Other sugars	12.5	17.1	5.1	18.8
HAA	0.9	6.5	9.1	0.9
Pyrolytic lignin	19.2	25.7	18.8	17.9

2.6.2 Effects of additives

Research into the effects of additives have looked at the suppression of volatiles formation and the promotion of char forming reactions for the development of flame retardents as researched and reviewed by Shafizadeh (60). Extensive experiments were conducted by Shafizadeh et al. on the effects of temperature and pretreatment on the yields of chemicals. Few of the studies cover typical fast pyrolysis conditions, but serve to show the influence of additives on the yields of liquids as shown in Table 2.17 (29).

Shafizadeh also showed the effects of other additives on the pyrolysis of cellulose and xylan (56, 138). The results showed that levoglucosan yields could be maximised by acid washing the biomass to remove alkali metals which are know to reduce the formation of levoglucosan, as discussed earlier. Yields were typically increased from 14 to 50% by acid washing of cellulose (56). The effects of 10 wt% $ZnCl_2$ addition to the xylan were investigated and the results showed that the yield of 2-furaldehyde was increased from 4.5 to 10.4 wt% at 500°C; NaOH had the reverse effect and lowered the yield to 1.6 wt%. In both cases, char yields were increased from 10 wt% to 26 wt% and 21 wt% respectively. Water yields were also dramatically increased from 7 wt% to 21 wt% and 26 wt% for $ZnCl_2$ addition and NaOH addition respectively. Furfural formation is promoted by the presence of $ZnCl_2$ but NaOH

promotes furfuryl alcohol formation. Levoglucosan formation was lowered by traces of NaCl, but glycolaldehyde formation increased in conjunction with acetic acid.

Table 2.17
Pyrolysis products from cellulose and treated cellulose at 550°C [wt%]

Product	Cellulose	+ 5% H_3PO_4	+ 5% $(NH_4)_2HPO_4$	+5% $ZnCl_2$
H_2O	11	21	26	23
Char	5	24	35	31
Organic liquids	66	16	7	31
Acetaldehyde	1.5	0.9	0.4	1.0
Furan	0.7	0.7	0.5	3.2
Propenal	0.8	0.4	0.2	tr.
Methanol	1.1	0.7	0.9	0.5
2-methylfuran	tr.	0.5	0.5	1.2
2,3-butanedione	2.0	2.0	1.6	1.2
1-hydroxy-2-propanone/glyoxal	2.8	0.2	tr.	0.4
Glyoxal				
Acetic acid	1.0	1.0	0.9	0.8
2-furaldehyde	1.3	1.3	1.3	1.3
5-methyl-2-furaldehyde	0.5	1.1	1.0	0.3
CO_2	6	5	6	3

tr.: trace amount

This area has been further studied by Piskorz et al. (139), Richards et al. (140, 141) and has been reviewed by Radlein et al. (137). Similar studies on the effects of $ZnCl_2$ and NaOH on the pyrolysis product spectra of cellulose have been carried out by Pavlath (142).

Fung has also investigated the effects of H_3PO_4 on the formation of levoglucosenone [LGO] from cellulose pyrolysis over a range of temperatures from 350-840°C, and an additive concentration of 1% (143). A maximum yield of 34% was obtained at 430°C, decreasing rapidly to a minimum of 11 % at 820°C. Fung proposed that the formation of levoglucosenone was directly from cellulose not via levoglucosan, as at 320°C, levoglucosan decomposed almost completely in the presence of H_3PO_4 to give water, CO, CO_2 and a low quantity of levoglucosenone.

Work on the formation of glycolaldehyde [HAA dimer] from cellulose has been performed by Richards who showed that cellulose pyrolysed with addition of 22 wt% NaCl led to formation of HAA in preference to 1-hydroxy-propan-2-one at 350°C and under high vacuum (140). The maximum yield of glycolaldehyde was 9.2 wt% from pure cellulose, decreasing to 4.8 wt% from the salt impregnated cellulose. This led to the hypothesis that hydroxyacetaldehyde was a direct product from cellulose decomposition derived from C_5 or C_6 in the glucose unit in cellulose, possibly via a dehydration followed by a retro Diels-Alder reaction (140).

From Table 2.09, transition metals [Fe and Cu] were found to increase the yield of levoglucosan, up to 15.8% from wood exchanged with iron, although the yield of char also increased significantly. With salt adsorption, similar effects were observed, but to a lesser degree, especially after acid washing. Copper and iron chlorides were found to benefit levoglucosan yields. Low levels of sorbed $FeSO_4$ tended to catalyse levoglucosan and levoglucosenone formation to char. In summary, use of ions such as Fe or Cu [or their salts] increase yields of levoglucosan, but have the penalty of increasing char yields.

The mechanism of levoglucosan formation from wood in the presence of transition metals is not known. Richards proposes that levoglucosan formation is possibly linked with lignin. Low yields of levoglucosan from wood, it is proposed, is due to K and Ca inhibition in conjunction with lignin as experiments with $CuAc_2$ and cellulose led to a drop in yield from 41.5 to 31 %. When wood had been acid washed to remove ions, the levoglucosan yield was only 5.4%: 10.8 of the maximum theoretically possible from the cellulose component of the wood, i.e. 41.5 wt% yield by simple depolymerisation of the cellulose polymer. Richards tentative hypothesis is that the presence of transition metals decreases the interference of lignin during cellulose conversion to levoglucosan. Such transition metals are proposed to form complexes with phenol groups in the lignin.

2.6.3 Effect of reactor process parameters

2.6.3.1 Reactor temperature

Several studies have looked at the influence of reactor temperature on the yields of chemicals. The main conclusion is that other factors such as ash in the feedstock have a more significant influence on their yields [see Tables 2.08, 2.15, 2.16]. Work on fast pyrolysis for chemicals by Scott et al. has show that there is some effect for yields of anhydrosugars and their related compounds with reactor temperature (144). The reader is referred to the extensive results reported by Halling (96).

Work was carried by Vasalos et al. in a fluidised bed to examine the optimum conditions for the production of phenols at reactor temperatures of 400-750°C and particle size ranges of 300-425 μm and 500-600μm (145). He showed that the optimum temperature for the production of phenols was 15 wt% at 490°C for the 300-425 μm particle size.

2.6.3.2 Gas/vapour product residence time effects on chemical yields

The gas/vapour product residence time also influences the chemical composition of the product liquids, due to secondary gas phase reactions. Therefore, if particular chemicals are required, the residence time may have to be accurately controlled. Particular interest has focused on two chemicals: hydroxyacetaldehyde and levoglucosan. These two chemicals may be found in fast pyrolysis liquids in significant yields which are influenced by the reactor temperature [see Figure 2.10], the gas/vapour product residence time, the feedstock and ash/additives in the feed. The effects of residence time on liquids composition have also been investigated by Scott et al. and their conclusions was that it does not have such a significant influence as the reactor temperature (71). Results from the work by Palm et al. on sweet sorghum bagasse are shown in Table 2.18 (144).

Table 2.18
Variation in chemical composition with gas/vapour product residence time for sweet sorghum bagasse, 10.05 % water, 9.2% ash [dry basis], at 525°C [yields, % m.a.f. basis]

Residence time [s]	0.22	0.30	0.38	0.44	0.50	0.78	0.98
Char	10.38	8.92	12.98	13.28	12.72	17.28	18.67
Gas	9.24	11.76	12.36	12.89	12.00	15.03	15.9
Organics	61.43	62.25	55.11	59.54	57.95	53.07	47.40
Water	7.59	12.45	14.4	12.6	11.4	10.8	14.1
Acetic acid	1.68	1.90	2.04	2.58	2.50	3.44	2.77
Acetol	1.04	--	0.60	1.55	0.86	2.02	1.58
Cellobiosan	0.52	0.57	0.36	0.48	0.50	0.38	--
Diacetyl	0.49	0.00	0.61	0.78	0.00	0.93	0.80
Formaldehyde/formic acid	0.49	0.51	1.85	2.06	1.68	2.47	1.72
Glyoxal	0.55	0.64	1.05	1.14	1.22	1.74	0.79
Hydroxyacetaldehyde	6.25	6.96	6.54	7.99	6.98	7.35	4.92
Levoglucosan	0.93	1.00	1.53	1.81	1.71	2.19	1.55
Pyrolytic lignin	17.1	22.7	15.1	12.0	14.0	18.0	16.1

2.6.3.3 Pressure effects on yields

The effects of pressure on the yields of chemicals have been shown in Table 2.14; lowering the pressure increases the yields of anhydrosugars by lowering the enthalpy required for volatilisation of the liquids. Pressure does not appear to have a significant influence on chemical yields at typical fast pyrolysis conditions.

2.7 Summary of optimal process parameters for fast pyrolysis for liquids

From the extensive review of previous work carried out on the fast pyrolysis of biomass, the designer of a reactor for the production of liquids for use as an alternative fuel and/or a source of chemicals should use the following parameters as a guide in the design of a reactor. This is limited to some extent by the reactor configuration chosen and the feedstock.

2.7.1 For liquid fuel production

For production of pyrolysis liquid as an alternative fuel, the following process parameters and pretreatments are recommended:

reactor temperature:	450-625°C
gas/vapour product residence time:	< 2 s
gas/vapour product temperature:	400 - 500°C
reactor pressure:	atmospheric
biomass particle size:	< 2 mm fluid bed; < 5 mm transport, entrained or circulating fluid bed; any size for an ablative reactor
biomass pretreatment:	yes- 1% acid washing to remove ash
biomass moisture content:	< 10 wt%, d.a.f. basis, preferably lower than 5%

2.7.2 For chemicals production

The following process parameters and pretreatments are recommended for the production of specific chemicals:

reactor temperature:	~450-500°C, depending upon the feedstock
gas/vapour product residence time:	< 1 s
gas/vapour product temperature:	400 - 500°C
reactor pressure:	atmospheric or lower
for levoglucosan:	mild H_2SO_4 washing + $CuCl_2$ [~0.46% Cu], cellulose feedstock, no K or Na
for hydroxyacetaldehyde:	>0.01 wt% K^+ in feedstock

for phenolics:	hardwood feedstock, small particles [< 425 μm]
for levoglucosenone:	acid washing + $FeSO_4$ additive, 1 bar pressure
for acids, ketones, aldehydes	ash remains in material or addition of K, Na

These parameter ranges are used to place some limits on the design of the ablative pyrolysis reactor as detailed in Chapter 5, in particular for the production of liquids for fuels.

The area of additives in feedstocks to enhance product yields is an area requiring further work, in particular for the production of speciality chemicals. This must also be balanced against the disposal or recovery of the additives after pyrolysis.

Chapter 3. Kinetics and Mechanisms of Biomass Pyrolysis

3.1 Introduction

The proposed pathways of cellulose pyrolysis are reviewed along with the reaction mechanisms for cellulose, lignin and hemicellulose. The pyrolysis kinetics of each component are summarised and whole wood fast pyrolysis pathways and kinetics reviewed. Secondary gas/vapour decomposition kinetics are also analysed and discussed. The chapter is structured as follows:

- review of cellulose pyrolysis pathways and cellulose, hemicellulose and lignin decomposition mechanisms [Section 3.2]
- whole wood fast pyrolysis and mechanisms [Section 3.3]
- mathematical modelling of pyrolysis [Section 3.4]
- summary of biomass pyrolysis kinetics [Section 3.5]

Biomass pyrolysis is a complex set of chemical and physical processes. To date, no model or reaction pathways have been proposed which account for all of the wide range of products formed during pyrolysis and the relative influence of the process parameters and feedstock characteristics. Global models which "lump" the rates of formation of products into solids, liquids and gases are the most common as some intermediate steps cannot or have not been determined due to experimental and/or equipment limitations. A number of studies have shown that the main components of most biomass types, i.e. cellulose, hemicellulose and lignin, are chemically active at temperatures as low as 150°C (147, 148, 149, 150, 151). Wood, it is claimed, begins pyrolysis at 250°C although the actual rate is very slow (152).

3.2 Pathways of biomass component pyrolysis

3.2.1 Cellulose pyrolysis pathways to 1980

The component of wood which has received the most attention is cellulose due to its high abundance in most biomass types [see Table 2.01] and in the belief that it is representative of whole wood. Cellulose has a well defined structure which allows its easy purification and separation (20 59, 60, 69, 102, 141, 152, 153, 154, 155, 156, 157, 158). Until 1980, research was related to flame retardents and fire research, e.g. as reviewed by Shafizadeh (60) and by Byrne et al. (159).

It was generally considered that primary pyrolysis of pure cellulose occurred by two competing pathways: one involving dehydration and the formation of char, CO_2 and water and the second involving fragmentation and depolymerisation resulting in the formation of

liquid products consisting mainly of levoglucosan (20, 141, 152, 153, 154). At temperatures greater than 300°C, fragmentation or transglycosylation takes place and involves the conversion of cellulose into predominantly a liquid product consisting of levoglucosan and other anhydrosugars. Some of the principle research in the area is summarised below.

One of the first notable studies carried out on cellulose pyrolysis in 1956 was that by Madorsky et al. who proposed that cellulose could decompose by two pathways: one pathway preserved the hexose monomers by depolymerisation and a second pathway led to fragmentation of the monomers by dehydration and condensation reactions to a char product, CO_2, CO and water (160). Kilzer and Broido later reviewed cellulose pyrolysis in 1965 and proposed the reaction mechanism depicted in Figure 3.01 (153).

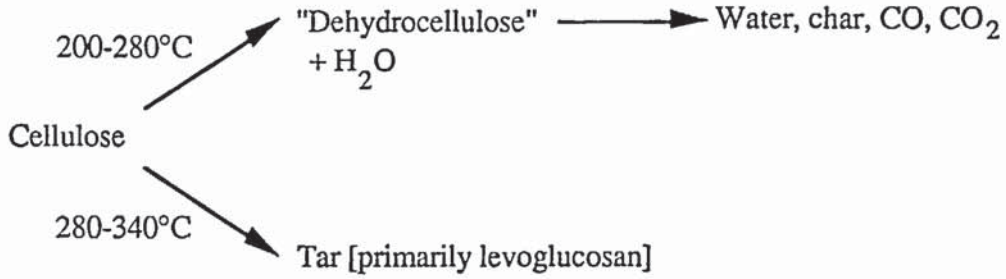

Figure 3.01. Pure cellulose pyrolysis pathway of Kilzer and Broido [1965]

Kilzer and Broido thought that the lower temperature pathway was evident at temperatures less than 280°C with a loss of water at approximately 220°C to form a "dehydrocellulose". The structure of this "dehydrocellulose" was thought to involve a tetrahydro-5-hydroxymethylfurfural system which upon decomposition would yield 5-hydroxymethylfurfural, as detected in the product liquids. Above 280°C, depolymerisation of the cellulose occurred with the formation of levoglucosan as the main volatile product. They also highlighted the formation of other anhydro-derived compounds such as 1,4-anhydro-α-D-glucopyranose, and 1,6-anhydro-β-D-glucofuranose [furanose isomer of levoglucosan]. Kilzer and Broido were also one of the few to note the significant effects of ash [in particular alkali earth metals] on the pyrolysis of cellulose with the addition of $KHCO_3$ catalysing dehydration reactions leading to increased formation of CO, CO_2 and water as confirmed in other studies discussed later in this section.

Byrne et al., who also reviewed cellulose pyrolysis work, agreed with the reaction pathways proposed by Madorsky and Kilzer and Broido and attempted to identify some of the chemicals using gas-liquid chromatography [GLC] (159). From their analyses, anhydro-derived sugars, as noted by Kilzer and Broido, were identified in products formed at pyrolysis temperatures of 350-500°C. They then attempted to elucidate a mechanism for the formation of volatile carbonyl compounds to explain the lower temperature route proposed by Kilzer

and Broido, i.e. less than 300°C. This proposal in their paper proved to be wrong as the experiments were carried out at 420°C and the product yields and composition were therefore not representative of the lower temperature route, i.e. less than 300°C. Byrne et al. assumed that the carbonyl compounds reacted via condensation reactions to produce ethylenic crosslinking with water elimination to form char, water, CO_2 and CO. They also noted the presence of 19 carbonyl compounds in the liquids and highlighted that hydroxyacetaldehyde was an important and significant [in terms of yields] "intermediate", since shown to be a direct product formed by a competing pathway [see Section 2.4.1.3].

Shafizadeh during the course of his extensive research recognised that the products of pyrolysis were also influenced by process parameters and intrinsic effects including ash [and its composition], degree of polymerisation, crystallinity and morphology although generally these were ignored in his discussions. Shafizadeh proposed a more detailed reaction pathway than that proposed by Kilzer and Broido for cellulose pyrolysis. Each pathway was postulated to depend upon the pyrolysis temperature as shown in Figure 3.02 (60). Shafizadeh proposed that pathway 1 occurs at temperatures below 280°C, the main products being water, char, CO and CO_2, due to dehydration reactions. Pathway 2 is favoured at temperatures of 300-500°C with depolymerization [glycosidic bond cleavage, transglycosylation and rearrangement reactions] giving levoglucosan as the main product. Pathway 3 is for temperatures above 500°C resulting in the formation of low molecular gases and volatile products. Shafizadeh purports that the volatiles and gases are formed by fission, dehydration, disproportionation, decarboxylation and decarbonylation reactions. The volatile products he assumed were primarily hydroxyacetaldehyde, furaldehydes and glyoxal. From his work, Shafizadeh presented considerable evidence for the formation of products from the first two pathways. However, he seldom discussed the formation of volatiles and gases as competing reactions and lumped them into the temperature dependent pathway 3.

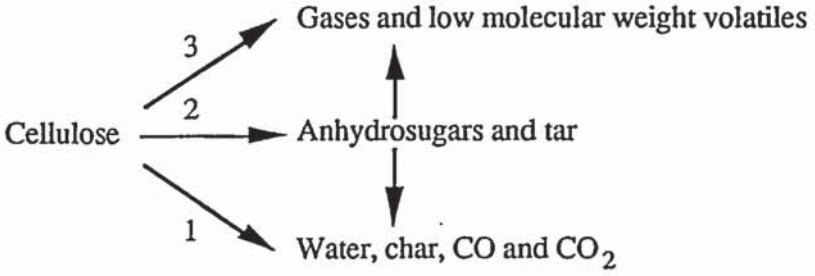

Figure 3.02. Shafizadeh's first cellulose pyrolysis pathway [1968]

Shafizadeh later attempted to increase yields of organics liquids, in particular to enhance yields of levoglucosan, by water washing which met with limited success [see Table 2.04]. Later when the cellulose was acid washed and then washed with de-ionised water to

neutrality, yields of levoglucosan and liquids were found to increase more significantly than water washing alone [see Table 2.04] (56). Shafizadeh was unsure whether the increased yields were due to the removal of the ash, the addition of small quantities of acid to the cellulose structure or a modification of the cellulose structure or a combination of all three. Shafizadeh still had difficulties reconciling the production of low molecular weight species with temperature and as secondary degradation products. He therefore attempted to explain their formation in a second pathway as shown in Figure 3.03 (154, 161).

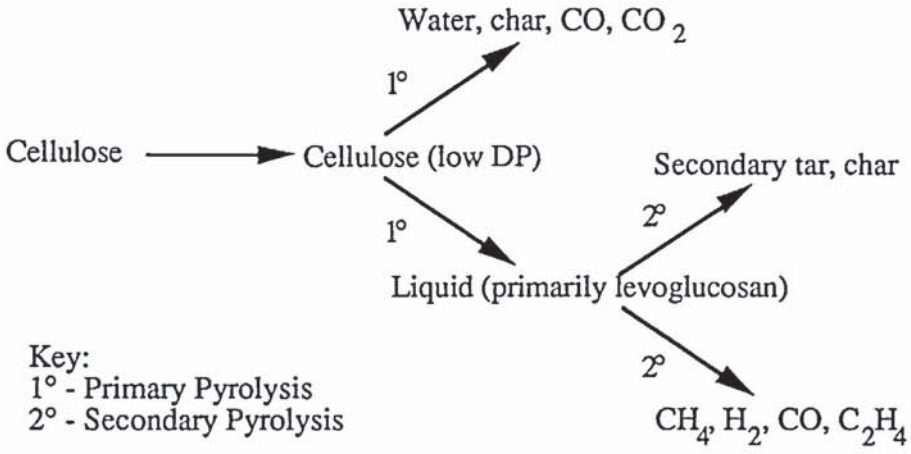

Figure 3.03. Shafizadeh's second cellulose pyrolysis pathway [1979] (20, 60, 102, 162)

In this second approach, the cellulose appears to go through an "active" state where the cellulose has a low degree of polymerisation [DP] of about 200 and chemicals such as acetic acid, aldehydes and ketones are secondary liquids. Shafizadeh accounts for formation of low molecular weight components such as aldehydes and ketones as sequential reaction products and not dependent upon a competing reaction.

3.2.2 Cellulose pyrolysis pathways from 1980

Much of the ambiguities in both cellulose primary decomposition have been resolved by the extensive research of Scott et al. (e.g. 58, 163, 164) and Richards et al. (e.g. 65, 140) and Evans and Milne (69, 158)

3.2.2.1 University of Waterloo cellulose pyrolysis pathway

Piskorz et al. (139) were originally of the view that chemicals such as hydroxyacetaldehyde were secondary decomposition products from the degradation of levoglucosan, in agreement with the mechanism proposed by Shafizadeh [Figure 3.03]. They recognised that the formation of hydroxyacetaldehyde and levoglucosan was related and that the reactor temperature had an influence on their relative yields [see Section 2.5.1.2] (59, 95). Piskorz et

al. (59) have proposed the Waterloo cellulose pyrolysis pathway, similar to that proposed by Shafizadeh in 1968, and this is shown in Figure 3.04. This pathway takes into account two major competing pathways for the pyrolysis of cellulose. Each pathway is capable of minor rearrangement reactions to account for the variety of different products produced due to intrinsic effects, i.e. cellulose morphology, degree of polymerisation and presence of alkali cations, and also the process parameters of temperature, heating rate and pressure (59).

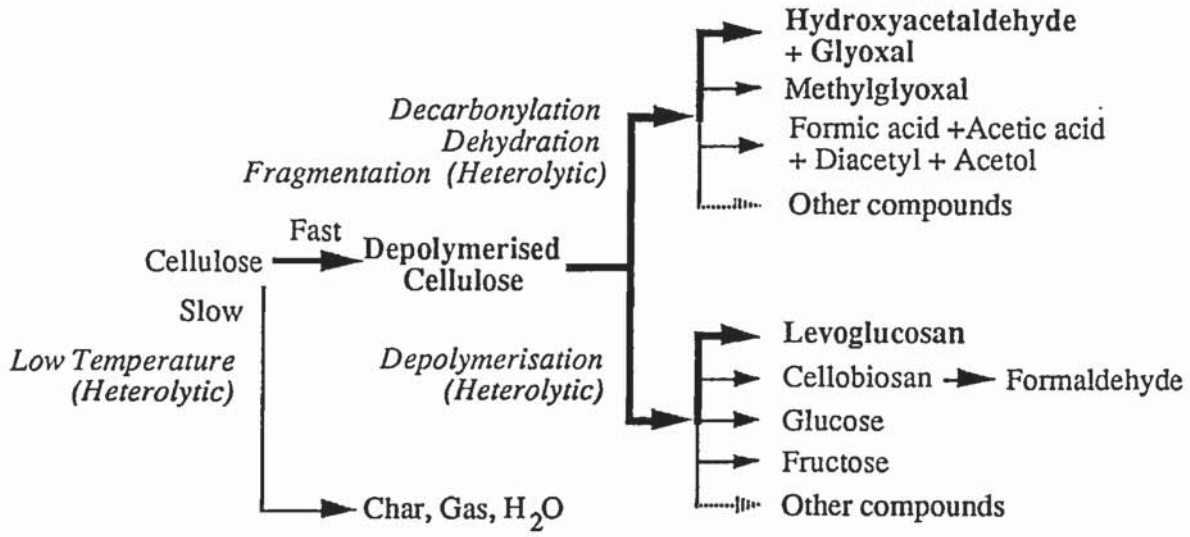

Figure 3.04 . University of Waterloo Reaction Pathway [1988]

Piskorz et al. are of the same view of Richards that the competing pathway for HAA formation occurs by direct cleavage of a glycosidic ring (140). Research such as that of Basch and Lewin (165) and Halpern and Patai (166) identified cellulose decomposition as being "unzipping" of the cellulose polymer once the free chain ends have been activated. Piskorz proposed that this process is blocked by the presence of alkali earth metals, possibly by their high polar charge, a view similarly supported by Essig et al. (167). Piskorz also noted that the proportion of free chain ends is similar to the alkali cation content [0.05-0.06 wt%]. The influence of ash, in particular alkali or alkali earth metals on the chemical composition was identified in 1967 by Kilzer and Broido (153) and earlier by Arseneau in 1951 (168).

3.2.2.2 University of Montana

Although the work of Shafizadeh and then Richards has focused on the chemistry of cellulose pyrolysis, Richards has attempted to unify the theory on cellulose pyrolysis mechanisms for the production of levoglucosan and he performed a thorough series of experiments which were carried out to assess the effects of alkali metals, pressure and chemical linkages and orientation on the yields of hydroxyacetaldehyde and levoglucosan . He originally favoured

the heterolytic scission of the glycosidic linkage of the cellulose polymer, as proposed by Shafizadeh, in the formation of levoglucosan (65). However, in subsequent work he has proposed the alternative hypothesis that mid chain heterolytic scission of the cellulose polymer leads to shortened chains which terminate in a resonance stabilised glucosyl cation which either stabilises as the 1,6 anhydride or leads to further transglucosylation.

Richards et al. also studied the effects of linkage position and orientation on the pyrolysis of polysaccharides: natural [1,3-, 1,4- and 1,6- linkages, α and β orientations] and synthetic glucans [all possible linkage positions and orientations] were used to elucidate the reaction mechanisms for LG formation (65). They showed that if the glucan was relatively free of inorganics, the yield of LG was relatively insensitive to the position and anomeric orientation of the glucosidic linkages. For natural glucans and the synthetic glucans, the LG yield varied from 36-55%, thus eliminating the possibility of S_N2CB reactions; this finding confirmed earlier results on the pyrolysis of acid washed glucans which refuted the theory that LG formation by displacement reactions [S_N2CB] as had been proposed by Antal (20). The formation of LG was proposed to be by subsequent glucosidic scission of terminal units. Richards recognises that one of the limitations of the heterolytic approach is that his reaction mechanisms are applicable to pure cellulose. Evans and Milne are also in general agreement with the hypotheses of Shafizadeh and Richards that a concerted displacement reaction occurs (69).

Independent of how the exact chemical reactions occur, at present the available mechanisms do not offer a definitive reaction pathway which has been generally accepted. The Waterloo reaction pathway is a very useful approach which does explain the range of products formed during pyrolysis and accounts for the effects of ash and the degree of polymerisation.

3.2.3 Hemicellulose pyrolysis

Hemicellulose has received less attention due to its lower abundance, variety of constituents, high reactivity and rapid degradation at low temperatures [150-350°C]. It is believed that the intermediate levoglucosan [from cellulose] is replaced by a furan derivative [from hemicellulose] (34, 169). This may be due its lack of crystallinity and lower DP such that fragmentation rather than depolymerisation occurs (34). Hemicellulose is the more likely source of furan derivatives and gives higher yields of char, water and acetic acid during pyrolysis due to its higher reactivity compared to that of cellulose. Soltes and Elder suggested a two step degradation process where the first step is depolymerisation to water soluble fragments, subsequently followed by decomposition to volatile components (170). Varhegyi et al. proposed that xylan, a component of hemicellulose, begins thermal degradation at 200°C and the presence of methanol and 2-furaldehyde in the products, they suggested, was due to

demethoxylation of 4-O-methyl-D-glucuronic units and dehydration of pyranose units. They also suggested that these reactions were occurring via the α-glycosidic bonds as the β-glycosidic bonds are less sensitive to thermal degradation. Varhegyi et al. proposed that the formation of 2-furaldehyde at low temperatures [250-300°C] was probably due to dehydration of the pentose units which were formed from uronic acid units by decarboxylation.

The dehydration reactions also form moieties having double bonds, carbonyl groups and conjugated double bond carbonyl groups. These moieties are thought to rearrange, condense and fragment to generate CO, CO_2, formaldehyde and other chemicals such as acetic acid. The identification of the chemicals produced by xylan pyrolysis have been reviewed by Evans and Milne (158). Other research on hemicellulose has been carried out by Ramiah (171), Williams and Besler (172) and Varhegyi et al. (173, 174, 175) based upon DTA studies, although they do not present any work on possible global reaction pathways or comprehensive mechanisms. The author has not found any global reaction pathways for hemicellulose pyrolysis.

3.2.4 Lignin pyrolysis

The complex structure of lignin has led to a lack of understanding of the pyrolysis of this biomass component. Lignin is the most thermally stable component of wood but its chemical structure varies according to its source and the method of isolation. To date, most work in lignin pyrolysis has been obtained from model compounds in the belief that they will mimic the behaviour of lignin during pyrolysis. Minor decomposition begins at 250°C but most significant lignin pyrolysis occurs above this temperature (34, 102, 155). High molecular weight compounds such as coniferyl alcohol and sinaptyl alcohol are formed during the initial stage of pyrolysis by the formation of double bonds in the alkyl side chain of the lignin structure [see Figure 2.06]. The field of lignin research may be generally characterised into temperature regimes: above 600°C and below 600°C which are reviewed below.

3.2.4.1 Lignin pyrolysis below 600°C

Pyrolysis of lignin below 600°C has received considerable attention (e.g. 3, 43, 69, 102, 158, 176, 177, 178, 179, 180). Detailed work using Kraft lignin has also been carried out by Jegers and Klein who identified and quantified 33 products [12 gases, water, methanol, and 19 aromatic compounds such as phenol, cresol and guaiacol] at a range of temperatures from 300 to 500°C (181, 182). They reported that monohydroxyl phenolics were favoured by long pyrolysis times and high reactor temperatures. Iatridis and Gavalas studied the pyrolysis of Kraft lignin at 400-700°C using a captive sample reactor, obtaining a total volatiles yield of 60 wt% (183). Nunn et al. have also carried out work in this area at temperatures from 330 to

1100°C, obtaining a maximum of 53 wt% liquid at 625°C, again in a captive sample reactor (85). Whereas hemicellulose and cellulose, on heating, break down readily at the glycosidic linkages to form volatile products, lignin yields a considerable amount of char because of the greater stability of the aromatic rings (e.g. 29, 172).

3.2.4.2 Lignin pyrolysis above 600°C

High temperature pyrolysis of lignin [> 600°C] leads to complex cracking, dehydrogenation, condensation, polymerisation and cyclisation reactions resulting in the formation of products such as CO, CH_4, other gaseous hydrocarbon, acetic acid, hydroxyacetaldehyde and methanol. Polyaromatics, benzene, phenylphenols, benzofurans and naphthalenes are formed by secondary reactions depending on the temperature (20, 69, 85, 102, 158, 176, 177, 184). Jegers and Klein reported that guaiacols and catechols were unstable intermediates which could further react to form CH_4 [from catechol degradation] or undergo coking reactions in preference to the formation of phenols (185).

Other work has been carried out with model compounds followed by modelling simulations to obtain possible reaction mechanisms and reaction kinetics for lignin pyrolysis. Klein and Virk have proposed a reaction mechanism derived from the pyrolysis of the model compound phenolphenyl ether (102, 182, 183). Mathematical modelling of lignin pyrolysis has also been attempted using the Monte Carlo simulation technique (186, 187). The overall simulation is comprised of two Monte Carlo simulations: one comprising the lignin structure and the second the degradation of its oligomers. The simulation contained model compound reaction pathways and kinetics in a Markov-chain based simulation of the reaction of lignin polymers which subsequently produced yields of various hydrocarbons and oxygenated compounds. No comparison with actual results was presented, however, and the validity of the model was not discussed in detail. Other mathematical models have been developed by Solomon et al. (177, 189) to predict the molecular weight distribution of the tars and Anvi (176, 190) who predicted the rate of evolution of lignin pyrolysis gases. The results of their simulations were in very good agreement with tar evolution rates and product yields. The simulation of gas compositions with experimental results were in good qualitative agreement. Only one reaction pathway to account for the complex pyrolysis of lignin has been proposed: similar to the reaction pathway of cellulose [see Figure 3.02], this is due to Antal and is shown in Figure 3.05 (102). Similar to the Shafizadeh cellulose pathway with each pathway being related to the temperature, Antal's reasoning was that both cellulose and lignin have thermally stable rings interconnected by ether linkages with thermally labile hydroxyl functions; therefore, during pyrolysis, they should exhibit similar behaviour in terms of decomposition pathways and reactions.

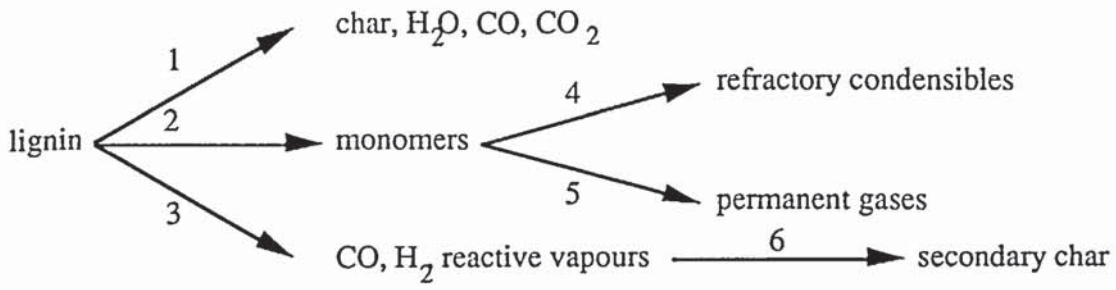

Figure 3.05. Antal's proposed lignin reaction pathway [1985]

Pathway 1 is a low temperature process with dehydration being an assumed dominant reaction although there is no conclusive experimental evidence. At higher temperatures, pathway 2 dominates and a variety of lignin monomers are formed. Unlike cellulose pyrolysis [pathway 2, Figure 3.02], the pathway governing monomer formation [phenylpropane units] from lignin is not well differentiated from the lower temperature pathway. High heating rates and low pressures appear to favour pathway 2.

Antal then further suggested pathways 4 and 5 which become evident at temperatures above 500°C due to monomer degradation in the vapour phase. Pathway 4 was proposed to be a lower temperature route [not defined] with the formation of refractory condensible materials. Pathway 5 is the higher temperature route resulting in monomer cracking to CO, CH_4 and higher hydrocarbons. Antal also notes that experimental evidence suggests there may be competitive dehydration and decarboxylation reactions in pathway 5. He also suggests that a fraction of the volatile matter which undergoes vapour phase cracking via pathway 5 reacts to produce only CO, irrespective of the temperature, although further experimental work is required to confirm his hypothesis. The two remaining pathways, 3 and 6, are believed to exist at very high heating rates where char is formed by secondary gas phase reactions. Antal acknowledges that his proposed pathway for lignin pyrolysis is highly controversial and has noted that more experimental results are required to develop a suitable reaction pathway for lignin pyrolysis.

The work of Nunn et al. on milled wood lignin has been used to elucidate some of the proposed pathways by Antal on lignin pyrolysis. Nunn et al. confirmed pathway 5 with the formation predominantly of CO from the secondary vapour phase cracking of the volatile matter above 1000 K [7 wt% increase in CO yield from 1000-1440 K for a corresponding 8 wt% drop in the liquid yield with slight increases in CH_4 and CO_2 yields] (85). Nunn et al. have, however, shown that at low temperatures light oxygenated liquids [formaldehyde, methanol and acetaldehyde] are also formed primarily below 770K in conjunction with water, with char yields reaching an asymptotic yield of 14 wt% above 1050 K. CO_2 appears to be predominantly a lower temperature product as correctly proposed by Antal, as Nunn observed

that the CO_2 yield only increased from 3.6 wt% to 4.1 wt% for a temperature increase from 1000 K to 1440K. A proposed modified lignin pathway is shown in Figure 3.06 below.

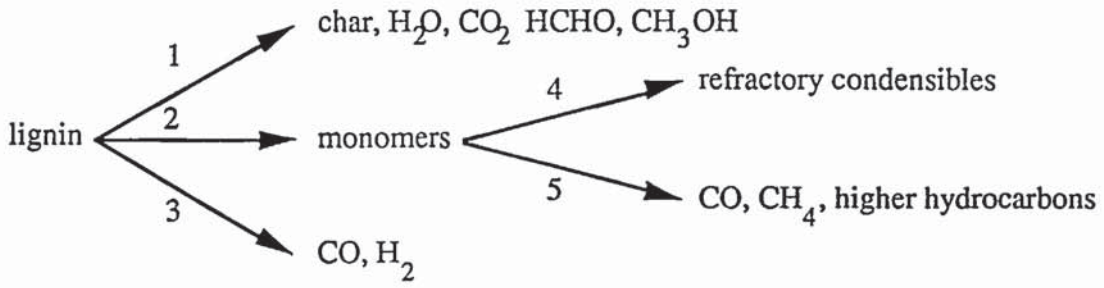

Figure 3.06. Proposed lignin reaction pathway based upon the literature

In summary, further experimental results are required to elucidate the pathways of lignin and hemicellulose decomposition, although the selection and preparation of globally representative samples is difficult due to composition variability from biomass to biomass.

3.3 Whole wood fast pyrolysis

3.3.1 Introduction

The pyrolysis of the three main components of most biomass types has been briefly reviewed above. It could therefore be expected that the pyrolysis of wood would exhibit similar characteristics to the pyrolysis of its components. From TGA, DTA and DSC work, it has been concluded that the results of wood pyrolysis may be approximated by a linear combination of the pyrolysis of the three main components (102, 152, 155, 157, 161, 162, 174, 191, 192, 193, 194, 195, 196). The focus of this section is fast pyrolysis of wood which has been accounted for in three major proposed reaction schemes which are discussed below in chronological order.

3.3.2 Fast Pyrolysis of Biomass Workshop, October 1980

The first comprehensive reaction scheme to account for the fast pyrolysis of wood was the general consensus of pyrolysis specialists attending a workshop on the Fast Pyrolysis of Biomass, at the Solar Energy Research Institute [now National Renewable Energy Laboratory, NREL], in October 1980 (197). This is depicted in Figure 3.07. This was the first model to take into account the influence of heating rate, temperature and pressure with regards to biomass pyrolysis. The focus of the model is the formation of hydrocarbons, CO, CO_2, H_2 and H_2O as the interest at that time was in olefins for the chemicals industry.

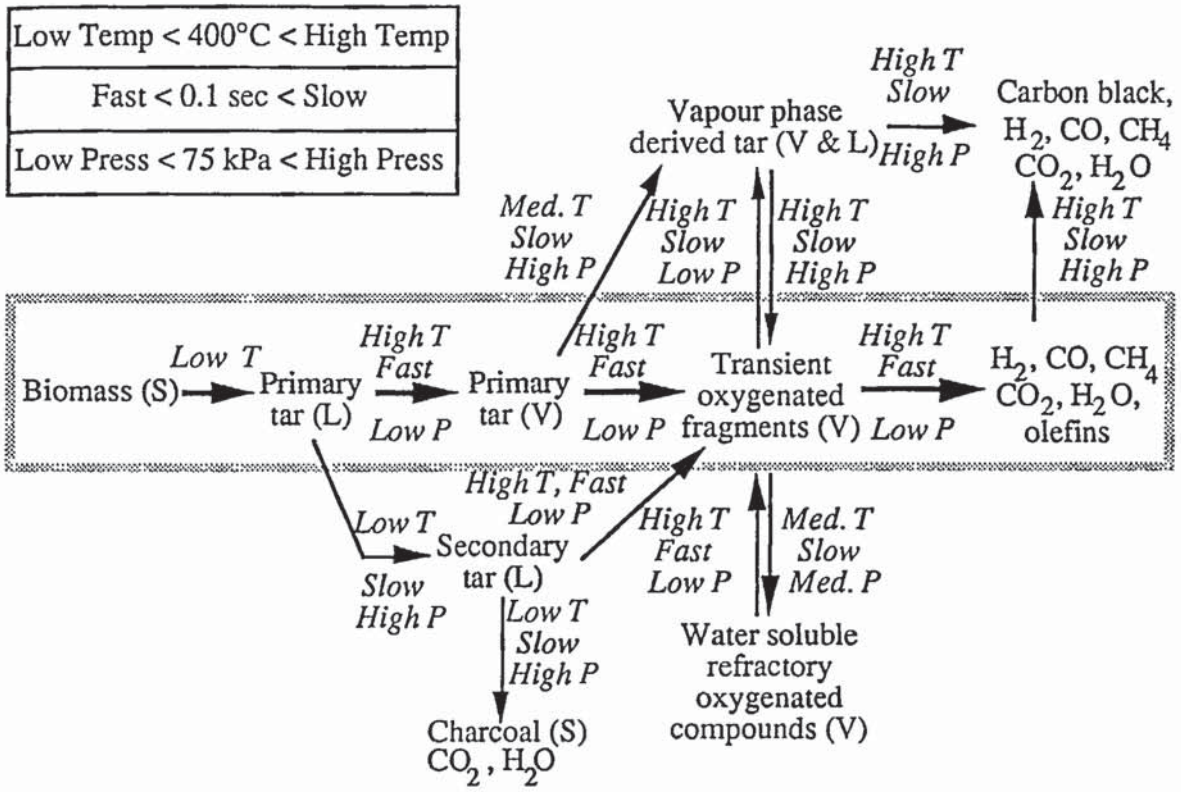

Figure 3.07. Fast pyrolysis of biomass proposed pathway [1980]

3.3.3 Diebold proposed modified reaction scheme

Diebold then proposed a simplified global reaction scheme in that the biomass initially decomposed to a viscous primary precursor [oligomeric liquids] with an elemental structure similar to wood (198). This primary liquid can vaporise to primary vapours, as shown in Figure 3.08. The phenomenon of a "molten state" has been confirmed by Diebold (121) and Lédé et al. (51, 199) who have shown that under ablation conditions [high applied pressure], the wood may appear to have a specific "fusion" temperature. This pathway does not have a step accounting for the formation of secondary char from secondary gas/vapour phase reactions which are known to occur (200).

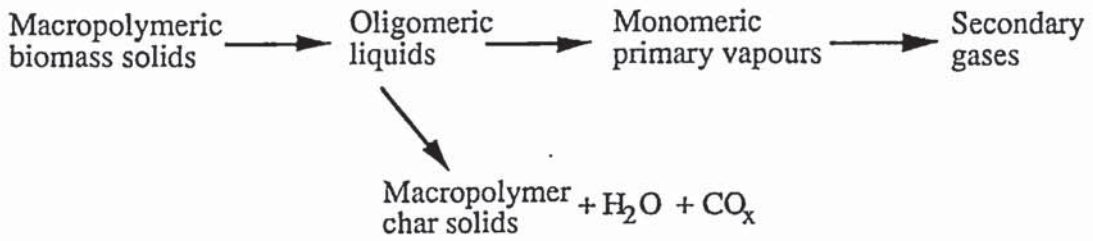

Figure 3.08. Diebold modified reaction scheme [1985]

3.3.4 Evans and Milne wood pyrolysis pathway, 1987

A reaction scheme has been proposed by Evans and Milne as shown in Figure 3.09 (169). Similar to the Copper Mountain reaction scheme [see Figure 3.07] in terms of considering the influences of pressure and temperature, the influence of "pyrolysis severity" is considered as the increase in temperature, heating rate and vapour residence time. Under high pressure conditions, the direct formation of a liquid product is due to the wood appearing to change to a "plastic" or "active" state. At low pressure, however, it is not clear whether a liquid phase exists, after the primary decomposition of the biomass.

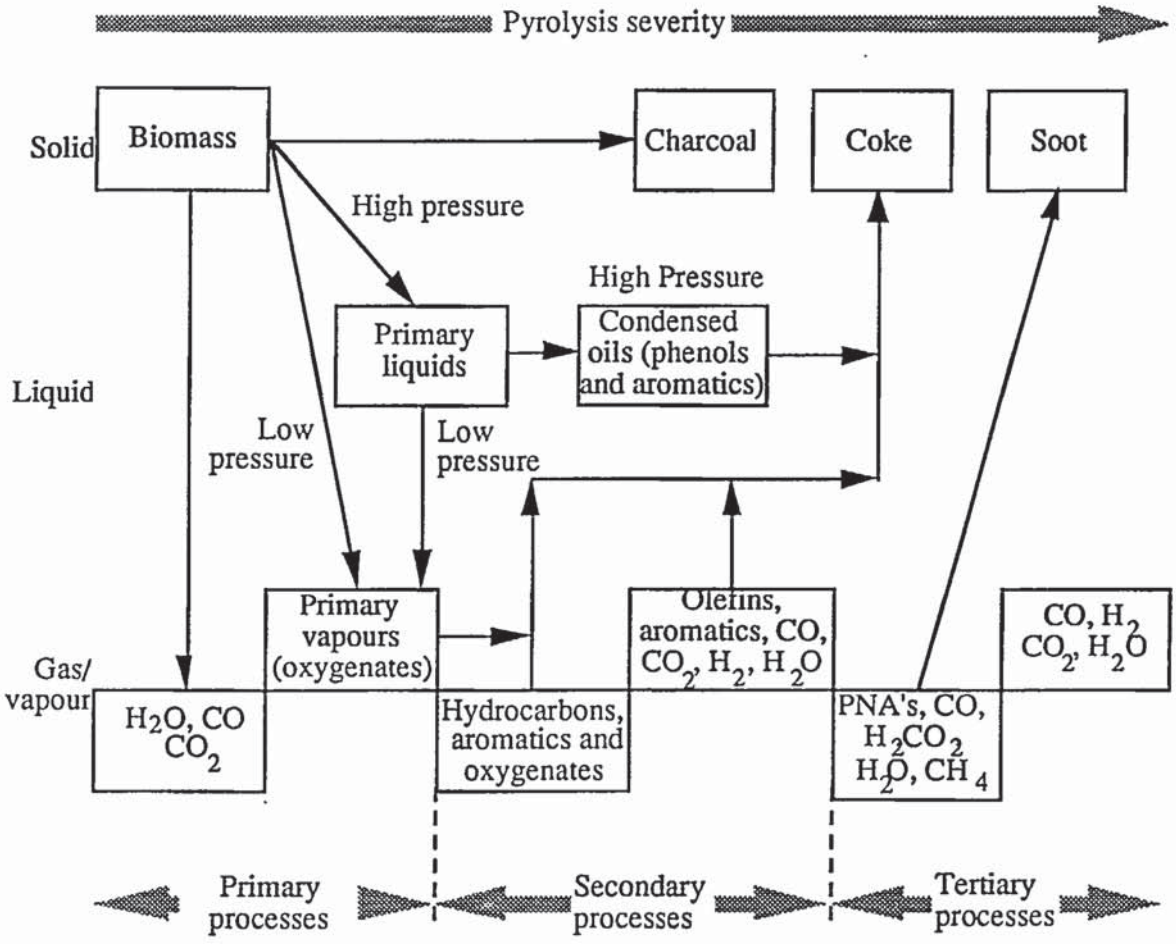

Figure 3.09. Evans and Milne proposed reaction pathway [1987]

3.3.5 Discussion of fast pyrolysis mechanisms for wood and cellulose

Cellulose has been the easiest component to study due to its ease of purification and separation. Lignin and hemicellulose cannot be separated in their pure forms in a similar way as their composition varies widely from one biomass to another. The recent work of Piskorz et al., Diebold and Richards as described previously [see Sections 3.2.2.2, 3.2.2.2 and 3.3.3]

originally applied to lower temperature pyrolysis has aided understanding of processes occurring in fast pyrolysis. The Waterloo model provides an elegant and simplistic interpretation of the primary decomposition of cellulose by two competing pathways. This work has also demonstrated that depolymerisation reactions are favoured at temperatures below 450°C and fragmentation above 500°C, although the yields can be influenced by cationic effects. If non-treated biomass is being considered, then the pathways of fast pyrolysis must involve the competing steps of fragmentation and depolymerisation, taking into account the process parameters and the intrinsic nature of the feedstock. It is apparent from the review of fast pyrolysis that there are limited pathways which can account for the products formed.

To complete the reaction pathways, more information is required on the fast pyrolysis of lignin and hemicellulose to allow for the further development of reaction mechanisms. The area of whole wood fast pyrolysis mechanisms can only remain speculative as intermediate products and reactions cannot be determined.

3.4 Mathematical modelling of pyrolysis

3.4.1 Introduction

Mathematical modelling may be defined as the art of obtaining a solution, given specified input data, that is representative of the response of the process to a corresponding set of inputs (201). The development of a mathematical model can be mechanistic (theoretical) using physico-chemical principles, empirical based on experimental data, statistical or judgmental as in an expert system or a combination of the above. Mathematical modelling is utilised in pyrolysis for several end results, primarily to assess the effects of the interaction of parameters on the yields and compositions of the final products. The objectives of a mathematical pyrolysis model should include:

1 the development of a diagnostic tool in order to evaluate the importance of the process parameters on the products;
2 the prediction of the effects of process parameters, i.e. heating rate, reactor temperature, particle size, moisture content, gas/vapour product residence time and temperature on the product yields and characteristics in order to aid optimisation of the pyrolysis process;
3 the development and establishment of better reactor design techniques,
4. the optimisation of the parameters for the desired end product.

Models of interest are kinetic models for primary products yields and secondary vapour phase decomposition kinetic models for the gas phase reactions of the product vapours before

recovery as liquids. Analytical models are beyond the scope of this thesis, but a comprehensive review may be found in Bridge (202) and in the recent work of di Blasi et al. (52, 203, 204). There are four types of model: empirical, kinetic, analytical and stagewise.

3.4.2 Empirical modelling

This is the simplest approach in that the model is based on the overall mass balance as shown in equation {3.01}.

$$\text{biomass} \dashrightarrow \alpha\ \text{char} + \beta\ \text{liquid} + \gamma\ \text{gas} \qquad \{3.01\}$$

where α, β and γ are the mass fractions of the products at given conditions. Such models provide a simple stoichiometry specific to the reactor conditions used and are therefore highly specific and of limited use. Functional or empirical relationships between yields and the process parameters may be derived but the model requires a substantial amount of experimental data.

3.4.3 Kinetic modelling

The complexity of the pyrolysis process implies that there are numerous homogeneous and heterogeneous reactions occurring either simultaneously and/or consecutively depending on the reactor conditions. Kinetic modelling is therefore an attempt to represent the overall kinetics as individual reaction pathways.

Kinetic models are derived from experimental studies using Thermogravimetric Analysis [TGA], Differential Scanning Calorimetry [DSC], Differential Thermal Analysis [DTA]. The kinetics of wood degradation and its respective components have been and still are obtained by measuring the rate of weight loss of the sample as a function of time and temperature. The most common technique for this investigation is thermogravimetric analysis [TGA]. TGA involves continuous weighing and recording of data obtained from a sample, heated at either constant temperature or a fixed heating rate, enclosed in a furnace (e.g. 102, 148, 149, 150, 151, 152, 161, 162, 173, 191, 192, 193, 194, 195, 196). These experiments are normally carried out under vacuum or in a nitrogen atmosphere at both low temperatures and heating rates. Some workers have used steam as the gaseous environment in their experimental system (195, 196, 205). As there is no provision for the collection of volatile pyrolysis products, the TGA data are normally used to derive overall kinetic expressions. The global thermal degradation process can be described by a simplistic reaction scheme as shown in equation {3.02}.

biomass —> char + volatiles {3.02}

The rate of the above reaction is then described in the form of a first order Arrhenius type rate law as shown in equation {3.03}.

$$-\left(\frac{dW}{dt}\right) = [W - W_f]\, A \exp\left(\frac{-E}{RT}\right) \quad \{3.03\}$$

where: W is the initial weight fraction, W_f is the final weight, A is the pre-exponential [frequency] factor [s^{-1}], E is the activation energy [J/mol], R is the universal gas constant [J/molK], T is the reactor temperature [K].

If the sample is heated at a constant rate M, then:

$$-\left(\frac{dW}{dt}\right) = \left(\frac{A}{M}\right)[W - W_f] \exp\left(\frac{-E}{RT}\right) \quad \{3.04\}$$

$$M = \left(\frac{dT}{dt}\right) \quad \{3.05\}$$

Sometimes the weight term is replaced by a density term, usually assuming that no shrinkage occurs during char formation. Table 3.01 shows some selected kinetic parameters for overall reaction rate expressions. The Arrhenius kinetic parameters, the activation energy E [J/mole] and the pre-exponential [frequency] factor, A [s^{-1}] are derived by obtaining best fit curves through the experimental data and solving the Arrhenius rate law, using a least squares method. The kinetic constant for first order reactions is then used to predict the change in mass or composition of the original material by the equation {3.06}:

$$V = V^*[1 - e^{-\kappa t}] \quad \{3.06\}$$

where V^* is the maximum attainable yield at temperature T [K], V is the yield at time t, and κ is the rate constant determined from equation {3.07}:

$$\kappa = A \exp\left(\frac{-E}{RT}\right) \quad \{3.07\}$$

A comparison of the different kinetic parameter estimation methods has been made by Vovelle et al. and they highlight the variability in the values obtained using different methods (206). To demonstrate the variability of kinetic data due to differences in sample size, shape and origin, a range of kinetic data are also given in Table 3.01.

Table 3.01

Experimental kinetic parameters for overall reaction rate expressions

Source	Sample	Temperature Range [°C]	Activation Energy [kJ/mol]	Frequency Factor [s^{-1}]
Akita & Kase (207)	α Cellulose	250-330	224.0	1.0×10^{17}
	Modified cellulose	250-330	134.0	1.7×10^{10}
Bilbao et al.(148, 149	Cellulose	230-300	54.3	5×10^{17}
150, 151)	Xylan	< 280	10.2	9.8
	Lignin	< 325	17.8	2.6×10^{3}
	Pinaster pine	290-325	16.4	6×10^{2}
		> 325	52.9	1.7×10^{16}
	Barley straw	240-270	12.5	42
		>270°C	25.7	8.2×10^{6}
Broido (208)	Cellulose	226-328	221.6	1.7×10^{15}
Brown & Tang (209)	Ponderosa	---	149.9	
Chatterjee (210)	Cotton	---	227.3	138.1
Kanury (211)	α cellulose	100-700	79.5	1.7×10^{5}
Lewellen et al. (212)	Cellulose	---	139.8	6.8×10^{9}
Simmons et al. (213)	cellulose	---	36	1.6×10^{10}
Stamm (214)	Douglas fir sawdust	110-220	104.7	2.4×10^{5}
	α Cellulose	110-220	108.8	6.0×10^{5}
	Hemicellulose	110-220	111.8	7.1×10^{6}
	Lignin	110-220	96.3	1.1×10^{4}
	Coniferous wood	95-250	123.5	6.2×10^{7}
Thurner et al. (89)	Oak sawdust	300-400	106.5	2.5×10^{6}
Tran & Rai (194)	Douglas fir bark	100-850	101.7 + 142.7 X **	2.1×10^{8}
	Catalysed bark *	100-850	102.6 + 86.2 X **	2.3×10^{8}
Salazar et al.(215)	lc hemicellulose		54	165.9
	cellulose		166	1.1×10^{12}
	sc hemicellulose		83.6	1.5×10^{4}
	cellulose		417.6	2.4×10^{33}
Samolada et al. (87)	fir wood	400-500	56.5 v	136
			94.5 g	2.4×10^{4}
Varhegyi et al. (173)	Avicel cellulose	---	205 #,	1.26×10^{15}
		---	222 §	6.3×10^{16}
		---	234 ∞	4×10^{17}

Williams et al. (172)	cellulose	5 °C/min	187.6	1.45×10^{13}
		80°C/min	260.4	6.49×10^{19}
	hemicellulose	5 °C/min	258.8	1.86×10^{22}
		80°C/min	125.1	1.61×10^{9}

*	bark with 15% K_2CO_3	**	X denotes fractional conversion
#	10C°/min heating rate	g	total gases
§	80C°/min heating rate	v	total volatiles
∞	preheated, then 10C°/min heating rate	lc	large cylinder sc small cylinder

Kinetic parameters estimated by the researchers given in Table 3.01 show a wide variability in the values, even for similar feedstocks and similar conditions. Some of the variability in the parameters may be accounted for by the neglect of temperature variation of the sample during heat up and the use of the steady state temperature as the overall reaction temperature, as highlighted by Williams and Besler (172). Some kinetic modelling has also been performed with large biomass samples where the effects of mass and heat transfer cannot be neglected. This is evidenced by Salazar who gives different value for the pre-exponential factor and the activation energy for two differing cylinders of eucalyptus (215). Other researchers have used two or more consecutive steps of zero and first order reactions to describe the pyrolytic degradation of the biomass (e.g. 101, 155, 160, 216, 217, 218, 219).

Other discrepancies arise from too simplistic modelling and the presence of impurities or ash which may influence the decomposition kinetics. Varhegyi et al. have investigated the effect of NaCl, $FeSO_4$ and $ZnCl_2$ on the pyrolysis of Avicel cellulose under different conditions with four different modelling approaches which agreed well with the experimentally derived weight loss curves (173).

3.4.4 Stepwise models

This modelling approach allows for the formation of intermediate components and their subsequent conversion to final products, as shown in equation {3.08}.

biomass ---> product component j {3.08}

where the rate of formation of component j with a yield V_j at a given time t is given by equation {3.09}:

$$\left(\frac{dV_j}{dt}\right) = [V_j^* - V_j]\, k_{oj} \exp\left(\frac{-E_j}{RT}\right) \qquad \{3.09\}$$

where V_j^* is the ultimate attainable yield of product j, i.e., the yield at high temperature and long residence times (e.g. 220). The constants k_{oj}, E_i and V_j^* cannot be predicted beforehand and must be estimated from experimental data, a problem that increases as the number of reactions postulated increases. The model provides a simple scheme that can be used to predict product yields and this approach has been used by Krieger et al. (80). Some kinetic models have taken into account the competitive nature of some of the pyrolysis reactions which have been postulated to account for the variations in product yield. One example is that of Bradbury et al. for cellulose as shown in Figure 3.10 (161).

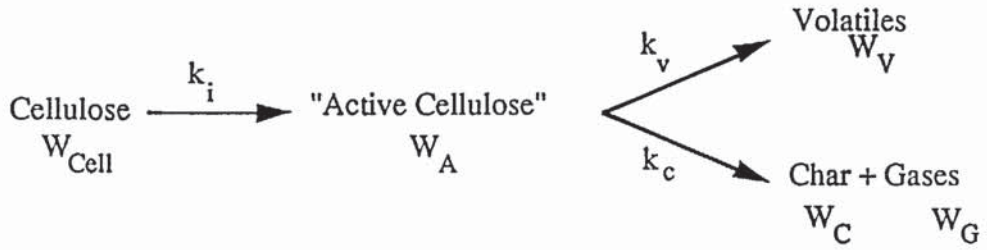

Figure 3.10. Bradbury's competing kinetic model for cellulose pyrolysis

where:

$$-\left(\frac{dW_{cell}}{dt}\right) = k_i\, [W_{cell}] \qquad k_i = 1.7 \times 10^{21} \exp\left(\frac{-58000}{RT}\right) \text{min}^{-1} \qquad \{3.10\}$$

$$-\left(\frac{dW_A}{dt}\right) = k_i\, [W_{cell}] - (k_v + k_c)\, [W_A] \qquad k_v = 1.7 \times 10^{16} \exp\left(\frac{-47000}{RT}\right) \text{min}^{-1} \qquad \{3.11\}$$

$$-\left(\frac{dW_C}{dt}\right) = 0.35\, k_c\, [W_A] \qquad k_c = 1.7 \times 10^{11} \exp\left(\frac{-36000}{RT}\right) \text{min}^{-1} \qquad \{3.12\}$$

Bradbury's model as shown above was based on the pyrolysis of pure cellulose. Theoretical and experimental results for weight loss agreed to within ± 5%. As a consequence this model has generally been used to account for char yields in the models of large particle pyrolysis (e.g. 80, 104, 221, 222).

Koufopanos et al. (192, 193) proposed that the biomass pyrolysis rate could be related to the individual pyrolysis rates of the biomass components by equation {3.13}:

$$\text{biomass} = \alpha\, [\text{cellulose}] + \beta\, [\text{hemicellulose}] + \chi\, [\text{lignin}] \qquad \{3.13\}$$

- bracketed terms [ ] represent the fractions of the biomass components not transformed into gases or volatiles
- α, β, and χ are the weight fractions of the corresponding biomass components in the virgin biomass.

The reaction scheme of the individual components then followed a similar reaction scheme as shown in Figure 3.10. Theoretical and experimental results for the weight loss agreed to within ± 10%. However, there was no indication in the model of Koufopanos et al. that it could be used to predict product yields (192, 193). Nunn et al. (220) found that, in general, the calculated values fitted laboratory data within ± 7% for temperatures up to about 950-1000°C. Similar modelling approaches using the kinetic pathways and data of Bradbury et al. have been adopted by other researchers, e.g. Simmons and Lee (213), Salazar and Conner (215), Samolada and Vasalos (87) and Varhegyi et al. (174) with reasonable agreement between experimental and predicted results.

3.4.5 Analytical models for large particles

Kinetics are sufficient to predict the reaction rate in small particles [< 100 μm]. However, for large particles, both the physical and the chemical changes are essential for obtaining a global pyrolysis rate. To formulate an analytical pyrolysis model, the known parameters that can influence the pyrolysis process must be considered in conjunction with the processes occurring during pyrolysis:

- heat transfer from the reactor environment to the particle surface by convection, and/or radiation and/or conduction,
- heat transfer from the outer surface of the particle into the interior of the particle by conduction and in a few situations to a lesser degree by convection,
- convective heat transfer between the volatile reaction products leaving the reaction zone and the solid matrix,
- primary pyrolysis leading to conversion of the biomass to gas, char and a primary liquid product,
- secondary and tertiary pyrolysis leading to conversion of the primary product to a gas, char and a secondary liquid product,
- changes in physical properties, enthalpy and heats of reaction of the biomass,
- changes in the enthalpy of the pyrolysis products,
- diffusion of volatiles out of the solid and away from the particle surface. Pressure gradients may also occur due to vapour formation in larger particles.

These processes are all temperature dependent and, since temperature changes with time and space, they will also be time and spatially dependent. Furthermore, they will also be

dependent on the physical structure of the particle along with its properties such as density, thermal properties, size and the grain orientation of the particle. A more detailed study of single particle models which includes the formulation and assumptions made in the models has been compiled by Bridge (202) and is beyond the scope of this thesis.

3.4.6 Vapour phase kinetics and primary liquids formation

After the formation of the primary vapours, they are subject to a particular time-temperature history before their subsequent recovery as liquids. This will therefore determine the final yield of organic liquids. Secondary pyrolysis kinetics are essential in the design of a reactor for the optimal production of organic liquids and the following areas are reviewed:

- primary liquids formation and secondary decomposition,
- general gas/vapour cracking kinetics.

3.4.6.1 Primary liquids formation and secondary decomposition

Models for the primary formation of organic liquids followed by secondary decomposition have been proposed by Liden et al. (83), Diebold (205) and Gorton and Knight (223). Lidén and Diebold using different reactor configurations, proposed similar kinetic models. Their reaction scheme is shown in Figure 3.11.

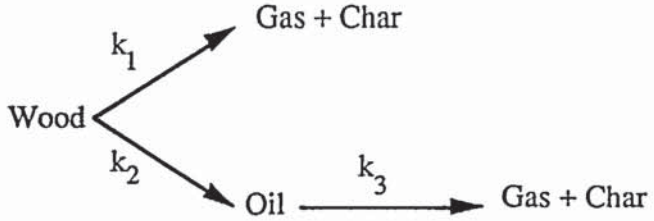

Figure 3.11. Reaction scheme used by Liden et al. and Diebold

The kinetic expression used for the estimation of the yield of liquid products and the values of the kinetic parameters used for each model are listed below:

$$x = x_o \left(\frac{1-\exp(-k_3\theta)}{k_3\,\theta} \right) \qquad \{3.14\}$$

where:

k_3: the reaction rate constant for the liquid decomposition step [s^{-1}]

θ: the mean residence time for the liquid decomposition [s]

x_o: the theoretical 'ultimate' oil yield [wt%]

x: the yield of liquids [wt%]

with:

$$k_3 = 4.28 \times 10^6 \exp\left(\frac{-107500}{RT}\right) \qquad x_o = 0.703 \qquad \{3.15\}$$

$$k_3 = 1.55 \times 10^5 \exp\left(\frac{-87634}{RT}\right) \qquad x_o = 0.78 \text{ or } 0.76 \qquad \{3.16\}$$

for Lidén and Diebold respectively. The reaction scheme used by Gorton and Knight (223) is shown below in Figure 3.12 with the reaction rate expression shown in equation {3.17}:

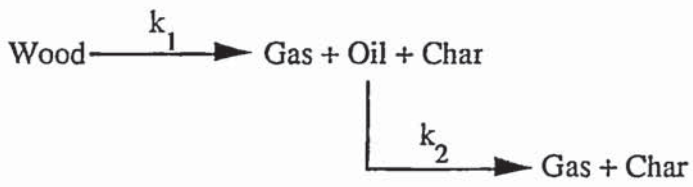

Figure 3.12. The reaction scheme of Knight et al.

$$x = \left\{\frac{k_1 b_5}{(k_2 - k_1)[\exp(-k_2\tau)]}\right\} \qquad b_5 = 0.811 \qquad \{3.17\}$$

with:

$$k_1 = 1.483 \times 10^6 \exp\left(\frac{-21380}{RT}\right) \qquad \{3.18\}$$

$$k_2 = 23.12 \exp\left(\frac{-7060}{RT}\right) \qquad \{3.19\}$$

where:

k_1: reaction rate constant for the first order production of liquid [s^{-1}]

k_2: reaction rate constant for the first order decomposition of liquid [s^{-1}]

b_5: maximum fractional conversion of wood to liquid [wt%]

τ: residence time [s]

Vasalos et al. (224) and Piskorz et al. (81) tested the above models using their own experimental data. Vasalos et al. found that using Lidén's parameters, they obtained a better fit of the liquid yields of ±20% for the particle size range 300-425 μm, while Diebold's parameters gave a better fit of ± 10% for the particle size range 500-600 μm. Knight's et al. model did not predict satisfactorily liquid yields for either particle size range when used by Vasalos et al. (224). They concluded that the variations between the predicted values and the experimental results could be attributed to the exclusion of the water yield in the reaction mechanism, the residence times used, and the type and size of biomass tested.

Scott et al. (95) found, when testing the models of both Lidén and Diebold, that the predicted liquid yields agreed with achieved yields within ± 10% for the temperature range 500-700°C with residence times of up to 1 second. Low predictions of liquid yields at the highest

temperature were attributed to the assumed water yield [2-5 wt% for cellulose], the constant x_0 parameter or errors due to the total yield being normalised to 100%.

3.4.6.2 Secondary gas phase decomposition

Primary wood pyrolysis vapours are stable below 500°C but they do begin to undergo secondary reactions above this temperature (20). Antal proposed that the conversion of primary vapours to either gases or tars occurred by the temperature based competitive reaction scheme shown in Figure 3.13.

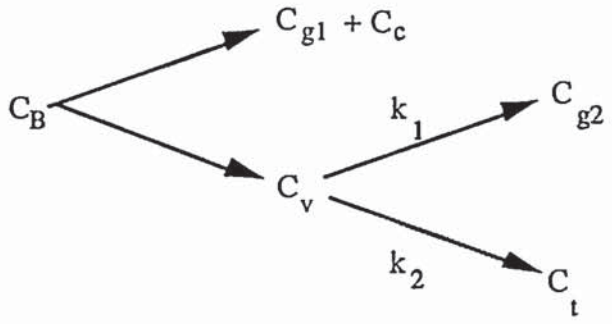

Figure 3.13. Antal's Proposed Reaction Scheme for secondary reactions

where:

- C_B: mass fraction of carbon in biomass,
- Cc: mass fraction of carbon in the char,
- C_v: mass fraction of carbon composing the reactive volatile matter [carbon in volatile matter/carbon in sample pyrolysate],
- C_{g1},C_{g2} the mass fraction of carbon composing the permanent gases,
- C_t: the mass fraction of carbon composing the refractory condensible materials, including the secondary liquids.

The first reaction produces more permanent gases by cracking the reactive volatile matter to smaller, less reactive species. The second reaction produced refractory condensible materials, which may be tar or some combination of water-soluble organic compounds.

Work has been carried out on the fast pyrolysis of biomass for the production of olefins at high temperatures due to cracking of the product vapours to non-condensible gases (e.g. 35, 225, 226).

Several studies have looked at the decomposition of pyrolysis products with temperature and residence time. These are detailed in Table 3.02 although different approaches have been used in analysing the experimental data and the decomposition pathway used generally follows the model of Liden and Diebold [see Section 3.4.6.1]. Secondary decomposition kinetics research has been conducted by Antal where a range of feedstocks were pyrolysed in a 3 stage reactor which allowed the decomposition of the vapour products to be studied and summarised in detail (196). A recent similar study by Boroson et al has highlighted that the gas/vapour product temperature of the products is more significant for liquids than the residence time (227). In the equipment of Boroson et al., the vapours were produced under conditions which are not typical for fast pyrolysis conditions; however, the results qualitatively agree with the expression and kinetic constants derived by Diebold and Liden.

Table 3.02
Vapour phase decomposition kinetics for pyrolysis liquids

Researcher	Feedstock	Temperature Range [K]	Activation Energy, E	Pre-exponential factor, A	Reference
Antal et al.	cellulose	773-973	204.3	2.07×10^8	195
	softwood	773-973	100.9	7.5×10^5 *	196
Boroson et al.	softwood	773-1073	99.3	8.91×10^5	227
Diebold	softwood	923-1073	87.6	1.55×10^5	205
Gorton et al.	wood	NK	7.1	23.1	223
Graham	cellulose	923-1173	100.8	1.1×10^6	39
Hajaligol et al.	cellulose	923-1073	133.4	2×10^8	119
	hardwood	NK	69	3.4×10^4	119
Lidén et al.	poplar	773-1073	107.5	4.28×10^6	83
Nunn et al.	hardwood	598-1403	49.4	5.6×10^2	228
Scott	cellulose		107.5	3.1×10^6	84
Stiles et al.	cellulose	673-873	81.0	7.9×10^3	229
	silver birch	723-873	73.0	5.3×10^3	229
Thurner et al.	hardwood		106.5	2.5×10^6	89

* ratio of activation energies for parallel gas and tar formation reactions

The products can be held at relatively long residence times if the gas/vapour product temperature is less than 500°C with only relatively slow cracking of the products. Most anhydrosugars are stable in the vapour phase at about 500°C (102). Therefore, for the

production of liquids as a fuel, relatively long residence times [~2 s] can be tolerated if the gas/vapour product temperatures are less than 500°C.

There is a wide variation in the kinetic parameters. It is apparent that the rate of liquids decomposition is considerably less than the rate of primary liquids formation. The most generally accepted parameters are those of Diebold, Liden and Boroson. The reader is also referred to the work of Chang and Kyihan (230), Bohn and Benham (225), Figueiredo et al. (231), Nunn et al. (219), Vassilatos (94) and Samolada and Vasalos (87) on secondary cracking reactions of biomass pyrolysis liquids in the vapour/gas phase.

The main results from a study of the kinetics is that for the production of liquids in high yields, low gas/vapour temperatures are required [400-500°C] and short vapour product residence times [less than 2 s].

3.5 Summary of biomass pyrolysis kinetics

As pyrolysis is a very complex process and the different intermediates formed are difficult to collect and identify, various approaches have been used to develop kinetic models. Most predict weight loss rather than product yield and distribution. The kinetic parameters vary from one model to another because they are very sensitive to experimental conditions. One research group found that even a decrease of 4.2 kJ/mol [from 133.1 kJ/mol to 18.9 kJ/mol] in the activation energy of tars caused the predicted value of the liquid yield to increase by approximately 16 % (233). One other problem which is not generally addressed by first order kinetic models is the prediction of the ultimate yield of liquid products. The maximum value is usually a "theoretical" value based upon experimental evidence or an assumed value. Also, there is no inclusion in the primary liquids formation for the variation of water yields with temperature and this is an area requiring further research.

The main benefit of these various kinetic studies have been the optimisation of process parameters, the prediction of yields, improved reactor design approaches the assessment of variations in product yields with gas/vapour phase temperature and time. There is a trade-off between reactor temperature and gas/vapour product residence time that has not yet been fully explored with regars to product yields and liquid quality. Recent efforts notably by Boroson, Scott et al. and Liden et al. have helped to elucidate some of the experimental results.

Chapter 4. Review of Ablative Pyrolysis of Biomass for Liquids

4.1 Introduction

This chapter reviews work which has made a contribution to the field of ablative pyrolysis. In this chapter, fundamental heat transfer relationships are reviewed and then processes by reactor throughput. Mass balances, reactor parameters, design correlations and operational information are given where possible and results compared with other fast pyrolysis processes. The research reviewed includes:

4.2 Centre Nationale des Recherches Scientifiques, University of Nancy

4.2.1 Background

The reason why this work was conducted is unclear: it appears to have developed from an analysis of the criteria for fast pyrolysis and then ablative pyrolysis was viewed as fulfilling the requirements of high heat transfer rates coupled with minimal char production. The results of this work were fundamental to the design of the reactor presented in Chapters 5 and 6, although there are discrepancies in the correlations and results as discussed in Section 4.2.4. Detailed heat transfer relationships were derived by Lédé from empirical results and the application of fundamental heat transfer theory. This has been the only fundamental work known by the author to have been published on ablation heat transfer with specific application to wood pyrolysis and is therefore a major contribution to the field.

4.2.2 Description of the rotating disk experimental rig

Lédé et al's. experimental system is shown in Figure 4.01 overleaf (50, 51, 115, 199, 233). A stainless steel disc of 7.5 cm diameter, spinning at a constant and controlled speed, was heated by four gas burners. Wood rods of diameter 2 to 10 mm, were pressed vertically onto the hot surface by weights and ablated for a preset time with the change in rod length noted. The average rate of ablation was then determined and the reaction zone measured by microscopic

examination of the rod end. To prevent volatiles combustion, an argon jet was directed at the contact point of the wood rod on the heated disk. The methodology, however, did not allow for overall product recovery for mass balance determinations.

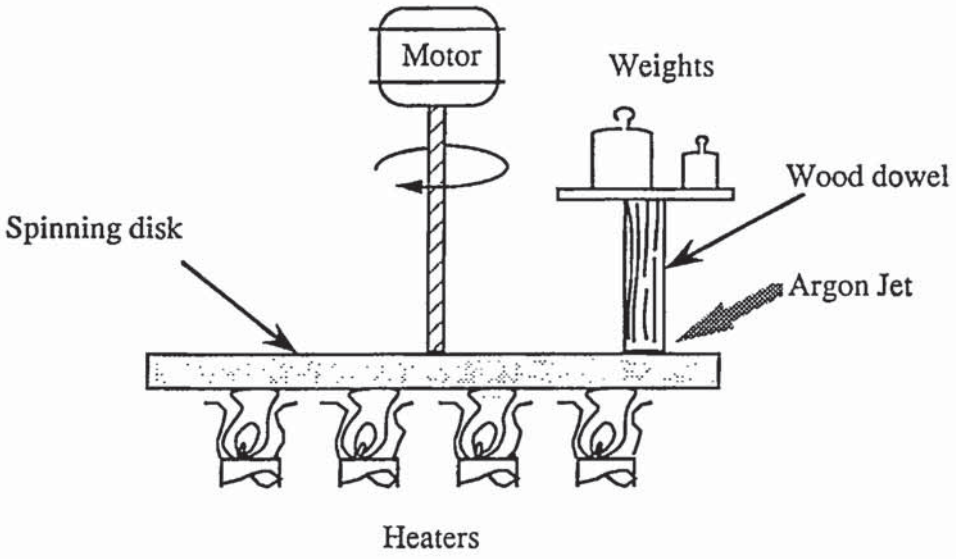

Figure 4.01. Lédé's spinning disc pyrolysis apparatus

By measuring the ablation rate of the rod in conjunction with the heated disk temperature, degree of relative motion and the applied pressure of the rod on the heated disk various fundamental correlations and relationships were obtained (51, 233, 234). Ablation rates were measured for a range of disk temperatures from 550°C to 900°C, relative motion [between the contacting biomass and the heated disk] at velocities from 0.3-3 m/s, and applied pressures of 2 x 10^5 to 3.5 x 10^6 Pa. Separate experiments were also carried out under conditions of no relative motion between the biomass and a heated metal surface (235).

4.2.3 Results of the work

A range of correlations were then determined for the ablation rate, the heat transfer coefficient, the wood decomposition temperature and other related parameters from the empirical results and the application of fundamental heat transfer equations. These are presented below.

4.2.3.1 Ablation rate, V

The ablation rate [rate of linear shrinkage of the wood rod applied to the metal disk] was measured for the range of experimental conditions noted in Section 4.2.1 and it may be calculated from equation {4.01}:

$$V = \hat{A}p^F \qquad \{4.01\}$$

where V is ablation [melting] rate, [m/s], $\hat{A}$ is a function of the reactor heated surface temperature, [m/sPaF], p is the applied pressure, [Pa], F is a constant dependent upon the solid [approximately equal to 1 for wood]. The ablation variable, $\hat{A}$, was empirically derived by Lédé et al. and is dependent on the reactor heated surface temperature (51). Lédé et al. determined values of $\hat{A}$ for four different disk temperatures [873, 973, 1073 and 1173 K] by a logarithmic plot of V against p. The term F is a variable that is dependent on the heated disk temperature and was derived in a similar way as $\hat{A}$ by Lédé et al. from the same logarithmic plot of V against p. In conjunction with determination of V, reasons for the dependency of the ablation rate on F are not fully explained by Lédé, but he has proposed the following relationship empirically determinedrelationship:

$$F = \frac{C_p(T_d - T_o)}{C_p(T_d - T_o) + \Delta H_{pyr}} \qquad \{4.02\}$$

where ΔH_{pyr} is the enthalpy of pyrolysis [J/kg]. Recently, Lédé has returned to the problem of endothermal volatilisation of particles in gas-solid environments, i.e. during convective heat transfer and compared his model prediction with measured values for V (103). Lédé's conclusions were that estimations of the ablation velocity were similar conditions for the range of conditions studied, i.e. for a measured wood rod ablation rate of 7×10^{-4} m/s, the calculated value was 6.92×10^{-4} m/s. The reader is referred to the above paper for the exact analytical approach used.

It was also found that the ablation rate, V, was related to the degree of relative motion between the contacting solid and the heated disk (235), with V reaching an asymptotic value at a relative velocity greater than 1.2-1.3 m/s. For conditions where there is no relative motion between the rods and the heated surface, equation {4.01} becomes:

$$V = \hat{A}p^{0.25} \qquad \{4.03\}$$

4.3.2.2 Heat transfer coefficient, h

The heat transfer coefficient, h was determined by equations {4.04} or {4.05}:

$$h = \Re\, p^F \qquad \{4.04\}$$

$$h = V\rho_w C_{pw}\left(\frac{T_d - T_o}{T_w - T_d}\right) + V\rho_w \Delta H_{pyr} \qquad \{4.05\}$$

where $\Re$ = 0.017 [W/m^2KPa^F], ρ_w is the dry wood density [kg/m^3], C_{pw} is the dry biomass heat capacity [J/kgK], T_d, T_o and T_w are the fusion [decomposition], datum and wall temperatures respectively [K]. Lédé neglects the enthalpy of pyrolysis, ΔH_{pyr}, in his calculations as it comprises only 3.6% of the total energy requirement to pyrolyse the wood. Actual values of F were determined from 0.982 to 1.01 depending upon the decomposition temperature. If equation {4.04} is to be used, a new value for $\Re$ should be determined for the biomass to be used as detailed by Lédé et al. (234). Heating rates of 4 x 10^6C°/s were claimed (51, 235).

4.3.2.3 Biomass decomposition temperature, T_d

For his range of experiments carried out, Lédé postulated T_d to be an average of 739 K within the experimental conditions studied of an average heat transfer coefficient of 10000 W/m^2K, heated disk temperatures of 500-900°C and applied pressure of 1 x 10^5-3.5 x 10^6 Pa. Lédé proposed an analytical solution for the wood decomposition temperature from his results. Lédé assumed that during steady state ablation, a superficial reaction layer of thickness ê moved at a constant velocity V towards the unreacted core of the wood. He then assumed that the temperature inside the reacting volume êS [where S is the rod cross sectional area] was constant at the decomposition temperature, T_d. The equation for the mass balance inside the reacting wood volume is given by equation {4.06} (234):

$$\kappa \hat{e} S \rho_w = V S \rho_w \qquad \{4.06\}$$

where κ is the assumed first order kinetic constant for the decomposition of wood [s^{-1}] at T_d. Lédé then assumed that Vê was equal to the solid thermal diffusivity, α_w, [m^2/s] to give equation {4.07}:

$$\kappa = \left(\frac{V^2}{\alpha_w}\right) \qquad \{4.07\}$$

For a known heated surface temperature and heat transfer coefficient, in conjunction with the biomass properties, T_d may be estimated by equation {4.08} based upon the mathematical manipulation of equations {4.05-4.07}:

$$T_w = T_d + \frac{T_d - T_o}{h}\sqrt{(\kappa \lambda_w \rho_w C_{pw})} \qquad \{4.08\}$$

where λ_w is the dry wood thermal conductivity [W/mK]. Lédé assumed that the reacting volume had a constant decomposition temperature [a reasonable assumption as the products are

being formed at this temperature] and that the endothermal decomposition was an assumed first order reaction, as various kinetic studies on primary wood and cellulose decomposition have shown [see Table 3.01]. Lédé et al. proposed that wood decomposition occurs at a specific "fusion" temperature under ablation conditions. If the heat for pyrolysis is provided at a temperature T_w from the metal surface, a theoretical increase in the surface temperature to T_d, the decomposition temperature, would lead to a subsequent increase in the heat flux demand. This high energy demand would only be satisfied by an equal external heat flux supply from the metal surface if the temperature gradient is high, i.e. large T_w-T_d differences. The result of this is that T_d appears to reach a stable value, resembling a constant melting point during biomass decomposition.

4.2.3.4 Liquids devolatilisation time

One other important result from this work was an estimation of the lifetime for liquid decomposing/vaporising on the heated disk. For the vaporisation of liquids to volatiles the kinetic constants of $A = 2.7 \times 10^7\ s^{-1}$ and $E = 116$ kJ/mol were obtained. These are in agreement with parameters determined by Diebold for the decomposition of "active wood" to vapours or "active wood" to char (205). This is discussed in Chapter 9.

4.2.4 Critique of Lédé's design correlations

The design parameters are those used in the specification of an ablative pyrolysis reactor in terms of the reactor heated surface temperature, the wood "fusion" temperature, datum temperature, heat transfer coefficient, applied particle pressure; from these, the ablation rate and consequently the required heat transfer area for a given reactor throughput and known biomass thermal and physical properties can be estimated. Those for which Lédé derived expressions or values are discussed below in Sections 4.2.4.1-4.2.4.4. Due to publishing errors, care must be taken in assessing the data (51).

Lédé's experiments were not accurate enough to determine whether or not rod diameter influenced the ablation rate. It was indicated that increasing wood diameter appeared to decrease the ablation rate, all other factors being constant. Lédé has modelled the endothermal volatilisation of cellulose for a range of temperatures, heating rates and enthalpies. His main conclusions were that in the chemical regime, the temperature at which the endothermal devolatilization begins varies within relatively close limits, typically ~407-483°C; this is consistent with his prior findings described in Section 4.2.2, even for widely varying conditions [heat transfer coefficients from 100-10000 W/m^2K, reactor temperatures from 900-1500 K and enthalpies of decomposition varying from 0 to 40000 J/kg].

4.2.4.1 The ablation velocity, V

Calculation or determination of the ablation rate is essential in the design of an ablative pyrolysis reactor. It will determine the reactor throughput for a given set of parameters. The ablation rate is the linear regression rate of the biomass as it decomposes if continuous removal of the products occur. At temperatures less than 600°C, empirically derived values for V should be used, due to unquantifiable errors in the estimation of the ablation rate. New data for measured ablation rates at 500°C are presented in Chapter 9.

4.2.4.2 Heat transfer coefficient, h

Lédé et al. recognised that h was subject to other influences such as vapour formation below the biomass inhibiting heat transfer, although this was not included in his equations for the estimation of h. This is apparent in the estimation of V where equation {4.01} does not accurately predict the values below 600°C.

Lédé proposed that Vê = constant, i.e. that the product of the linear ablation rate and the reaction layer ê were directly related. This was modified to a preheating zone e' [from ambient to 200°C, at which point chemical reactions were assumed to begin] and a reaction layer ê [from 200°C to the wood decomposition temperature]. Lédé's first assumption was that the reaction zone was the point from 100°C to the wood decomposition temperature. Under typically fast pyrolysis conditions, the feedstock is pre-dried to reduce the moisture content of the biomass to less than 10%: therefore, the wood heats rapidly from ambient temperature to ~ 466°C and then degrades as proposed at T_d. The interaction of the reactor parameters and their evaluation in the design of an ablative pyrolysis reactor are detailed in Chapter 5. No mass balances for the experiments using the spinning disk apparatus in terms of liquids and gases have been published. Lédé claims that little or no char is produced: only some white residue which is wood ash. It is likely that the hot product char oxidises once removed from the reaction area. The estimates of the heat transfer coefficient have a slight error due to the enthalpy of pyrolysis having been neglected in the calculations of the heat requirement.

4.2.4.3 Theoretical fusion temperature, T_d

The wood decomposition temperature is defined as the temperature at which the wood undergoes a phase change to a reactive "active wood" state, i.e. the primary wood components are reacting at significant rates to form fluids and char. The wood decomposition temperature may be used in reactor design for evaluating energy requirements and the kinetics of biomass decomposition for evaluating the minimum reactor temperature at which biomass decomposition

begins. The concept of the formation of "active" wood has also been proposed by Diebold (121) and Kothari and Antal (104). Reed proposed a similar theory that wood is heated to 773K without any significant reaction, depolymerises and then melts to form a liquid which subsequently vaporises or degrades (49).

Lédé has pointed out that strictly the "fusion" model for wood decomposition is not appropriate and that the induction period for the formation of an "active wood" does not occur at a constant "fusion temperature". The value of 739K is a best fit for the range of temperatures and heat transfer coefficients determined for Lédé's specific experimental conditions of applied pressures from 1 x 10^5 to 3.5 x 10^6 Pa, disk temperatures of 550-900°C and relative motion > 1.2 m/s (51). In subsequent work, Lédé et al. noted that T_d varies by ± 30K about 739 K within his range of experimental conditions and values may be determined from equation {4.08} (51). As noted Lédé has determined, by more detailed mathematical modelling, that T_d may vary from 407-483°C for cellulose decomposition, depending on reactor parameters (103). His more recent modelling work has elucidated some of his prior findings:

- For biomass decomposition to fluids, there is a competition between heat flux required for solid heating and the chemical reactions which have not been clearly defined.
- For biomass fast pyrolysis, the reactions occur during a short time and solid temperature has no time in which to increase to a large extent, i.e. analogous to sublimation.
- for most fast pyrolysis conditions, the effective fusion temperature [subsequently modified to an effective reaction temperature, T_e] is different to the external hot medium temperature with differences up to 700°C depending on the reactor temperature.

The importance of the wood decomposition temperature is that under fast pyrolysis conditions the biomass does not achieve the reactor temperature and that determination of kinetics for fast pyrolysis above 500°C may not be possible using current techniques. At conditions outside those studied by Lédé, no independent experimental work has been carried out.

4.2.5 Current status

The practical work on ablative pyrolysis of wood stopped at the University of Nancy in 1988.

4.3 Colorado School of Mines, USA

4.3.1 Background

The objectives of the work were to produce pyrolysis vapours for catalytic treatment as a parallel study to the ablative pyrolysis work being performed at NREL [see Section 4.6] using

the same principle of contacting biomass with a heated surface under conditions of high relative motion and applied pressure. The work was basic in experimental approach in assessing the requirements for ablation and preliminary yield data were obtained. Two sets of apparatus were constructed: initially, a heat flux concentrator to investigate rates of ablation and product distribution and secondly an engineering reactor to develop a method of particle ablation, derive some basic heat transfer mechanisms and mass balances and assess the reactor potential.

4.3.2 Description: heat flux concentrator

Reed and Cowdrey initially constructed a "heat flux concentrator" to investigate ablative pyrolysis. This comprised a drill press which forced and rotated wood dowels into a 1.2 cm diameter tapered hole in a heated copper block (236). The vapours and gas products emerged through 12 holes in the bottom of the block: liquids were collected in traps and gases recovered in a burette by water displacement. It was intended that the char product would exit through the holes in the copper block. The heated block temperature range used was 500-700°C and total liquid yields of over 50 wt% on an as fed basis were obtained. The forced contact of the wood in the concentrator, however, caused the holes to be plugged after about 10g of wood was fed.

4.3.3 Description: contact pyrolysis mill

A "pyrolysis mill" was then constructed as shown in Figure 4.02 derived from the principles of a conventional grain mill (107, 236, 237, 238). The pyrolysis mill had a stationary upper "stone" and a rotating lower "stone" which were both copper and both in contact with fixed electrical heaters. The lower plate was rotated at speeds up to 80 rpm, the contact pressure on the wood particles being controlled with a spring.

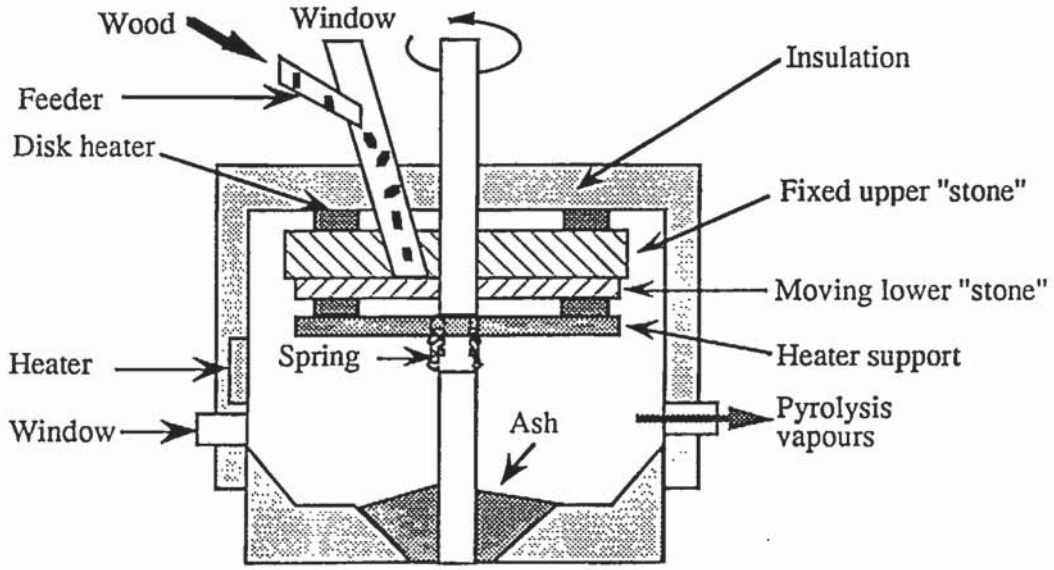

Figure 4.02. Reed and Cowdrey's ablative pyrolysis mill

The reactor wall was heated to 300-400°C to prevent pyrolysis vapour collection inside the reactor. Wood particles entered the reactor through the upper plate and the vapours escaped through holes in the plate to a series of four liquid traps consisting of a cooled condenser and a sulphuric acid trap to remove water vapour. Char and ash accumulated inside the reactor after the particles were ablated.

The problems with the system employed by Reed was that the escape of the pyrolysis vapours through the plates was prevented by plugging of the holes in the disc. Unreacted feed and char remained in the hot reactor environment to undergo more conventional pyrolysis. No residence time values are quoted. The concept is good, but the problem with using disks is that variable particle size causes processing problems due to disk spacing. Smaller particles will therefore not be ablated and will more slowly carbonise on the hot plates. Relative motion between particles and disk could not be maintained as the particles tended to stick to one surface and not move as intended and the installation of ribbed disks did not solve the problem. A low percentage of the heat transfer area was utilised due to poor distribution of the wood chips. The copper plates were susceptible to deformation despite the low temperatures. Even distribution and efficient use of the heat transfer area proved difficult.

4.3.4 Results for the contact pyrolysis mill

Some results for the contact pyrolysis mill are presented in Table 4.01. Using this reactor system, total liquid yields of up to 54 % of liquid based on dry feed have been achieved. The only feedstock tested was bone dry wood. Feed rates of up to 0.2 kg/h were achieved with run times up to 1.5 hours. The mass balance closures varied from 75.1-114.9% although exact reasons for the poor mass balance closures are not given. The yields of liquids are much lower than those obtained from fast pyrolysis processes and the high losses do not allow a complete evaluation of the results to be made [see Chapter 8 for gas analysis comparison].

Cowdrey estimated the average heat flux in the first reactor to be 6.8 W/cm^2 compared to 5.08 W/cm^2 in the second reactor (238). Diebold has quoted heat fluxes of 6 W/cm^2 for a commercial ablative pyrolysis plant and the ablative pyrolysis reactor used in this work has a calculated heat flux of 11.4 W/cm^2 at 600°C as discussed in Chapter 5 (46). The best organic yield was 54.4 wt% although the residence time is not known.

4.3.5 Current status

No further work has been carried out or is planned and the reactor has been dismantled (239).

Table 4.01

Results for the ablative pyrolysis mill for reactor disk temperatures 450, 550 and 600°C

Run Number	105	106	107	109	110	111
Reactor Temperature [°C]	450	550	550	550	550	600
Throughput [g/h]	123.7	62.2	145.4	101.5	52.8	13.0
Char	58.3	31.5	14.1	18.0	16.0	5.5
Liquid	24.1	33.5	48.6	38.5	42.8	54.4
Gas [N_2/Ar free]	9.9	49.9	19.8	18.6	35.1	23.2
Closure	92.3	114.9	82.5	75.1	93.9	83.1
Gas composition [N_2/Ar free basis]						
H_2	8.50	1.03	0.00	1.82	0.00	2.95
CO_2	61.09	38.97	50.33	30.53	36.57	30.54
CO	29.29	45.99	40.3	48.92	47.15	44.39
CH_4	1.00	9.13	7.4	12.47	10.58	14.81
C_2H_4	0.00	0.09	0.00	0.12	0.00	3.11
C_2H_6	0.00	1.18	0.00	1.63	1.68	1.88
C_3H_6	0.11	0.95	1.58	1.32	0.41	1.71
C_3H_8	0.02	0.27	0.39	0.33	0.38	0.31
1-butene	0.00	0.20	0.00	0.25	0.32	0.30
C_4H_8	0.00	0.09	0.00	0.12	0.00	0.00

4.4 University of Twente, the Netherlands

4.4.1 Background

This work was instigated under the JOULE programme to develop a new reactor technology for the pyrolysis of biomass by sliding and pressing the particles on a heated surface, thus achieving the key elements of ablation. Ablative pyrolysis was originally meant to be achieved in a heated rotating cone where the particles could "slide" across a heated metal surface and the pressure could be generated by the centrifugal action of the particles on the rotating heated wall. This concept was partially realised as described below.

4.4.2 Description: conceptual design

The concept is that biomass particles are fed onto a vaned impeller which is mounted at the base of the heated rotating cone and are then flung on to the heated surface with the final char and ash residue flung out of the top of the cone. The applied particle pressure was to be achieved by the particles being flung along the wall with the centrifugal motion generating the pressure. Particle ablation was expected to occur by heat transfer from the heated cone as the particles bounced and slid across the surface (240). This is depicted in Figure 4.03.

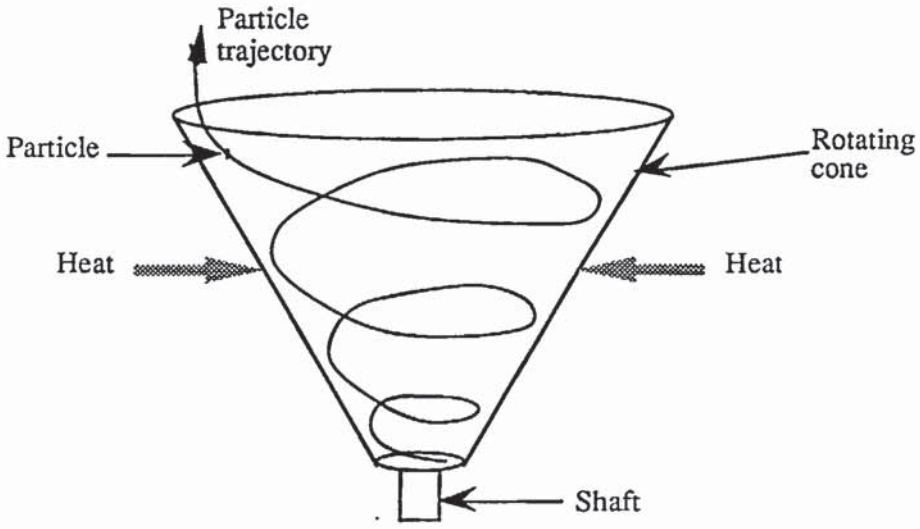

Figure 4.03. Principle of particle behaviour in the rotating cone

A cold flow experimental cone was constructed to investigate the dynamic behaviour of particles in the intended reactor. Nearly spherical mono-sized PVC particles, diameter 140-780 μm, and density 1.1 g/cm^3, were used as they could be easily seen and photographed (240). This work was carried out in two cones of angle 60° and 90°. Cone rotational speeds up to 1800 rpm were used to determine the influence of gas flow on the residence time and motion of the particles at ambient conditions with particle motion recorded using an endoscopic camera. PVC particles greater than 400 μm appeared to be unaffected by gas viscous forces and the residence time of the particles was almost independent of the particle diameter. For particles smaller than 200 μm, viscous forces became dominant and the residence time of the particles was strongly dependent on the particle diameter. Particle residence times were 0.01-0.3 s as determined from high speed photographic measurements (241).

4.4.3 Description: heat transfer model

A heat transfer rig was constructed and tested with the same cone dimensions as the 60° cone to investigate the heat transfer to the particles ablatively "sliding" on the cone surface (240, 242).

MISSING

PAGES

NOT

AVAILABLE

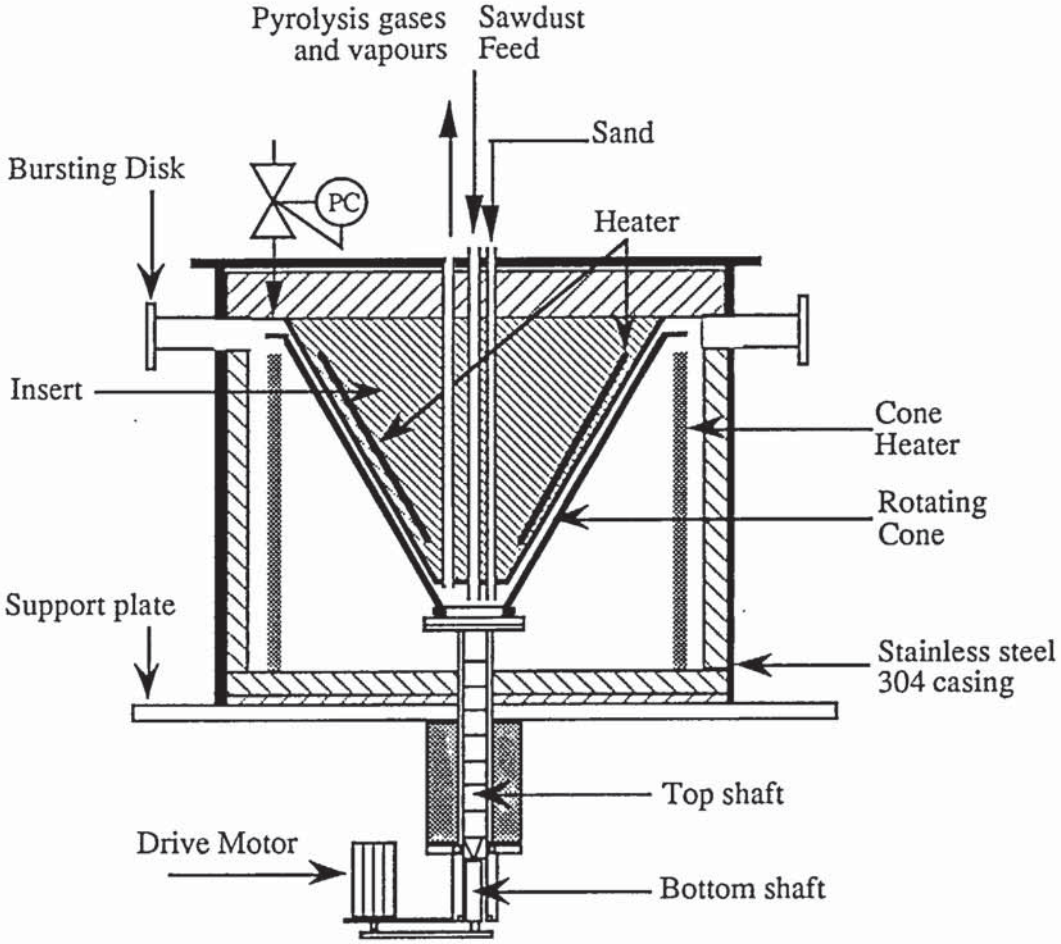

Figure 4.05. University of Twente modified rotating cone reactor

The fitting of the internal cone reduced the operational volume from 0.25 m^3 to 0.003 m^3. To remove the problem of particle adhesion to the reactor wall, sand was added in a mass ratio of 10 or 20:1 sand to biomass fed. The collection space outside the heated zone was designed only to accommodate a low yield of char from the reactor; therefore, run times were restricted to a maximum of 10 minutes. The liquids were collected in a condenser system consisting of six condensers in series followed by gas filtering. Gas analysis was performed by GC on batch gas samples.

4.4.5 Results for the rotating cone reactor

Results from the modified reactor, shown in Figure 4.05, have been obtained for softwood, hardwood and rice husks and are summarised in Table 4.02 below (244). Due to isothermal operation of the rotating cone reactor, a significant proportion of the product vapours were cracked to non-condensible gases. The overall closures are also slightly lower than would be expected, probably due to the formation of low molecular weight liquids which proved difficult to recover.

Table 4.02

Results for the rotating cone reactor, reactor temperature 600°C [wt% dry feed basis]

Feedstock	Char	Organics	Water	Gas	Closure
soft wood	10.0	31.0	15.5	35.5	92.0
hardwood	7.0	19.0	21.0	38.0	85.0
rice husks	18.0	11.0	20.5	32.0	81.5

Reactor throughputs are claimed to be 7.2 kg/h of biomass; this is high as the sand has a high thermal input to the system, helping to pyrolyse the fine biomass particles. As noted earlier, the original intention of particle ablation by centrifugal action of the particles on the heated rotating cone has not been fully achieved. The action of the sand is partly as a heat carrier, similar to a fluid bed and partly to remove product char from the cone wall.

4.4.6 Current status

The reactor is to be modified so that the sand is removed from the reactor with the char, followed by combustion and recycling of the hot sand to the reactor. The research is continuing on biomass feedstocks and scale-up of the reactor.

4.5 BBC Engineering and Research Ltd., Canada

4.5.1 Background

This work was instigated to assess fast pyrolysis as an alternative method for the disposal of tyres. The primary objective was to demonstrate that short residence times and high heating rates could produce high yields of liquids from rubber at moderate temperatures of 400-600°C in an ablative reactor. A 10-25 kg/h unit was constructed to investigate the reactor parameters of surface temperature, gas/vapour product residence time and particle size. A larger scale system of 25 t/d has been reported using wood, although no details are available yet. The details of particle ablation have not been disclosed.

4.5.2 Description: continuous ablation reactor

Only limited details of the continuous ablation reactor [C.A.R.] are available: ablation is said to be due to sliding contact of rubber particles on a hot metal surface and meets all the criteria of

high applied pressure, high relative motion and high heating rates (245). Tests on a 50 kg/h pilot reactor have demonstrated efficient heat and mass transfer and a smaller test unit is presently operating at a throughput of 10 to 25 kg/h, although more typically throughputs of 16 kg/h. Particles up to 6 mm have been used with liquid recovery in a two stage direct liquid quench of the product vapours with recycled liquids after char removal in a high temperature cyclone. The system is shown in Figure 4.06 overleaf.

Tyre rubber, primarily of particle size 1-3 mm is used, although tests have been carried out using 6 mm particles. The feeder is mounted on load cells, comprises a pressurised lock hopper with a variable speed discharge screw which feeds the reactor. The reactor has staged external heating for zonal temperature control and catalysts can be added to the reactor. Vapour product residence time in the reactor is controlled by the addition of nitrogen and the vapours are separated from the char and metal in a cyclone before quenching in a baffle plate column. Liquids are then collected in a sump tank and are returned to the column via a water cooled heat exchanger, with a proportion being pumped to storage. The first column is operated at 100°C exit temperature for the vapour/gas products. The second column is similar to the first with a final gas exit temperature of 40°C. Gas analysis is done both on-line and on a batch basis.

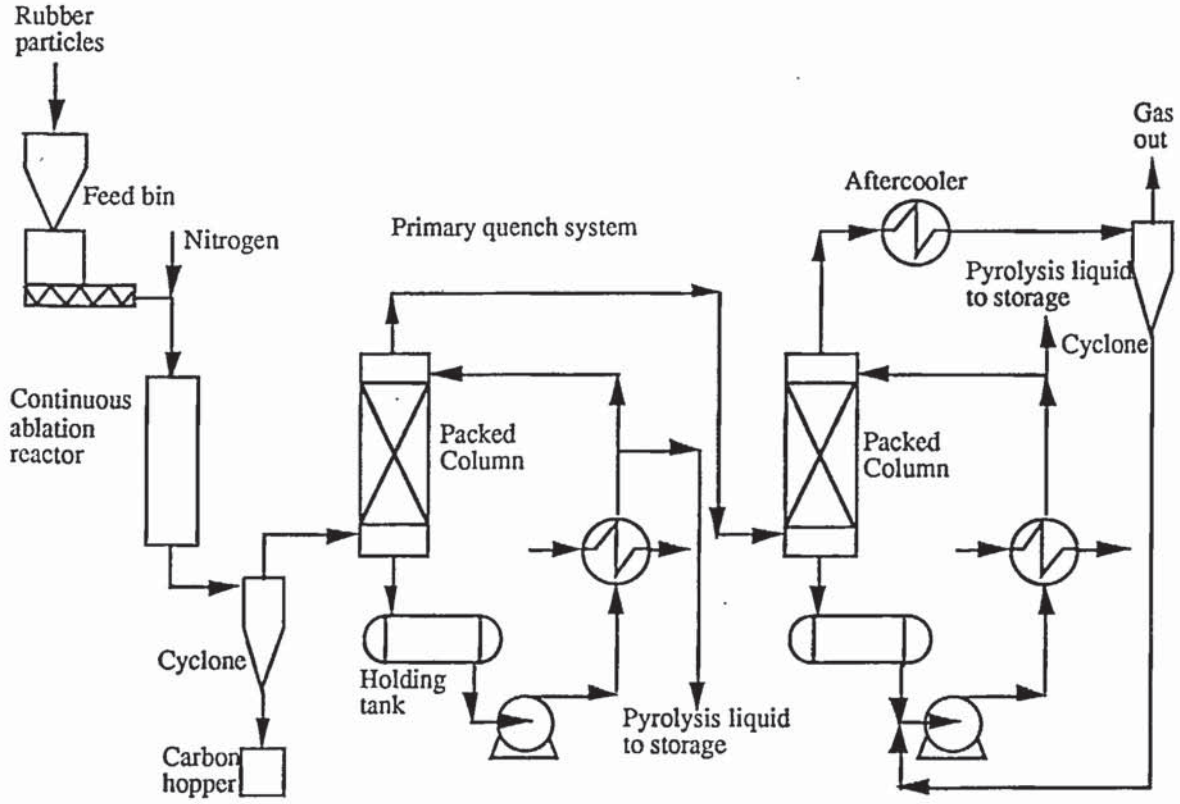

Figure 4.06. Black's continuous ablation reactor system

4.5.3 Results

Liquid yields of 54 wt% have been obtained at 470-540°C at 0.88 s residence time and for 1.3 mm particles. These yields are comparable to those obtained by Roy et al. with their vacuum pyrolysis apparatus who for a similar reactor temperature of 500°C achieved yields of: char, 35.5 wt%, oil 56.22 wt%, water 4.0 wt% and gases 4.3 wt% on wt% tyre as received basis (246). A liquid composition for the continuous ablation reactor is given in Table 4.03. Some mass balances are presented in Table 4.04 (247).

Table 4.03
Analysis of the liquid product from the continuous ablation reactor, run Apr 2b, [wt % of liquid]

Benzene	0.135	Styrene	1.3
Toluene	0.95	Limonene	0.35
Ethylbenzene	0.24	Naphthalene	0.15
Xylenes	1.12	Total aromatics	26.00

Table 4.04
Mass balances for the continuous ablation reactor [wt% dry basis]

Run Number	Apr 2b	Apr 2a	Apr 1e	Mar 31d
Feed ash content [wt %]	7.1	7.1	7.1	8.8
Reactor Temp. [°C]	450	475	515	535
Residence Time [s]	0.925	0.965	0.881	0.925
Char	52.9	41.2	30.1	37.5
Liquid	39.1	48.1	54.3	50.2
Gas [inert free]	8.0	10.8	15.6	12.3
Closure	100.0	100.1	100.0	100.0

Problems have occurred during sustained periods of operation where the fine carbon black {< 3 μm} gradually made the recycled liquid in the first collection column too viscous to pump after 2 hours. Approximately 30% of the char formed was too fine to be efficiently recovered by the cyclone. A particle size analysis of the product char showed it all to be less than 10 μm.

Modification of the liquids recovery system, which has not been detailed, allowed operation to be extended to 3 hours. Black proposed filtering of the liquids which may prove difficult in view of the particle size of less than 10 μm.

4.5.4 Current status

The plant described is still operational and trials on a 25 t/d plant using wood are presently ongoing.

4.6 NREL Entrained Flow Vortex Reactor

4.6.1 Background

This work developed from exploratory research at the Naval Weapons Research Centre at China Lake instigated in 1975 to evaluate the production of automotive fuel from organic wastes (226). Results indicated that high yields of unsaturated hydrocarbons [C_2H_4, C_3H_6 and C_4H_8] up to 24 wt% on a dry feed basis were obtainable (248, 249). A continuous flow pyrolysis reactor produced hydrocarbon gases for subsequent separation and gasoline synthesis. A bench scale reactor comprising a 38 mm internal diameter heated coil, lengths 2 and 6 m, through which biomass particles were entrained by CO_2 with a throughput of 5 kg/h was used. Unsaturated hydrocarbons were then further processed by conventional techniques to produce gasoline. Subsequent to this project, Diebold conducted further tests with the heated coil entrained flow reactor described using pure cellulose and birch flour as the feedstocks. This second phase at China Lake, funded by the Solar Energy Research Institute [SERI], had the objective of determining olefin yields from lignocellulosic feedstocks using the same equipment (226).

From this work, Diebold continued his research into pyrolysis at SERI, now the National Renewable Energy laboratory [NREL]. The phenomenon of ablative fast pyrolysis was demonstrated by Diebold in 1980 when he showed that when biomass was moved relative to a red-hot nichrome wire, the wire appeared to "cut" the wood (121). The pyrolysis rates attained by this technique were estimated to be three and a half orders of magnitude greater than slow pyrolysis rates at a similar temperature. Heating rates of 5 x 10^5C°/s were reported (121). Subsequently, a 50 kg/h entrained flow ablative pyrolyser was designed and constructed, using an externally heated horizontal vortex tube as the reactor, which is described and discussed below. This is one of the first developed ablative reactor technologies and research has been ongoing for 14 years into ablative pyrolysis.

4.6.2 Description: vortex cyclone reactor

Figure 4.07 shows the current reactor system configuration at the NREL laboratory. The reactor functions as a horizontal cyclone with wood chips, ~ 5 mm metered into the system by a screw feeder, entrained by a recycle stream of inert gas and pyrolysis products into a supersonic jet of hot carrier gas [steam or nitrogen]. A long entrainment tube is used to allow the particles to accelerate to the high entering velocities of over 400 m/s. The particles enter the vortex reactor tangentially generating high centrifugal forces, up to 2.5 x 10^5 "g's", which press the particles on the wall. For a particle size of 5 mm, an assumed wood density of 500 kg/m^3, a reactor radius of 0.067 m and particle velocity of 420 m/s, the generated pressure on the reactor wall is calculated to be 6.58 x 10^6 N/m^2.

The 316 stainless steel reactor has an internal diameter of 13.4 cm, a length of 70 cm, and is heated by three wall heaters. The gases, vapours and char fines leave the reactor through the axial exit, which extends part way into the reactor. The typical carrier gas to biomass mass ratio is in the range of 0.7-1.5. Relevant updates on the initial reactor performance, commissioning and experimentation are to be found in proceedings of the U.S. D.o.E. Biomass Thermochemical Conversion Contractors' Meetings (250, 251, 252, 253, 254).

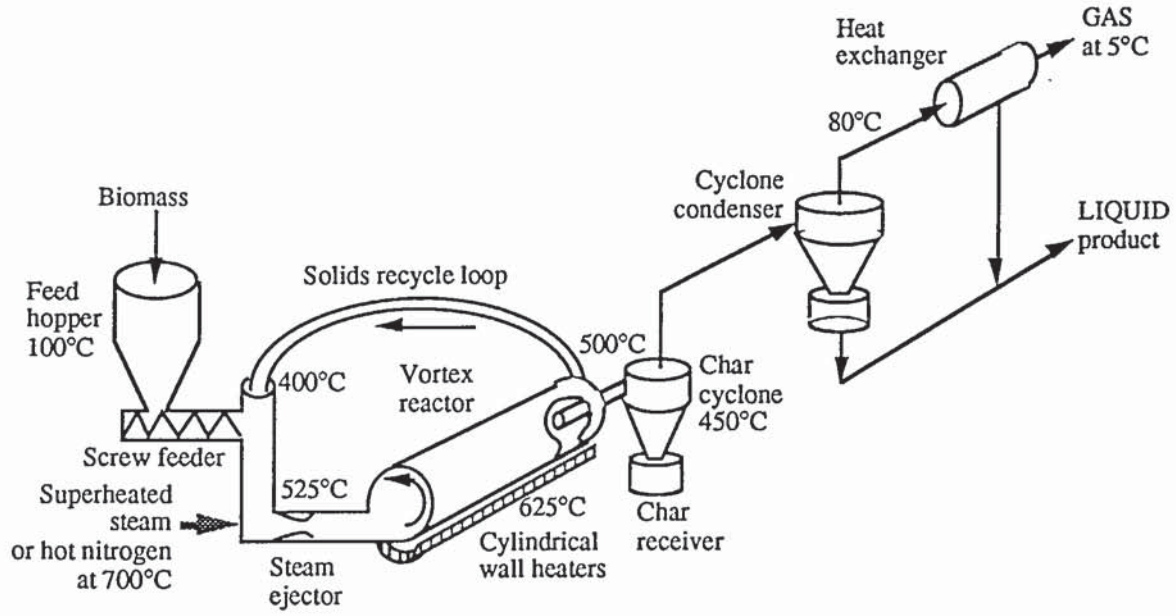

Figure 4.07. NREL [formerly SERI] ablative pyrolysis system (116)

4.6.3 Modifications to the original reactor design

To date, four different internal configurations have been used:

1. a smooth walled reactor with no recycle loop,
2. a smooth walled reactor with a gas recycle loop,

3. a ribbed walled reactor with no recycle loop,
4. a ribbed reactor with a solids recycle loop.

Cold flow studies confirmed that approximately only 20% of the available heat transfer surface in the smooth walled reactor was covered by wood chips in the first and second reactor configurations (252). A fabricated helix was placed inside the reactor to force the biomass to flow over the entire reactor heat transfer area. This was partially effective but a proportion of the biomass passed below the helix due to non-ideal sealing of the helix against the reactor wall. Diebold noted that at lower temperatures, [< 625°C], 30% of the feedstock remained partially pyrolysed on a once through basis despite the helix increasing the contact area of the wood particles with the reactor wall (250). In order to reduce the char yield, a solids recycle loop was added and a new reactor built with an integral helix having a pitch of 25 mm, width 6 mm and height 3 mm.

Installation of the solids recycle loop reduced, in conjunction with the ribbed reactor, the char yield to 7-10%, compared with the previous values of 30% at a wall temperature of 625°C. With the present ribbed reactor configuration, a 5 mm particle was calculated to be recycled 23 times to achieve a final thickness of 50 μm, at which point it would be entrained out of the reactor with the gas and vapour products. Assuming only ablative pyrolysis to be significant a particle would ideally be ablatively pyrolysed in 0.7 s (116). In practice, the particle pyrolysis time is much longer as the particle tangential velocity and thickness decrease along the length of the reactor to 100 m/s and then the particle is recycled (116). Unlike other entrained flow reactors, recycle of the partially pyrolysed biomass is not difficult and the solids residence time is decoupled from the gas/vapour product residence time. A proportion of the product vapours and gases must, however, be recycled. No values have been published for the ratio of recycle gas/vapour products to exit gas/vapour products. The recycle loop functions due to the steam or nitrogen entering the reactor via a venturi ejector which causes a suction effect on the recycle stream.

As part of the development work to investigate particle trajectory in the reactor, a cold flow replica of the smooth wall reactor was constructed. Diebold measured the particle velocity with high speed photograph measurements of 4000 fps in the cold flow model and observed that the particles lost their high initial tangential velocity of 120 m/s very rapidly to 12 m/s. Diebold concluded that, in the cold flow model, the particles were in a dry friction condition and hence would not slide smoothly on the wall. However, during ablative pyrolysis as the particles degrade, the liquid products act as a thin lubricating film upon which the particles slide. It has been confirmed by Lédé in his experiments that frictional resistance to motion is almost negligible (51). To test this, Diebold measured the exit velocity of the particles from his reactor

and determined the frictional coefficient of the particles in the reactor. The frictional forces on the particle can be estimated using equation {4.09} by Diebold:

$$F_f = \frac{\mu A_c u_r}{t_f} \qquad \{4.09\}$$

where F_f is the frictional force [N/m], μ is the pyrolysis liquid film viscosity [Ns/m^2], A_c is the particle contact area [m^2], u_r is the particle tangential velocity [m/s] and t_f is the pyrolysis liquid film thickness [m]. The liquid film thickness t_f [m] can be calculated by equation {4.10}, assuming total conversion to liquids:

$$t_f = \frac{\lambda_l (T_w - T_d)}{\rho_w C_p V (T_d - T_o)} \qquad \{4.10\}$$

where λ_l is the liquid film thermal conductivity [W/mK], T_w is the reactor wall temperature [K]. Diebold estimated the frictional forces using equation {4.09} to evaluate what would occur for individual particle pyrolysis in the vortex reactor. From calculated values of the frictional coefficients, it was determined that a single particle would rapidly slow down from its high initial velocity of over 400 m/s in the reactor to approximately 40 m/s, similar to cold flow model results if pyrolysed on a once through basis: this is because the pyrolysis liquid film produced would not be sufficient for particle "sliding" to occur. From Diebold's observations, the particles lost only a small proportion of their high initial velocity in the reactor, i.e. the particles were being lubricated during the ablation process. By constructing a mass balance based upon the ablation rate of an isolated particle, as shown in equation {4.10}, a film thickness 25 times thicker than that formed from the path of a single particle would be required for such a low drop in the particle velocity during actual operation, i.e. the particles are sliding on an accumulated liquid/vaporising film of pyrolysis products.

Diebold proposed that the pyrolysis liquid film may be composed of large oligomeric components which either cannot vaporise or can be degraded sufficiently to form lower molecular weight compounds which can vaporise more readily (51). The liquids formed which can rapidly vaporise are assumed to be carbohydrate derived [cellulose and hemi-cellulose] and have a "half-life" or volatilisation time of 836 and 15 ms at wall temperatures of 466°C and 625°C respectively. Kinetic constants for the volatilisation of cellulose derived liquids were presented in Section 4.2.3.4. Diebold suggested that the larger oligomeric components are lignin derived and are more thermally stable than carbohydrate-derived liquids; therefore, they require longer [more energy] to be thermally reduced to smaller molecules and/or vaporised from the surface. At temperatures greater than 625°C, it was noted that the liquids rapidly

degrade to produce a coke on the heated wall which reduces the heat transfer coefficient, increases the surface friction and consequently reduces the reactor throughput.

Estimation of the pyrolysis liquid viscosity at reactor temperatures is very difficult and no one has yet proposed a measured value for pyrolysis liquid. A value of 30 mPa s $\pm$ 20% has been used as an estimate as this is an average value for vaporising organic liquids, by Diebold and Power (116). Lédé proposed a value of 72.5 mPa s at 466°C, for an assumed liquid density of 500 kg/m^3 (234). The organic vapours are postulated to be formed from the liquid at the wall temperature rather than from the liquid formed at ~466°C assuming Lédé's fusion model is assumed to be correct [see Section 4.2]. The liquids are therefore in a good, "boiling mode," of evaporation. From discussions with Dr. Diebold, the ash is scraped or rubbed off by the biomass particles and entrained with the char out of the reactor (255).

4.6.4 Heat transfer in the vortex reactor

Diebold (254) and Reed (49) have reviewed methods for supplying heat to the metal reactor wall for ablative pyrolysis. Diebold considered several ways of improving the heat transfer, one of which was to condense sodium vapour on the outside of the reactor tube. This method of achieving high heat transfer rates was not implemented due to a potential problem of H_2 diffusion through stainless steel at high temperatures (256). Heat transfer is important as ablative pyrolysis systems typically have a fixed heat transfer area; therefore, the heat flux must be maximised to achieve high specific throughputs. For the vortex reactor, the specific throughput is estimated at 115 kg/m^{2}h for a wall temperature of 625°C, based upon a throughput of 36 kg/h. It should be noted that the specific capacity is dependent upon the reactor wall temperature, the biomass density and the ablation rate.

For the specific case of particle ablation in a centrifugal environment, as the particles decrease in mass and thickness, the ablation rate decreases as the centrifugal forces on the particle decrease; consequently, the contact pressure decreases, as determined by equation {4.11} (116):

$$p = \frac{F_r}{A_c} = \frac{t_p \rho_w u_r^2}{r} \qquad \{4.11\}$$

where F_r is the radial force on the particle [N], t_p is the particle thickness to the heat transfer surface [m] and r is the reactor radius [m]. Therefore as particle thickness decreases, the heat transfer coefficient and the reactor specific throughput decrease.

4.6.5 Results

Using the experimental set-up described in Section 4.6.2, the highest published total liquid yield is 67% [including moisture] or 55 % [dry oil/dry feed basis] based on direct measurement (116). The yields are comparable with those produced by fluid bed fast pyrolysis technologies [see Table 8.02]. The design throughput, however, has not been achieved: the maximum throughput achieved is 36 kg/h dry wood. Overall mass balances are given in Table 4.05. The liquid has a reported higher heating value of 22.3 MJ/kg (198, 257), comparable with other fast pyrolysis liquid which range from of 21.6-24.6 MJ/kg (258, 259, 260). Experiments have been carried out with thermal cracking of the vapour products, but the exact conditions of thermal cracking temperature and product yields and compositions are not given (109).

Table 4.05
Mass balances for the NREL vortex reactor [wt% dry feed basis]

Feedstock	Organic liquids	Char	Gases	Water	Reactor temp.(°C)	Residence time (s)	Reference
Aspen poplar	53.4	12.0	16.0	10.9	500	0.75	184
Aspen poplar	55.4	13.1	13.8	11.8	625	--	47

Detailed analysis by HPLC, ^{13}C NMR [Nuclear Magnetic Resonance] and elemental compositions have been compiled by McKinley (184). Selected elemental and chemical analysis for the liquids are given in Tables 4.06 and 4.07 below.

Table 4.06
Elemental analysis of NREL pyrolysis liquids [wt% dry basis]

Reactor temp. (°C)	C	H	O	N	C/H molar	Density [g/cm^3]	H_2O [wt%]	Ref.
450-500	48.6	7.2	44.2	<0.1	1.13	1.23	--	184
480-485	53.3	6.2	39.6	NK	1.38	1.28	16.1	91
500	57.3	6.1	34.9	1.3	1.27	1.22	17.0	184

Table 4.07

Chemical analysis of NREL pyrolysis liquids, [wt% chemical in biomass liquid] (184)

Chemical	Yield	Chemical	Yield
Acetol	4.08	Glycolic acid	0.54
2 furaldehyde	0.66	Formic acid	0.97
Furfuryl alcohol	0.10	Acetic acid	4.08
Phenol	0.73	Propionic acid	0.33
5-methyl furfural	0.06	Butyric acid	0.43
4-butyrolactone	0.26	Valeric acid	0.26
Methyl cyclopenten-l-one	0.44	Hexanoic acid	0.26
p-cresol	0.09	Heptanoic acid	0.03
m-cresol	0.04		
eugenol	0.13	Levoglucosan	1.99
2,6-dimethoxyphenol	0.66	Syringaldehyde	0.37

4.6.7 RDF Pyrolysis

RDF [Refuse Derived Fuel] has been used as a feedstock, after initial laboratory experiments by Levie and Diebold, to optimise the parameters for liquids production in a single particle reactor (261, 262). The use of RDF in the vortex reactor has been detailed by Scahill and Diebold with the product collection system modified as shown in Figure 4.08 (263).

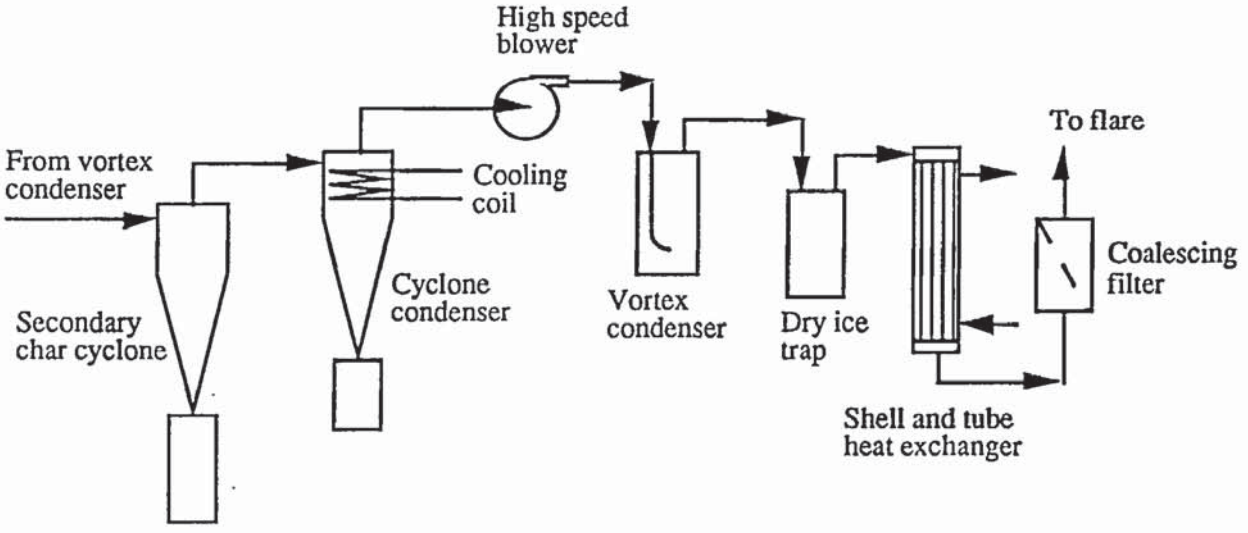

Figure 4.08. NREL RDF liquid collection system

Feed rates of 10.6 kg/h at a wall temperature of 625°C were attained. Blockages were encountered in the liquids collection system and substantial modifications were made to account for problems of highly viscous condensates and stable aerosols. RDF derived liquid was found to be 4 orders of magnitude more viscous than a wood derived pyrolysis liquid produced under similar conditions. The modifications included doubling the transfer line diameter after the first cyclone condenser to 5 cm, use of a high speed centrifugal blower to mechanically remove the aerosols in the vapour stream at 100°C after the second cyclone condenser and use of an additional cold trap to enhance collection as shown in Figure 4.08. The remainder of the condensation train consists of the vortex condenser with vapours exiting at 50°C, the dry ice trap at 10°C and the coalescing filter with products entering at -3°C. With RDF feed, the physical action of the vortex reactor segregates low density, friable char from higher density attrition resistant metals and debris. It has been observed in particular that aluminium flakes concentrate in the reactor and can be separated from the other inert metals.

Table 4.08
RDF derived pyrolysis products [wt% dry basis] (257, 263)

Run number	Char and Ash	Condensates	Gas	Closure, wt%	Losses
Run 104	17.2 (0.9)*	24.6	--	41.7	58.3
Run 105	14.6 (1.9)*	44.1	15.8	74.5	25.5
Run 107	18.6 (2.1)*	41.6	12.4	72.6	27.4

* tramp solids fraction in char/ash, wt% dry basis

The RDF pyrolysis vapours have also been catalytically upgraded over a commercial ZSM-5 catalyst [C-12] (264). To maintain high hydrocarbon yields, a secondary catalytic reactor is used for benzene alkylation to produce high octane compounds such as cumene. Yields of C_2+ hydrocarbons of 20.5% [wt % of RDF fed], 6.3 w% primary gasoline, 6.2% primary fuel oil and 3.4 % secondary gasoline are quoted. Product yields for RDF are given in Table 4.08.

Closures for RDF pyrolysis are poor due to the difficulty in recovering the product vapours and their removal from the product collection system. The actual liquid yield is anticipated to be greater than 50 wt%. The high losses noted using RDF would suggest that the product vapours have a much lower molecular weight than those of wood-derived liquids. This may be due to the presence of plastics and lacquers in the RDF which volatilise to alkenes [C_nH_{2n}].

4.6.8 Current status

Recent work has looked at the production of ethers for use as petrol additives using RDF as the primary feed (265). The product vapours from the vortex reactor are catalytically treated over HZSM-5 and then reacted with methanol or ethanol to produce ethers (266). This work is still ongoing. Commercial development of the NREL process by Interchem is discussed in Section 4.7. Due to commercial interests, little information is published on yields and process design.

4.7 Interchem Industries Inc., USA [formerly Pyrotech]

4.7.1 Background

Interchem Industries Inc. was founded in 1985. Initial work to scale up the ablative fast pyrolysis process was carried out by Pyrotech Corporation to solve an energy deficit problem at a pulp mill at Samoa, California, as detailed by Ayres based upon the ablative fast pyrolysis technology developed by NREL (267, 268). The company entered into agreement with Midwest Research Institute Ventures, a subsidiary of Midwest Research Institute, of which NREL is a division, and a consortium of Fortune 500 companies in 1989 to commercially develop the technology (269). The primary objective of the consortium is to develop and exploit the commercial potential of the NREL pyrolysis process to produce a phenol adhesive substitute and an alternative fuel. Interchem obtained a licence to construct a scaled up reactor based upon the NREL vortex reactor, although NREL were not involved with providing any technical expertise at this stage. Construction of the 32.7 t/d facility for the production of fuel oil and charcoal, referred to as a Petroleum Synthesis Unit [PSU] was completed in September 1990 with testing until January 1991 (270, 271).

4.7.2 Description: first generation Petroleum Synthesis Unit

The first plant was built in Missouri for the conversion of sawmill wastes and the flowsheet is depicted in Figure 4.09. The reactor wall is heated by the combustion of recycled non-condensible pyrolysis gases and the product vapours from the reactor are directly quenched in a 6 tray column, initially using diesel and then product liquids. The collected liquids are split: part is recycled to the quench column and the rest is transferred to a storage tank. The remaining gases and vapours are recycled to the reactor and part is combusted for process heat.

Figure 4.09. Interchem Petroleum Synthesis Process, Mountain View, Missouri [1990]

This first plant was closed down in late 1992 and decommissioned as operational and technical problems could not be solved using the existing equipment. The design capacity of 1360 kg/h was not achieved. The process had some operational difficulties which were (272):

- the furnace refractory for the vortex reactor had been damaged during initial transport,
- particle recycle problems,
- unreacted particle carryover into the product collection system,
- low particle velocities in the reactor leading to low throughputs,
- plugging of the plate heat exchanger in the product collection system,
- gas leaks from the reactor.

4.7.3 Results

The pretreatment and handling units have been retained and the product recovery system has been improved. Interchem have now relocated the wood handling equipment to Kansas City and are building the second reactor tube. Initial throughputs of only 90 kg/h were achieved due

to the problems noted earlier in this section. No quantitative results of the operation of the first plant have been published. Various modifications were then made to the process:

- the plate heat exchanger was replaced with a shell and tube exchanger to remove the blockage problems,
- rebuild the recycle loop was rebuilt in order to retain the particle kinetic energy and improve the process efficiency,
- the reactor exit cyclones were placed in series to improve particle collection efficiency,
- the furnace refractory was repaired to minimise leaks and improve heat transfer.

These modifications and repairs only increased the throughput to 180 kg/hr, 13.2 % of the design capacity. The reasons for the low throughput were then surmised to be due to construction problems detailed as:

- loss of particle velocity upon entering the reactor due to the initial 0.6 m of the reactor tube not being heated, i.e. the particles were experiencing dry friction and consequently lost a significant proportion of their velocity,
- insufficient recycle gas reheated in the condenser,
- the recycle loop was overloaded with unreacted particles.

4.7.4 Current status

The second reactor system based upon the operational experiences obtained with the first system have been accounted for in the second plant and is due for restart in late 1993 with the collaboration of NREL. The new process is shown in Figure 4.10 overleaf (272).

4.8 Other approaches to ablation

4.8.1 Frictional heating to produce pyrolysis vapours

Other work of interest which involves frictional heating of wood to produce wood vapours is in the field of wood smoking. In the 1950's patents were filed for the ablation of wood rods to produce a liquid smoke with heating achieved by friction (273, 274). The apparatus consisted of a grooved disc rotating at speeds of 1400 rpm and frictionally heating wooden posts. The vapours produced were washed with a water spray and used to smoke meats. This patent was then modified and reapplied for as the "Smoke Generator" (275). The process reached commercialisation, but the manufacture of wood post to the correct size and shape from hardwoods proved expensive and the process was then superseded by slow pyrolysis techniques for the production of food flavourings.

Figure 4.10. Second generation Interchem Petroleum Synthesis Process, Kansas [1993]

4.8.2 Ultrapyrolysis

Another approach in which ablation makes up a significant proportion of the overall heat transfer coefficient is in the Ultrapyrolysis work of the University of Western Ontario and its commercial development by Ensyn Engineering Associates. In their reactor, hot sand is impinged directly with a stream of solid particles and the jets are destroyed simultaneously to generate highly turbulent conditions during which the biomass particles are fast pyrolysed. The original intention of using high velocity sand was purely as the heat carrier to the biomass; however, the abrasion of the product char had the added effect of increasing the heat transfer rates. The work at the University of Western Ontario has been carried out at temperatures primarily above 650°C to produce gases (35, 38, 40, 42).

4.9 Requirements and features of ablative pyrolysis

The main requirements and features of ablative flash pyrolysis have been derived from the work of Diebold et al. [Section 4.6], and Lédé et al. [Section 4.2] and can be summarised as:

- high particle pressure on the heated surface [typically greater than 5 x 10^5 N/m^2 for appreciable ablation rates greater than 1 mm/s],
- high relative motion between the heated surface and the biomass particles [greater than 1.2 m/s as the ablation rate increases asymptotically to a maximum at a relative velocity of greater than 1.5 m/s] to maximise the heat transfer rate [from Lédé (51)],
- a reactor heated surface temperature not greater than 625°C [from Diebold (116)],
- relatively easy scale up.

The key requirements are depicted in Figure 4.11. Similarly, the key features relevant to such a design are:

- very high heating rates [greater than 1000 C°/s],
- little or no particle transport or carrier gas,
- short vapour product residence time [less than ~0.8 for chemicals and less than 2 s for liquids for fuel (Scott et al.(57, 59,72)].

It may also be preferable to perform the pyrolysis reactions under a slightly reduced pressure to remove pyrolysis products and reduce the extent of secondary reactions by allowing more controllability over the residence time of the vapours. As noted, the presence of a diluting gas reduces secondary degradation reactions in the gas phase. It is these requirements and features which have formed the basis for the reactor design as discussed in Chapter 5.

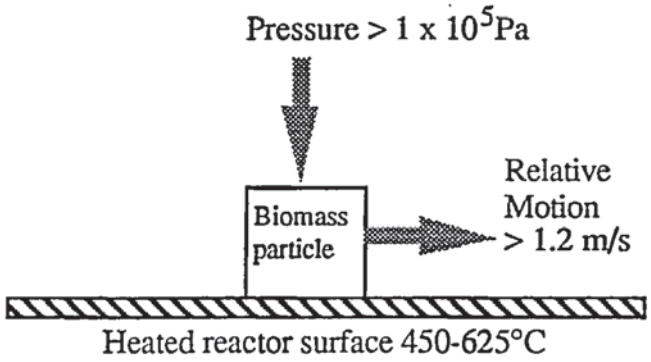

Figure 4.11. Principle of ablative pyrolysis

Ablative pyrolysis offers the possibility of having a compact reactor design with high heat transfer rates and high specific reactor throughputs. The key feature of ablation is that the products are rapidly removed from the reaction interface and this allows large biomass particles to be used compared to those used in conventional fluid bed processes.

Chapter 5. Ablative Pyrolysis Reactor Design

5.1 Introduction

In Chapter 4, the requirements and features of ablative fast pyrolysis were summarised. This chapter describes the design procedure for the ablative pyrolysis reactor that was subsequently built and operated as discussed in Chapters 6 and 7. The essential specifications for the design are [Chapter 2]:

- maximum reactor heated surface temperature, T_w [625°C]
- high particle pressure on the heated surface, p [as high as possible]
- high relative motion between biomass and the heated reactor surface, V_r [> 1.2 m/s]
- gas/vapour product residence times [less than 2 s]
- gas/vapour product temperatures [less than 500°C]

Modelling and reactor design related to the ablative fast pyrolysis process have been researched primarily by Lédé et al. (50, 51, 233, 234). Diebold et al. have specifically developed equations for the vortex reactor based upon discussions with Lédé et al. and which have been described in Chapter 4 (116). The design has been based primarily upon the work of Lédé et al..

5.2 Ablative fast pyrolysis reactor design summary

The result of the design is specification of the biomass contact area and heat transfer area for a given heated surface temperature, T_w; applied particle pressure p; and high relative velocity V_r. The procedure described below details the steps required in the design of a reactor for the optimal production of liquids. The starting point is with the specification of values for the following:

- velocity of the biomass relative to the heated surface, V_r [greater than 1.2 m/s]
- applied particle pressure, p [greater than 5×10^5 Pa]
- reactor heated surface temperature, T_w [typically between 450 and 625°C]
- the datum temperature, T_o [K] [assumed as 273 or 373 K]
- the pre-exponential factor, A [1.48×10^{10}s - see below]
- activation energy, E [112700 J/mole - see below]
- biomass specific heat capacity, thermal conductivity and density [typically 0.1 W/mK and 2800 kJ/kg, density by direct measurement]
- the heat of pyrolysis at the selected reactor temperature, ΔH_{pyr} [typically 40 kJ/kg]
- the required dry biomass throughput, B_r [kg/h]
- the biomass volume throughput, V_b [m^3/s]

The following parameters then need to be determined from either relationships from the literature such as by Lédé et al (50, 51, 234, 299) and Diebold (116, 198) or basic heat transfer relationships which are described and discussed in detail below:

- the ablation variable, $\hat{A}$ [m s/PaF] [calculated]
- the frequency factor, F [dependent on T_w]
- the ablation rate, V [empirical or calculated]
- heat transfer coefficient, h [W/m^2K] [calculated]
- the biomass decomposition temperature, T_d [K] [calculated or assumed]
- the heat flux density, Ø [W/m^2] [calculated]
- heat requirement to pyrolyse the biomass, Q_{pyr} [W] [calculated]
- the kinetics of biomass decomposition, κ, [s^{-1}] [calculated]

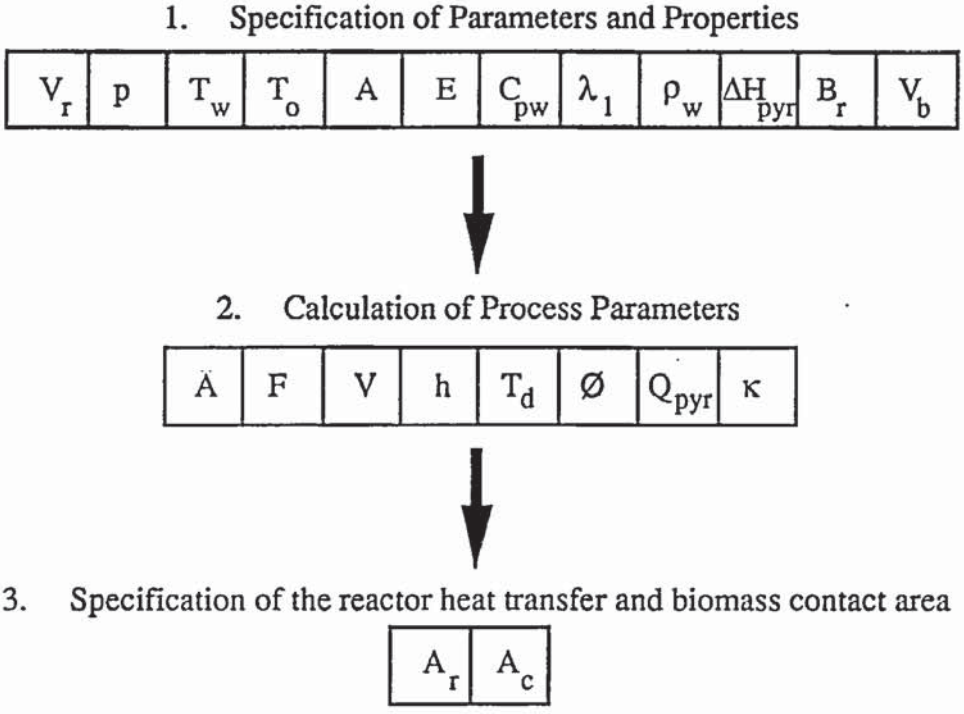

Figure 5.01. Design methodology for an ablative pyrolysis reactor

The required heated transfer area, A_r, is then determined by basic heat transfer relationships from:

- the calculated heat flux density Ø, [W/m^2],
- the heat requirement to pyrolyse the biomass, Q_{pyr} [W],

Finally the required biomass contact area, A_c is calculated from relationships by Lédé et al. [see Section 4.2] based on:

- the ablation rate V, [m/s],
- the required biomass volume throughput, V_b, [m^3/s],

The required heated transfer area A_r, must be greater than or equal to the required biomass contact area A_c to achieve the desired throughput. The results of the design procedure are a required biomass contact area and a required heat transfer area for a given biomass throughput. This is essentially a reactor specific capacity [kg/h/m^2], i.e., the mass of pyrolysing dry biomass per m^2 of available heat transfer area per hour. This should, therefore, be used as a major criterion in the evaluation of ablative pyrolysis reactors for similar reactor parameters and biomass properties.

The physical properties used for in the reactor design are summarised in Table 5.01, based upon data used by other researchers for experimental work on ablative pyrolysis. The sensitivity of the design procedure to variations in the process parameters and related properties is summarised in Section 5.5.

Table 5.01
Biomass physical properties (51, 121, 116, 198, 233)

Property	Symbol	Value
heat capacity	C_{pw}	2800 J/kg K
density	ρ_w	531 kg/m^3
thermal diffusivity	α_w	8.2 x 10^{-8} m^2/s
thermal conductivity	λ_w	0.1 W/mK

5.3 Reactor design

The purpose of the author's work as described in Chapter 1 was to design, construct and operate a novel ablative pyrolysis reactor for the production of liquids. The maximum design capacity for the reactor was specified as 5 kg/h; therefore, this formed the starting point for the reactor design at a maximum reactor heated surface temperature of 600°C.

5.3.1 The ablation variable Â [m/sPaF],

The ablation variable, Â, is a variable that was empirically derived by Lédé et al. (51) that is a function of temperature and provides an intermediate step in the calculation of V, the rate of ablation (see section 4.2.3). Lédé et al. determined values of Â for four different disk temperatures [873, 973, 1073 and 1173 K] by a logarithmic plot of V against p as previously

described [see Section 4.2.3.1]. In order to obtain values of Â in the operational temperature range selected, it was necessary to extrapolate known data. The values obtained by Lédé et al. are plotted in Figure 5.02 (233) with an additional value at a temperature at 823 K [550°C] from his direct measurement (233). The value of R^2 indicates the goodness of fit of the curve to the data, 1 being a perfect fit, 0 indicating no correlation. Figure 5.02 represents the best relationship that could be obtained and it is appreciated that at lower temperatures the potential errors increase. Â may be calculated by equation {5.01} for any temperature.

$$\hat{A}\ [m/sPaF] = 4.7317 \times 10^{-11} \times 10^{0.0020438\ T_w\ [K]} \qquad R^2 = 0.935 \qquad \{5.01\}$$

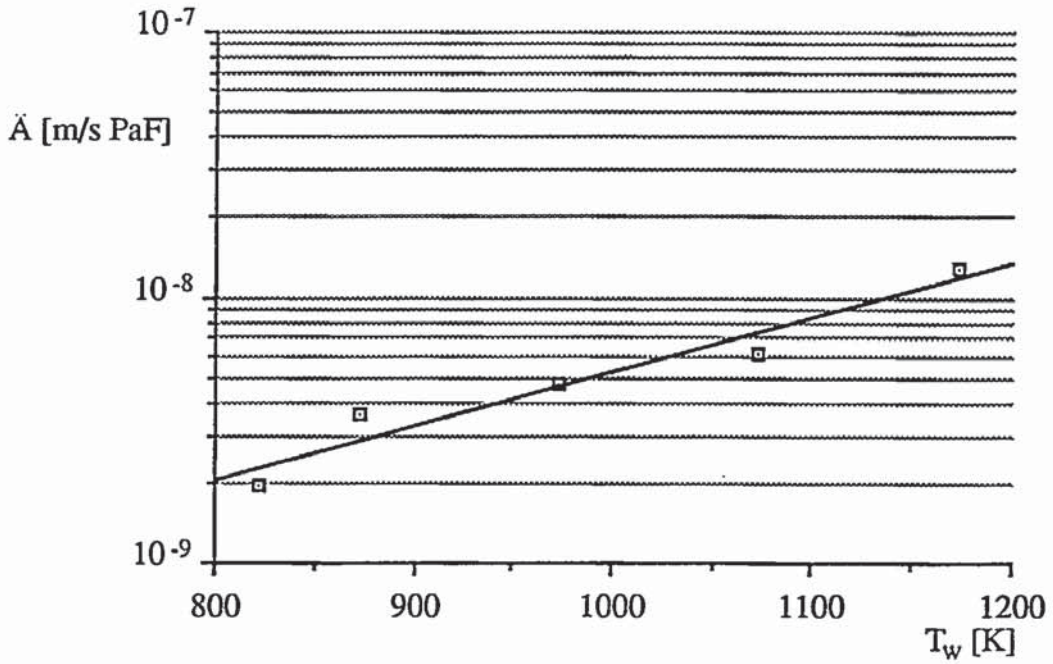

Figure 5.02. Variation of Â with reactor heated surface temperature, T_w

5.3.2 Frequency factor F

The frequency factor F is a variable that is dependent on the heated disk temperature and was derived in a similar way as Â by Lédé et al. from a logarithmic plot of V against p [see Section 4.2.3]. F varies from solid to solid as shown by experiments conducted on Rilsan, paraffin wax and ice and may be determined experimentally with temperature; Lédé et al. assumed F was constant and equal to about 1.0 for wood. No other independent evidence has been offered for its evaluation, until derived as part of this thesis [see Chapter 9]. The specificity of F for each compound has not been fully explained although Lédé also empirically determined F from equation {5.02} in an attempt to explain its meaning:

$$F = \frac{C_p\,(T_d - T_o)}{C_p\,(T_d - T_o) + \Delta H_{pyr}} \qquad \{5.02\}$$

where ΔH_{pyr} is the enthalpy of pyrolysis [J/kg] for wood. Lédé's values for F are given in Table 5.02 which shows that extrapolation to lower temperatures is not meaningful. A value of 0.993 was assumed in this design for the maximum reactor temperature of 600°C.

5.3.3 Estimation of ablation rate, V

Using the arbitrarily specified applied particle pressure, p, the calculated value of Â from equation {5.01} and the assumed value of F for a selected heated surface temperature, the rate of particle ablation, V, is calculated (51, 233, 116) under conditions of relative motion where V_r is greater than 1.2 m/s by equation {3} [see Section 4.2]:

$$V = (4.7317 \times 10^{-11} \times 10^{0.0020438\, T_w}) * p^{0.993} \qquad \{5.03\}$$

It may also be measured empirically, but this was not done for this design. However, new empirical values of V for 500°C were derived later in this work and are presented in Chapter 9.

Table 5.02
Variation of F with heated disk temperature

Heated disk temperature, K	873	973	1073	1173
F	0.993	0.997	1.010	0.982

5.3.4 Estimation of the heat transfer coefficient, h

The conductive heat transfer coefficient, h, is estimated from Lédé's work which showed that it could be related to the contact pressure, p; ablation rate, V; datum, wall and decomposition temperatures; and biomass thermal properties by equation {5.04}. This assumes that the liquid product is mechanically wiped away from the biomass-heated surface interface (51, 233):

$$h = \frac{\rho_w V\{C_p(T_d - T_o) + \Delta H_{pyr}\}}{(T_w - T_d)} \qquad \{5.04\}$$

Assuming that ΔH_{pyr} is negligible compared to the heat requirement to bring the biomass to its decomposition temperature, T_d; equation {4} may be reduced to equation {5.05}:

$$h = \frac{\rho_w V C_p (T_d - T_o)}{(T_w - T_d)} \qquad \{5.05\}$$

From equation {5.03}, where $V = \hat{A}p^F$, equation {5.05} becomes:

$$h = \frac{\rho_w \hat{A} P^F C_p (T_d - T_o)}{(T_w - T_d)} \qquad \{5.06\}$$

As $\hat{A}$ is a function of T_w, and as ρ_w, C_p and the temperatures are not functions of p, the heat transfer coefficient is a function of the applied pressure, as shown in equation {5.06}. Assuming that F = 1.0:

$$h = \Re p \qquad \{5.07\}$$

Lédé calculated a value for $\Re$ of 0.017 W/m^{2}KPa from a substitution of biomass density, biomass specific heat capacity and the datum temperature [720 kg/m^3, 2800 kJ/kgK and 373 K respectively] in equation {5.06} and using measures values of V with p. T_d was approximated as 739 K (51) [see Section 4.3.2.3 and 5.3.5]. From the experimental work he calculated $\Re$ to be 0.017 W/m^{2}KPa and F = 0.995 from a logarithmic plot of h against p. The value of $\Re$, therefore, varies from biomass to biomass and may be calculated using equation {5.06} for different solids.

5.3.5 Estimation of the biomass decomposition temperature, T_d

The biomass decomposition temperature is dependent on the heat transfer coefficient, the biomass physical and thermal properties and the reactor temperature and is calculated by equation {5.08} (233):

$$T_w = T_d + \frac{T_d - T_o}{h}\sqrt{(\kappa \lambda_w \rho_w C_p)} \qquad \{5.08\}$$

where κ is the assumed first order kinetic constant for the decomposition of wood calculated by equation {5.09} (233):

$$\kappa = A \exp\left(\frac{-E}{RT_d}\right) \qquad \{5.09\}$$

Values for A, the pre-exponential constant and E, the activation energy are presented in Table 3.01. The kinetic data used in this work are those of Thurner and Mann of $A = 1.48 \times 10^{10}$ and E = 112700 J/mole as these are one of the few sets of values derived for wood at the fast pyrolysis temperatures used in this research (89). The calculated heat transfer area, the biomass contact area and the related parameters are presented in Section 5.4.

5.3.6 Estimation of the heat flux, Ø

The heat flux, Ø [W/m^2], was calculated from equation {5.10} by Lédé et al. (51, 116):

$$Ø = h\,(T_w - T_d) = \rho_w \hat{A} p^F C_p (T_d - T_o) \qquad \{5.10\}$$

This is the heat flux across the reaction layer. However, it does not predict the overall heat flux from the reactor wall to the biomass. Equation {5.11} was, therefore, used for the estimation of the overall heat flux into the wood:

$$Ø = h\,(T_d - T_o) \qquad \{5.11\}$$

The value estimated by this method will not be an exact solution as the abrasion of the product char from the wood will give some intermediate temperature which cannot be evaluated at this stage. Ø should be greater than the heat required for pyrolysis over the contact heat transfer area as given in equation {5.12}.

$$Ø \geq \frac{Q_{pyr}}{A_r} \qquad \{5.12\}$$

The energy required for biomass pyrolysis, Q_{pyr}, is estimated from equation {5.13}.

$$Q_{pyr} = B_r(C_p(T_d - T_o) + \Delta H_{pyr}) \qquad \{5.13\}$$

where B_r is the required dry biomass throughput [kg/s]. The contact heat transfer area A_r should be greater than the biomass contact area to achieve the desired throughput where A_c is the contact area calculated from equation {5.14}, i.e. $A_r \geq A_c$.

$$A_c = \frac{V_b}{V} \qquad \{5.14\}$$

5.4 Application of design procedure

The above procedure was constructed as a spreadsheet so that the various parameters could be manipulated and their effects on the overall design evaluated in terms of the biomass throughput or the required heat transfer area. A printout of the spreadsheet used for the design as a base case is given as Table 5.03.

Table 5.03

Design of ablative pyrolysis reactor

Specification of properties		Symbol	Value	Units
Biomass data				
	specific heat capacity	Cpw	2800	J/kg
	biomass dry density	ρω	530	kg/m^3
	thermal conductivity	λ	0.1	W/mK
	thermal diffusivity	α	6.739E-08	m^2/s
Reactor Parameters				
	required throughput	Br	5	kg/h
	biomass volumetric throughput	Vb	2.621E-06	m^3/s
	reactor temperature	Tw	873	K
	datum temperature	To	298	K
	applied particle pressure	p	500000	N/m^2
	activation energy	E	112700	J/mole
	pre-exponential factor	A	1.48E+10	s-1
	heat of pyrolysis	ΔHpyr	40000	J/kg
Calculation of parameters				
	ablation variable	A	2.881E-09	m/sPaF
	frequency factor	F	0.993	
	ablation velocity	V	0.0013142	m/s
	heat transfer coefficient	h	8500	W/m^2K
	biomass "fusion" temperature	Td	710.2	K
	heat flux density	Ø	3.50	W/cm2
	decomposition kinetic constant	κ	76.099	s-1
	heat requirement for pyrolysis	Qpyr	1659	W
Calculation of the required heat transfer area				
	required heat transfer area	Ar	473	cm^2
Calculation of the required biomass contact area				
	calculated biomass contact area	Ac	20	cm^2
Requirement is that Ar > Ac				

From the spreadsheet, the interactions of the process parameters could be more easily assessed and the iteration of the heat transfer coefficient and the biomass decomposition temperature carried out. Using this design, there is flexibility in the specification of the required biomass contact area and the required heat transfer area. The one assumption which was made in the design was that the available contact area between the biomass and heated surface would be fully utilised with no apparent "voidage". At this stage, the effects of particle distribution in the reactor could not be determined or accounted for since the reactor configuration had not been specified. The most important factors affecting the design values were studied by carrying out a sensitivity study on the reactor throughput as described overleaf.

From the design procedure presented in Table 5.03, the variation of reactor throughput [kg/h] with the reactor temperature and the contact pressure, assuming that the contact area is fixed, was plotted as shown in Figure 5.03 below.

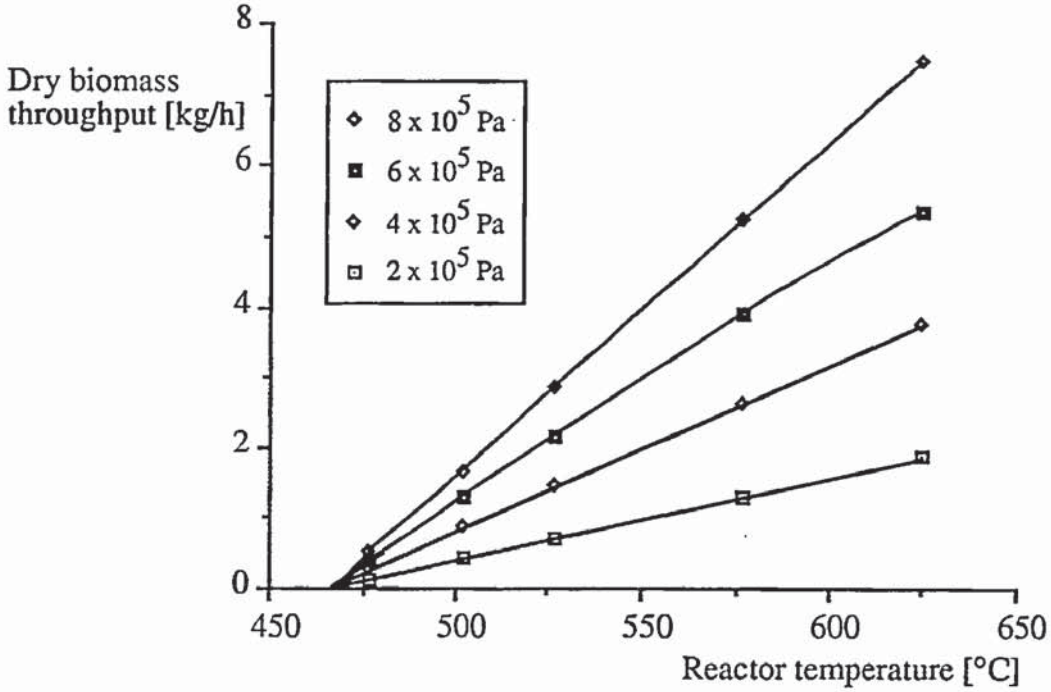

Figure 5.03. Variation of the theoretical reactor throughput with reactor temperature and contact pressure

Form this, the required throughput for a given temperature could be estimated. The results shown in Figure 5.03 were used during the initial commissioning experiments as discussed in Section 7.4.

5.5 Reactor design sensitivity

The design procedure presented in Section 5.3 can be used to assess the sensitivity of the required heat transfer surface for a required biomass throughput, to changes in the parameters. The parameters listed in Table 5.03 above were varied by ± 5% and ± 10% and the relative change in the biomass throughput noted. The standard case was for 5 kg/h of dry wood [maximum declared throughput], ρ_W = 530 kg/m^3, specific heat capacity = 2800 J/kg, thermal conductivity λ_W = 0.1 W/mK, reactor temperature T_W = 600°C, applied particle pressure p = 5 x 10^5 Pa, frequency factor F = 0.993. The results are shown in Table 5.04 below with the other variables upon which they are dependent. The reactor heat transfer area was fixed and it was assumed that the required heat flux could be achieved.

Table 5.04

Sensitivity of reactor throughput to parameter variations: base case value of throughput, 5 kg/h

Variation	-10%	- 5%	0	+ 5%	+10%	Dependent
Parameter			% variation in B_r			
F #	-72.8	-47.9	0	+ 91.9	+ 268.1	T_w, ΔH_{pyr}
F ± 2.5%		- 27.9	0	+ 38.6		
Â	-10.0	-5.0	0	+ 5.0	+ 10.0	T_w
V	-10.0	-5.0	0	+ 5.0	+ 10.0	p, Â, F
h	+ 8.9	+ 4.1	0	- 3.6	- 6.7	T_d, T_w, T_o, ρ_w, C_{pw}, λ_w, p
p	- 9.9	-5.0	0	- 5.0	-9.9	h, V
T_w	- 24.6	- 13.2	0	+ 15.1	+ 32.5	
T_o	+ 0.9	+ 0.5	0	- 0.5	- 0.9	
ρ_w	- 3.9	- 1.9	0	+ 1.9	+ 3.8	
λ_w	- 3.9	- 1.9	0	+ 1.9	+ 3.8	
C_{pw}	- 3.9	- 1.9	0	+ 1.9	+ 3.8	
A	- 3.9	- 1.9	0	+ 1.9	+ 3.8	
ΔH_{pyr}	0	0	0	0	0	T_w

10% variation in F most unlikely

The results show that the most significant influence is the frequency factor F and then the reactor temperature T_w; therefore, these should be carefully considered in the design of the reactor. The frequency factor F has a cumulative effect on the design and its specification is difficult for reactor temperatures below 600°C, since there are available. It is recommended that empirical data for V should be obtained for cases were the design is for reactor temperatures less than 600°C. New values for ablation rate variation with temperature and relative motion are presented in Chapter 9.

5.6 Summary of the reactor design procedure

The dominant design parameters to be calculated are the area for biomass contact and the area required for heat transfer which require specification of the following process parameters:

- ablation rate, V, [empirical or calculated]
- contact pressure, p, of the biomass on the heat transfer surface, [specified]
- biomass velocity relative to the hot reactor surface V_r, [specified]

- biomass decomposition temperature, T_d, [calculated]
- contact heat transfer coefficient, h, [calculated]
- reactor heated surface temperature T_w, [specified]
- required biomass throughput, B_r, [specified]
- required biomass volumetric throughput, V_b, [m^3/s] [calculated]

Starting with these and following the design procedure outlined above, the required biomass contact area and heat transfer area can be calculated. For the maximum design capacity of 5 kg/h at 600°C, the required heat transfer area was calculated to be 473 cm^2 and the required biomass contact area was calculated to be 20 cm^2. The actual construction of the reactor and the engineering aspects of its construction are discussed in Chapter 6.

In summary, the ablative pyrolysis reactor design was based upon the fundamental equations derived for wood rod ablation experiments. These equations were then modified and manipulated into the design procedure presented. It is acknowledged that there may be errors in the prediction of V at temperatures below 600°C, due to a lack of empirical data to confirm extrapolations to lower reactor temperatures and for biomass of different density and properties.

Chapter 6. Reactor Dimensions

6.1 Introduction

Chapter 5 presented the theoretical design and specified the process parameters of an ablative pyrolysis reactor for a maximum throughput of 5 kg/h of dry wood. The engineering design is summarised in this chapter which is structured as:

- review of approaches to biomass ablation [Section 6.2]
- generation of a new ablative pyrolysis reactor concept [Section 6.3]
- the rotating blade concept [Section 6.4]
- estimation of the gas/vapour product residence time [Section 6.5]
- specification of the reactor dimensions [Section 6.6]

6.2 Approaches to biomass ablation

Given the key requirements of ablative pyrolysis, five approaches to ablative pyrolysis have been used by other researchers which are described in Chapter 4. The principles are depicted in Figure 6.01 overleaf and were described in Chapter 4.

High relative motion has been achieved by:

- moving the biomass relative to a fixed heated surface either mechanically [e.g. Colorado School of Mines] or hydrodynamically [e.g. NREL, BBC Engineering],
- moving the heated solid relative to the fixed biomass mechanically [e.g. University of Nancy] or hydrodynamically [none tried or known],
- moving the heated solid and the biomass relative to each other mechanically [e.g. Colorado School of Mines] or hydrodynamically [University of Western Ontario and University of Twente].

The high contact pressure between the biomass particles and the heated solid may be achieved by mechanical [P_m] or pneumatic [hydrodynamic, P_{ce}] pressure. Both methods have been used:

- mechanical pressure [Colorado School of Mines and University of Nancy],
- pneumatic pressure [University of Twente, NREL, BBC Engineering and the University of Western Ontario].

The University of Western Ontario is mentioned as ablation is a key component of the heat transfer and reaction mechanism used in its systemalthough this was not an express objective of the technology developed. The reader is referred to the literature for further details (35, 41, 42). This approach is also used in the reactor system of Ensyn Technologies (276).

1. NREL, University of Twente and BBC Engineering

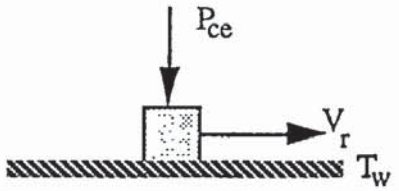

2. CNRS, University of Nancy

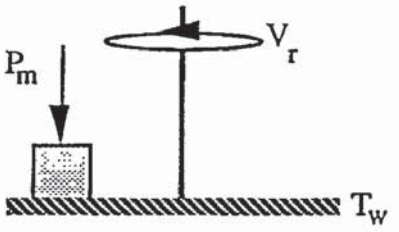

3. Colorado School of Mines v1

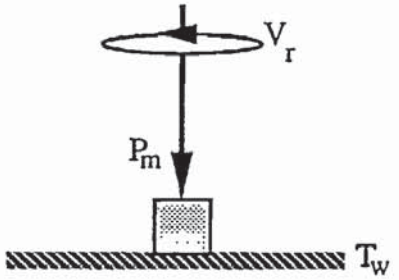

4. Colorado School of Mines v2

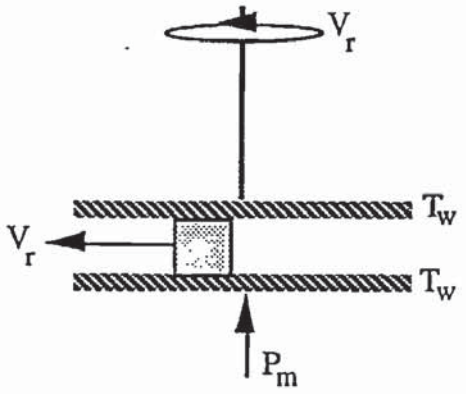

5. University of Western Ontario

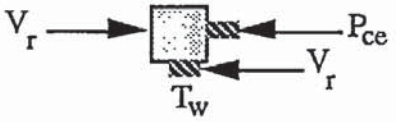

Figure 6.01. Biomass ablation approaches

6.3 Generation of new ablative pyrolysis reactor concept

In order to generate new, potentially usable ablative pyrolysis concepts, practical design criteria were summarised in addition to the key ablation requirements [see Chapters 2 and 4]. Some of the practical criteria considered were derived from the literature and from discussions with other researchers in the field. It can be seen from the approaches used that the reactor heat transfer surface must vary between a flat plate [Colorado School of Mines, University of Nancy] through an inclined surface [University of Twente] to a cylinder [NREL, BBC Engineering]. The design criteria are:

Key requirements of ablation

- high relative motion between biomass and hot surface to remove the reaction products and abrade off the product char layer to maximise heat transfer,
- high pressure between biomass and hot surface to increase the rate of pyrolysis.

Practical and general fast pyrolysis considerations

- ability to process a range of biomass particle sizes to reduce pretreatment steps such as size reduction, screening and re-chipping,
- ease of scale-up of the ablation concept,
- fixed reactor heated surface for good temperature control and high energy fluxes,
- no pneumatic biomass transport into the system or heat transfer gas,
- rapid removal of the product char and vapours from the reaction zone to minimise secondary reactions,
- reduce gas/vapour product temperatures to less than 500°C as quickly as possible to minimise secondary reactions,
- control gas/vapour phase residence time with the aid of a diluting gas, e.g. nitrogen, recycled non-condensable gas or combustion products, or by the use of partial vacuum.

With these criteria in mind, a horizontal rotating blade reactor concept evolved as described below. Various other configurations and cocepts were generated, although they were not believed to have the range of advantages which the concepts presented overleaf have.

6.4 Rotating blade concept

6.4.1 Selection of the rotating blade concept

Based upon the work of Reed and Cowdrey (107, 236) and Lédé et al. (51), a modified or hybrid concept was derived to overcome some of the operational difficulties arising from their approaches. The concept derived uses a fixed heated surface and uses a second non heated rotating surface to press the biomass particles onto the heated surface, generating the applied pressure. There are two approaches which fit into this category:

1. a rotating blade to generate a mechanical pressure on a horizontal surface [depicted in Figure 6.02]. In this approach, the resistance to motion of the particles on the heated surface causes the blades to exert a mechanical force on the particles leading to rapid ablation. As the particles ablate and are reduced in size, they move towards the back of the blade and are finally reduced to fine char, in theory dependent on the blade clearance from the reactor surface. The rotating blade approach utilises the available heat transfer area by continuously sweeping the particles across all of the metal surface and allowing a wide range of particle sizes to be simultaneously ablated.
2. generation of a centrifugal force on a vertical surface [depicted in Figure 6.03]. This approach generates a centrifugal pressure by "skimming" the particles over a heated surface as shown in Figure 6.03.

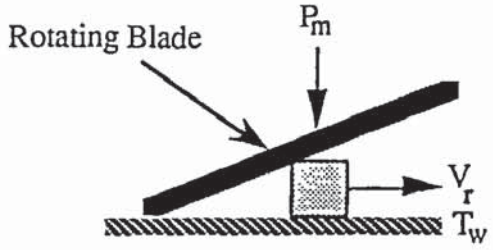

Figure 6.02. Rotating blade concept to generate a mechanical pressure [side view]

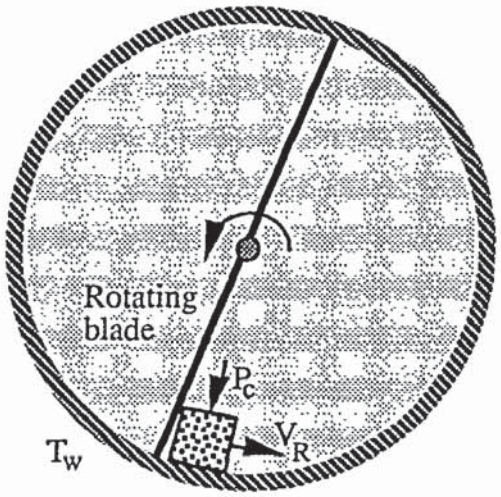

Figure 6.03. Rotating blade concept to generate a centrifugal pressure [top view]

The horizontal rotating blade concept was selected in the belief that it met all the criteria listed above. The following design features were considered and are discussed below after carrying out a series of cold flow experiments to determine basic solids handling properties:

- blade clearance from the heated reactor surface to control final char particle size,
- control of the gas/vapour product residence time and temperature,
- orientation of the heated surface and hence the rotating blades,
- removal of ablative char and ash from the heated surface,
- particle dynamics in the reactor with the reference to char removal.

It was considered that char handling and removal from the reactor would present the most significant problem if pneumatic solids transport was not used. The theoretical design procedure assumed that the available contact area below the blades would be fully utilised and that there would be no "voidage". This aspect will be assessed further in Chapter 9.

6.4.2 Cold flow experiments

To assess blade size, shape and number, a small cold flow rig was constructed. This allowed an empirical assessment of the effects of blade number, angle and rotational speed on the

behaviour of the particles. Up to four blades 5 cm long and of variable angle relative to a horizontal metal surface could be positioned radially from a drive shaft and rotated above the metal plate. A series of experiments were carried out to examine these operational parameters.

The small test rig used is shown in Figure 6.04. The flat horizontal surface had an internal diameter of 150 mm with a variable speed drive motor on the shaft. One or two blades could be mounted each 50 mm in width and 30 mm deep on pivoting holders so that various blade angles could be used with the blade edge scraping the metal surface. The blade angle to the metal surface could be varied to assess the behaviour of the particles at different angles, rotational speeds and with or without a lubricating oil film.

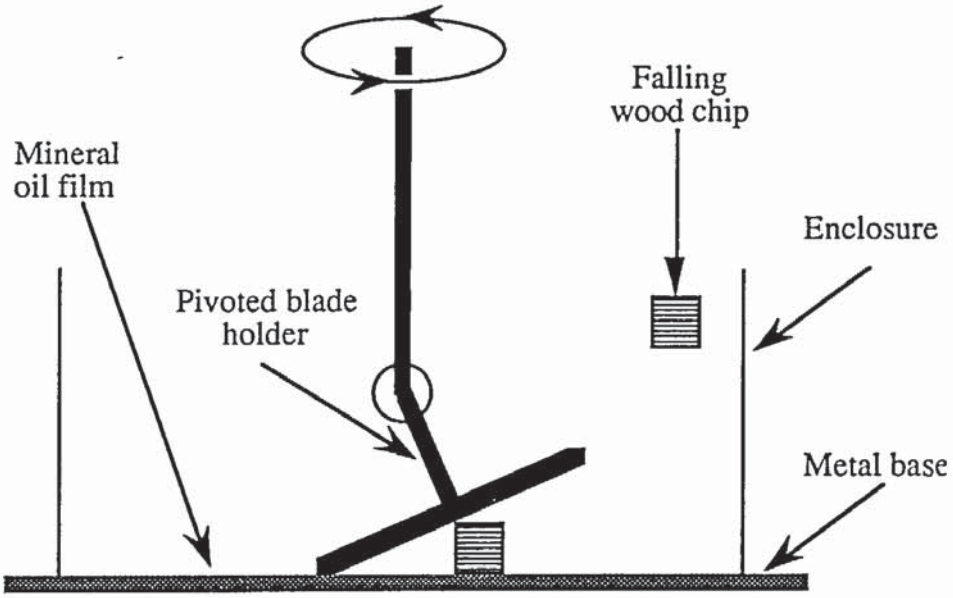

Figure 6.04. Small cold flow test rig used to study particle motion

6.4.2.1 Effect of number of blades

The purpose of this study was to assess if multiple blades would be more beneficial than one large blade. To this end, one or two blades were used and the effects studied. With one blade, when several particles were added, the blade would tilt laterally and scrape the metal base plate. At high rotational speeds [above 2 rps] and when two blades were used, as the particles fell into the blade area, the blades would "bat" approximately 50% of the particles outwards against the enclosure wall, before falling uniformly and randomly below the blades. The tilting with two blades tended to be smoothed out as the distribution of particles became more uniform.

The results from these experiments demonstrated that regularly spaced blades would be highly beneficial in giving uniform particle distribution, maximising the available heat transfer area for the particles on the surface and minimising the effects of voidage due to uneven particle packing below the blades. For the final design, four blades were specified in order to study the effect of thenumber of blades and tilting effects. More blades could not be used due to space and manoeuvrability limitations.

6.4.2.2 Effect of blade angle

Blades angles up to 60° relative to the metal surface were studied to assess the generation of pressure on the biomass particles and also particle motion below the blades. At blade angles greater than 30° relative to the metal surface, the particles were simply pushed around with no resistance to motion and therefore no contact pressure. At angles of less than 20°, the blades tended to rise up over the biomass particles suggesting that there was resistance to lateral motion and hence a contact pressure was being generated on the particles. This was due to dry friction caused by the downward force of the rotating blades pressing the lubricating oil film out from below the wood particle, therefby increasing the contact pressure. The main conclusion was that low blade angles which move the particles and generate high mechanical pressure should be used. For the purpose of this work the blade angle was fixed at 10° relative to the heated surface to allow particles up to 6.35 mm to be used as this was the maximum particle size which could be handled in the screw feeder.

6.4.2.3 Effect of blade rotational speed

The purpose of studying the blade rotational speed was to assess if the particles would be moved laterally along the blades by centripetal forces. There was also the key requirement of high relative motion as it had been demonstrated that high relative velocities greater than 1.2 m/s maximised ablation rates [see Section 4.2].

At low rotational speeds of less than 20 rpm and blade angles above 20°, the blades only pushed the particles around on the surface. This was due to the oil film not being displaced and the particles sliding with or without the mineral oil film. When the blades were rotated at any speeds and at any angle up to around 60°, the biomass particles remained in their original position below the blades and did not slide outwards along the blade. The blades did, however, tend to rise up over the particles after a few minutes, once the mineral oil had been displaced to the side. A study of the mechanics of the particle motion due to centripetal forces suggested that the particles would not move out along the rotating blades due to contact pressure generated by a low blade angle. The results of this study were that the blades could be rotated at relative velocities of up to 2.5 m/s without any problems.

6.4.2.4 Effects of blade orientation

To avoid the use of a particle transport gas, i.e. to remove product char from the reactor, it was decided to investigate the possibility of mechanically transporting the char from the reactor using the blades and at the same time ablate the biomass particles. The action of char removal would therefore have to be selective such that non-reacted wood would remain in the reactor. From practical considerations, removal of the char from one point is to be preferred. It was decided to investigate the possibility of mechanical char transport from the reactor by positioning the blades asymmetrically to the normal axis of rotation on the drive shaft. To study this during the operation of the reactor, the blades were positioned such that their front edge lay on the normal rotational axis. From simple cold flow experiments, indication were that this would lead to some transport of char towards the axis of rotation, i.e. towards the centre of the reactor. The reactor outlet was, therefore, positioned below the blade holder near the centre of the reactor.

6.4.2.5 Effect of blade clearance

If the rotating blades are allowed to scrape the heated metal surface there may be excessive blade and surface wear with blade "tilting" contributing to this. This problem must be offset against the specification that the final char size will be determined by the blade clearance from the heated reactor surface. To reduce the problem of tilting, there are several possible solutions:

- have several feed entry points to smooth out the effects of a large number of particles entering the reactor - high rotational speeds would aid this,
- have a suitable enough blade clearance from the heated reactor surface,
- multiple blades to "smooth" out possible tilting effects,
- design the blades, holder and drive shaft to minimise deformation,
- have a fixed blade angle to reduce the possibility of distortion.

It was concluded that the blade holder, fitted to a 25 mm diameter shaft, should have a capacity for up to four blades mounted on adjustable holders to vary the blade angle and clearance relative to the reactor surface and during operation. Only one inclined biomass feed point would be used to randomly distribute the particles across the full width of the blades. The determination of the optimal blade clearance and its effect on the final ablative char particle size would be determined experimentally. The blades would be locked in position using locking nuts in the blade holder. To calculate the pressure generated by the rotating blades on the particles, single particle experiments would be carried out. The results of these measurements are discussed in Chapter 9.

6.4.3 Particle dynamics

An estimate of the particle motion during ablation is necessary to determine an effective blade depth - the distance from the front edge of the blade where the biomass particle initially enters to the back edge where the char exits - to ensure complete ablation of the particle to a fine product char. There are two possible particle ablation processes which can occur during operation of the reactor:

1 as the particles pyrolyse, they remain in their original radial position below the blade and gradually move to the back edge until they are totally consumed. Other biomass particles continually enter below the blades as soon as the particle begins to move backwards, i.e. a dynamic replacement of reacted particles,

2 the particles move to the back of the blade as above but no other particles enter the same position under the blade until the previous particle has been pyrolysed.

These effects controls the "voidage" below the rotating blades and hence the reactor specific capacity. The former can be encouraged to dominate by overfeeding but this can reduce fast pyrolysis at the expense of carbonisation of the feed. The available reaction area under the blades can be estimated by assuming that the particle enters at the front of the blade, begins ablation and then gradually moves backwards. Using the design values from Table 5.03, the particle ablation rate for an applied particle pressure of 5×10^5 Pa at 600°C would be 1.31 mm/s. A 5 mm particle would therefore take 3.8 s to completely ablate. Assuming that another particle does not enter the same position until the first particle is ablated [process 2 above] and that a maximum blade angle of 10° is to be used, then the blade width should be a minimum of 28 mm to accommodate the reduction in particle height during ablation for an assumed final char size of 0.5 mm. The blade depth was specified as 35 mm to allow a variety of blade clearances and angles to be studied.

The other consideration was to mechanically transport char from the reactor by the rotational action of the blades. This could be done in two ways: either allow the char to be carried outwards towards the edge of the blades by new particles mechanically displacing the char or orientate the blades such that the char would be transported towards a central collection point for a horizontal heated circular base. The efficiency of mechanical char transport was be monitored during the initial commissioning experiments: the success of which is discussed in Chapter 7.

6.4.4 Variation of ablation rate with radial distance along the rotating blades

Since ablation rate varies with relative velocity, temperature and applied pressure for which there is very limited data at temperatures below 600°C, there will be some degree of error in

the final design specifications which cannot be quantified at this stage in the work. Lédé demonstrated that above 600°C, wood rod ablation rates reached an asymptotic value at relative velocities above 1.2-1.3 m/s, depending upon the exact temperature used (51). Using his empirical data, the variation of wood rod ablation rate with the relative velocity was plotted in Figure 6.05 for a reactor temperature of 600°C and an applied pressure of 5 x 10^5 Pa.

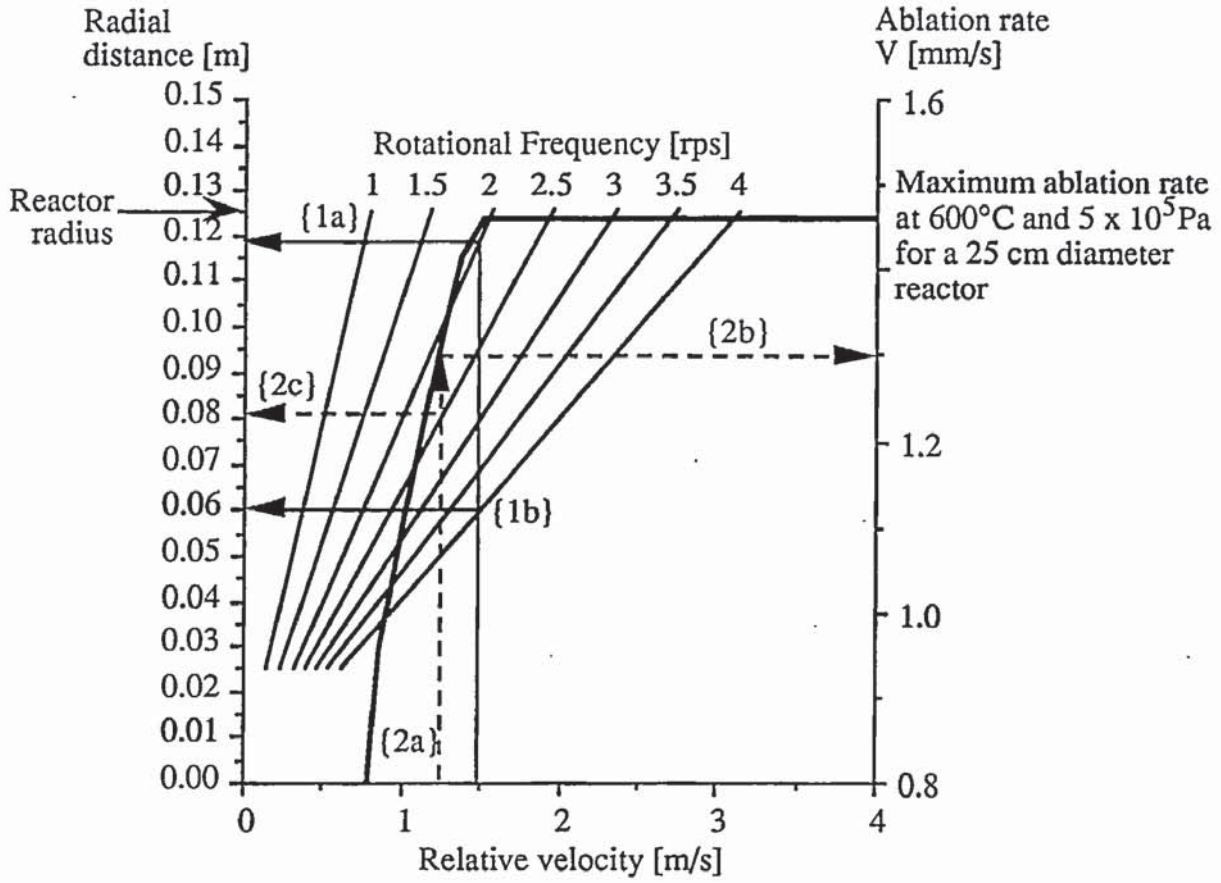

Figure 6.05. Variation of ablation rate with relative velocity, rotational speed and radial distance

Figure 6.05 shows that the maximum ablation rate increases to a maximum of 1.45 mm/s for a relative velocity of 1.5 m/s. The axis of the left shows the radial distance from the centre of the reactor and for various rotational frequencies, the relative velocity with radial position can be measured. As an example, indicated by line {1a} for a rotational speed of 2 rps, the maximum ablation rate is achieved at 0.117 m from the centre of the drive shaft and for 4 rps, line {1b}, the maximum ablation rate is achieved 0.06 m from the drive shaft. For relative velocities less than 1.5 m/s, as given for example by line {2a} at 1.25 m/s, the ablation rate can be measured for a given rotational freuqency, i.e. for 2.5 rps, the ablation rate is 1.3 mm/s, as indicated by line {2b}, and occurs at 0.08 m from the centre of the drive shaft, as indicated by line {2c}. To maximise the capacity of the reactor, the rotational speed and

contact pressure should be as high as possible. To avoid operation in the regime of reduced ablation rates for low rotational speeds, the diameter of the reactor could be increased.

6.5 Estimation of the gas/vapour product residence time

The gas/vapour product residence time has been defined in Section 2.5.2 as the ratio of net empty reactor volume [m^3] to the pyrolysis vapour/gas product formation rate plus the carrier gas/diluting gas volume [m^3/s], at the reactor gas/vapour phase temperature. The importance of the gas/vapour product residence time is that it influences the liquid yields and composition in conjunction with the temperature as previously discussed [see Section 2.5.2]. From a review of fast pyrolysis processes, most researchers do not describe their methods for calculating the residence time, neither what they consider to be the "reactor" operational volume, nor the assumed average molecular weight of the product vapours. This leads to comparisons between residence times which may not have been calculated on the same basis, leading to incorrect conclusions or wrong assessments of results.

In fluidised bed and entrained flow reactors, a first approximation is to use the heat transfer/fluidising gas at the reactor temperature to determine the apparent residence time, e.g. the University of Waterloo estimate the gas/vapour products to comprise only 10-15% of the total gas and vapour volume exiting the reactor (106, 277). Similar approaches are made by NREL (252) and the University of Western Ontario (39).

The volume of the pyrolysis products should therefore be taken into account to reduce errors in gas/vapour product residence calculations. For the reactor design, the condensible pyrolysis products have an assumed average molecular weight of 100, noted by Reed as a reasonable average (49). The gas densities may be calculated from equation {6.01}:

$$\rho_n = \frac{M_n P}{RT} \qquad \{6.01\}$$

where M_n is the molecular weight of the species [kg/mole], P is the reactor pressure [N/m^2], R is the gas constant [J/molK] and T is the reactor gas/vapour phase temperature [K]. The gas yields are then used in conjunction with the detailed compositions and the gas/vapour phase temperature to calculate the volume of products exiting the reactor per second. One problem is that as the pyrolysis of the biomass particle continues, the gas/vapour products continue to react and thermally degrade in the vapour phase (278, 279, 75, 205). This has been taken into account in the work of Graham, who included in his estimation of the residence time the linear decomposition of the primary vapours from a molecular weight of 100 to 24 over the reactor length (39). To determine the precise residence time of the

products would require a detailed molecular weight distribution of the pyrolysis products with time and temperature. To date, no such study has been performed and it is beyond the scope of this thesis. For the purpose of estimating the gas/vapour product residence time in this work, a spreadsheet was constructed to calculate the residence times for a different gas/vapour temperatures and different degrees of dilution with nitrogen. The basis of the spreadsheet was:

- mass balance data based upon the results of Diebold et al. for fast pyrolysis at 500°C [see Chapter 4],
- a gas/vapour product temperature assumed to be the same as the reactor temperature,
- an assumed volume of 0.00018 m^3 for the reactor internals comprising the rotating blades, the blade holder and the drive shaft,
- liquid pyrolysis products have an average molecular weight of 100 Da and obey the Ideal Gas law [equation 6.01],
- all non-condensible gas products behave ideally at atmospheric pressure,
- diluting nitrogen is added to the reactor at the same temperature as the heated surface,
- a maximum dry biomass feedrate of 5 kg/h.

When using the spreadsheet, the following procedures are carried out:

1 the reactor diameter for a required biomass throughput of 5 kg/h is entered,
2 the assumed volume for the reactor internals is entered,
3. the net reactor operational volume is calculated using an assumed reactor internal height and the cross sectional area of the reactor,
4. the reactor temperature is specified and the gas/vapour products are assumed to be formed/volatilised at the reactor temperature,
5. the reactor gas phase pressure is specified,
6. the experimental run time is set,
7. typical mass balance data for the reactor temperature are entered and the mass yields of product for the experimental run time are calculated,
8. the quantity of nitrogen product diluent is specified and its volume at the reactor temperature is calculated,
9. the rate of formation of gases and vapour products is calculated based upon the molecular weights and the ideal gas law at the reactor pressure,
10. the gas/vapour product residence time is calculated from the rate of formation of gas and vapour products and the addition of diluting nitrogen and the reactor operational volume.

The estimate for the reactor internal height was 65 mm and a sample printout of the spreadsheet is shown in Table 6.01.

Table 6.01

Sample printout of the gas/vapour product residence time spreadsheet

Calculation of Gas/vapour product residence time and Reactor Volume					
Reactor Specifications					
Reactor diameter:	0.25	m			
Reactor cross sectional area:	0.04909	m^2			
Reactor height:	0.065	m			
Empty reactor volume:	0.00319	m^3			
Estimated internals volume:	0.00018	m^3			
Operational volume:	0.00301	m^3			
Reactor parameters					
Datum temperature:	293	K			
Reactor temperature:	873	K			
Reactor pressure	101325	Pa abs.			
Gas/vapour outlet temp:	873.0	K			
Gas/vapour residence time:	**0.930**	s			
Experimental run time:	60	mins			
Biomass feedrate and Yields					
Feed	Wet	Dry	H2O	Ash	Total
	Wood	wood	0.100	0.005	1.105
Wood as fed to reactor (kg):	5.5	5	0.500	0.026	5.526
Products	Char	Organic	Water	Gases	Closure
		liquids			
% yields, wt% dry basis:	15	54	15	16	100
Mass yields, kg [wt% d.b.]	0.75	2.7	0.75	0.8	
Purging Nitrogen to Control Residence Time					
volume added per minute:	30	l/min			
density at datum temperature	1.1646	kg/m^3			
mass per minute:	0.035	kg			
density @ reactor gas/vapour temp.:	0.39087	kg/m^3			
volume at reactor temperature:	5363	l/hour			
Calculation of gas and vapour properties					
	H2	**CO**	**CO2**	**CH4**	**C2H4**
yield, wt%	0.10	5.34	4.78	0.41	0.19
mass yield, wt%	0.01	0.27	0.24	0.02	0.01
density at reactor outlet temp.	0.03	0.39	0.61	0.22	0.39
volume ex. reactor, l	179	683	389	92	24
	C2H6	**C3+**	**C4+**	**H2O**	**Organics**
yield, wt%	0.04	0.01	0.01	15	54
mass yield, wt%	0.00	0.00	0.00	0.75	2.7
density at reactor outlet temp.	0.42	0.59	0.78	0.25	1.40
volume ex. reactor, l	5	1	1	2985	1934
total gas/vapour volume from reactor	11656	l			

6.6 Specification of the reactor diameter and blade dimensions

The equipment parts for the reactor - the reactor shell and heated base, the reactor lid and sightglasses and the rotating blade dimensions used to achieve particle ablation - are described below. During the course of the practical work, various changes were made to the reactor and peripheral equipment to improve reactor operability. The original reactor specification is given in this chapter and subsequent modifications are described in Chapter 7. In the equipment described, all parts were made of 316L stainless steel unless otherwise stated. The detailed reactor and peripheral equipment are described below.

6.6.1 Reactor shell and heated base

The ablative pyrolysis reactor has an internal diameter of 258 mm with an internal height from the heated base to the interior of the reactor lid of 65 mm. The reactor cross section is shown in Figure 6.06 overleaf. The outlet from the base of the reactor is a 28 mm diameter threaded hole for a 15 mm internal diameter fitting The reactor flange and bolting dimensions are given in Figures 6.06 and 6.07.

There is a side inlet point for the addition of nitrogen at the reactor surface level to act as a thermal quenching medium and for the possibility of entraining fine char particles towards the reactor exit point. The top view of the open reactor is shown in Figure 6.07 with the reactor outlet hole. The external reactor wall is heated with a band knuckle heater rated to 2.25 kW at 450°C to minimise the deposition of product vapours on the wall during an experiment. The reactor base is heated with 14 x 400 W compact cartridge heaters as shown in Figure 6.07.

The cartridge heaters generate a heat flux of 11.4 W/cm^2 at 600°C. The temperature of each heater can be measured with an integral type K thermocouple. Two of the thermocouples are used in conjunction with the reactor heated surface temperature controller: one as the set point control thermocouple and the other as an overload to prevent the maximum operational temperature of the heaters being exceeded. Four other type K thermocouples are used to check the reactor temperature profile during reactor operation to ensure that the surface is uniformly heated.

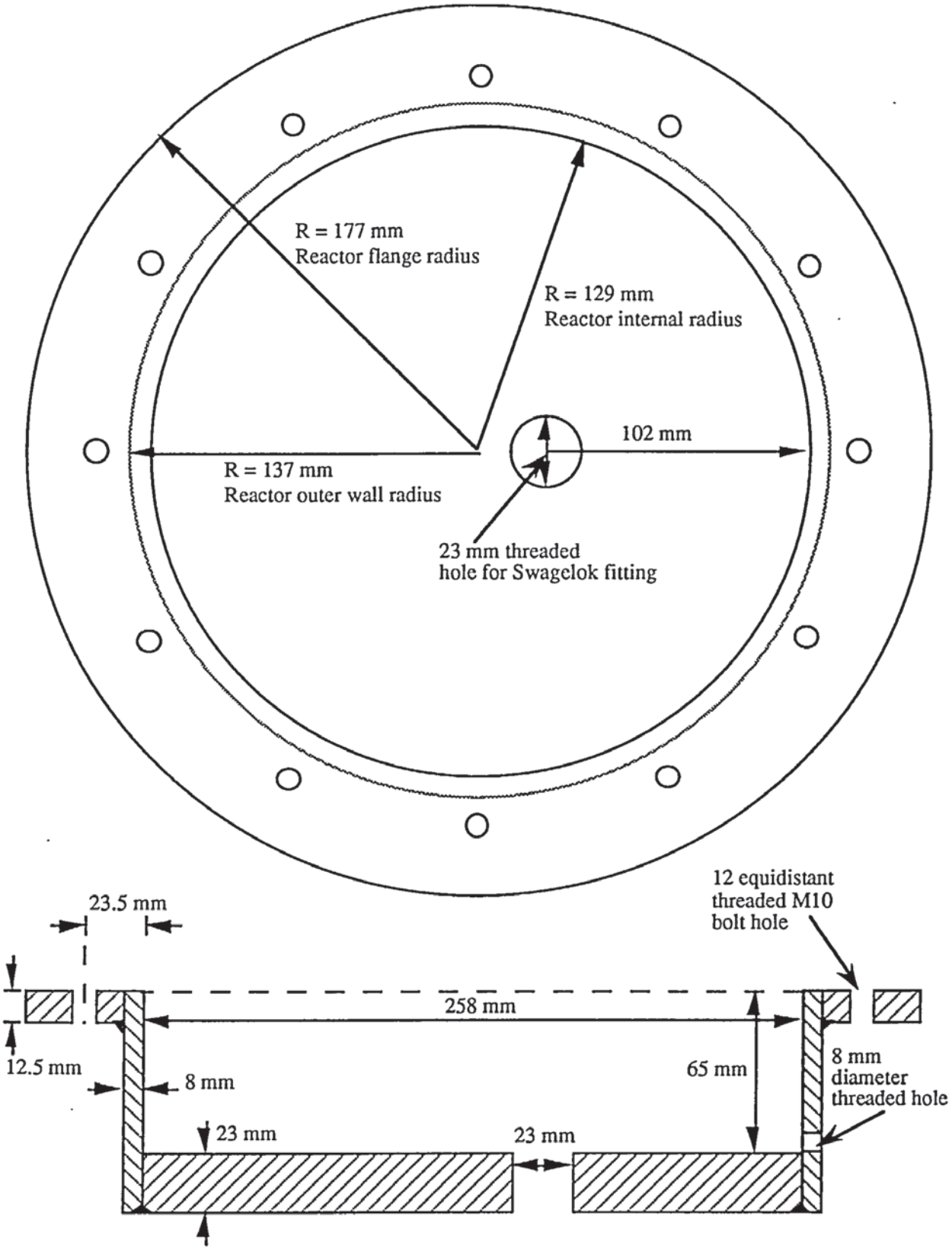

Figure 6.06. Reactor cross section with lid position and sightglass ports

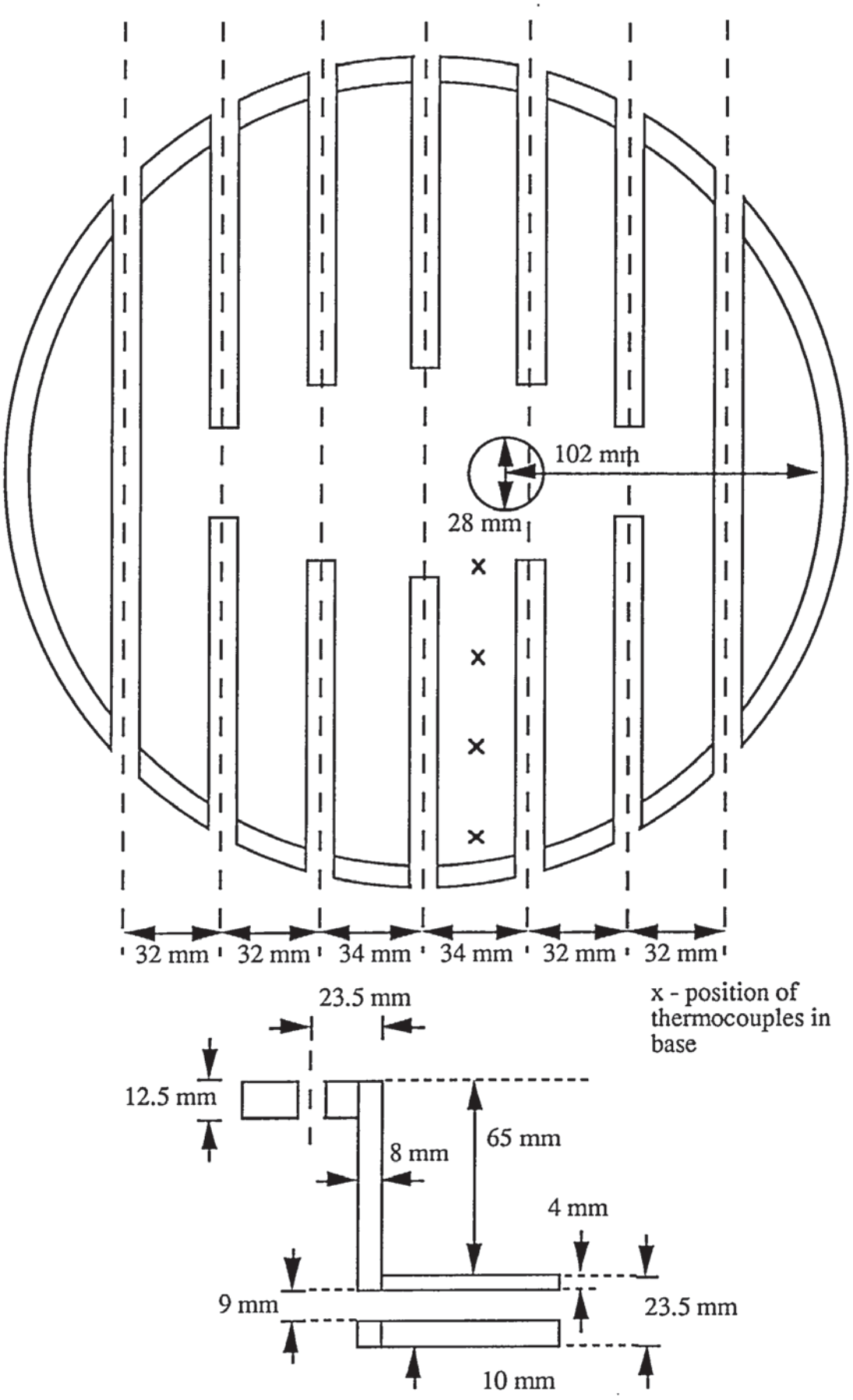

Figure 6.07. Position of heaters in reactor base

6.6.2 Reactor lid and sightglasses

The top view of the reactor lid is shown in Figure 6.08. The outer flange diameter is 353 mm by 12 mm. The lid has 12 M10 bolt holes which are equally spaced as shown. Two sightglasses ports have been fitted to allow the reactor interior to be studied during and after an experiment. Each 2 mm thick quartz sightglass has a 55 mm viewing diameter and a 3 mm nitrogen supply line to reduce the build up of pyrolysis vapour products on the glass during operation. The inclined sightglass can also be turned through increments of 45° to allow different parts of the interior to be seen. Figure 6.09 shows the side view of the reactor lid with the inclined sightglass and the flat sightglass used during the experiments. The carbon bush holder contains two small carbon bushes to seal the drive shaft during the experiments.

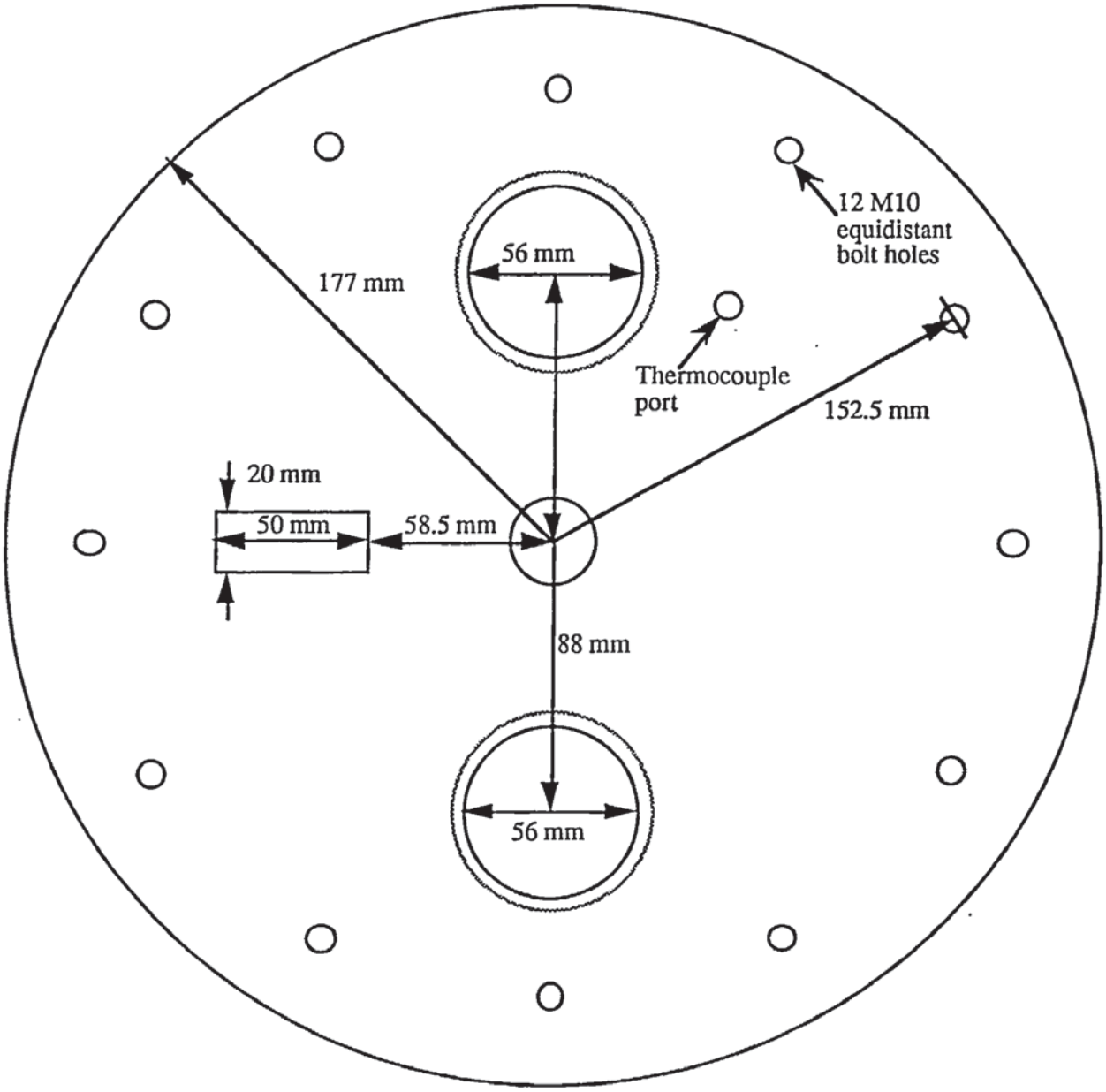

Figure 6.08. Top view of the reactor lid

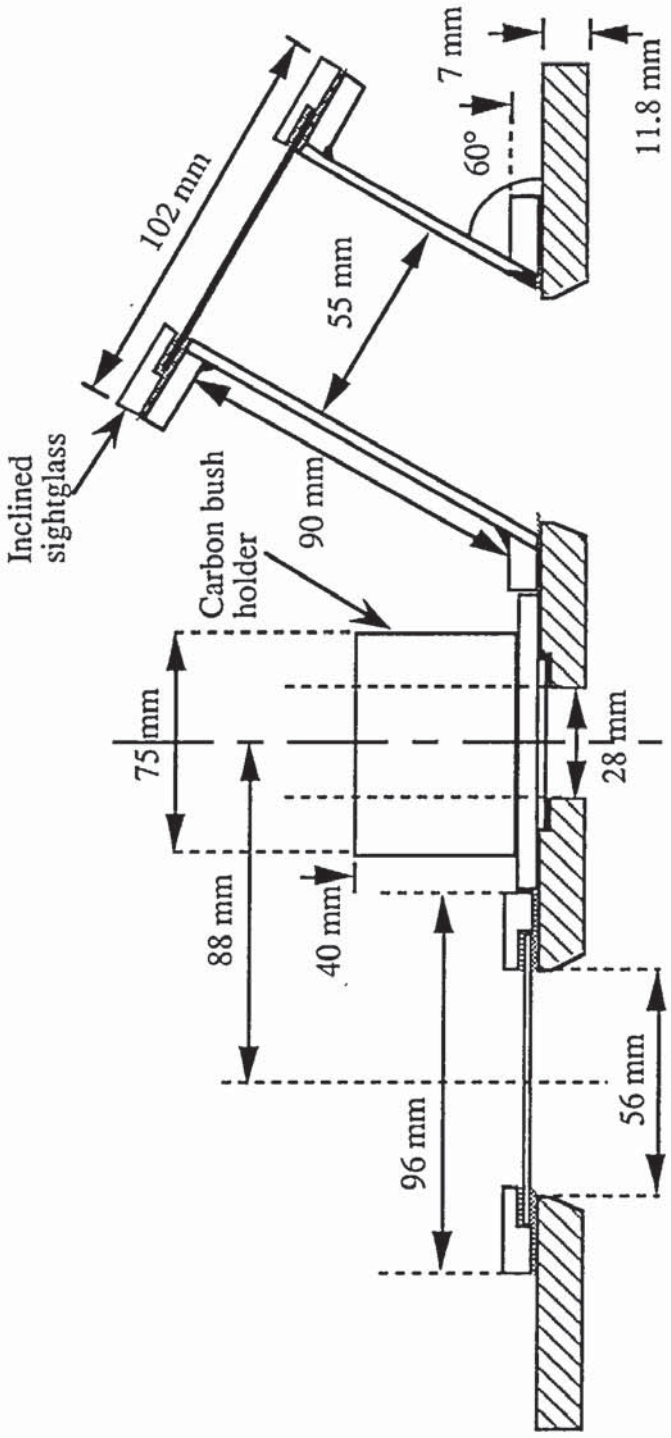

Figure 6.09. Side view of reactor lid and the original sightglasses and the carbon bush holder

6.6.3 Rotating blades and holder

Particle ablation is achieved by the action of four rotating blades, positioned asymmetrically on a metal holder. Each blade is independently mounted and the blade angle relative to the heated base can be varied. One blade is shown in Figure 6.10 with the blade holder.

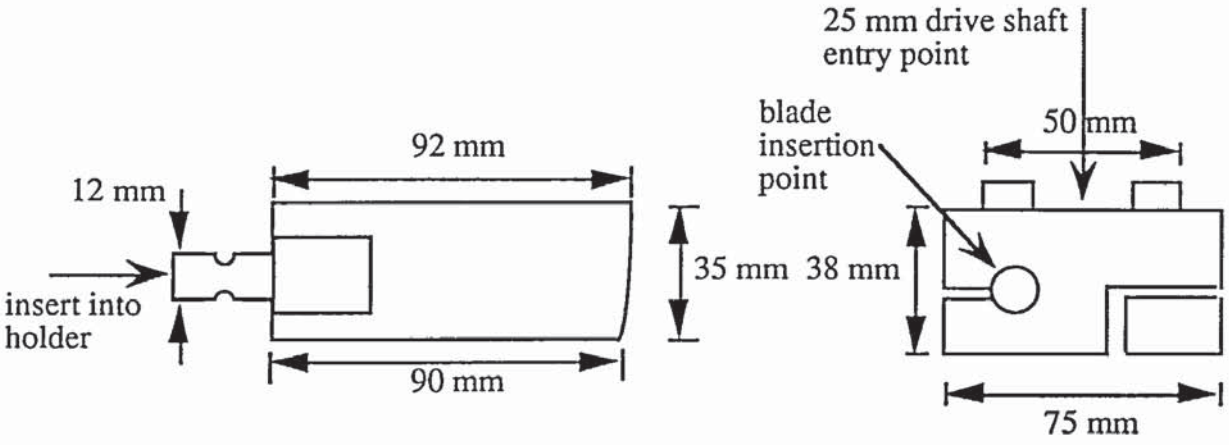

Figure 6.10. Single blade used to achieve particle ablation and the blade holder

The blades are inserted into the holes in the holder and secured with an M8 bolt through the holder. The drive shaft which fits into the recess in the top of the holder is secured using a locking nut in the bottom of the holder.

6.6.4 Biomass feed inlet point

In order to impart a random motion to the particles entering the reactor and distribute the particles along the length of the rotating blades, the inclined [60°] feed inlet is a 20 mm by 50 mm slot as shown in Figure 6.08. The feed tube to the inclined feed tube has a sightglass to visually check that the biomass is being fed to the reactor.

6.6.5 General reactor features

For all the above parts which use bolted flanges, sealing is done using 1.5 mm laminated graphite. The drive shaft bearings are positioned 0.15 m from the top of the reactor lid and the drive shaft is rotated by a 5:1 speed reducer powered by a 1.5 kW electrical motor with variable speed control. The biomass is fed into the reactor from a sealed nitrogen purged screw feeder with an inventory of up to 10 kg of dried biomass. The screw on the feeder limits the particle size to 6.35 mm and this was the maximum particle size range used during the experiments. The final constructed reactor is shown in Figure 6.11.

It was realised that there may be some subsequent modifications might be required to the reactor, the blades or the peripheral equipment. The reactor was constructed to allow some flexibility in its operation. In Chapter 7, the practical results are described and the modifications made to the reactor and product recovery systems are detailed. This includes the five initial commissioning runs and the following eleven experiments for which detailed mass balances were obtained [see Chapter 8].

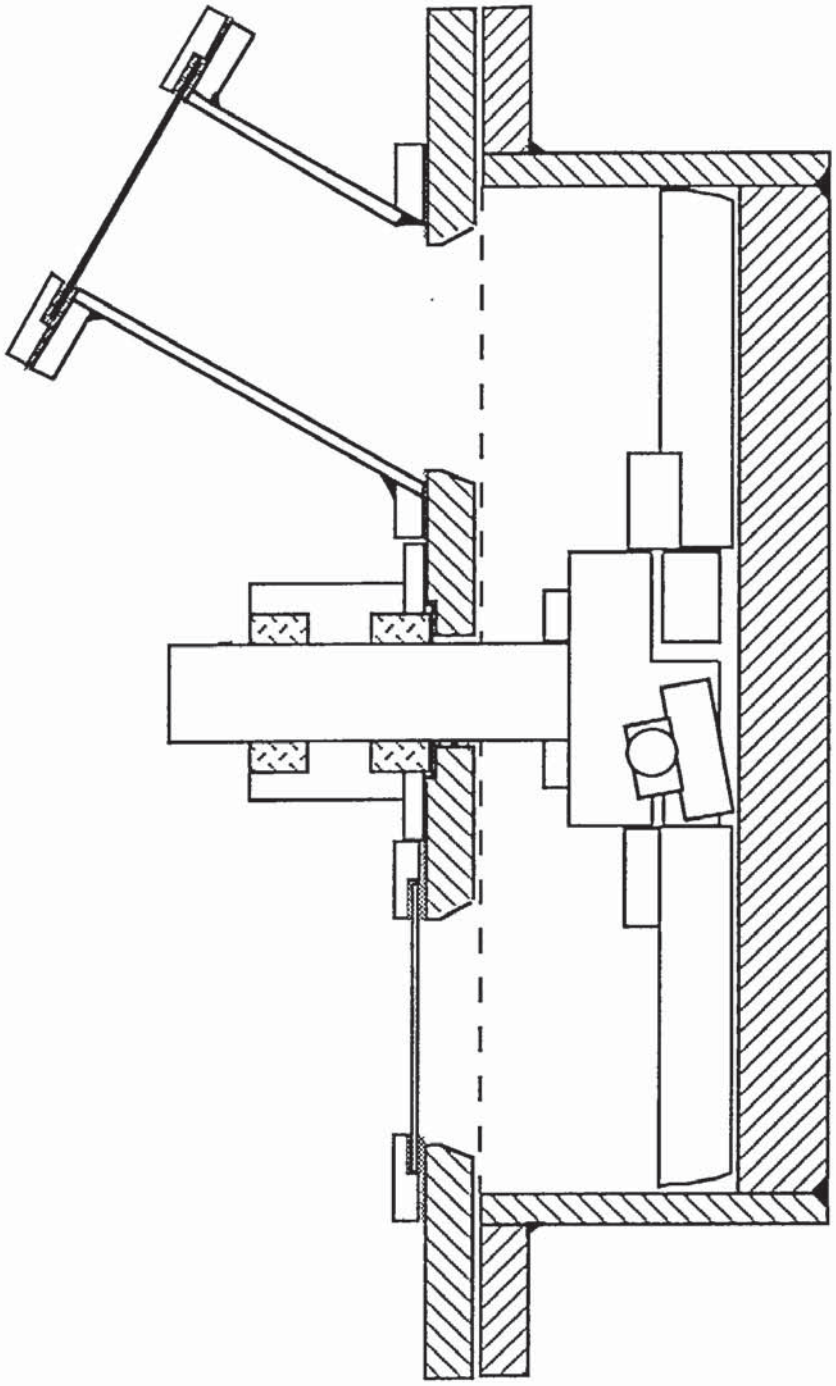

Figure 6.11. The assembled pyrolysis reactor with the rotating blades and holder

The reactor design presented above is a compact one with inherent advantages of even temperature distribution and control. Solids residence time is decoupled from the gas/vapour product residence time and this allows the degree of product dilution to be moderated and controlled using an inert gas, such as nitrogen.

Chapter 7. Operation of Reactor and Product Recovery Systems

7.1 Introduction

Chapter 6 presented the rotating blade approach used to achieve particle ablation and detailed dimensions of the constructed reactor. In this chapter the experimental results are discussed with respect to the operability of the reactor system, including product separation and collection. The chapter is structured as:

- pyrolysis liquids collection [Section 7.2]
- gas handling and analysis [Section 7.3]
- char separation and collection for runs CR01-CR05 [Section 7.4]
- reactor operation, modifications and results for runs CR01-05 [Section 7.5]
- reactor operation, modifications and results for runs CR06-12 [Section 7.6]
- reactor and product collection system operation for runs CR13-16 [Section 7.7]
- discussion of the reactor operation [Section 7.8]
- conclusions for the reactor and product recovery system [Section 7.9]

7.2 Pyrolysis liquids collection

7.2.1 Pyrolysis liquids collection processes

This section describes the evolution of a successful product separation and recovery system. As discussed in Chapter 2, three products are formed during pyrolysis: a solid char/ash residue, a vapour/gas product from which the organic liquid and water is condensed and a non-condensible gas which is defined as products which exist as gases at 25°C. The gas/vapour products of pyrolysis appear as a dense white "smoke" with characteristics of a suspension of micron sized aerosols and droplets which are highly conductive. To collect the liquid products, three processes are required:

- transport of the vapour to the collection system,
- rapid cooling of the vapours,
- coalescence of the aerosols and droplets to form a free flowing liquid at an arbitrary upper temperature of 50°C.

Many systems employ an inert particle transport gas or heat carrier gas for conventional fluidised bed reactors, such as nitrogen, so typically the condensible vapour products are present in low volumetric concentrations, estimated to be 10-15 vol.% of the total gas/vapour product volume (277).

Although all fast pyrolysis processes have necessarily included liquids collection, little attention has been paid to the fundamental design of these systems which, in fact, have posed considerable difficulties in achieving high collection efficiencies. The systems generally used are summarised in Table 7.01. No information has been found on the design or performance of liquid cooling and collection systems for pyrolysis liquids, and the only study known to have been carried out is based on a set of model compounds (280). Although there has been extensive work on hot gas clean up for gasification products for tar removal, this is directed at the gas as the valuable product and no work has been found which focuses on liquids collection in analogous situations.

Table 7.01

Pyrolysis technologies and liquids recovery systems

Institution	Product Collection System	Section	Reference
Alten	direct quench in recycled product water		281
BBC Engineering Ltd.	direct liquid quench	4.5	247
Colorado School of Mines	3 stage condenser system	4.3	236
CPERI	2 stage condensation		145
CRES	direct liquid quench in product oil		282
Egemin B.V.	direct liquid quench in product oil		283
Encon Enterprises	direct liquid quench in product oil		284
GTRI	direct liquid quench in product oil		260
INETI	water cooled condenser		75
Interchem Industries	direct liquid quench in hydrocarbon liquid	4.7	285
NREL	water quench in scrubber cyclone	4.6	116
Union Electric Fenosa	3 stage condensation with liquid contact		286
University of Aston	2 stage condensation and gas filtration		this work
University of Leeds	3 stage condensation		48
University of Twente	6 stage condensation	4.4	242
University of Waterloo	2 stage condensation and gas filtration		106

From this summary, it was apparent that there is a preference for direct liquid-gas contact to quench the vapours with a liquid to fulfil the requirements of cooling and collection in demonstration or commercial scale plant, usually using pyrolysis liquids as the quenching medium. The vapour liquid contact can be achieved by rapidly mixing the vapours and gases

with a liquid of similar composition, e.g. pyrolysis oils in a spray or packed column. For small scale systems, i.e. less than 10 kg/h, there is a preference for indirect heat exchange due to the problems of liquids handling and mass balance closure.

7.2.2 Product recovery systems used

The product separation and recovery system used are described below. No mass balances were obtained for runs CR01-CR05. The product separation and recovery system comprised four stages for runs CR06-CR16:

- char removal from the product vapours,
- liquids cooling and collection,
- gas filtration with aerosol removal,
- gas drying.

7.2.2.1 Product collection system for runs CR06-CR12

The first system for runs CR06-CR12 inclusive is shown in Figure 7.01. The product vapours and char exited from the reactor base, at 250-420°C, into a receiver [for run CR06 a steel pot was used, for CR07-12 a 1 litre ice-cooled flask was used]. Char and unablated wood remained in the receiver and the remaining cooled product vapours entered the first ice-cooled condenser at 160-250°C. The cooled and stabilised vapours then passed through a U tube which connected the two condensers where they collected as liquid. Remaining cooled and stabilised vapours and aerosols then entered the second condenser. The persistent aerosols and liquids which exited the second condenser at 25-50°C passed through a cotton wool filter with the remaining gases going through a column of 3Å molecular sieve [pre-dried at 105°C for 24 hours] to remove any residual water vapour. The non-condensible gases were drawn through the system using a vacuum pump which then discharged the gas through a volumetric flowmeter before entering the on-line gas analysers for CO, CO_2, CH_4 and H_2. Calibration and operation of the gas analysers and related equipment is described in Appendix II. Batch gas samples were taken every few minutes for GC analysis. The proportion of vapour products to diluting nitrogen are given in Table 7.02 overleaf for runs CR06-16.

Recovery of low molecular weight compounds has been investigated by Scott and Piskorz who showed that a variety of products could escape collection and recovery (90). It is therefore important to have a low final exit gas temperature to minimise the loss of low molecular weight components.

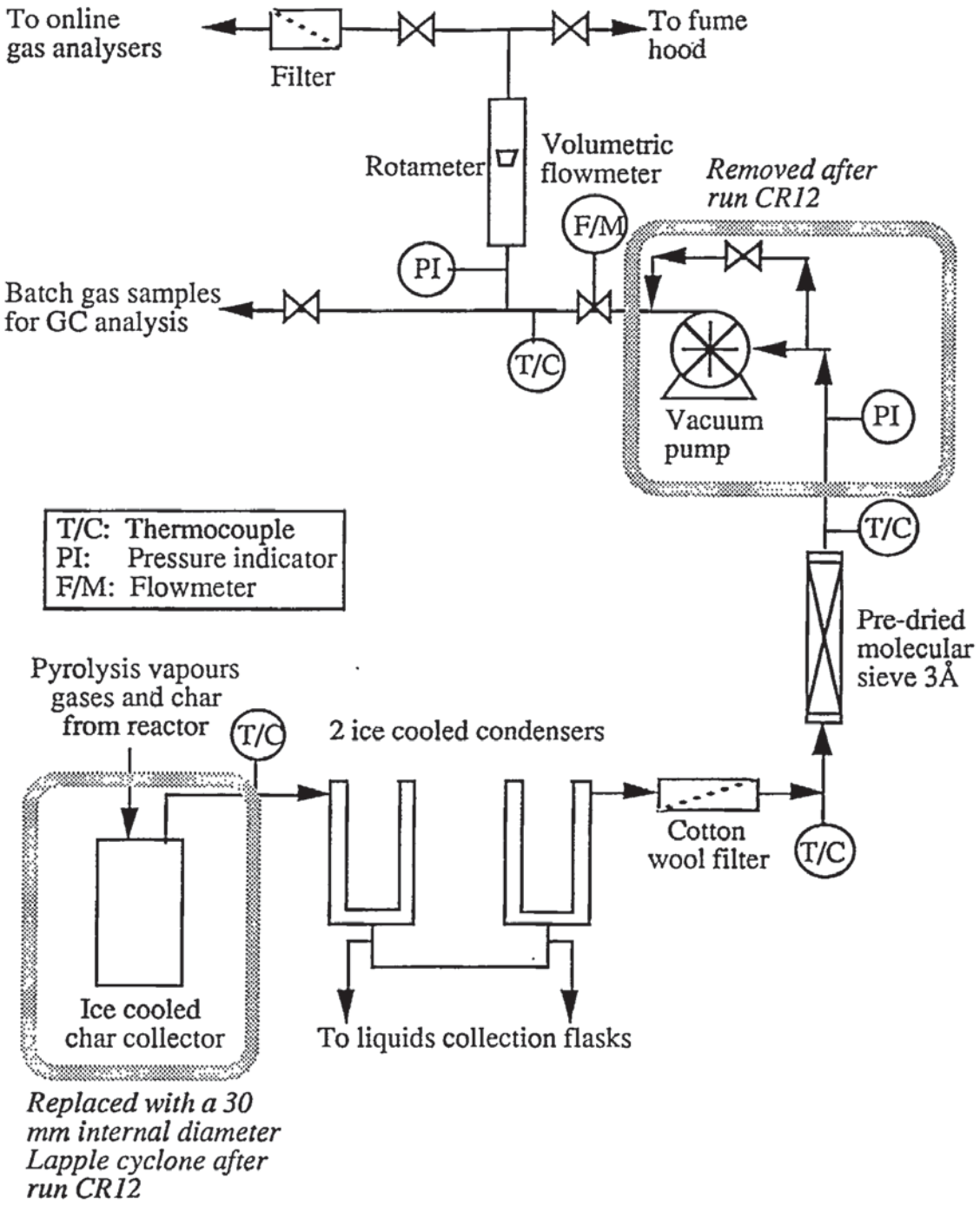

Figure 7.01. Product collection and separation system

7.2.2.2 Second product collection system for runs CR13-CR16

For runs CR13 onwards, the significant modification to the system was the replacement of the char receiver with a trace heated cyclone and trace heated pipes for hot char removal. The char cyclone is of standard dimensions with an upper cylindrical internal diameter of 0.03 m (287). The char cyclone is slightly oversize to allow large particles which may be carried out of the reactor to fall into the char pot to reduce blockage problems. The vacuum pump was also removed and the cotton wool filter was reduced from 60 g dry cotton wool to 15 g.

Table 7.02

Flow of diluting/purging nitrogen in the experimental runs for CR06-CR16 [wt N_2: dry wood and volume N_2:pyrolysis products at reactor exit temperature]

Run number	CR06	CR07	CR08	CR09	CR10	CR11
N_2:dry wood as fed	0.18	0.42	1.27	5.47	1.32	1.36
N_2: pyrolysis products	0.23	0.77	3.68	13.61	3.45	3.29
second condenser exit temperature [°C]	19.4	21.7	41.3	27.8	38.9	40.7

Run number	CR12	CR13	CR14	CR15	CR16
N_2: dry wood as fed	2.32	1.82	5.9	2.35	2.11
N_2: pyrolysis products	6.83	0.98	2.31	0.78	1.06
second condenser exit temperature [°C]	40.2	24.7	6.9	9.1	11.5

7.3 Gas handling and analysis

The dry gas was analysed continuously and by batch sampling. On-line continuous analysis was performed using LIRA 3000 infrared analysers for CO, CO_2 and CH_4 and a Leybold Heraus thermal conductivity analyser for H_2. Batch gas samples were taken every 3-5 minutes during steady state operation of the reactor. For batch gas analysis the following equipment and conditions were used [the integrator is a Spectra-Physics SP 4100 with helium carrier gas]:

- O_2, N_2, CO, CH_4 and H_2: 80-100 mesh molecular sieve 5 Å column [6.35 mm o.d., 1500 mm long], thermal conductivity detector [Pye Unicam 204 chromatograph], column temperature 70°C, detector and injector temperature 200°C.
- CO_2, C_2H_4 and C_2H_6: same equipment but with a Porapak N column [6.35 mm o.d., 1829 mm long] at 60°C.
- C_1-C_5: 0.19% picric acid on Graphpac-GC column [6.35 mm o.d, 1500 mm long], flame ionisation detector [Perkin-Elmer Sigma 2B chromatograph], column temperature 30°C, detector and injector temperature 150°C.

7.4 Char separation and collection for runs CR01-CR05

In order for the reactor to perform correctly the product char has to be removed to allow more biomass to enter below the blades for reaction. There are three possibilities for the location of product extraction and a number of possibilities for aiding this removal:

Location:

- remove all products [i.e. both char and vapour products] from the base of the reactor,
- remove all the char from an outlet in the reactor base and extract the gas and vapours from the top of the reactor,
- remove the ablative [fine] char and product gas and vapours from the reactor top and other solid products from the base,

Method:

- mechanical transport of all char to a reactor base exit,
- enhanced pneumatic transport [with nitrogen] of fine char to reactor top exit,
- enhanced pneumatic transport of fine char to reactor base exit.

The parameter values studied during runs CR01-CR05 are shown in Table 7.03 using air dry wood, 10-12 wt% water on a dry basis. From Figure 5.02, presented in Chapter 5, a temperature of 550°C and a feedrate of 2.5 kg/h were used to provide the required information for operation and initial assessment of the performance of the ablation concept.

Table 7.03
Operational values used in runs CR01-CR05

Run No.	Biomass fed [g, dry]	Run Time [min]	Relative velocity [m/s]	Reactor pressure [bar g]	Blade clearance [mm]	N_2 [l/min]
CR01	230.8	8	0.26	-0.15	0.38	7
CR02	377.4	16	0.62	-0.25	1.27	4
CR03	1464.8	42	0.65	-0.1	1.27	2
CR04	1244.1	30	0.83	-0.17	1.27	1.8
CR05	718.7	15	0.83	-0.25	1.54	4.3

The configuration of the product outlet systems for the first six runs is shown in Figure 7.02. In each experiment the outlet pipes from the reactor were insulated to a thickness of 20 mm, internal diameter 15 mm. Nitrogen quoted during runs CR01-05 was used to try and keep the reactor sightglasses clear, the success of which is discussed in Section 7.5.2.1.

7.4.1 Run CR01

The first two runs were used to evaluate removal of all the products from the reactor base outlet with char removal in the cyclone, i.e. with the rotating action of the blades transporting the product char to the centre of the reactor along with the gas/vapour products. This is depicted in Figure 7.02. A pipe with a 90° elbow was fitted to the reactor base and then into the cyclone. After the run, it was observed that particles were trapped in the elbow of the pipe due to a lack of transport by the nitrogen purge. The reactor contained unreacted wood chips suggesting that the reactor was being overfed or char removal was inefficient or ineffective. Blade tilting caused the rotating blades to scrape into the reactor surface with visible scoring.

7.4.2 Run CR02

Run CR02 was operated under the same conditions as run CR01, except that the blade clearance was increased from 0.38 to 1.27 mm to prevent blade tilting, as observed during run CR01. The qualitative results for this run were the same as for run CR01.

7.4.3 Run CR03

Since the mechanical transport of product char from the reactor was of limited success, the alternative of entraining fine ablatively produced char in the gas/vapour products as they exited the top of the reactor was tested. This was not successful as larger char particles were also entrained out by the product gases and vapours. It was evident from the first three runs that some limited mechanical transport of char to the reactor outlet was occurring as char was recovered in the char pot connected to the reactor base. It was noted that the clearance of the bottom of the blade holder from the reactor surface was only 2 mm, inhibiting the transport of char from the reactor. For the next run, CR04, 4 mm was removed from the base of the blade holder to increase the blade holder clearance from the heated reactor surface to 6 mm.

7.4.4 Run CR04

The cyclone was close coupled to the exit pipe on the reactor lid to remove larger particles entrained by the gas and vapours, as observed during Run CR03. The same quantitative results were obtained as for the previous three runs, but a larger proportion of char was transported into the char pot connected to the reactor base. The cyclone on the top, however, was blocked with large char particles.

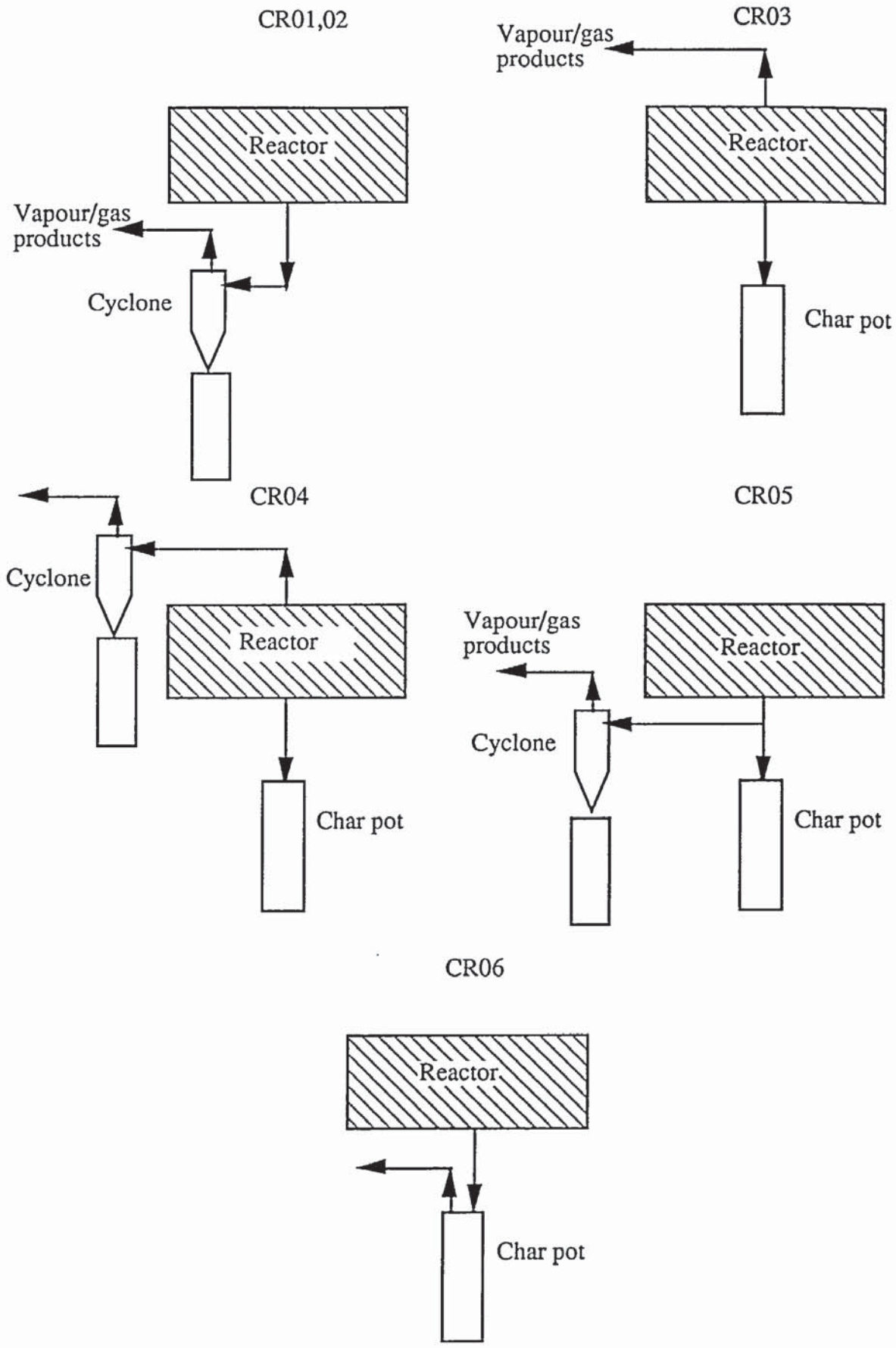

Figure 7.02. Product char separation systems tested during runs CR01-CR06

7.4.5 Run CR05

The approach for this run was to allow the relatively large particles to fall in to the char pot connected to the reactor base with the fines entering the cyclone for separation. This proved more successful with a larger proportion of char transported out of the reactor; however, the cyclone was blocked completely. The reason for the poor performance of the cyclone was due to product vapours adhering to the wall of the cyclone leading to eventual blockage.

7.5 Results and conclusions from runs CR01-CR05

7.5.1 Reactor operation

From the first five runs, the following results were obtained:

- particle ablation was evident with the rapid formation of product vapours visible via the sightglasses,
- char transport from the reactor was a significant problem,
- blade clearance did not appear to influence the final particle size, implying that there is intraparticle attrition leading to the formation of fine, ablatively produced char,
- mechanical transport of char wasnot efficient enough to cope with throughputs,
- char and product vapours should exit from the reactor base,
- the nitrogen flow was too low for the cyclone to operate correctly,
- for temperatures of 500°C and above, a thin layer of degraded liquids was visible on the heated reactor surface,
- the feedrate was too high for each run,
- estimated gas/vapour residence times were 10 s; therefore to reduce the residence time of the gas/vapour products, additional nitrogen would be used,

7.5.2 Modifications to the reactor

7.5.2.1 Use of the reactor sightglasses

From Figure 6.09 in Chapter 6, two sightglass configurations were used to observe the reactor interior during an experiment and observe the particles during ablation. Trials during experimentation proved partially successful at maintaining visibility of the reactor interior using both sightglasses. The flat sightglass proved extremely difficult to keep clear as product vapours rapidly condensed and degraded to form a black glassy char, despite the impingement of nitrogen at 25-50°C onto the inside of the quartz sightglass. The 60° inclined sightglass gave better qualitative results with no nitrogen. With no nitrogen to the sightglass, the lower 25 mm of the inclined tube, and also the sightglass, became coated with liquids;

however, this pale straw coloured liquid was fluid enough to drain off the glass and allow the interior to be seen. After a run, this liquid could be easily washed off with acetone or methanol. Although the white product vapours are too opaque to allow the particles to be seen, blade rotation could be observed. For run CR06 onwards, the sightglasses were not used and the view ports were blanked off.

7.5.2.2 Blade clearance and the blade holder

The initial blade clearance of 0.38 mm proved unsatisfactory with blade tilting occurring. The blade clearance was increased and set at 1.54 mm for the rest of the experimental program.

7.5.2.3 Blade holder modifications

It was originally intended that the blade holder would selectively allow fine char particles to pass below the blade holder and exit from the reactor with the larger unreacted particles remaining in the reactor. The initial clearance for the bottom of the blade holder from the reactor surface of 2 mm inhibited the transport of char from the reactor by the rotating blades. To alleviate the problem, 4 mm were subsequently removed from the blade holder bottom. With the blade clearance fixed at 1.54 mm, the clearance of the base of the blade holder from the reactor surface was 6 mm.

7.5.2.4 Reactor pressure

During the first five runs, the reactor was operated at pressures below atmospheric to reduce the reactor residence time and also remove the products from the reactor. This, however, caused several feeding problems; therefore, all subsequent runs were carried out at atmospheric pressure.

7.5.2.5 Surface blow line

Complete removal of product char was possible by the rotational action of the blades. A 2 mm diameter blow line was fitted at the surface of the reactor at the nearest point to the outlet in the reactor base, as shown in Figure 6.06. This was used to selectively entrain fine product char towards the outlet in the reactor base. The final reactor configuration for char removal from the reactor consisted of a vertical outlet tube from the reactor base into the product collection system. For run CR06, the initial char separator was a stainless steel pot, but this was replaced for runs CR07-12 with a 1 l round bottom flask and subsequently with the 0.03 m diameter cyclone for runs CR13-16 as previously described [see Section 7.2.2.2].

7.6 Reactor and product collection operation, modifications and results for CR06-CR12

The general outline of the reactor operation is given below and the reactor is shown schematically in Figure 7.03. The full detailed procedure for setting up the reactor, calibrating equipment and testing the system is given in Appendices II and III.

7.6.1 Reactor preparation and system operation

The rotating blades are set at the desired clearance and the reactor lid sealed. The biomass feeder tube is connected to the inlet pipe and the feeder filled with a pre weighed mass of oven dried wood. The feeder is sealed and the nitrogen flows are set at atmospheric pressure before the condenser system is connected to the vertical outlet pipe on the base. During purging, the reactor is heated to the set point temperature. The blades are allowed to heat up and rotated at speeds up to 200 rpm. When the reactor temperature is stable at the set point, biomass is then continuously fed in from the sealed and nitrogen purged screw feeder.

The product collection system is weighed before and after the run and then washed with methanol to remove liquids from the condensers and the cotton wool. The total liquid yield is then the mass difference of the product collection system, including the mass differences in the cotton wool and molecular sieve adsorbent, less the char recovered in a pre weighed dried filter paper after liquids filtration. The wet char is oven dried to remove the methanol. The wood fed to the reactor is determined after the run by reweighing the wood in the hopper and re measuring the wood moisture content.

After the reactor has cooled down to 50°C, the lid is removed and the reactor contents examined. A thin film of about 1 g of material was observed on the reactor base for runs at 550 and 600°C. For the runs at 450°C, this layer was only visible as a faint grey colour on the reactor base. This is in accord with claims that the liquid product film on the reactor surface is around 100 μm from work on the mechanisms of ablative pyrolysis (116). This grey deposit can be scraped off the surface and washes off easily with acetone. Fine char is easily removed from the lid and constitutes less than 2 g per run.

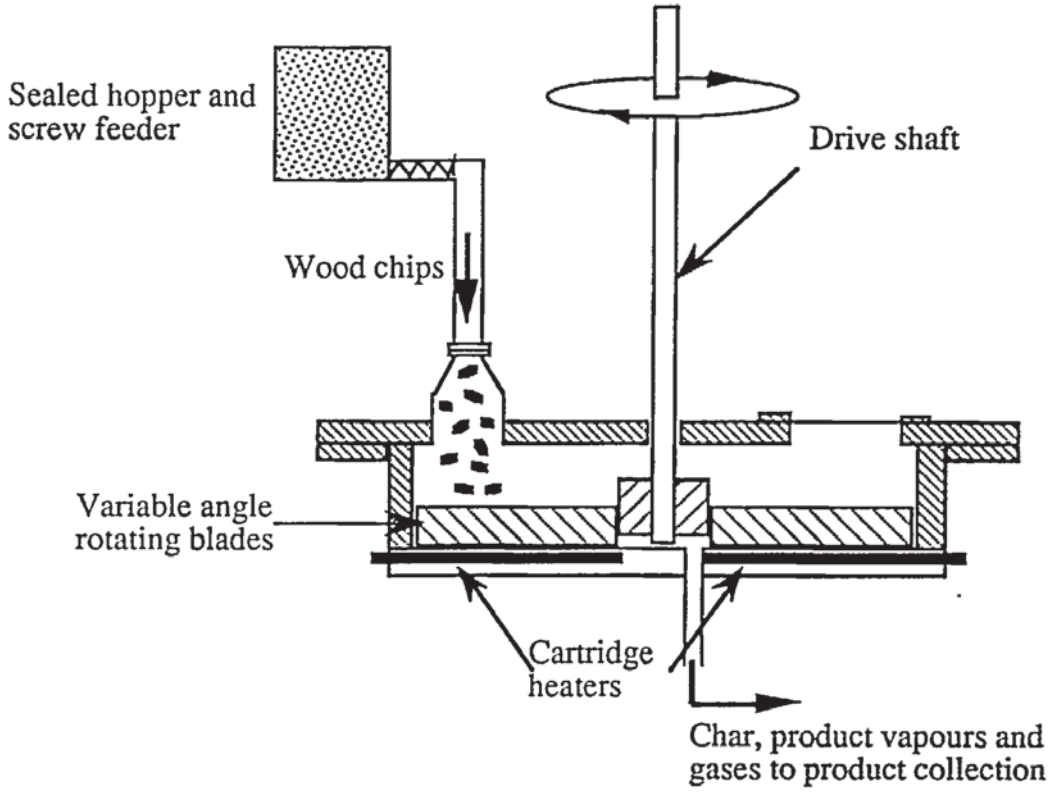

Figure 7.03. Schematic of the ablative pyrolysis reactor for runs CR06-CR16

7.6.2 Reactor operational results for runs CR06-CR12

The experiments for this second phase were the first to yield mass balance data as the product collection system had been changed [see Section 7.4.1] to recover the liquids for analysis and separate the char from the product vapours. Run CR06 was the first run to use significant quantities of nitrogen [greater than 6 l/min] as a gas/vapour product diluent and assist in transporting product char from the reactor. The quantities of reactor char and product collection char were measured to assess the success of the surface blow line and these are shown in Table 7.04 for runs CR06-16. The nitrogen surface blow line required some degree of optimisation to prevent unreacted particles from being entrained out of the reactor. This has generally been achieved with low ratios of reactor to product collection system char for most runs. Reasons for high ratios of reactor char to product collection system char are that the biomass feedrate was not optimised and overfeeding occurred for some runs, leading to a build up of material in the reactor. In general there were no operational problems with the reactor, the drive shaft and drive motor or the feeder when operated at atmospheric pressure.

Operational results are presented in Table 7.05 with the total quantities of wood fed, the experimental run time, the average blade velocity and the reactor pressure. Operating the reactor at reduced pressures was discontinued after CR07 as the lining of the feeder was pulled around the feed screw causing damage to the lining.

Table 7.04

Mass of recovered char fractions for runs CR06-CR16

Product Collection System Char [PC] Average Sieve Size [mm]	CR06	CR07	CR08	CR09	CR10	CR11	CR12	CR13	CR14	CR15	CR16
0.0375	9.70	2.94	12.76	3.27	1.72	0.71	2.50	5.43	1.47	9.10	5.67
0.0905	4.53	4.76	41.46	5.07	3.16	0.65	3.06	7.17	2.47	6.52	5.52
0.1780	1.78	11.26	34.11	7.11	13.91	8.39	10.13	5.51	4.61	13.68	9.22
0.3025	0.11	2.20	20.00	2.72	5.58	4.08	5.43	1.46	1.16	6.98	4.36
0.4775	0.25	3.14	23.13	3.40	7.47	5.36	10.88	1.27	1.70	3.20	4.12
0.8900	0.81	4.53	45.05	7.77	9.71	9.26	13.17	1.25	2.57	7.75	1.91
1.2900	0.24	1.92	19.09	1.69	4.27	4.01	5.93	0.34	0.52	1.11	0.50
1.5500	0.47	3.18	13.23	1.82	3.25	4.47	5.45	0.48	0.41	0.94	0.46
2.5250	0.64	16.27	39.03	8.36	21.34	23.82	52.28	2.70	1.07	3.01	1.54
4.4500	1.04	9.54	7.22	39.33	19.36	16.59	78.54	2.37	0.17	0.43	0.06
mass sieved [g]	19.57	59.74	255.08	80.54	89.77	77.34	187.37	27.98	16.15	52.72	33.36
Reactor Char [RC] Average Sieve Size [mm]	CR06	CR07	CR08	CR09	CR10	CR11	CR12	CR13	CR14	CR15	CR16
0.0375	1.20	1.36	0.28	0.00	0.16	0.42	0.17	0.89	0.43	0.55	3.19
0.0905	1.35	1.11	0.45	0.02	0.13	0.40	0.07	0.52	0.73	1.81	1.93
0.1780	7.83	2.68	1.79	0.10	0.35	1.75	0.29	1.04	0.98	3.72	3.54
0.3025	4.39	1.54	1.17	0.07	0.17	1.06	0.28	0.47	0.67	1.82	1.00
0.4775	6.04	3.70	3.02	0.25	0.27	1.99	0.17	1.13	1.28	2.22	1.59
0.8900	8.33	10.46	7.61	1.15	0.45	8.57	0.24	4.39	2.76	6.21	2.24
1.2900	1.36	5.09	1.76	0.52	0.22	4.04	0.29	1.36	0.67	1.91	0.54
1.5500	1.05	6.10	1.60	0.62	0.33	4.45	0.18	2.13	0.63	1.53	0.52
2.5250	6.72	21.17	5.82	3.89	2.34	15.22	1.64	15.69	1.44	2.70	0.06
4.4500	6.95	5.50	9.33	13.89	4.45	7.44	3.18	26.18	1.64	4.36	0.09
mass sieved [g]	45.22	58.71	32.83	20.51	8.87	45.34	6.51	53.80	11.23	26.83	14.70
Ratio: RC/PC	2.31	0.98	0.13	0.25	0.10	0.59	0.03	1.92	0.70	0.51	0.44

The longest run time was 45 minutes for CR09 and other runs have been shorter than this to prevent over pressurisation due to a gradually increasing pressure drop across the cotton wool filter and the reduction in transfer pipe diameter at the interface between the condensers and the metal outlet pipe. To reduce the vapour product residence time, the reactor operational volume was reduced followed by a reduction the quantity of nitrogen used for diluting the gas and vapour products. This is described in Section 7.7.

Table 7.05
Operational values and results for runs CR06-CR16

Run No.	Biomass fed [g, wet]	Wood H_2O [wt% dry basis]	Run Time [min]	Average relative velocity, V_r	Reactor Pressure [kPa abs.]
CR06 [597°C]	467.5	9.25	12	1.39	76.0
CR07 [550°C]	505.5	2.44	15	1.39	91.0
CR08 [550°C]	1106.6	2.08	33	1.39	101.9
CR09 [456°C]	352.8	2.86	45	1.2	101.9
CR10 [602°C]	454.3	1.99	14	1.11	102.7
CR11 [550°C]	466.0	1.86	15	1.39	101.6
CR12 [554°C]	679.2	3.21	21	0.83	100.9
CR13 [505°C]	325.7	1.21	18	1.39	100.4
CR14 [458°C]	124.2	1.37	27	1.39	101.3
CR15 [501°C]	318.2	1.2	35	1.39	100.4
CR16 [551°C]	288.5	0.36	41	1.39	100.5

7.6.3 Product collection system operation for runs CR06-CR12

Use of the ice cooled char collection flask and the two ice-cooled condensers have highlighted several qualitative points with regard to liquids recovery, char separation and product cooling:

- a thick and very viscous liquid tended to deposit in the connecting pipework from the char receiver to the condensers and in the first condenser. This was believed to be due to a partial cooling of the vapours to a temperature low enough for lignin-derived macromolecules to condense. These liquids which were fluid initially during collection in the first condenser were solid after cooling and required soaking in methanol to dissolve them.
- As the pyrolysis products passed through the equipment, the aerosol droplets if impinging on a surface at less than 400°C tended to adhere and remain stuck. Fine char entrained in the products became stuck in the droplets and this process repeated itself until the transfer pipe finally blocked. Typically experimental runs were stopped after 45 minutes to prevent blockage problems.

- A significant proportion of the liquids remained as stable aerosols after the products passed through the two ice cooled condensers and a U tube of condensed liquids. About one third of the pyrolysis liquids were typically recovered in the cotton wool filter.
- Use of unheated transfer lines can lead to their eventual blockage due to the deposition of liquids and char on their inner surface.

The recovery of the pyrolysis liquids is not a simple condensation process. Rapid cooling of the product vapours leads to the formation of stable aerosols and micron size droplets, possibly with polar molecules bonded onto the surface of water droplets. Impingement and coalescence of the product vapours must therefore be an essential feature in the liquids recovery process.

The material found in the char receiver on the outlet of the reactor contained non-ablated wood and product char. The non-ablated wood becomes partially reacted by the hot product vapours coming in contact with the material as it exits the reactor, leading to slow pyrolysis by convective and radiative heating. These particles have a "scorched" brown surface, but the particle interior is fresh wood. These non-ablated particles typically lost 18% of their dry mass by this process, primarily by dehydration and possibly hemicellulose degradation due to their contact with the hot product gases and vapours as they exited the reactor base.

7.6.4 Modifications to the reactor and product collection system for CR13 onwards

7.6.4.1 Drive shaft seal

The graphite carbon bushes used in the original drive shaft seal were replaced after run CR12 with a polymer composite seal and water-cooled jacket. This has proved very effective during subsequent reactor operation.

7.6.4.2 Reactor interior plate

In order to reduce the gas/vapour product residence times and the quantity of nitrogen used to dilute the products, an internal plate was fabricated for attachment to the reactor lid to reduce the reactor operational volume by 54%. Other modifications to the product collection system have been detailed in Section 7.2.

7.7 Reactor and product collection system operation for runs CR13-16

The main change in reactor operation for runs CR13-16 was the installation of a metal blank inside the reactor to reduce the operation volume after CR12. This had the effect of reducing the reactor operational volume by 54%.

7.7.1 Second product collection system for runs CR13-CR16 and proposed modifications

The trace heated char cyclone worked very well with minimal build up of fine product char on the walls of the cyclone and the connecting pipe from the reactor base to the cyclone inlet. For the connection between the cyclone and the condensers, collection of viscous liquids and char has occurred. It appears that once the product vapours "contact" a cooler area, e.g. the inlet to the condenser, they will rapidly adhere to the surface, whether it is trace heated or not.

Some trials have been carried out with additional cotton wool in the second condenser, typically 7-8 g of pre-dried cotton wool to reduce the loading on the cotton wool filter, [runs CR15 and CR16]. This has proved useful in recovering more of the raw liquids and allows a smaller cotton wool filter to be used. The remaining stabilised aerosols, non-condensible gases and vapour exit the second collector into the cotton wool filter with a temperature of less than 10°C and this has improved the mass balances. The cotton wool filter removes any residual aerosols and the gas is passed over a fixed bed of 3mm molecular sieve 3Å pellets [pre-dried at 200°C for 48 hours] before passing through a volumetric gas meter. As for runs CR06-CR12, The gases passed to the on-line gas analysers for analysis with batch samples being taken every few minutes. The operation of the final liquid collection system was entirely satisfactory and gave very good mass balance closures as will be shown in Chapter 8.

7.7.2 Proposed modifications to the reactor and product collection system.

From the qualitative results, the rotating blade approach has proved effective in meeting the requirements of ablative pyrolysis. There are some limited changes required to the reactor and product collection system:

- the fitting of a rotary valve to prevent pressure build up in the feeder and prevent products migrating up the feed tube,
- modification of the connection between the condensers and the cyclone outlet,
- alteration of the feedscrew in the biomass feeder to allow larger particles to be fed to the reactor,
- the preheating of the nitrogen flows to the reactor to 400°C,
- modification of the connection between the condensers so that a U tube of liquid can collect to "scrub" the stabilised pyrolysis vapours as they pass through the system,

- heating of the reactor lid to improve the temperature control of the gas/vapour products.

7.8 Discussion of the reactor operation

From the qualitative results presented, the rotating blade concept has proved effective in rapidly ablating the biomass particles under conditions of high relative motion and applied particle pressure. To date, 53 % of the theoretical design throughput has been achieved, factors contributing to the reduced reactor throughput being:

- low biomass density [396 kg/m^3 compared to the design value of 530 kg/m^3],
- low biomass thermal conductivity [90% of particles found to ablate across the grain],
- non-uniform distribution of biomass particles below the rotating blades,
- product char inhibiting biomass particle ablation and removal from the reactor,
- variable ablation rates with relative velocity,
- variable contact pressure generated by the rotating blades on the biomass particles.

7.8.1 Effect of lower biomass density on the reactor throughput

The density of the wood used during the course of this research was 74.7% of the original design value specified [396 kg/m^3 compared to design value of 530 kg/m^3-see Table 5.01] on a dry basis. Therefore, the influence on the reactor throughput is a reduction of 74.7% to a maximum reactor throughput of 3.7 kg/h dry biomass. As discussed in the reactor design sensitivity in Section 5.5, the biomass density has a direct influence on the reactor specific throughput. The reactor throughput could be increased by using wood of higher density.

7.8.2 Effect of biomass thermal conductivity

The particles used in the experiments are regular cuboids with a potential 66% of the particles experiencing heat transfer across the grain, due to 4 sides of the 6 sides of the particle being across the grain in terms of orientation of the wood structure. From single particle experiments [described in Chapter 9] using uniform cuboid particles, over 90% of the biomass particles were ablatively pyrolysed across the wood grain. This also had an influence on the reactor throughput and operation as the cross-grain thermal conductivity is 2-2.5 times less than the value of the perpendicular thermal conductivity (24). Therefore, the biomass throughput was adversely affected by this decrease in the thermal conductivity due to reduced heat transfer, possibly by up to 40%. This is discussed in Chapter 9.

7.8.3 Non-uniform distribution of biomass particles below the rotating blades

One of the original assumptions used in the design procedure in Chapter 5 was that the contact area below the rotating blades was fully utilised in terms of perfect distribution of the biomass particles. This has proved not to be the case. From observation of the char inside the reactor for some experiments, the remaining particles consisted of a mixture of ablatively produced char and slowly carbonised particles. This showed that the product char was being carried around by the blades if not mechanically transported or "blown" out of the reactor.

7.8.4 Product char inhibiting biomass particle ablation

The product char was not completely removed by mechanical action of the rotating blades. However, the addition of a nitrogen blow line which was gradually optimised to selectively entrain ablatively produced char from the reactor did reduce the quantity of char remaining in the reactor after an experiment. Further optimisation is required.

7.8.5 Unquantifiable variable ablation rates

As discussed in Chapter 6, the ablation rate varies with radial distance from the centre of the reactor. There are no data available for temperatures below 600°C. However, new empirical data obtained from the experimental programme is presented in Chapter 9.

7.8.6 Generated particle pressure

The other significant influence on the results was the pressure generated by the rotating blades on the biomass particles. The design value of 5×10^5 Pa was not always achieved. Estimates for the pressure generated from empirical results on single particle and wood rod experiments are detailed in Chapter 9.

7.9 Conclusions for the reactor and product recovery system

The reactor concept has been tested and proved effective in ablating wood particles, with throughputs of approximately 53% of the design capacity. Possible explanations for the lower biomass throughput have been discussed; the main reason for this was the lower density of biomass compared with the figure assumed in the original design procedure presented in Chapter 5. The product recovery system proved to be very effective after some initial modifications. Mass balances and product analyses are presented in Chapter 8.

Chapter 8. Experimental Mass Balances and Results Analysis

8.1 Introduction

This chapter presents the mass balances for 11 experimental runs with analyses of char, liquids and gas samples with results comparison where possible with other fast pyrolysis work. The chapter is structured as follows:

- basis for the determination of product yields [Section 8.2]
- product yields and mass balances [Section 8.3]
- selected char elemental analyses [Section 8.4]
- selected liquids analysis: elemental, GC-MS and HPLC analyses [Section 8.5]
- gas analyses by on-line infra-red, thermal conductivity and gas chromatography [Section 8.6]
- discussion of the results [Section 8.7]

8.2 Basis for the determination of product yields

Product yields are expressed on a dry ablatively pyrolysed wood basis. During operation, however, not all the wood is ablatively pyrolysed. A small proportion of the particles bypass the rotating blades and leave the reactor unconverted; some particles remain in the reactor but are slowly carbonised and remain in the reactor after shutdown. In addition, in some early runs [CR07 to CR11] some particles were partially dried and partially devolatilised in the product collection system due to contact with the hot product vapours in the char knock out pot as previously described. The assessment method for ablative char and the mass balances are detailed in Appendix IV. The wood used was a typical pine wood used in the building industry, obtained in the form of 50 mm x 50 mm cross section lengths which were then cut, comminuted and sieved to a size fraction of 4.75-6.35 mm before use in the reactor. The dry wood composition is: carbon 49.84; hydrogen 6.09; nitrogen 0.05; oxygen [by difference] 43.54; sulphur trace; and ash 0.48.

8.3 Experimental mass balances

The product yields on a dry ablatively pyrolysed wood basis are shown in Table 8.01. Only the ablatively pyrolysed wood is used for the estimation of performance as in a scaled up system, the ablation phenomenon will be maximised: carbonisation and residual reactions will be minimised through process design and longer run times respectively. The volatiles contribution from non-ablated particles is estimated to be less than 4.3 wt% to the total volatiles yield. Therefore, although the closure values presented in Table 8.01 are slightly high, they are realistic and achievable yields.

Table 8.01

Mass balances for the ablative pyrolysis reactor [yields, dry ablatively pyrolysed wood basis]

Run number	CR09	CR14	CR15	CR13	CR07	CR08
Reactor surface temperature [°C]	456	458	501	505	550	550
Wood H_2O [wt %, dry basis]	2.86	1.37	1.2	1.21	2.44	2.08
Gas/vapour temperature [°C]	318	323	350.3	278	389	366
Reactor pressure [kPa, abs.]	101.9	101.3	100.4	100.4	91.0	101.9
Run time [min]	45	27	35	18	15	33
Ablated wood [wet]	260.4	117.2	301.7	264.6	412.4	1003.1
Residence time of gas/vapour products [s]	2.45	5.83	6.57	2.73	2.83	2.02
Char	12.8	18.8	22.1	12.2	13.8	21.1
Organic liquid	60.3	50.4	41.4	56.6	58.3	48.6
Water	17.7	20.3	17.4	24.5	22.7	10.3
Gas [N_2 free]	10.0	5.8	6.0	12.9	9.0	6.6
Closure	100.7	95.4	86.9 *	106.2	103.8	86.6 ∞

Run number	CR11	CR16	CR12	CR06	CR10
Reactor surface temperature [°C]	550	551	554	597	602
Wood H_2O [wt %, dry basis]	1.86	0.36	3.21	9.25	1.99
Gas/vapour temperature [°C]	294	289	418	415	368
Reactor pressure [kPa, abs.]	101.6	100.5	100.9	76.0	102.7
Run time [min]	15	41	21	12	14
Ablated wood [wet]	370.2	284.9	480.9	441.4	384.3
Residence time of gas/vapour products [s]	1.97	--	0.76	5.85	1.75
Char	13.7	15.9	10.9	12.6	12.4
Organic liquid	55.4	46.9	63.0	47.4	65.9
Water	18.1	13.7	11.4	25.7	11.5
Gas [N_2 free]	8.5	2.24	10.2	9.3	9.2
Closure	97.5	78.8 *	98.6	95.0	98.9

∞ bypassing of cotton wool filter * leak from feeder

Mass balances for other fast pyrolysis processes are given in Table 8.02 for comparison purposes.

Table 8.02

Comparison of fast pyrolysis mass balances [yields, wt% % dry wood basis]

Group Feedstock	Organic liquids	Char	Gas	Water	Total liquids	Closure	Temp. [°C]	Ref.
Aston University								
Pine wood [CR10]	65.9	12.4	9.2	11.5	77.4	98.9	602	
NREL								
Aspen poplar	--	--	--	--	64.3		500	184
Aspen poplar	55.4	13.1	13.8	11.8	67.2	94.1	625	47
Waterloo University								
IEA poplar	65.8	7.7	10.8	12.2	78.0	96.5	497	288
Poplar	51.1	8.9	19.0	17.8	68.9	96.8	600	289
Ensyn Technologies Inc.								
maple		16.6	10.9	--	72.6	100.1	500	290
poplar		17.0	10.0	--	73.0	100.0	500	290
poplar		9.0	27.8	--	63.2	100.0	600	290
IEA poplar		7.5	32.9	--	61.7	102.1	650	108
Georgia Tech Research Institute								
wood	60.0	12.0	10.0	18.0	78.0	100.0	550	291
Twente University								
softwood	10.0	31.0	15.5	35.5	66.5	92.0	600	244
Leeds University								
pine wood	43.3	17.2	14.3	24.7	68.0	99.5	550	292

It can be seen that the product yields are comparable with those obtained for other fast pyrolysis processes. The mass balance closures are generally good and those greater than 105% are due to the small contribution of volatiles from non-ablated wood. The organic liquid yield for CR10 is comparable to the best result obtained for untreated wood achieved by the University of Waterloo of 69.54 wt% organics (106). All of the product yields for the work described in this thesis are by direct measurement and recovery and no yields were assumed or calculated on a "by difference" basis [see Appendix III].

8.4 Char yields and analysis

The ablative char yields for this work are generally comparable to those of other fast pyrolysis processes as shown in Table 8.01. Char analyses were carried out, since, in a scaled up or commercial pyrolysis system, the product char would probably be used for the generation of process heat for drying of the feedstock prior to pyrolysis or heating of the reactor. Char is present in the reactor after a run, the product collection system and the condensed liquids. Char was recovered from the product collection system by washing the system with dry methanol and recovering the char by filtration. In some cases, a small quantity of the char, less than 0.5 wt% of the wood fed, was not filtered due to agglomeration after washing and subsequent drying. Product char was recovered from the raw condensed liquid by filtration and added to that recovered from the product collection system.

The reactor char is hygroscopic, adsorbing 3-5 wt% water if exposed to air for 24 hours. The core of large particles that passed through the reactor [> 2 mm] was unreacted wood. Detailed analyses for sieved reactor char produced at 550°C [CR16] and 600°C [CR10] are given in Appendix IV [Table IV.01]. Analysis of char for CR10 is compared in Table 8.03 with char analyses for other fast pyrolysis processes: CR10 was characterised by the highest organic liquid yield and had a good closure. Reactor char typically has a high carbon content due to prolonged heating after reactor shutdown with reactor surface char having a high carbon content, typically 85 wt% carbon.

Table 8.03
Analysis and comparison of fast pyrolysis chars (293, 106)

Analysis	C	H	O	N	S	Cl	Ash
Ablative Char, Aston University, pine wood [CR10]							
602 °C	82.53	3.10		0.09			
Ablative Char, NREL, softwood feed							
625°C	81.8	3.7	11.5	0.01	0.02	0.01	2.84
Fast Pyrolysis Char, University of Waterloo, poplar aspen feed							
625°C	73.16	2.33		0.43			9.5
541°C	69.99	2.80		0.30			6.5
500°C	66.77	3.90		0.35			3.2
465°C	59.28	5.25					2.0
425°C	55.13	5.48					3.4

From Table 8.03, the ablative char from this work has a higher carbon content than that of the NREL char from the vortex reactor system. The char produced in the fluid bed pyrolysis work of the University of Waterloo shows that the char carbon content increases with reactor temperature, although it is lower than that of the ablative pyrolysis char at similar temperatures [see Appendix IV]. This would imply that the ablative pyrolysis char is more highly devolatilised and hence more highly reacted.

8.5 Pyrolysis liquids analysis

8.5.1 Selection of analytical techniques

Analysis of the pyrolysis liquids is essential for their evaluation as a liquid fuel and as a potential source of chemicals. A variety of analytical techniques have been applied to the condensed liquids and the liquids recovered in methanol. Part of the analytical work was carried out in a collaborative study with Imperial College in London to assess the effects of reactor configuration on product yields and liquids composition from the ablative pyrolysis reactor and a wire-mesh reactor which is described in Appendix IB. The liquids have been analysed by several different methods:

- elemental analysis of the raw condensed liquids,
- Fourier Transform-infra-red [FT-ir] for the identification of functional groups,
- size exclusion chromatography [SEC] for the determination of molecular weight distribution of the pyrolysis liquids,
- ultra-violet [UV] fluorescence for the determination of chemical structural differences,
- gas chromatography-mass spectroscopy [GC-MS] for the quantification of a limited number of volatile components,
- high performance liquid chromatography [HPLC] for the quantitative identification of water soluble chemicals,
- Karl Fischer titration for water determination.

Details of the analyses for FT-ir, SEC and UV-fluorescence are given in Appendix IB. The results of the elemental analyses, Karl Fischer water determination, GC-MS and HPLC are detailed in the sections below.

8.5.2 Elemental analyses of the condensed pyrolysis liquids

The condensed pyrolysis liquids for some of the experiments have been analysed and the results are shown in Table 8.04. The elemental analyses of the condensed liquids are comparable to those from other fast pyrolysis processes.

Table 8.04

Elemental analysis of the pyrolysis liquids [wt% dry basis, water yields on a wet basis]

Reactor temp. [°C]	C	H	O	N	H/C molar	Specific gravity	H_2O [wt %]	Ref.
NREL								
450-500	48.6	7.2	44.2	<0.1		--	--	295
480-485	53.3	6.2	39.6	--	1.38	1.28	16.1	91
500	57.3	6.1	34.9	1.3	1.27	1.22	17.0	184
Georgia Tech.								
424-477	52.1	6.2	41.4	0.2	1.42	1.27 *f*	11.0	91
Waterloo University								
500	51.8	6.7	41.3	0.2	1.55	--	--	72
500	65.9	6.1	28.0	<0.1	1.12	1.11 ø	24.3	295
500	55.2	6.1	38.7 §	--	1.33	--	--	296
500	55.1	6.4	32.2	--	1.39	1.23	19.2	184
Ensyn Technologies Inc.								
510 *	55.5	6.7	37.7	0.1	1.45	1.21 ≈	23	259
Raw condensed liquids from this work								
450-CR14	46.8	7.0	46.2	0.0	1.11		30.6	
500-CR13	52.5	6.7	40.7	0.0	1.31		31.9	
500-CR15	47.7	7.1	45.2	0.0	1.12		33.5	
550-CR16	47.5	7.1	45.4	0.0	1.12		26.8	
600-CR06	53.4	6.3	40.3	0.0	1.41		17.8	

f at 23°C ≈ at 25°C ø at 55°C § by difference

8.5.3 FT-infrared spectroscopy of the pyrolysis liquids

FT-ir is a fast scanning, medium/high resolution, high signal-to-noise ratio, non-destructive analytical technique which is routinely used to ascertain the presence [or absence] of specific functional groups in pyrolysis liquids and to identify spectral features of certain classes of organic compounds by comparison with neat, or mixtures of, authentic samples, or by reference to an FT-ir spectral library. It does not, however, give information about the number of atoms [e.g. H, C, O, etc.] present. Since C, H and O are the main constituent elements of biomass and its thermally derived products, analysis of FT-ir spectra [in the mid-infrared

region, 4000 cm^{-1} - 200 cm^{-1}] of pyrolysis oils provides a quick and simple qualitative technique to identify the major organic classes present: saturates, unsaturates, aromatics and oxygenates. The results and their discussion may be found in Appendix IB. The liquid products have similar chemical groups to those obtained by other researchers with some minor structural differences. Characterisations by size exclusion chromatography and FT- infrared spectroscopy have suggested greater extents of secondary reactions in liquids from the ablative pyrolysis reactor which show lower degrees of substitution of aromatic structures. This may be due to the formation of lighter organic chemicals during slower heating of a small proportion of the feedstock in the reactor, as a consequence of non-optimised reactor operation, or as a result of cracking of lignin-derived macromolecules form the reactor heated surface. Comparison of the ablative liquids with those from other ablative pyrolysis reactors show similar trends in molecular mass distributions and structures suggesting that the ablative pyrolysis process inherently cracks some liquids during volatilisation (184).

8.5.4 Molecular mass distributions of the liquids

The use of size exclusion chromatography allows two analytical results to be obtained: analysis of chemical structures and the determination of the molecular weight distribution of the pyrolysis liquids. The degree of liquid cracking can be assessed, either to lower molecular weight liquids or to gases by the concentration of low molecular weight liquids. The analyses of McKinley on fast pyrolysis liquids are compared in Table 8.05 (184).

Table 8.05

Comparison of molecular weight distributions of liquids obtained from different reactors

Temperature [°C]	Number Average [Da]	Weight Average [Da]
Run CR07 [pine]		
550	240	360
NREL [IEA poplar]		
500	340	450
University of Waterloo [IEA poplar and aspen poplar]		
504	460	740
500	410	640
University of Western Ontario [IEA poplar]		
700	330	510

A lower number and weight average was obtained for the pyrolysis liquid from run CR07, suggesting secondary reactions produced smaller molecular weight liquids, i.e. by gas phase reaction or initial cracking upon vaporisation from the reactor surface. The differences between this work and the NREL vortex reactor products are less noticeable than the differences between this work and that of the University of Waterloo. It would appear that the long residence time for the product vapours in CR07 led to a significant reduction in the quantity of large molecular components, possibly by secondary condensation reactions. From HPLC work presented in Section 8.6 large quantities of low molecular weight liquids such as formic acid and related compounds were detected.

8.5.5 GC-MS of the liquids

The techniques detailed in Sections 8.3 and 8.4 allow the identification of differences in the chemical structures of the liquids. The use of analytical techniques such as those described in the following sections allow the quantification of actual chemical compounds in the liquids.

Gas chromatography-mass spectrometry [GC-MS] involves the separation and measurement of ions according to their mass-to-charge ratio. Both molecular weight and molecular formulae are readily determined using very small quantities of material in this destructive analytical method. Fragmentation of the molecules gives rise to ions leading to information about the structure of the parent molecule. This method is useful for volatile and non-volatile compounds, liquids and solids using appropriate ionising sources. Samples are introduced directly into the spectrometer either via a heated inlet [for volatile liquids] or directly using suitable probes for volatilisation. In GC-MS, volatile liquids are injected first into a gas chromatographic system to separate [by a chromatographic column] them into fractions which are carried through [by a carrier gas] into the ion source of the MS spectrometer. Analysis of minute quantities eluting from the column is therefore feasible using the mass spectrometer acting as a mass/charge detector. GC-MS allows a liquid to be rapidly "finger-printed" to allow initially a qualitative comparison of liquids obtained from different feedstocks or comparison of liquids produced under widely varying process parameters, i.e. different residence times or reactor temperatures. Only limited quantification is possible due to the instability of certain chemicals upon vaporisation and considerable experience is required in the interpretation and quantification of the peaks identified.

The detailed analysis has been performed by the University of Waterloo, Canada, using a mass spectrometer, FID detector, column DB-5 with average response factors obtained by direct injection of phenol, guaiacol, eugenol and vanillin. Sample traces for run CR08 and CR13 are shown in Figure 8.01 and 8.02 respectively with a tentative chemical identification listed in Table 8.06 for the peaks indicated.

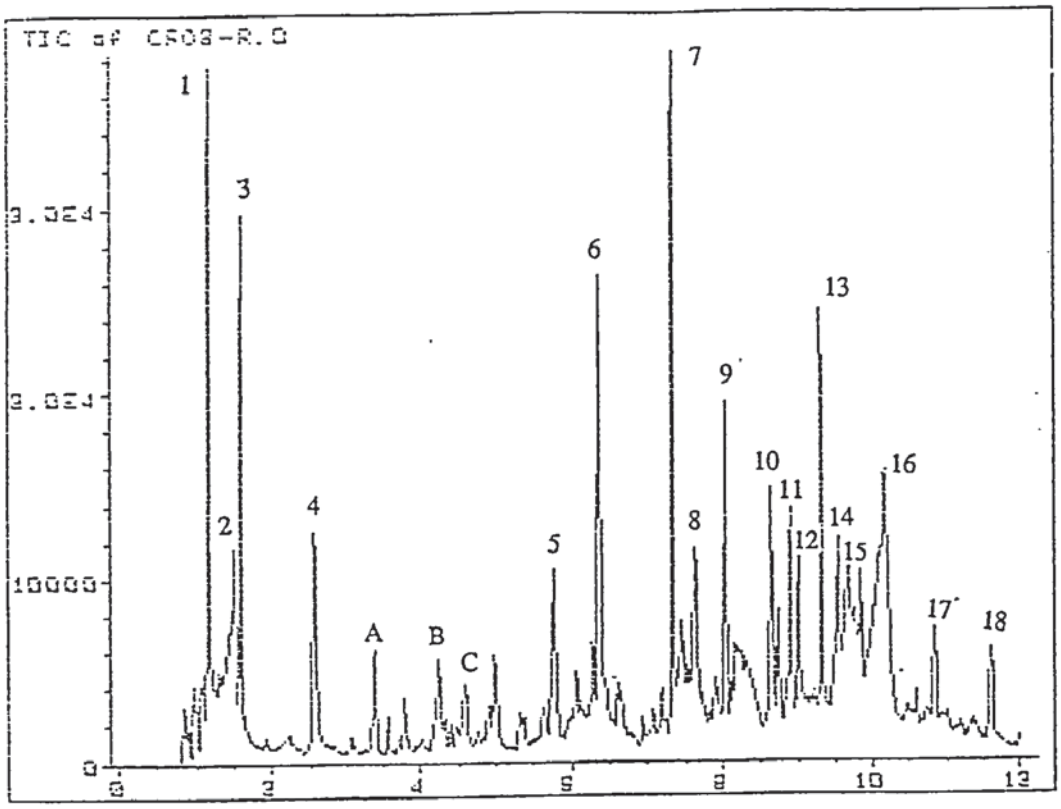

Figure 8.01. GC-MS analysis of the raw liquids for run CR08

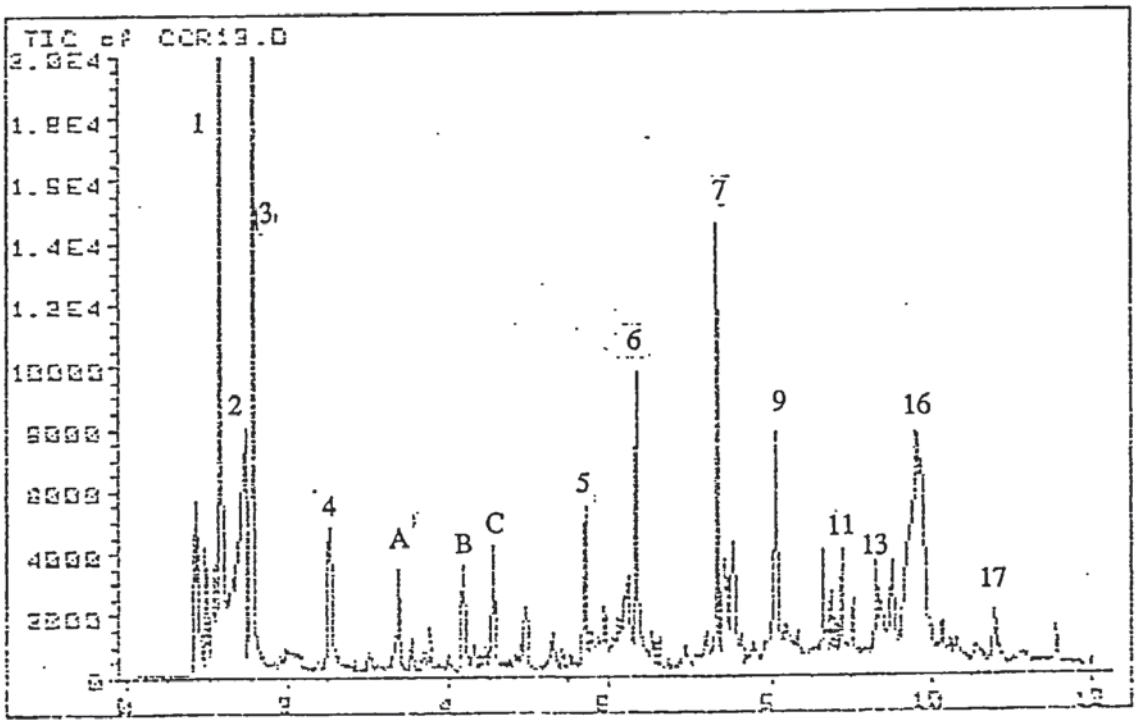

Figure 8.02. GC-MS analysis of the raw liquids for run CR13

Table 8.06

Peak identification in the ablative pyrolysis liquid-peak number and respective chemical component

1.	hydroxyacetaldehyde	10.	phenol, 2-methoxy-4-(2-propenyl)
2.	acetic acid	11.	benzaldehyde, 4-hydroxy-3-methoxy
3.	acetol	12.	phenol, 2-methoxy-4(1-propenyl)
4.	hydroxypropanal [?]	13.	phenol, 2-methoxy-5(2-propenyl)
5.	1,2-cyclopentanedione, 3-methyl	14.	ethanone, 1-(4-hydroxy-3-methoxyphenyl)
6.	2-cyclopenten-1-one, 2,3,4 trimethyl	15.	anhydrosugar [anhydroglucofuranose?]
7.	benzene, 1,4 dimethoxy	16.	levoglucosan
8.	*no match found*	17.	benzene acetic acid, 4-hydroxy-3-methoxy
9.	phenol, 4-ethyl-2-methoxy	18.	benzene, 1,2-dimethoxy-4-(2-propenyl)

Others

A.	2-furancarboxaldehyde	B.	2(3H)-furanone	C.	angelicalactone

The GC-MS trace for CR08 raw condensed pyrolysis liquid contains roughly 1% lignin derived peaks which are monoaromatic. There are few di-methoxy phenols in the liquid indicating that the feedstock is coniferous as coniferous wood lignins contain exclusively guaiacylpropyl units (1-methoxy) whereas deciduous wood lignins contain both guaiacyl- and syringylpropyl (di-methoxy) moieties (28). The peak 18 is however a syringyl moiety. The traces show similar chemical components to those obtained by Faix et al. by GC-MS for wood derived products (297).

8.5.6 High Performance Liquid Chromatography [HPLC]

This chromatographic technique can be used to analyse extremely small concentrations of compounds separately, or in mixtures, using highly sensitive detectors. The components of a mixture are separated on a packed column according to the magnitude of their interaction with the packing [solid] material and the mobile [liquid] phase. Specifically, analysis of degradation products of biomass, e.g. sugars, alcohols, aldehydes, etc., can be achieved on reversed-phase columns using a combination of specific properties [e.g. UV absorption] and universal bulk properties [e.g. refractive index] for detection purpose. This is a non-destructive method of separation which can be applied to neutral, ionic, low and high molar mass solutes present in aqueous or organic phases. It is, therefore, ideally suited to pyrolysis liquids since these

comprise a complex mixture of several classes of organic compounds with widely different volatilities, and chemical and thermal stabilities: separation is normally carried-out at ambient temperatures and does not therefore interfere with the physical and chemical nature of the liquid. The separated fractions can be isolated for further examination by other techniques.

The analyses have been performed by the University of Waterloo, Canada, using an Aminex HPX 87H column, isocratic 0.007 N H_3PO_4 as the eluent at a flow rate of 0.8 ml/min and a temperature of 65°C using a Waters R401 refractive index detector using n-propanol as the internal standard. Quantitative values are given in Table 8.07 compared with results for the University of Waterloo and NREL (184).

The analyses presented in Table 8.07 do not allow any immediate trends with temperature to be made. Again effects of process parameters and feedstocks will influence the yields of products. Recovery of the products from methanol proved to be very difficult due to the loss of low molecular weight compounds such as acetic acid. The formation of levoglucosan is favoured by low pyrolysis temperatures of less than 500°C [depolymerisation] and the formation of hydroxyacetaldehyde by higher temperatures, in line with the Waterloo reaction pathways and trends [see Figure 2.10]. In the analyses shown, the ratio of levoglucosan to hydroxyacetaldehyde is 1.3 at 500°C, decreasing to 0.6 at 600°C. The gas/vapour product residence time is longer than those typically used to preserve certain chemicals and secondary condensation reactions may have occurred.

8.6 Pyrolysis gas analysis

The dry pyrolysis gases after drying were analysed by two methods: on-line [continuous sampling] and batch sampling [for GC analysis]. The on-line analysis allowed any possible variation in the gas composition with time to be monitored. The dried product gases were analysed on-line for CO, CO_2, CH_4 and H_2. Batch samples were used to compare the on-line analyses during steady state operation and allow for the determination of higher hydrocarbons up to C_4 gases.

GC and on-line analyses are presented in Table 8.08. The on-line gas analysers have a higher degree of error as they were originally used for a downdraft gasifier. The gas analysers have a large span compared to the gas quantities being analysed: CO_2: 35 vol.%, CO: 30 vol.%, CH_4 :10 vol.% and H_2: 20 vol.%. The pyrolysis gas concentration is usually less than 5 vol.%, therefore errors at low gas concentrations can become significant, as CO and CO_2 comprise over 90 vol.% of the pyrolysis gas products. The gas analysis by GC are more reliable and are given in Table 8.08 where possible. GC analyses for some runs were not carried out due to the non-availability of the equipment.

Table 8.07

Composition of pyrolysis liquids obtained by fast pyrolysis of wood [yields, wt% moisture free feed] (184)

	Waterl 1	Waterl2	NREL	CR09	CR13	CR07	CR06
Feedstock	poplar	maple	poplar	pine	pine	pine	pine
Moisture content	0	5.9	4.6	2.86	1.21	2.44	9.25
Particle size, mm	3.00	0.59	1.00	5.55	5.55	5.55	5.55
Temperature, °C	504	508	500	457	500	550	597
Pressure, bar	1	1	1	1.02	1.0	0.91	0.76
Residence time, s	0.48	0.47	0.75	2.45	2.73	2.83	5.85
Total liquids	77.0	77.2	64.3	80.2	82.1	83.0	79.9
Char	11.8	13.7	12.0	13.7	12.3	14.1	13.8
Non condensable gas	11.0	9.8	16.0	10.3	13.0	9.2	10.2
Closure	99.8	100.7	92.3	103.6	107.5	106.3	103.8
Some constituents in liquid [based on % weight of constituent in pyrolysis liquid]:							
Glycolic acid	0.55	0.66	0.54				
Glyoxal				0.8	0.32	0.55	0.3
Formic acid	1.48	1.48	0.97	6.03 *	4.72 *	5.62 *	1.33 *
Acetic acid	3.09	2.89	4.08	0.04	1.36	tr.	0.35
Levoglucosan	1.02	1.50	1.99	4.24	3.32	3.66	0.99
glycolaldehyde/HAA				3.81	2.65	4.36	1.7
cellobiosan				trace	0.02	0.26	0.22
Acetol	2.85	1.75	4.08	1.11	1.61	2.65	0.57
2-Furaldehyde	0.46	0.37	0.66				
2 cyclopenten-1-one							
2,3,4 trimethyl				0.02	0.34		0.22
benzene, 1,4 dimethoxy				0.02	0.39		0.26
phenol, 4 ethyl, 2 methoxy					0.18		
phenol, 2 methoxy-5(2 propenyl)					0.18		

* includes formaldehyde

Table 8.08

Comparison of pyrolysis gas analysis: this work and results from other fast pyrolysis processes [N_2 free basis, % vol.] (106, 198, 238)

Gas	H_2	CO	CO_2	CH_4	C_2H_4	C_2H_6	C_3H_6	C_3H_8	C_4H_8
Aston University [GC results]									
456°C [CR09]	tr.	44.2	55.8	tr.					
458°C [CR14]	--	49.1	45.4	4.8	0.75			0.04	
501°C [CR15]	--	47.6	43.7	7.1		1.0	0.66 $		
505°C [CR13]	--	44.4	48.6	5.9	0.02	0.55		0.49	0.08
550°C [CR07]	--	45.4	45.1	6.4					
550°C [CR08]	0.8	47.9	47.2	4.9					
550°C [CR11]*	8.5	43.4	41.6	6.5					
551°C [CR16]*	4.5	57.2	25.2	9.3					
554°C [CR12]*	4.5	52.6	35.1	7.9					
597°C [CR06]	0.1	38.5	47.7	8.5	1.54	0.8	3.1		
602°C [CR10]	3.6	52.0	36.1	5.7	1.2	1.0		0.4	
NREL [Run 34]									
625°C	3.4	46.2	43.1	4.6	1.3	0.3	0.4	0.1	0.3
Colorado School of Mines [Run 111]									
600°C	3.0	44.4	30.5	14.8	3.1	1.9	1.7	0.3	0.3
Waterloo [Run 13]									
500°C	5.9	57.8	26.2	8.4	1.6	0.1	0.1		

* Gas analyser results $ [$C_3H_6 + C_3H_8$]

The results for the different reactor temperature on a mass yield basis may be found in Appendix IV. It has been proposed that the reactor temperature during fast pyrolysis is the most significant influence on the composition of the gas products (84). For comparison with an analogous reactor to the rotating blade approach, the work of Reed and Cowdrey from the contact pyrolysis mill was chosen: the ratios of the mass yields of CO/CH_4, CO/CO_2 and $CO/(C_2H_4+C_2H_6)$ are shown in Figure 8.03 (238). To compare the extensive results compiled by Scott et al. the yields of CH_4 and CO with temperature were plotted as shown in Figure 8.04. The results for CH_4 and CO are similar to those obtained for the poplar and maple in a fluid bed reactor while the results for the ablative plate pyrolysis reactor and the contact

pyrolysis mill show similar qualitative trends. In the pyrolysis mill of Reed and Cowdrey, the yield of CO is higher at low disk temperatures of 450°C, but rapidly reaches a ratio similar to this work. In the contact pyrolysis mill, the ratio of carbon monoxide formation is higher suggesting that there may was some cracking of the primary product to non-condensable gases. This is confirmed by the lower liquid yields which have been reported in their work. The hydrogen yields from the ablative pyrolysis reactor are only significant at temperatures of 600°C and short residence times. The degree of cracking of product vapours to non-condensable gases appears to be low in this work due to the reduced gas/vapour product temperatures.

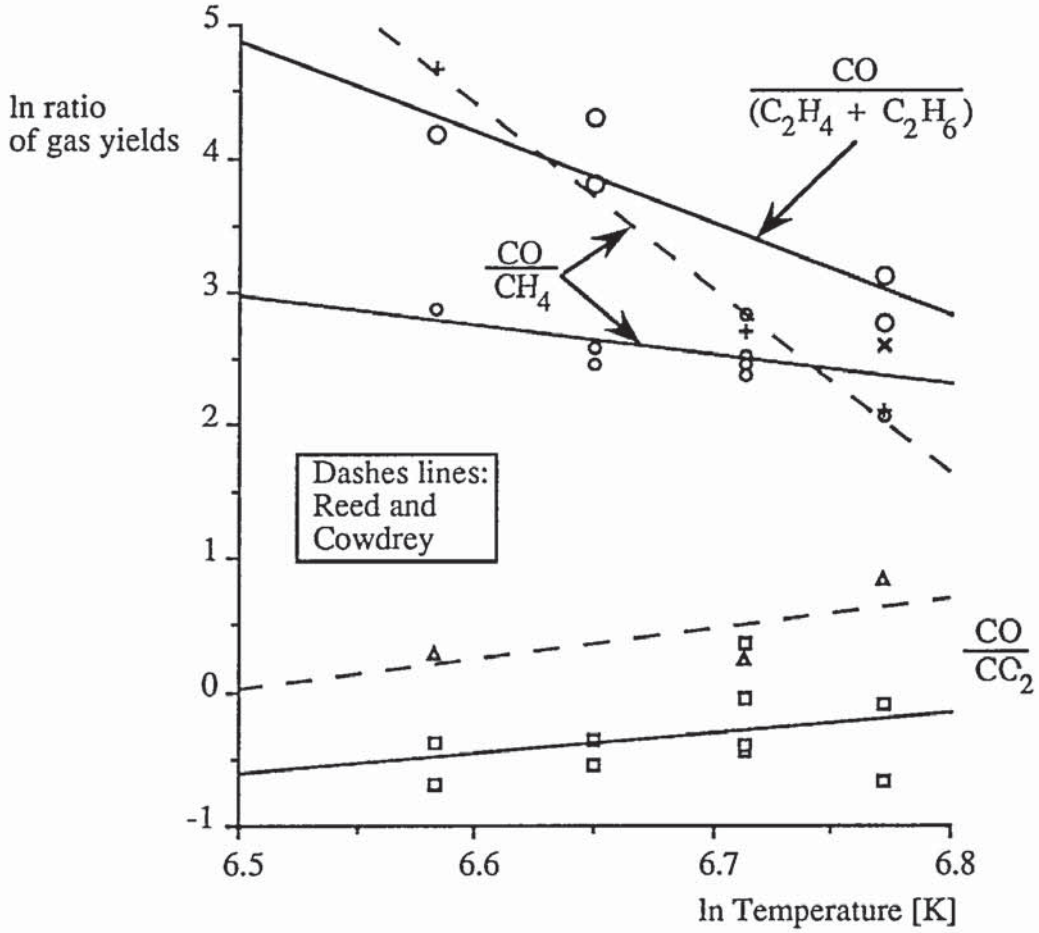

Figure 8.03. Comparison of the ratios of gas product for different reactor temperatures for the contact pyrolysis mill and the ablative plate reactor

CO_2 is seen as a primary pyrolysis product, formed during the initial decomposition of cellulose and hemicellulose which is a lower temperature route reaching a maximum around 450°C (84). With increasing reactor temperature, the formation of CO gradually increases. The formation of CO_2 as a primary pyrolysis product has been reported by Diebold (205) and Graham (39) as "prompt" gas. They have determined that under fast pyrolysis conditions approximately 4 wt% of the pyrolysis products are prompt gas consisting mostly of CO_2.

Results [not plotted] from the fluid bed pyrolysis reactor of Scott et al. for residence times less than 1 second show similar qualitative trends in gas compositions for similar reactor temperatures (62). For a comparison of the CH_4 and CO yields, the results of the University of Waterloo were compared in Figure 8.04 below. The ratio of CH_4 and CO are in very good agreement with the results of Scott et al. despite different reactor configurations, modes of heat transfer and feedstocks (62).

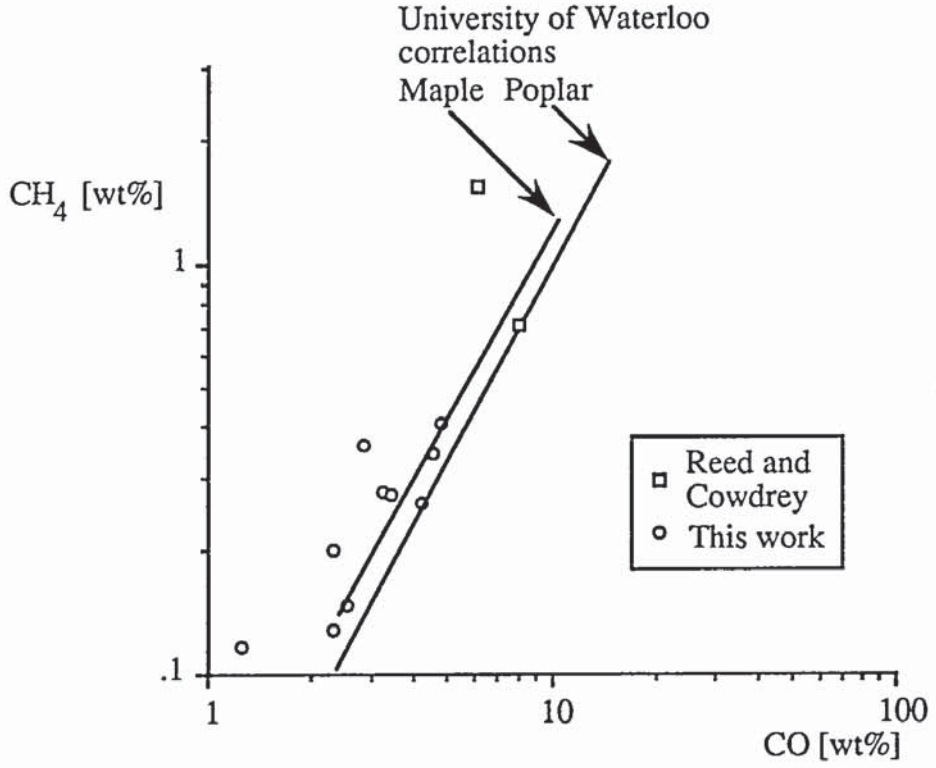

Figure 8.04. Comparison of CH_4 and CO yields for the ablative plate reactor and the Reed and Cowdrey pyrolysis mill with the University of Waterloo correlations for maple and poplar

The comparison of the wt % yield of CO and CH_4 are similar to those obtained by Scott et al. for poplar and maple, despite the differences in feedstock, reactor configuration, gas/vapour product residence times and particle size (57). This also shows that the gases are being produced under fast pyrolysis conditions. The differences for some of the runs are due to runs with low mass balance closures. The limited results from the work of Reed and Cowdrey do not allow any definite conclusions to be made. It is believed that the vapours were significantly cracked in the hot reaction zone before recovery. If the key requirements for fast pyrolysis can be achieved, then the same quantitative yields and compositions can be obtained. Differences will be due to the intrinsic nature of the feedstock and catalytic effects of ash and/or additives in the biomass.

8.7 Results discussion

8.7.1 Mass balances

The mass balance closures from the ablative pyrolysis reactor are generally very acceptable with low closures for three runs due to operational problems. The product collection system proved to be very effective in separating and recovering the products. The organic liquid yields from the work equal those of any other fast pyrolysis process using an untreated feedstock. The average mass balance closure for the runs, where there were no losses, was 99.5 wt%.

8.7.2 Char yields

There are three principal solid products: ablatively produced char, non-ablated wood and slowly carbonised char. As the optimisation of the reactor continued, the quantity of non-ablated char was continually reduced. From Table 8.01, the average ablative char yield during the experimental program was 15.1 wt% on a dry ablated wood basis, slightly higher than those obtained from fast pyrolysis process as shown in Table 8.01. The char has a higher carbon content than any other primary product char suggesting that it is highly reacted.

8.7.3 Organic liquid yields

The product yields were expressed on a dry ablatively pyrolysed wood basis. The reasoning was explained in Appendix IV and, as further operational optimisation is carried out, the amount of non-ablated material will be continually reduced. The actual contribution of the non-ablated material was very small and estimated to be a maximum of 3.7 wt% of the wood fed to the reactor or 4.3 wt% of the total volatile yield.

The highest organic liquid yield was obtained at 600°C-65.9 wt%. This is comparable to the high organic liquid yields obtained by the University of Waterloo-69.54 wt% for a non-pretreated wood feedstock (106)]. The yield was also much higher than that from the NREL vortex reactor for a similar temperature - 54.3 wt% at 625°C.

The high liquid yields were achieved by rapidly cooling and diluting the product vapours with nitrogen as soon as they had been produced in the reactor. The organic liquid yields for some runs were reduced, due to secondary condensation reactions which can occur below 400°C [see below]. As discussed in Appendix IV, the contribution of volatiles from the non ablated material is an average of 4.3 wt% of the total volatile yield, believed to be as carbon dioxide and water. The organic liquid yields are therefore realistic and are justifiably represented on an ablated wood basis only.

The normalised results for organic liquid yields and the water of pyrolysis are plotted in Figure 8.05. The results shown in Table 8.01 were normalised to allow a better comparison and evaluation of the product yields with residence time. The water of pyrolysis is defined as the total water in the product liquids less the original feed water. As discussed in Appendix IV, there is a small contribution from the non-ablated feedstock to the overall volatile yields which cannot be accurately quantified. Assuming that the contribution from this non-ablated material is constant for all temperatures the minimum asymptotic yields of organics is estimated to be 47 wt% organics and the maximum asymptotic water yield is estimated to be 24 wt% at residence times up to about 10 s. This is of interest for future reactor design with a particular specification for gas/vapour product residence times and temperature.

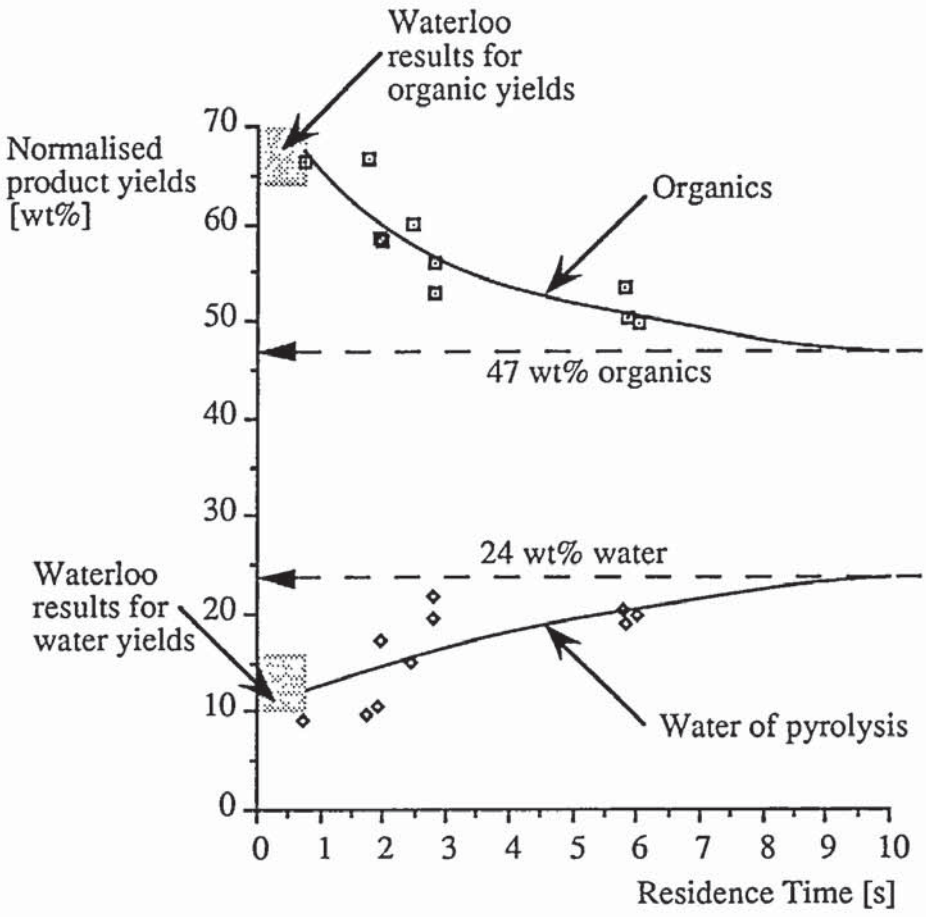

Figure 8.05. Normalised yields of organics and water of pyrolysis with residence time, gas/vapour product temperature range 280-420°C

The gas/vapour product temperature in the ablative pyrolysis reactor is too low. To minimise the yield of water during further experiments, the nitrogen used to dilute the product vapours will be heated to 400°C before entering the reactor operational volume. This will both lower the residence time, moderate the gas/vapour phase temperature and improve the yields of organics.

8.7.4 Water yields

The typical yield of water from fast pyrolysis processes is 12 wt%, as shown in Table 8.01. The water of pyrolysis yields are high [> 12 wt%] for eight of the runs due to long residence times leading to secondary gas phase condensation reactions. As shown in Figure 8.05, increasing residence time increases the water yields. The organic liquid yields also showed a corresponding decrease. From Figure 8.05, run CR12 gave the lowest water yield of 8.9 wt% at 418°C, 0.76 s gas/vapour product residence time. Further work is required to allow the more accurate prediction of water of pyrolysis yields with gas/vapour product temperature and residence time to aid in the optimisation of improving liquid quality in terms of its homogeneity, water content and composition.

8.7.5 Non-condensable gas yields

Gas yields from fast pyrolysis processes are approximately 12 wt% at reactor temperatures of around 500°C and residence times less than 1 s. The yields of gas are reasonable due to cooling and dilution of the products. Since the reactor is not operated isothermally, there is no additional energy supplied to crack the product vapours to CO, H_2 and higher hydrocarbons. At gas/vapour phase temperatures less than 500°C, minimal secondary cracking occurs [see Chapter 3]. Secondary reaction due to vapour contact with hot char could occur, but there is no substantive evidence to support this. Yields of gases such as hydrogen and higher hydrocarbons is very low suggesting that liquids degradation to gases is minimal and only occurs during devolatilisation from the reactor surface at temperatures above 550°C. From the results presented in Tables 8.01 and 8.08, the gas compositions and yields are comparable to those from other processes. CO and CO_2 comprise about 90 vol.% of the products with lesser amounts of CH_4.

8.7.6 Liquids composition

As the major focus of this work is on the optimal production of organic liquids for their subsequent use as a fuel and/or a source of chemicals, detailed analysis of the liquids is essential. The condensed liquids have similar elemental compositions to those obtained in other work and the chemical composition is also very similar with decreasing concentrations of anhydrosugars in favour of fragmentation compounds such as formic acid, hydroxyacetaldehyde and acetic acid with increasing reactor temperature. High yields of formic acid and formaldehyde at 450-550°C would imply that there is a high degree of liquid cracking to low molecular weight liquids on the heated reactor surface.

Chapter 9. Evaluation of the Ablative Pyrolysis Reactor

9.1 Introduction

In Chapter 5 the reactor design methodology was presented and applied to the design of a nominal 5 kg/h ablative pyrolysis reactor. In Chapter 8, the mass balances for the experimental program were presented and discussed. This chapter examines and evaluates the original design equations and proposes a simplified design methodology. Data are presented for single particle and wood rod pyrolysis with measured ablation rates at different reactor temperatures, relative velocities and calculated contact pressures. This chapter is structured as follows:

- investigation of the key process parameters [Section 9.2]
- modelling of wood rod ablation [Section 9.3]
- new simplified design procedure [Section 9.4]
- evaluation of the reactor throughput: theoretical and actual [Section 9.5]
- gas/vapour phase kinetics [Section 9.6]
- conclusions for the reactor and reactor modelling [Section 9.7]

9.2 Investigation of the key process parameters

9.2.1 Introduction

To confirm or refute certain assumptions in the design procedure presented in Chapter 5, an analysis of the key design parameters and equations used was conducted. A range of experiments were also carried out to compare predicted ablation rates with measured ablation rates at a range of temperatures, using both single particle experiments and wood rod ablation experiments. Due to contractual requirements, the primary aims of this work were the design, construction and operation of the reactor and the product collection system to obtain mass balances for evaluation of the rotating blade approach used in the reactor. Time constraints did not allow a full series of experiments to be carried out at different applied pressures, relative velocities and reactor temperatures. The results will be used to direct future work [see Chapter 11].

A limited number of experiments were carried out with two objectives:

- individual particle experiments at 450, 500, 550 and 600°C to mimic actual reactor conditions and the estimation of single particle ablation rates in the ablative pyrolysis reactor,
- wood rod ablation experiments using a wood of similar dry density to that used by Lédé et al. [645 kg/m^3 compared to 720 kg/m^3 used by Lédé et al (51)] to validate theoretical estimation of ablation rates at 500°C in a comparable experimental configuration.

The first set of experiments were required as direct measurement of the contact pressure generated by the rotating blades on the particles during an experiment was not possible. As discussed in Chapter 6, an analysis of the mechanics of particle ablation could only be carried out using empirical data.. The results from the single particle and the wood rod ablation experiments would be used to:

- determine of ablation rates at 450 and 500°C to improve predictions for the ablation velocity V with reactor temperature,
- calculate the contact pressure generated by the rotating blades on single particles at four different temperatures based upon the measured ablation rates from the single particle experiments,
- confirm the results of Lédé et al which originally demonstrated that the rate of ablation varied with the relative velocity until an asymptotic value was reached,
- modify the reactor design methodology where necessary to account for new empirical results,
- estimate the heat transfer coefficient, biomass decomposition temperature and the heat fluxes obtained during the experimental work and compare the results with the original design methodology,
- estimate the usage of the available contact area below the rotating blades,
- compare the theoretical reactor throughput with the experimental results.

9.2.2 Experimental procedure for single particle experiments

The evaluation of ablation rates is an essential design requirement as the reactor throughput is directly proportional to the ablation rate. One of the constraints of the ablative pyrolysis reactor was that, during experimental runs, the actual pressure generated by the rotating blades on the particles could not be measured [see Chapter 6]. By performing single particle experiments in the reactor, individual particle ablation rates could be measured and the contact pressure generated by the rotating blade estimated.

The ablative pyrolysis reactor was operated with an open top and the reactor base heated to the desired temperature, monitored using type K thermocouples located at various points in the reactor base. The empty reactor interior was continuously purged with nitrogen to prevent volatiles combustion. A single blade mounted on the blade holder used during the experiments, angled at 10° relative to the reactor surface, was rotated at a relative velocity greater than 1.5 m/s. A previously weighed, dimensioned [uniform cuboid of measured length, breadth and height] and dried wood particle [dry density 396 kg/m^3] was dropped in front of the rotating blade and ablated for 5 s. The ablated particle was then rapidly removed from the reactor using a suction line after stopping the rotating blade. Twenty particles were used for each of the four different temperatures, ten for initial trails and 10 for detailed ablation rate measurement. The

particles were re-weighed and their dimensions re-measured and the ablation rate calculated. Observation of the particle orientation to the heated reactor surface was also made.

9.2.3 Results for the single particle experiments

The average ablation rates and their variation with reactor surface temperature are shown in Figure 9.01 and Table 9.01 for those particles which could be used. The highest individual particle ablation rate was 0.63 mm/s measured at 550°C. The standard deviation of the measured ablation rates at each temperature indicates that the average ablation rate varies by approximately 20% at each temperature.

Table 9.01
Average single particle ablation rates with reactor temperature

Temperature [°C]	450	500	550	600
number of usable particles	7	7	6	2
Average ablation rate [mm/s]	0.33	0.44	0.50	0.43
standard deviation	0.06	0.11	0.11	--

Variation in particle ablation rate may be accounted for by particles not beginning ablation immediately, changes in wood structure and grain orientation to the reactor surface causing differing heat transfer rates to occur and different resistances to movement by the rotating blades. Some of the particles were deformed during pyrolysis or broken up by the grinding action of the blades, predominantly at 600°C where 80% of the particles were broken up, possibly due to increased frictional resistance to motion as more of the products formed as vapours and not liquids. Approximately 5% of the particles were ablated non-uniformly and at angles to the wood grain, 15 % were ablated along the grain and 80% of particles were ablated across the wood grain.

From these simple experiments, it would appear that operation of the reactor at 550°C would give the highest ablation rates without particle break up. The importance of particle break up is that relatively large biomass particles could be comminuted by the rotating blades with subsequent rapid ablation of the fragments. The formation of "fragments" could, however, reduce the reactor throughput by preventing other particles entering below the blades. Further experiments are required to confirm this theory.

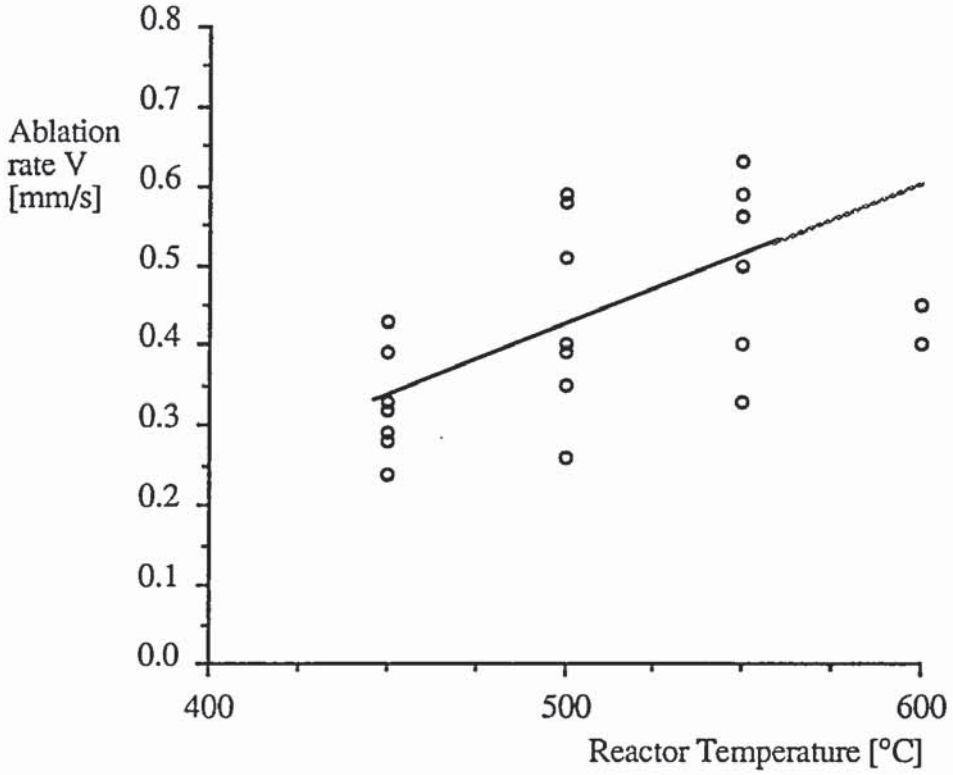

Figure 9.01. Variation of measured single particle ablation rates with reactor temperature, blade angle 10° relative to the reactor surface

From the measured single particle ablation rates shown in Figure 9.01, the blade angle of 10° was not generating the contact pressure required and hence the ablation rate originally specified from the design methodology of 1.3 mm/s for an assumed contact pressure of 5 x 10^5 Pa at 600°C was not being achieved. The significance of this to the throughput of the reactor is discussed in Section 9.7.

9.2.4 Experimental procedure for wood rod ablation experiments

To complement the single particle experiments, wood rod ablation experiments similar to those carried out by Lédé et al. [see Section 4.2] were performed. In this configuration, as shown in Figure 9.02, the wood rod was moved relative to the heated surface. The objectives of this complementary work were to:

- confirm the variation of ablation rate with relative velocity at temperatures below 600°C,
- determine the asymptotic ablation rate at 500°C to confirm prior theoretical estimations for the ablation rate V and for comparison with the single particle experiments previously described in Section 9.2.2,
- measure ablation rates similar to those obtained from the single particle experiments and calculate the pressure generated by the blades on the particles.

The variation of ablation rate with relative velocity and applied pressure was measured for wood rods, 6.35 mm in diameter rotated on the hot reactor base in a cylindrical holder with the contact pressure generated using a weight. The weight was suspended during rotation on a wire to prevent the weight from being imbalanced and pressing against the wall of the cylindrical guide tube. This is depicted in Figure 9.02.

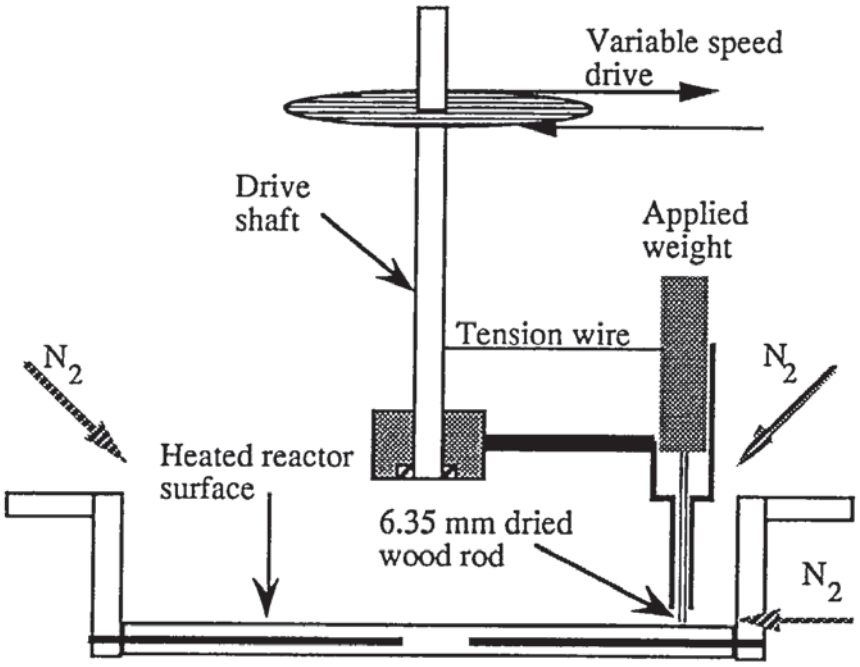

Figure 9.02. Wood rod ablation experimental set up

60 experiments were carried out for relative velocities varying from 0.1 to 1.97 m/s and the wood rod ablation rate measured. The wood rod was ablated for 60 s with the applied weight on top, the difference in length measured and the ablation rate calculated. Limited trials were conducted with an applied pressure of 385000 Pa and a relative velocity of 1 m/s as shown in Figure 9.03.

9.2.5 Results for the wood rod ablation experiments

A quick assessment was made of different applied pressures on the wood rod to give an estimate for the contact pressure which would give an ablation rate of 0.5 mm/s-the average ablation rate obtained at 500°C for the single particle experiments. A contact pressure of almost 200000 Pa was required [198770 Pa] to give an asymptotic ablation rate of 0.51 mm/s at 500°C. The results for variation of the ablation rate with relative velocity are shown in Figure 9.03.

It was evident that during ablation, the char/reaction layer was "thermally" pliable and the wood grain was visibly bent over a distance of 1-2 mm. At low relative velocities, the deformation of

the wood grain was more pronounced [2-4 mm into the wood rod] as more of the wood rod was allowed to heat due to reduced mechanical erosion of the char products and increased heat conduction. This suggested that the wood was undergoing a "phase change" or plastic stage. After cooling, ablation of the remaining partially reacted matrix proved extremely difficult with ablation rates reduced to 10% of their value for the same conditions using fresh wood. It is proposed that this partially reacted matrix is mainly lignin, which after going through an initial "plastic" stage becomes thermally stable. This is significant for ablative reactors where the particles are recycled after partial ablation, i.e. the partially reacted material imposes a significant resistance to ablation if allowed to cool and solidify. Completely reacted char is more friable and can be abraded off quite readily when the ablation rate is greater than 1.2 m/s.

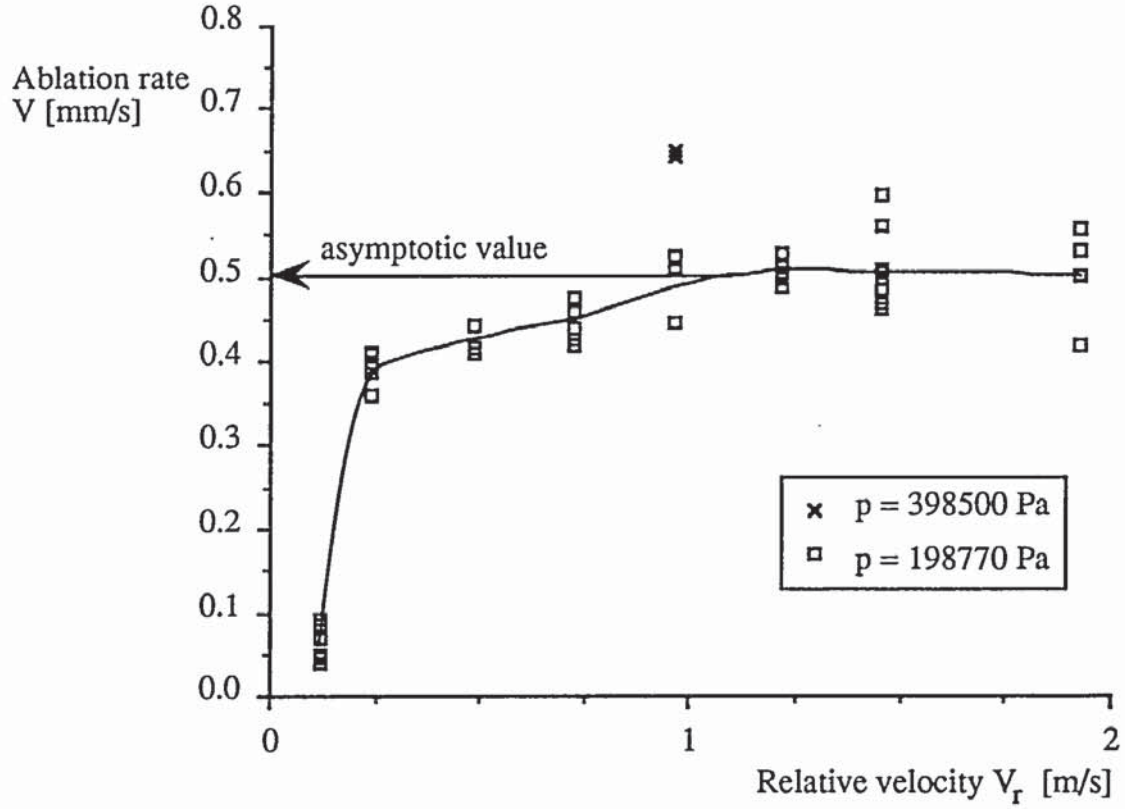

Figure 9.03. Variation of linear ablation rate with relative velocity for two contact pressures, 198770 Pa and 385000 Pa, T_w = 500°C, ρ_w = 645 kg/m^3

The determination of ablation rates below 600°C is an area requiring further work to improve reactor design procedures.

9.2.6 Estimation of the ablation rate, V and the ablation variable, Â

The ablation variable Â is calculated from the measured ablation rate V divided by the contact pressure for relative velocities above 1.2 m/s. The results of the single particle ablation and the

wood rod ablation experiments were described above. Based upon the wood rod ablation experiments, the theoretical calculation of the ablation rate and the actual measured ablation rate could be compared. The original equation for the prediction of V was:

$$V = \hat{A}p^F \qquad \{9.01\}$$

where:

$$V = (4.7317 \times 10^{-11} \times 10^{0.0020438\, T_w[K]}) \times p^{0.993} \qquad \{9.02\}$$

The calculated value using equation {9.02} for V using an applied pressure of 198770, and a temperature of 500°C was 0.33 mm/s: the empirically measured value from Table 9.01 was 0.51 mm/s, 155% higher than the calculated value. Measurement of the ablation rate at 455°C was 0.016 mm/s-apparently close to the lower limit for ablative fast pyrolysis. Comparison of the results of Lédé et al. are given in Figure 9.04 below based upon a ratio of the ablation rate and the measured pressure with temperature as this was the only basis on which the results from this work and that of Lédé et al. could be compared.

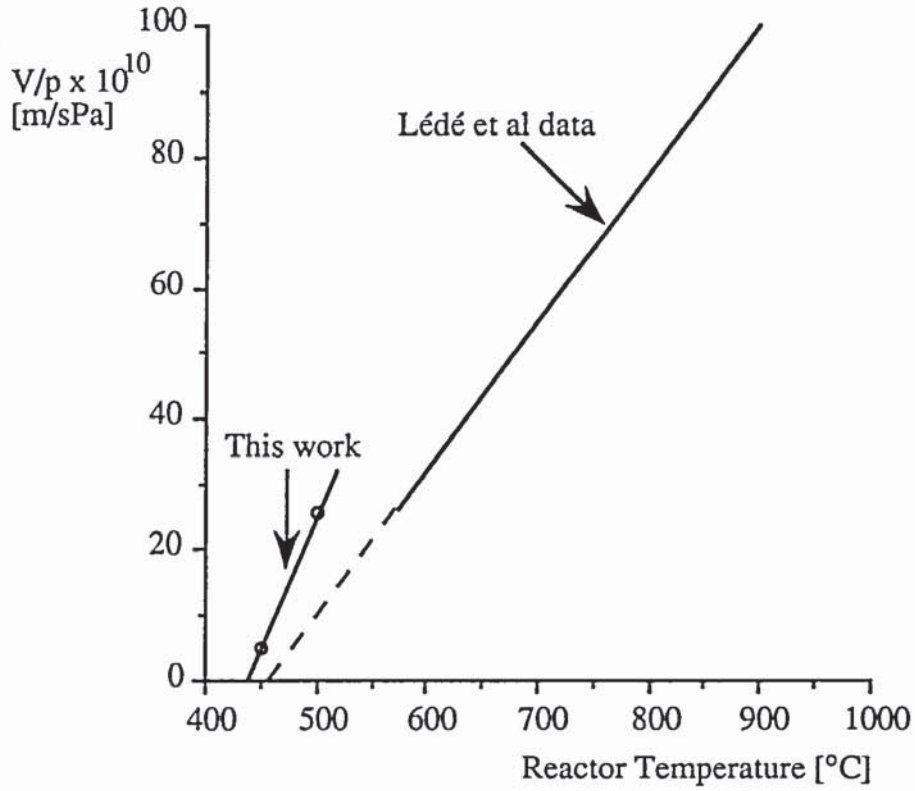

Figure 9.04. Variation of $^V/_p$ with temperature T_w. Comparison of measured values from this work and Lédé et al.

From preliminary data at 450 and 500°C, the ratio of $^V/_p$ is slightly higher than the empirical data of Lédé et al.; however the results exhibit similar trends. Preliminary results from Figure 9.04 would suggest that the minimum decomposition temperature, i.e. the temperature at which

the ablation rate V equals zero, under fast pyrolysis conditions, is approximately 435°C. The variation of the ablation variable Â with temperature was shown in Figure 5.01; new values from this work and the data of Lédé et al. are shown in Figure 9.05 below (51). Â was calculated using equation 9.01 and assuming F = 0.993.

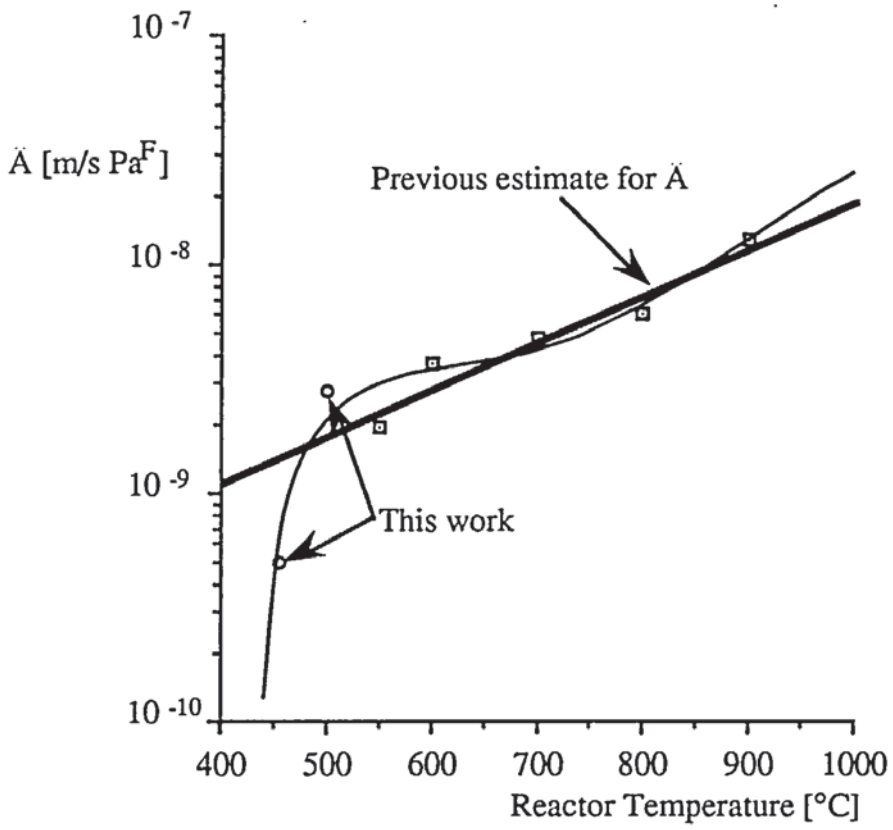

Figure 9.05. Variation of Â, the ablation variable with reactor temperature. Comparison with original estimation and data of Lédé et al.

The correlation for Â from Figure 9.05 is given as equation {9.03} where T_w is in °C:

$$\hat{A} = -9.262 \times 10^{-8} + 4.484 \times 10^{-10}[T_w] - 7.056 \times 10^{-13}[T_w]^2 + 3.7497 \times 10^{-16}[T_w]^3 \qquad R^2 = 0.98 \qquad \{9.03\}$$

Based upon equation {9.03} and assuming that F = 0.993, the average contact pressure generated by the rotating blades for the single particle measurements can be calculated. For the four temperatures studied, the calculated average contact pressures [based upon $p^{0.993} = V/\hat{A}$] are shown in Table 9.02 overleaf.

From these results, the highest contact pressures are generated at 450°C. However the ablation rates are minimal and the rate of liquid formation is low. Since the particles are being moved at relative velocities greater than 1.2 m/s, the liquid products form a very thin film on the reactor

surface and the action of the rotating blade generates a high contact pressure due to the high frictional resistance to motion.

Table 9.02
Results for the single particle experiments: calculated contact pressure

Temperature [°C]	450	500	550	600
Usable sample size	7	7	6	2
Average ablation rate [mm/s]	0.33	0.44	0.50	0.43
average contact pressure [Pa]	8.0×10^5	2.3×10^5	1.8×10^5	1.4×10^5

From the empirical data presented in Table 9.02, the frictional resistance of the particles can be estimated and also the thickness of the liquid product film upon which the biomass particles are sliding approximated. The force diagram for a uniform ablating wood particle is shown in Figure 9.06 where F_n [N] is the force generated on the particle by the blade, V_r is the relative velocity [m/s] and F_{fric} [N] is the frictional resistance to motion [N].

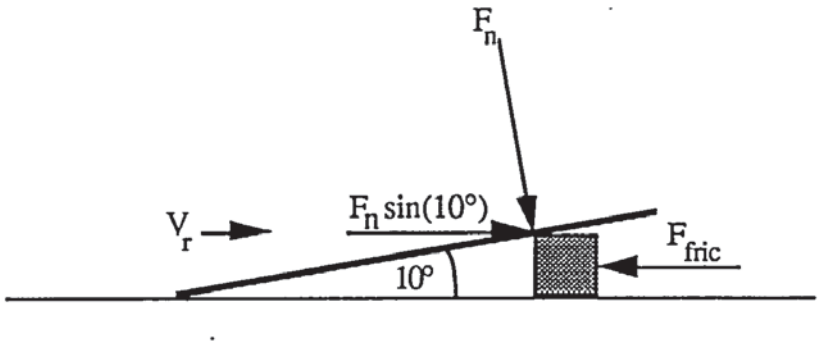

Figure 9.06. Force diagram for an ablating wood particle, blade angle 10° relative to the heated reactor surface, relative velocity > 1.2 m/s

Using the data presented in Table 9.02 for measured average ablation rates and applied pressures, the thickness of the liquid product layer and the frictional force exerted by the particles due to their resistance to motion is given in Table 9.03. The liquid film viscosity, μ_l, was assumed to be 0.07245 Ns/m^2 as estimated by Martin et al. (235). The frictional force was estimated by equations {9.04 and 9.05}:

$$F_n = \frac{p}{\cos(10) A_{pa}} \qquad \{9.04\}$$

$$F_{fric} = F_n \sin(10) \qquad \{9.05\}$$

The thickness of the liquid film, t_f [m] was then calculated from equation {9.06}:

$$t_f = \frac{A_{pa}\mu_l u_r}{F_{fric}} \qquad \{9.06\}$$

where u_r is the relative velocity of the particle [m/s], A_{pa} is the particle contact area [m^2] and F_{fric} is the frictional resistance of the particles to motion [N]. The values given in Table 9.03 are specific to the single particle experiments, but serve to indicate the possible range of pressures generated in the reactor during operation. The proportion of products which are produced directly as vapours or gases is not known and therefore the results could not be interpreted further for application to the reactor design.

Table 9.03

Estimated frictional force, F_{fric} and film thickness, t_f, for a uniform particle 5 mm x 5 mm

F_{fric} [N]	3.5	1.0	0.8	0.6
t_f [m]	6×10^{-7}	2×10^{-6}	3×10^{-6}	4×10^{-6}

The rate of liquids formation and deposition on the reactor surface at temperatures above 500°C is sufficient to lubricate the motion of the particles and consequently the pressure generated on the particles is reduced, although the ablation rate is increased due to the increased reaction rate. If this product film is allowed to evaporate before the biomass is applied on the same point on the heated surface, the contact pressures generated could be increased. From Table 9.03, it would appear that at 600°C the particles are well lubricated; therefore the reasons for the high mechanical comminution of the biomass to smaller particles is contrary to the predicted results. Reasons for the break up of the particles are hard to find: one possibility is particle and char interaction.

The rate of devolatilisation of the liquid products from the reactor surface was measured and compared with the results obtained by Lédé et al. the lifetime of the liquids on their heated disk. Lédé et al. estimated the lifetime of the liquid products from wood rod ablation experiments by direct observation and calculated the life time of the liquids by equation {9.07}(234); the results are shown in Figure 9.07 below and compared with the work of Diebold (205):

$$t_\infty = 2.7 \times 10^7 \exp\left(\frac{-11600}{RT_w}\right) \qquad \{9.07\}$$

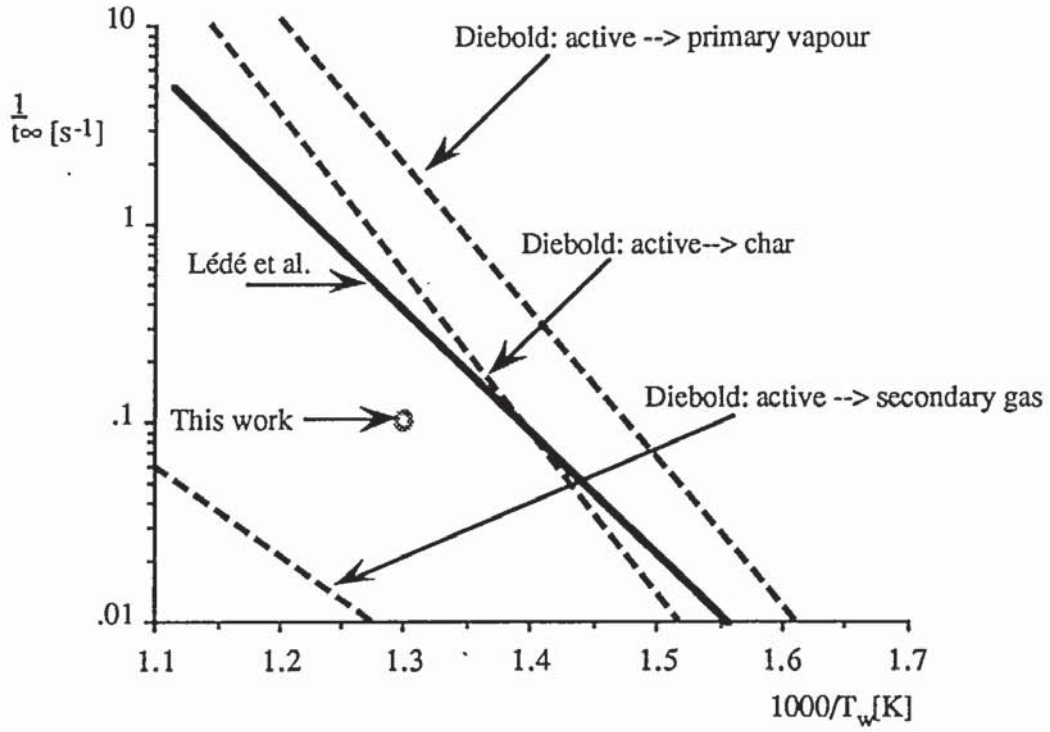

Figure 9.07. Estimation of liquids devolatilisation times with reactor temperature. Comparison with Lédé et al. and Diebold

The average measurement from the ablative pyrolysis reactor in this work was 10 s compared to 2.55 as estimated from equation {9.07}. Reasons for the discrepancy may be due to the data of Lédé being derived for reactor temperatures greater than 600°C; therefore, there may be errors at extrapolations to temperatures below 600°C. The intrinsic nature of the feedstock may also have an influence in terms of the chemical composition of the liquids.

Liquids formed during the wood rod experiments remained on the hot reactor surface longer than the estimates from the work of Lédé (234). The potential throughput of the ablative pyrolysis reactor could be increased if the liquids were allowed to vaporise before the particles were passed over the liquids, with corresponding high contact pressures being generated by dry friction. This is an area requiring further testing and evaluation.

9.2.7 Estimation of the heat transfer coefficient, h

The approach used in the original design procedure for the calculation of h involved the correlation of Lédé as given by equation {9.08} and based upon the assumption that the solid biomass was directly converted during pyrolysis to gas/vapour products:

$$h = \Re\, p = 0.017\, p \qquad \{9.08\}$$

The heat transfer coefficient can be estimated by the fundamental heat transfer equation {9.09}:

$$h = \frac{\rho_w V C_p (T_d - T_o) + \rho_w \Delta H_{pyr}}{(T_w - T_d)} \qquad \{9.09\}$$

which can be simplified to:

$$h = \Psi\, p^F \qquad \{9.10\}$$

where:

$$\Psi = \frac{\hat{A}\, \rho_w C_p (T_d - T_o) + \rho_w \Delta H_{pyr}}{(T_w - T_d)} \qquad \{9.11\}$$

Values for Ψ were calculated for 450 and 600°C using the design spreadsheet described in Chapter 5 and by iterating values for the heat transfer coefficient, h and the biomass decomposition temperature, T_d until a solution was reached. Values for reactor temperatures of 500 and 550°C [not shown] were within the bounds of the curves shown for 450 and 600°C. The results of this indicated that what was considered to be a constant, $\Re$ [equivalent to Ψ and equal to 0.017 W/m^{2}KPa by Lédé et al.] is variable with changing biomass decomposition temperature, reactor temperature and heat transfer coefficient (51). Using the biomass thermal properties previously noted in Table 5.03 and a wood density of 396 kg/m^3, the values of V, h and T_d were calculated and the values of Ψ plotted in Figure 9.08 against contact pressure.

From Figure 9.08, as the contact pressure increases, values for Ψ at 450°C increase at a rate greater than similar values calculated for a temperature of 600°C. This is due to the difference between the reactor temperature and the decomposition temperature (T_w-T_d) becoming smaller at low values of T_w compared to the difference in (T_d-T_o), hence the apparent increase in Ψ. From the values shown in Figure 9.08 and the temperature range of 450-600°C, as indicated by the dashed line in Figure 9.08 there is an almost linear correlation between Ψ and the applied pressure for the range of parameters studied and all values of Ψ are much lower than the constant of Lédé et al.. From these values for temperature in the range of 450-600°C and for the biomass physical and thermal properties noted in Table 5.03, the heat transfer coefficient can be plotted against the contact pressure and compared with the correlation of Lédé et al. Values for Ψ can be calculated from equation {9.12} for the temperature range 450-600°C:

$$\Psi = 2.058 \times 10^{-3} + 7.111 \times 10^{-9} p \qquad R^2 = 0.96 \qquad \{9.12\}$$

Equation {9.12} allows the heat transfer coefficient to be estimated if the process parameters, biomass physical and thermal properties and pressure are known and the iterative procedure for the calculation of T_d and h is carried out as described in Chapter 5.

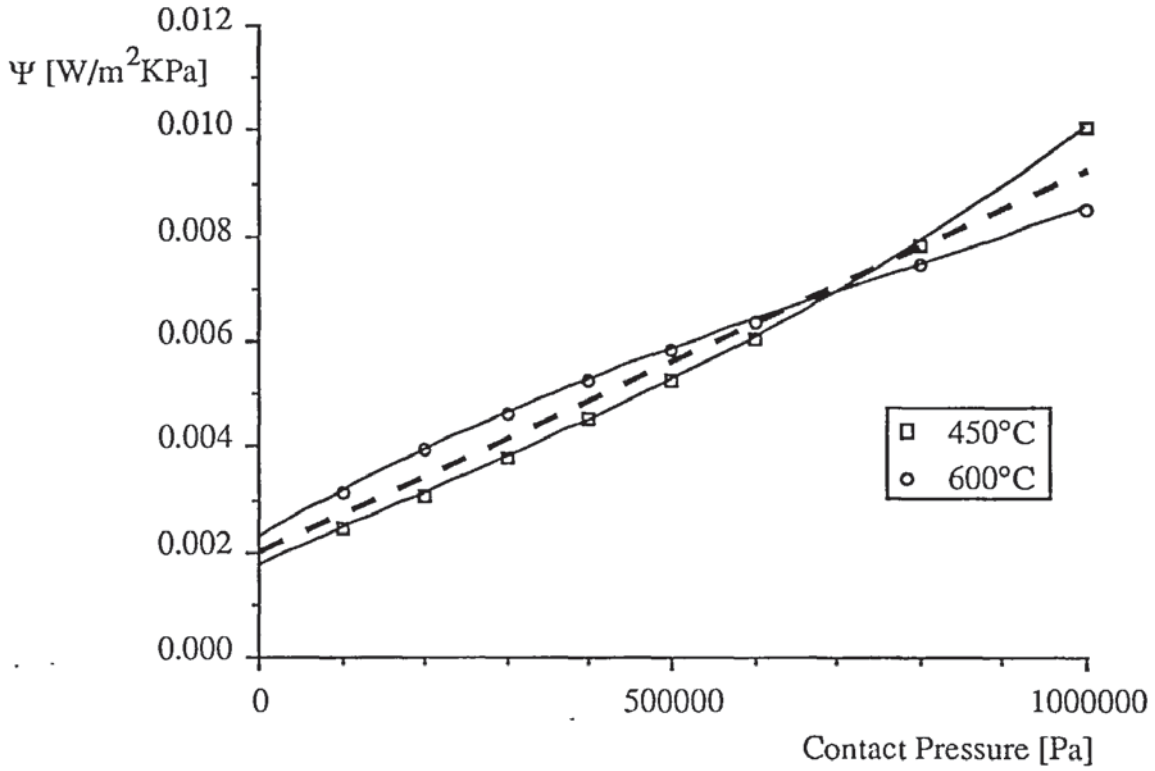

Figure 9.08. Variation of Ψ [W/m²KPa] with contact pressure, p [Pa]

The calculated values for the heat transfer coefficient, h against contact pressure using equation {9.12} were compared with the values calculated by Lédé using equation {9.07} and are shown in Figure 9.09.

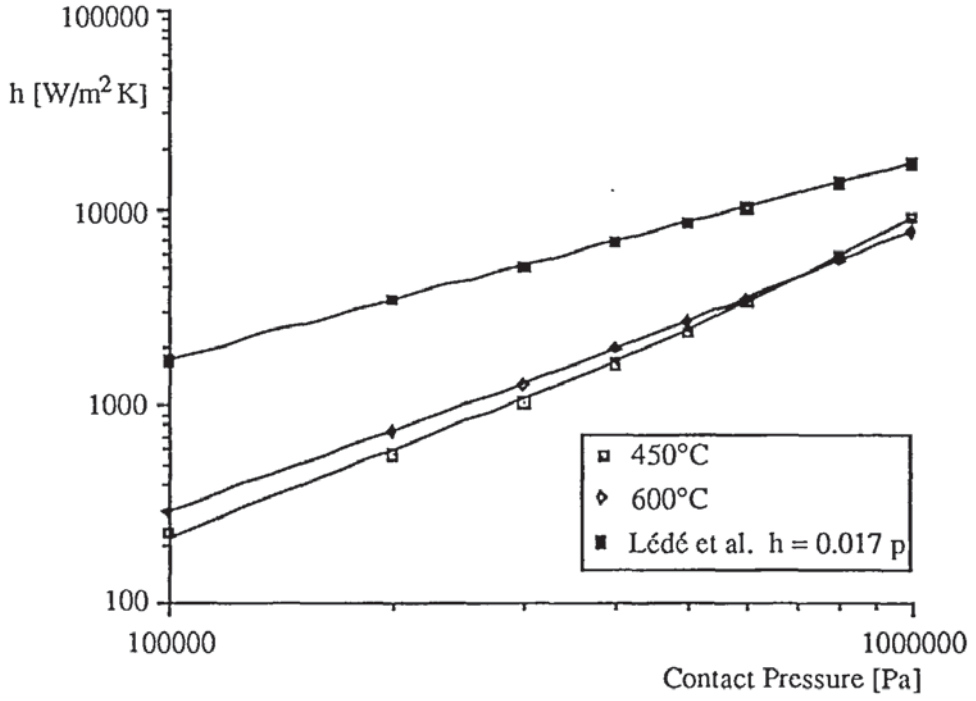

Figure 9.09. Variation of h with applied pressure. Comparison with Lédé et al. and this work

The heat transfer coefficient increases with temperature for 450-600°C but is consistently lower than the values estimated using the work of Lédé et al. (51). This has various implications for the design of an ablative reactor, i.e. the required heat transfer area may be underestimated due to the high calculated values for h. To calculate the required heat flux into the solid it was assumed that the solid would be heated from the datum temperature to the biomass decomposition temperature as shown in equation {9.13}:

$$\emptyset = h\,(T_d - T_o) \qquad \{9.13\}$$

This has been modified to represent the overall energy balance into the solid by basic heat transfer and account for the enthalpy of pyrolysis, ΔH_{pyr} during ablation [see Appendix V]:

$$\emptyset = \rho_w C_{pw} V (T_w - T_o) + \rho_w V \Delta H_{pyr} \qquad \{9.14\}$$

Calculated values for the heat flux in the single particle experiments are given in Table 9.04. The values indicate that heat fluxes higher than the maximum available from the heaters are being achieved. This is discussed in Section 9.3.

9.2.8 Estimation of the biomass decomposition temperature, T_d

As shown in Section 9.2.7, the evaluation of the heat transfer coefficient requires an estimate of the biomass decomposition temperature and its variation with the biomass properties and biomass decomposition kinetics. To demonstrate that at lower temperatures, the choice of kinetic parameters, in particular the values for the pre-exponential factor , A, and the activation energy, E, has a significant impact on T_d, four different sets were used to determine the biomass decomposition temperature, T_d at h = 10000 W/m^{2}K. A comparison of the biomass decomposition temperature for different kinetic parameters and reactor temperatures is shown in Figure 9.10 below, using the kinetic data of Liden et al. (83), Bradbury et al (161), Thurner and Mann (89) and Wagenaar (244).

Lédé based his estimates on the calculation of T_d using the kinetic data of Bradbury et al. for cellulose decomposition, which decomposes at temperatures lower than those for whole wood; also shown in Figure 9.10. The kinetic data predicts a gradual change in T_d with increasing reactor temperature for the work of Lédé et al., compared to the estimates from primary wood decomposition kinetics, as shown in Figure 9.10. For three sets of data for wood pyrolysis, there is significant variation in the estimation of T_d from 665 K to 835 K between the reactor temperature limits for the optimal production of liquids.

Only an average value of T_d over the reaction zone can be used as the pyrolysis reactions will occur from temperatures of approximately 250°C up to the temperature of the product char at the contact point with the heated surface. Analytical models are required for an accurate assessment of the temperature profiles in the ablating reaction layer and, as yet, no suitable model has been written, although a basic heat transfer approach allows a rapid estimation of the temperature profile in the solid to be made [see Section 9.3 and Appendix V].

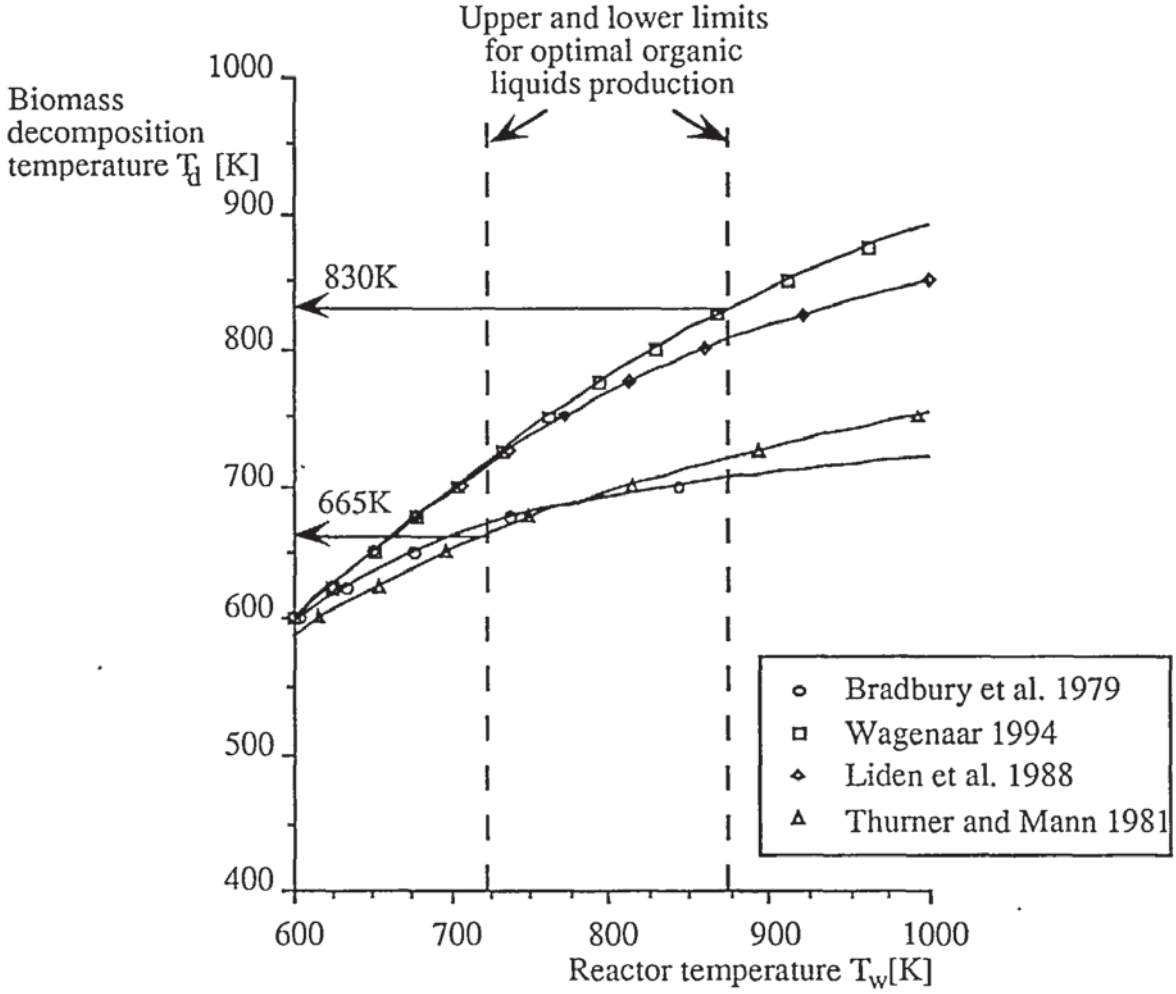

Figure 9.10. Variation of biomass decomposition temperature, T_d with reactor temperature, T_w. Heat transfer coefficient h = 10000 W/m²K

9.2.9 Conclusions of the re-evaluation of the key parameters

The main conclusions from the work described above are:

- the prediction of ablation rates below 500°C was not accurate and further empirical data are required,
- the lower limit for ablative pyrolysis is approximately 435°C,
- estimation of the ablation rate with pressure and reactor temperature has been improved,

- heat transfer coefficients predicted by Lédé et al. gave over estimates of up to 200% at contact pressures lower than 5 x 10^5 Pa,
- the generation of pressure by the rotating blades in the reactor is highest at 450°C due to the absence of a lubricating film of pyrolysis liquids on the reactor heated surface,
- the use of fewer blades may increase the reactor throughput as the liquids are given more time to volatilise from the hot reactor surface; a dry friction condition would increase the pressure generated by the blades on the particles and consequently the reactor throughput,
- the choice of biomass decomposition kinetics has a strong influence on the prediction of T_d and hence the required heat flux and heat transfer coefficients,
- the design methodology can be simplified based upon a re-assessment of the process parameters.

9.3 Modelling of wood rod ablation

An estimate of the thermal penetration into the wood rod during ablation would aid in the determination of the thickness of the product char layer, as the gas/vapour products of pyrolysis are known to react with the hot product char during release from the pyrolysing particle. By minimising the thickness of the char product layer, the extent of secondary intraparticle reactions could be reduced. The case for modelling of the temperature profile during ablation is well known in the literature and the derivation for wood pyrolysis is given in Appendix V. The heat conduction profile is schematically shown in Figure 9.11.

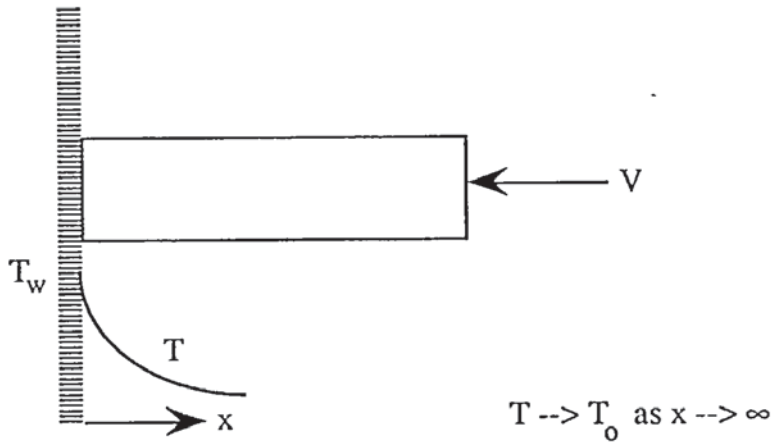

Figure 9.11. Schematic of wood rod ablation and theoretical temperature profile in the solid

From Appendix V, the temperature profile in the solid is given by equation {9.15}:

$$\frac{T_z-T_o}{T_w-T_o} = \exp\left(\frac{-Vz}{\alpha}\right) \qquad \{9.15\}$$

where z is the penetration distance into the solid [m] for a given temperature T_z. Therefore, z can be calculated by equation {9.16}:

$$z = \frac{\alpha}{V}\ln\frac{T_w-T_o}{T_z-T_o} \qquad \{9.16\}$$

To assess the thickness of the char layer before ablation from the particle surface, the biomass decomposition temperature was estimated and used in equation {9.16} to calculate the location of the reaction front within an ablating particle for the four reactor temperatures studied in the single particle experiments. The assumption is that the product char "matrix" in contact with the heated surface is at the same temperature as the heated reactor surface. The results are given in Table 9.04 and showed that the biomass decomposition temperature occurs at a distance of 0.0001 m behind the char product layer. Therefore the volatiles and liquids escape through a very thin char layer and this is constant for the temperature range of 450-600°C. These results are also shown in Figure 9.12 below with the temperature profiles calculated from the empirical ablation data of Table 8.01 and equation {9.16}.

Table 9.04

Variation of the heat transfer coefficients, heat flux and biomass decomposition temperature with reactor temperature

Reactor temperature, T_w [°C]	450	500	550	600
heat transfer coefficient, h [W/m^{2}K]	900	900	830	820
overall heat flux, Ø [W/cm^2]	15.6	23.2	29.1	27.4
biomass decomposition temperature, T_d [°C]	317	328	334	342
distance at which decomposition begins, z [m]	0.0001	0.0001	0.0001	0.0001

From Figure 9.12, the thickness of the thermal front can be measured, i.e. the thickness of the thermal front from the datum temperature in the solid to the reactor heated surface temperature at the interface between the char layer and the heated reactor surface. The thermal front is 1.65 mm at 450°C, rapidly decreasing to 0.5 mm at 600°C. The pyrolysis vapour gas products therefore have a very narrow char layer to pass through before escape from the solid matrix, although at 450°C, the depth of thermal penetration is high, suggesting that slower pyrolysis reactions may occur at this temperature. From Table 9.04, the biomass decomposition

temperature increases only slightly from 317 to 342°C for the temperature range of 450-600°C. The calculated values for the heat flux in the single particle experiments are high: higher than the maximum heat supply of the heaters of 11 W/cm^2 at 600°C. The high heat fluxes are achieved by moving the biomass over a large heated surface area, so that the temperature of the heated reactor surface remains constant. This is discussed in Section 9.4 with regard to the new and simplified design procedure.

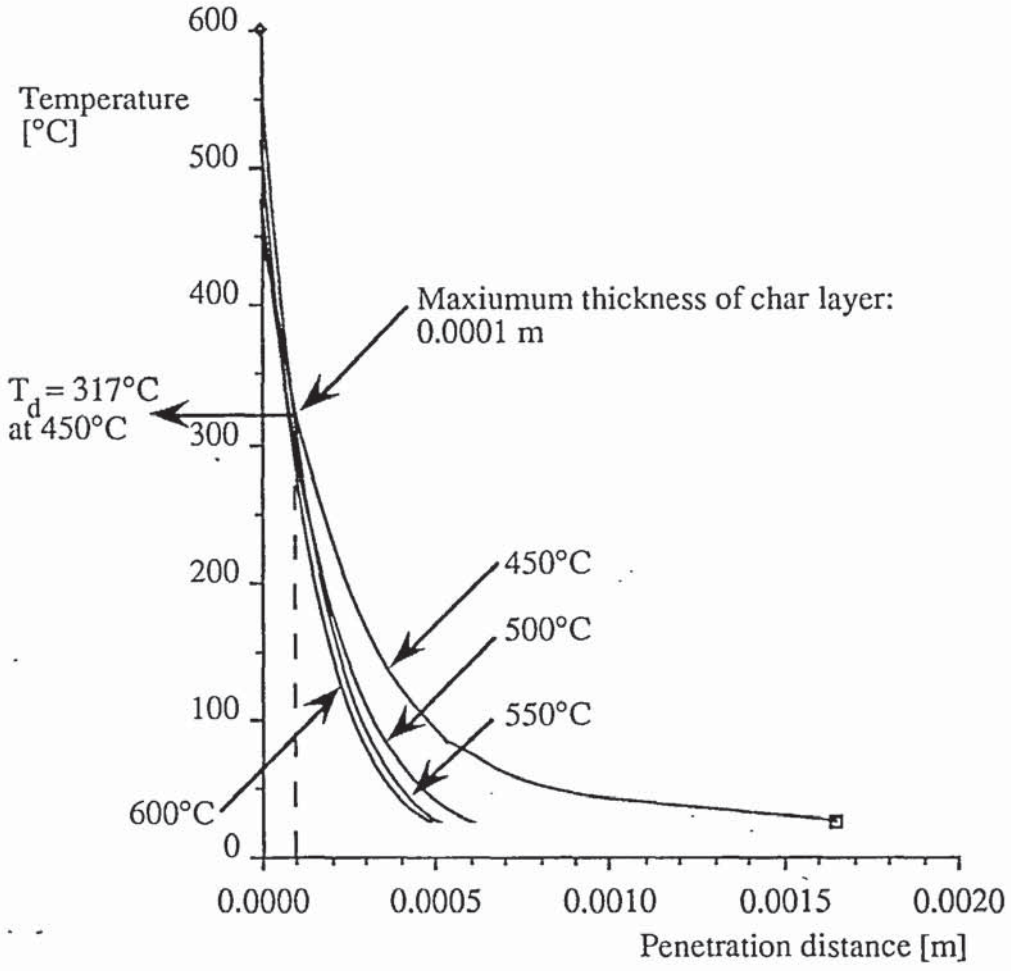

Figure 9.12. Variation of biomass temperature with distance into the solid for four reactor temperatures. Distance of reaction layer from heated surface indicated by thickness of char layer

The char layer thickness is small and constant, assuming that it is heated to the reactor heated surface temperature before abrasion. The determination of the mechanical energy required to abrade this product char layer would be useful in future design work to allow the specification of power requirements for an ablative reactor using a mechanical approach to achieve ablation. This is an area requiring further research.

9.4 Modified reactor design procedure

A reactor design methodology for an ablative pyrolysis reactor was described in relation to the specification and calculation of the process parameters and the prediction of reactor throughputs in Chapter 5. Based on the re-evaluation of the process parameters and the experimental results, the procedure was re-examined and simplified. The original procedure accurately predicted:

- ablation rate V for reactor temperatures above 500°C,
- the required biomass contact area A_c for reactor temperatures above 500°C,
- the biomass decomposition temperature T_d.

The original procedure did not accurately predict:

- the required heat transfer area A_r,
- the heat transfer coefficient, h
- the ablation rate V below reactor temperatures of 500°C,
- the heat flux required for pyrolysis, Ø,
- the contact pressure.

The model has been subsequently refined and improved based upon the empirical data and a detailed evaluation of the heat transfer process. The simplified model is dependent on values for:

- the ablation rate V [m/s] [calculated or empirically measured]
- the contact pressure p [Pa] [specified]
- the ablation variable $\hat{A}$ [m/sPaF] at the reactor temperature T_w [calculated]
- the reactor heat surface temperature T_w [°C] [specified]
- the available heat flux to the reactor heated surface E_{fl} [W/cm^2] [calculated]
- the biomass thermal and physical properties-specific heat capacity C_{pw} [J/kgK], the thermal conductivity λ_w [W/mK] and the biomass density ρ_w [kg/m^3], [specified]
- the required biomass throughput B_r [kg/s] [specified]

From the above parameters, the required biomass contact area A_c is calculated from:

$$A_c = \frac{B_r}{V\rho_w} \qquad \{9.17\}$$

where:

$V = \hat{A}p^F$ [or is empirically determined for T_w and p] $F = 0.993$ {9.18}

$\hat{A}$ [m/sPaF] is determined by:

$$\hat{A} = -9.262 \times 10^{-8} + 4.484 \times 10^{-10}[T_w] - 7.056 \times 10^{-13}[T_w]^2 + 3.7497 \times 10^{-16}[T_w]^3 \qquad R^2 = 0.98 \qquad \{9.19\}$$

The required heat transfer is calculated from the specified heat flux supplied to the reactor heat transfer surface. The value for the heat flux will be specific to the application and the required heat transfer area is dependent upon the overall heat flux for the biomass, as calculated from equation {9.20}:

$$\emptyset = C_{pw}\rho_w V(T_w - T_o) + \rho_w V \Delta H_{pyr} \qquad \{9.20\}$$

The required heat transfer area is then calculated from equation {9.21}:

$$A_r = \frac{\emptyset A_c}{E_{fl}} \qquad \{9.21\}$$

where E_{fl} is the calculated heat flux supplied to the reactor wall. From the calculated biomass contact area and the required heat transfer area, the basis for the reactor design is complete, taking into account engineering limitations of heat supply to the reactor heated surface. The reactor operational volume is then calculated to determine the gas/vapour product residence time as described in Chapter 7.

The reactor was resized based on the new design methodology presented above to see if it was heat transfer limited, assuming a heat flux of 11 W/cm^2 at 600°C. Assuming the same parameters as specified in Chapter 5, using the new wood density of 396 kg/m^3, a throughput of 5 kg/h, contact pressure 5 x 10^5 Pa, the required heat transfer area was calculated to be 203 cm^2. The actual reactor has an available heat transfer area of 477 cm^2, therefore the process is not heat transfer limited, but was limited by the contact pressure and char removal from the reactor as previously discussed in Chapter 7.

9.5 Evaluation of the reactor throughput: theoretical and actual

9.5.1 Biomass throughput

Based upon the original spreadsheet presented in Chapter 5, the reactor throughput [kg/h] can be plotted against the reactor heated surface temperature and the contact pressure. This allows a rapid evaluation of the reactor performance based upon the experimental data. In the original design procedure, a biomass density of 530 kg/m^3 was used. During the experimental work,

the dry biomass had a density of 396 kg/m^3. This therefore lowered the design capacity at 600°C and 5 x 10^5 Pa to 3.74 kg/h. Using the modified design procedure, the theoretical throughput assuming a biomass contact area of 20 cm^2, as specified in the original design, was calculated and the results presented in Figure 9.09.

The available contact area below the rotating blades was over 6.3 times the original specified area of 20 cm^2. The biomass throughput for each run was converted to a specific volumetric throughput and the theoretical contact area calculated. The "voidage" below the rotating blades was calculated and the results are presented in Table 9.05 for the original contact area and for the area available under the rotating blades used in the experimental work.

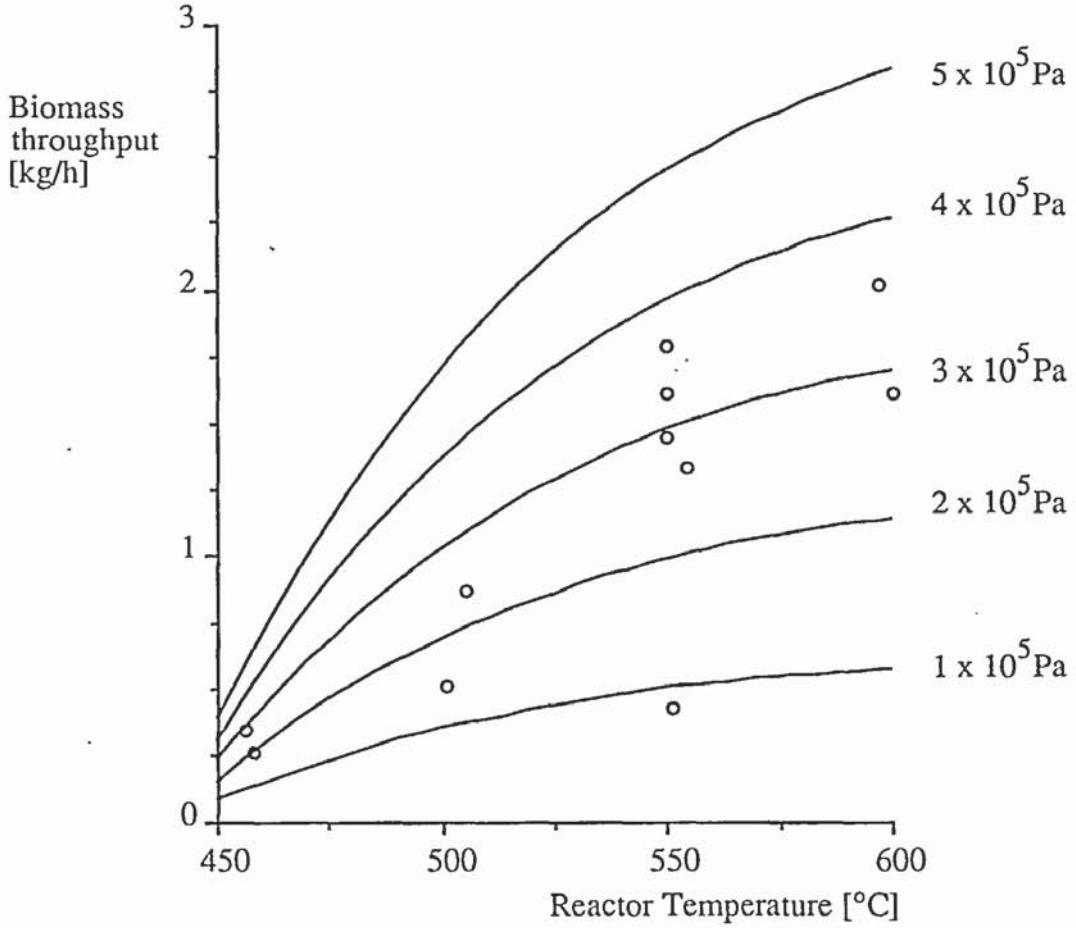

Figure 9.13. Theoretical variation of dry biomass throughput with applied pressure and reactor heated surface temperature. Comparison with experimental results

The results from Table 9.05 show that the usage of the actual contact area is low, probably due to the presence of product char below the blades preventing char from entering below the blades, mechanical comminution of the wood chips, and the inability of all of the available area below the blades to ablate the wood. These values show that the actual contact area usage

between the rotating blades and the heated reactor surface is very low, the highest value obtained being 10.8% of the available area. The results are also dependent on the assumption that all of the particles experience the same contact pressure, based on the values obtained from the single particle experiments. It is possible that due to fragmentation of the particles not all of the available contact is effectively used to cause ablation, with mechanically comminuted biomass and char particles which either remaining below the blade or passing out from the back of the blade. The presence of the liquid film may be such that only those particles at the front of the blade, i.e., facing the direction of motion are experiencing the pressures estimated from the single particle experiments. As four blades were used, an accumulated liquid product film may occur which subsequently reduces the ablation rate by lubricating the movement of the particles. This is an area requiring further investigation.

Table 9.05

Estimation of apparent usage below the rotating blades: actual blades with theoretical design

Run	Actual	Original	Run	Actual	Original
CR06	5.173	32.955	CR11	4.002	25.494
CR07	4.433	28.239	CR12	5.131	32.684
CR08	10.821	68.930	CR13	3.269	20.824
CR09	4.224	26.906	CR14	1.929	12.288
CR10	4.825	30.734	CR15	3.731	23.764
			CR16	3.126	19.913

The scale up assessment of the reactor cannot be completed until a further evaluation of the rotating bladé approach is made. However, the results from this work would suggest the rotating blade approach is successful in rapidly ablating wood chips and giving high yields of organic liquids. The basic approach is successful, however, further work is required to assess the pressures which may be generated and the ablation rates which may be achieved.

9.6 Gas/vapour phase kinetics

As noted in Chapter 3, gas/vapour phase kinetics are primarily concerned with vapour phase decomposition. In this work, the gas/vapour phase temperature did not go above 500°C; therefore, the application of secondary gas/vapour phase kinetics is of very limited use for the results obtained.

9.7 Conclusions for the reactor and reactor modelling

The reactor design procedure has been modified to account for new empirically derived data at 500°C. From this new data and the single particle experiments several important results have been derived:

- the contact pressure generated by the rotating blades during ablation at different reactor temperatures was estimated to varying from 1.6×10^5 to 8×10^5 Pa.
- actual reactor throughputs were compared with the new theoretical design limit based upon the ablation rates and the measured biomass throughputs; the usage of the blade contact area was calculated and this suggests that the available blade area is low at less than 10% of the available area,
- new ablation rates for relative velocities from 0.1-1.97 m/s were presented for a temperature of 500°C and used in the improvement of the estimation of the ablation rate with reactor temperature,
- the frictional force exerted by the particles [generated by the low angle blade] on the particles has been calculated and the related liquid film thickness approximated. The highest contact pressures were generated at 450°C and high frictional coefficients were obtained at this temperature. The significance of the calculation of the frictional forces was that if the product liquids are allowed to vaporise from the heated reactor surface, then the ablation rates and the biomass throughput can be increased,
- the biomass feedrate has still to be optimised and this is an area for future work,
- the blade angle is one of the parameters which requires further investigation which may also involve the modification of the rotating blades,
- testing of a range of blade angle and different numbers is required to assess the full potential of the rotating blade approach to ablate biomass particles,
- the new design methodology takes into account the limitations imposed by supplying the high heat fluxes required for fast pyrolysis by using the required heat flux for pyrolysis and the engineering heat flux which can be supplied to the reactor heat transfer surface,
- the single particle experiments have indicated what the possible ablation rates are that may be obtained in the ablative pyrolysis reactor. It is probable that not all of the biomass particles or their fragments are experiencing this pressure and that mechanical comminution and particle interaction is occurring. Further work is required in this area.

Chapter 10. Conclusions

An ablative reactor for fast pyrolysis of biomass has been successfully designed, built, and operated. The performance has matched that achieved by the best processes developed to date and new design concepts have been deduced that will improve both reactor design and liquid product quality. The rest of the conclusions are set out below:

10.1 Design

- The basic reactor design of using rotating blades to achieve ablation is good, with the ability to control the pressure on the biomass particles. The advantage of the rotating blade concept is that a feedstock of variable size can be used and the solids residence time is decoupled from that of the gas/vapour products.
- The approach to use the rotational action of the blades to transport char from the reactor proved only partially successful as the entry of biomass below the whole length of the blades inhibited transport of the char towards the centre of the reactor. The selective removal of ablatively produced char from non-ablated material was difficult, but has largely been resolved by the use of a nitrogen blow line across the reactor surface to the reactor outlet.
- The use of the drive shaft and blade holder were effective. The replacement of the carbon bush drive shaft seal with a polymer seal was completely effective in sealing the drive shaft at rotational speeds up to 200 rpm.
- The biomass feeder proved problematical at reduced pressures of -0.1 bar g due to the flexible lining. This has now been resolved with operation of the reactor at atmospheric pressure.
- The product collection system worked very well with good product recovery and high collection efficiency. The ice-cooled condensers were able to handle a wide range of gas flows and product temperatures. Dried cotton wool used in a small packed filter proved very effective for trapping the stabilised aerosols and residual vapour products if the product entering the filter are cooled to less than 10°C. From empirical measurements, dried cotton wool can remove three times its own weight of pyrolysis liquids from the gas/vapour stream before breakthrough occurs. Approximately 30 wt% of the condensable products remained as stable aerosols after cooling and collection in the two ice-cooled condensers and were subsequently trapped in the cotton wool filter.
- The use of the trace heated cyclone to remove char product was very effective with very low deposits of fine char [< 100 μm] inside the cyclone.
- The theoretical design procedure worked well to predict ablation rates and related parameters from 500-1000°C, based upon Lédé's empirically derived data. It also

successfully predicted the required biomass contact area, but it did not accurately predict the required heat transfer area, with an overestimate by a factor of 2.5. The procedure has now been modified, based upon empirical work on single particles and wood rods to improve calculation of the ablation rate with temperature, the required biomass contact area and the required heat transfer area provided the contact pressure, the reactor temperature and the biomass physical and thermal properties are specified. The modified procedure takes into account engineering limitations of heat supply to the reactor wall or surface, resulting in a more accurate and simplified design procedure.

- Only a limited number of basic reactor configurations are possible with any future developments being variations on established technologies. Differences will be related to the dominant mode of heat transfer to the biomass.
- Ablative pyrolysis offers an interesting approach to achieving high rates of heat transfer to the biomass with the possibility of compact reactor design and improved controllability of the process. A limited number of configurations are believed possible for ablation: flat plate, inclined surface and a cylindrical tube. Ablation offers the principle advantage of compact reactor design, high heat transfer rates and in certain configurations, no particle transport gas. Compared to conventional fluidised bed technologies, the degree of complexity may be higher, depending on the method used to achieve the key requirements of high relative motion, applied pressure and temperature.
- Ablation offers the significant advantage of rapidly removing the product char layer. This allows larger feedstocks to be used and takes advantage of the low thermal conductivity of the material. The pyrolysis reactions can occur in a narrow reaction interface which advances into the solid closely behind the thermal front. As the char layer is removed, secondary reactions caused by vapour and gas diffusion through the hot active char layer are minimised. The key engineering problem is heat supply to the reactor wall to cope with the high heat flux demands.
- From a review of the concepts, there are a limited number of ways of achieving the key requirements of biomass particle ablation. The rotating blade approach offers a solution to some of the operational problems encountered by Diebold [see Section 4.6] and Reed [see Section 4.3]. Operation has shown that the pressure generated by the rotating blades on the particles is generally a constant for the temperature ranges studied. This suggests that the throughput could be controlled by altering only the blade angle and the reactor heated surface temperature. It would appear that if the blades were increased in size and the angle was lowered, higher pressure could be generated.
- mechanical methods to achieve ablation increase the reactor complexity and also the need for high sealing temperature materials.

10.2 Construction and operability

- The reactor construction was relatively simple and compact. The only complexity is the sealing of the drive shaft which enters through the reactor lid. This was solved by locating the polymer drive shaft seal at a suitable distance from the reactor lid.
- The reactor construction is very compact and this has led to minor difficulties with the assembly. Due to its compact size, the reactor required specially fabricated parts which would be simplified on a larger scale unit.
- The basic reactor construction proved very reliable. The average temperature of the heated base during an experiment was within 1% of the set point and the band heater used to heat the reactor wall minimised vapour product deposition on the reactor wall interior at 400°C. The drive system was reliable.
- The use of sightglasses did not prove practicable as the product vapours and gases were too opaque to observe effectively the reactor interior.
- The reactor interior plate used to reduce the operational volume of the reactor was not heated, therefore, some deposition of organic liquids occurred during the experiments by heat loss through the interior plate. Fine char and liquids were found deposited in small quantities on the reactor liquids, typically 2 g during a run. To minimise the collection and subsequent degradation of vapours on the lid, it is proposed that the lid should be similarly heated to 400°C to minimise deposition and improve the temperature control of the reactor operational volume by reducing heat losses through the reactor lid.
- The use of a knock out pot to remove product char was not successful as the hot product vapours caused drying and partial reaction of the non-ablated wood. The use of the small trace heated cyclone to remove the product char and unreacted material from the hot gas/vapour products was successful. Use of the cyclone unheated caused the vapours to deposit on the interior and to eventual blockage of the cyclone. Transfer lines from the reactor to the liquids collection system should be heated to a minimum of 400°C to minimise the deposition of products inside transfer lines and char separation equipment.
- The biomass feeder requires modification to allow it to operate above atmospheric pressure. The cyclone has a pressure drop of 20000 Pa and therefore the reactor must be operated above atmospheric pressure. The biomass feeder hopper was not designed for operation above atmospheric pressure and was the cause of product losses during two of the runs. Either a feed system using to rotary valves or a new feeder designed to feed under pressure to the reactor is proposed.
- The need for a feed transport gas is removed as the particles are fed under gravity. Nitrogen can be used to control the residence time of the gas/vapour products.

10.3 Commissioning and Operation

- The main problems to occur during reactor commissioning were related to the separation of the product char from the non-ablated wood.
- Operation of the reactor system below atmospheric pressure caused various problems with feeding which have been resolved by operating at atmospheric pressure.
- The product collection system was relatively easy to operate. Initial char separation problems were soon resolved and the use of trace heated pipework and char separation equipment is required to minimise the deposition of liquids and subsequently char adhesion.
- The rotating blade concept was proved to be successful in ablating relatively large biomass particles in a 258 mm internal diameter reactor. Biomass throughputs of 2 kg/h dry biomass were achieved, 54% of the revised design capacity of the reactor for a wood density of 396 kg/m^3.
- Char removal from the reactor was eventually acceptable but not satisfactory and requires further development.
- There is a high "voidage" factor below the rotating blades if all of the theoretical contact area is considered.
- The rotating blade concept allows the gas/vapour product residence time to be decoupled from the solids residence time.
- A liquids collection system was developed which allowed the recovery and separation of the three product phases. Operation of the reactor and product collection system have produced a substantial number of qualitative conclusions which should be considered in the selection of the products recovery system:
  - distances from the cyclone outlet into the liquids collection system must be minimised to prevent the collection of product vapours on the walls of transfer lines,
  - an in line heater should be used to reduce the deposition of stabilised aerosols on the transition from the char separation system to the liquids collection system,
  - rapid cooling of the products leads to deposition of the pyrolytic lignin on surfaces, especially if they are not heated,
  - the time-temperature history of gas/vapour products is very important for the design and selection of a liquids product collection system.
- The recovery of biomass pyrolysis liquids is an area which is subject to qualitative design based upon fundamental chemical engineering principles. The characteristics of biomass pyrolysis vapours are influenced by:
  - temperature at which they exit from the reactor,
  - the gas/vapour product temperature,

- the degree of pyrolysis product dilution,
- the original reactor parameters which influence the yields of chemicals, non condensable gases and the average molecular weight distribution of the products,
- the physico-chemical nature of the vapour product which is, in fact, not really a vapour but is more like smoke or fume.

- The system proved reliable in recovering the majority of the products to give acceptable mass balance closures.
- For low gas/vapour temperatures from the reactor [< 350°C], the condensed liquid product had a high water content, typically above 25 wt%. For high gas/vapour temperatures from the reactor greater than 350°C, the condensed liquid product had a low water content of less than 25 wt%.

10.4 Results

- High liquid yields of up to 80 wt% on dry ash free feed have been achieved, comparable to those of other fast pyrolysis processes. For the eleven experiments, eight had acceptable mass balance closures. The losses which occurred during the other three runs were clearly identified-one due to a cotton wool filter which allowed the gas/vapour products to bypass it and two runs with leaks from the feeder.
- Increasing the residence time of the product vapours leads to secondary condensation reactions with an asymptotic yield of 47 wt% organic liquids at 10 s residence time and corresponding water yields of 24 wt%. For gas/vapour product temperatures between 280-420°C, the water of pyrolysis increases from 12 wt% at a residence time less than 1 s to approximately 24 wt% at 10 s. Organic liquid yields reach an asymptote and do not continue to decrease as has been described by other researchers, as long as the vapour product temperature is maintained below 500°C. At temperatures above 500°C, vapour phase decomposition occurs to non-condensable gases and char.
- The yields of gas and char were typical of fast pyrolysis processes. The gas products were typically 90 vol.% CO and CO_2 with the ratio of CO to CO_2 increasing with reactor temperature. The most significant minor component was CH_4 with small amounts of higher hydrocarbons. Hydrogen was only detected in significant quantities at reactor temperatures of 600°C. This is due to the reduced extent of cracking reactions which are known to form hydrogen and other hydrocarbons as products, probably due to cracking reactions as the liquids devolatilise from the hot reactor surface. Secondary gas phase cracking reactions were minimised by the use of nitrogen as a product diluent.

- Determination of the ablative char has proved difficult as the char fractions which were sieved were all highly reacted, i.e. they had high carbon contents compared to char from conventional fluid bed fast pyrolysis processes.
- The highest organic liquid yield is comparable to the highest values obtained in other conventional fast pyrolysis processes and higher than those obtained from other ablative fast pyrolysis processes under similar conditions.
- The degree of secondary gas/vapour phase cracking has been minimised by using nitrogen both as a product diluent and a temperature moderator, although lower temperature condensation reactions did occur [< 400°C]. At temperatures below 400°C, vapour phase condensation reactions were apparent with increased water yields above those normally expected of approximately 12 wt%. Gas/vapour product temperatures between 400-500°C are recommended.
- From the results of chapter 9, it would appear that the reactor would work better, in terms of biomass throughput, if one rotating blade was used and the liquids could vaporise from the heated surface to increase the frictional resistance of the particles, leading to increased contact pressures and increased ablation rates.
- The most difficult problem was the removal of the product char from the reactor. The rotating blades could not adequately transport the char from the area below the rotating blades to the centre of the reactor. The use of nitrogen pulses was required to selectively remove the product char from the reactor. This was largely successful; however the biomass feedrate, still requires optimisation.
- The feeder which was used was not ideally suited to the application. The feeder was intended for use at atmospheric pressure and its operation was problematical at reduced pressures and above atmospheric pressure.
- The maximum run time is about one hour due to the interface between the cyclone outlet and the inlet to the condenser eventually blocking. It is believed that this can be extended by heating the interface between the outlet of the cyclone and the condenser inlet to minimise liquids deposition.
- The reactor could be run without constant adjustment of flows and feedrates and reached steady state operation within 2 minutes.
- The reactor could accept a range of feed particle sizes and this is an important feature as the feed does not have to be sieved or screened.
- The reactor and the product collection system is in the initial stages of development and requires some modifications to improve their operability and optimise the biomass throughput. These modifications include:
    - modify the feeder tube by fitting a twin rotary valve system to allow the reactor to be operated above atmospheric pressure,
    - replace or modify the feeder to permit operation at a range of gas pressures,

- change the current blades with broader blades to allow lower blade angles and number of blades to be investigated,
- preheat the nitrogen flows to moderate the gas/vapour phase temperature from 400-500°C.

10.5 Reactor design and modelling

- A new design methodology for an ablative pyrolysis reactor has been described in relation to the specification and calculation of the process parameters and the prediction of reactor throughputs. The procedure accurately predicted:
  - ablation rate variation V with temperature above 500°C
  - the required biomass contact area A_c for reactor temperatures above 500°C,
  - the biomass decomposition temperature T_d.

  The model did not accurately predict:
  - the required heat transfer area A_r,
  - the heat transfer coefficient, h
  - the ablation rate V below 500°C, for a relative velocity between the biomass and the heated surface greater than 1.2 m/s,
  - the heat flux required for pyrolysis, Ø,
  - the contact pressure.
- The model has been subsequently refined and improved based upon the empirical data and a detailed evaluation of the heat transfer process. The simplified model is dependent on:
  - the ablation rate V [m/s],
  - the contact pressure p [Pa],
  - the ablation variable Â [m/sPaF] at the reactor temperature T_w ,
  - the reactor heat surface temperature T_w [°C],
  - the available heat flux to the reactor heated surface E_{fl} [W/cm^2]
  - the biomass thermal and physical properties-specific heat capacity C_{pw} [J/kgK], the thermal conductivity λ_w [W/mK] and the biomass density ρ_w [kg/m^3],
  - the required biomass throughput B_r [kg/s].

  From the above parameters, the required biomass contact area is calculated from:

$$A_c = \frac{B_r}{V\rho_w}$$

where $V = \hat{A}p^F$ [or is empirically determined for T_w and p] $F = 0.993$

Â [m/sPaF] is determined by:

$$\hat{A} = -9.262 \times 10^{-8} + 4.484 \times 10^{-10}[T_w] - 7.056 \times 10^{-13}[T_w]^2 + 3.7497 \times 10^{-16}[T_w]^3$$

This new correlation for $\hat{A}$ was derived to model the variation of ablation with reactor temperature from 450°C more accurately and so improve the design procedure. The required heat transfer is calculated from the specified heat flux supplied to the reactor heat transfer surface. The value for the heat flux will be specific to the application and the required heat transfer area is dependent upon the overall heat flux for the biomass:

$$\emptyset = C_{pw}\rho_w V(T_w - T_o) + \rho_w V \Delta H_{pyr}$$

The required heat transfer area is then calculated from:

$$A_r = \frac{\emptyset A_c}{E_{fl}}$$

From the calculated biomass contact area and the required heat transfer area, the basis for the reactor design is complete. This procedure is more simplified for the initial reactor design. The evaluation of the related parameters of biomass decomposition temperature, heat transfer coefficient and depth of thermal penetration into the biomass can be calculated as described in Chapter 9.

- The design sensitivity analysis shows that the estimation of the ablation rate V and the wood density have a direct influence on the reactor throughput pressure. More empirical data to validate results below 600°C are required.
- The interaction of relative velocity and ablation rate have not been adequately explored and no equations have been developed to account for the mechanical elimination of char from the reaction interface.
- The original design procedure presented in Chapter 5 was modified to account for new empirical data obtained at 500°C. This showed that the predicted ablation rate for below 500°C was 50% of the empirical value.
- The frictional force exerted by the particles on the rotating blade has been estimated from single particle experiments. This is approximately 1.1 N for a 5 mm x 5 mm biomass particle for a reactor temperature of 500°C, relative velocity 1.2 m/s and an applied pressure of 2×10^5 Pa.
- Biomass throughputs of 75 % of the revised design were achieved with estimated particle pressures of up to 3×10^5 Pa and maximum ablation rates of 0.6 mm/s.
- The heat transfer estimation method of Lédé gives over estimates at temperatures below 600°C and the new design procedure accounts for the variation of the heat transfer coefficient with varying process parameters.

- The overall heat flux into the biomass was defined as the heat transfer limiting factor and was estimated to be higher than value predicted by the method used by Lédé et al.
- Longer residence times can be tolerated without a significant depreciation in the overall liquids yield if the gas/vapour product temperature is carefully controlled to between 400 and 500°C. At temperatures less than 400°C, condensation reactions occur and organic liquid yields drop correspondingly, while above 500°C secondary cracking becomes significant, reducing product yield and quality. This is an area requiring further research and is a major recommendation. The criterion of short residence time [< 0.5 s] is not essential if the gas/vapour product temperature is 400°C. A minimum asymptotic yield of 47 wt% organics at 6-10 s residence time and gas/vapour product temperatures less than 500°C was estimated as discussed in Chapter 8.
- The calculated biomass throughputs, based on the single particle experiments, indicate that a low proportion of the available contact area is being effectively used for ablation. This may be due either to the presence of a relatively thick liquid product layer on the reactor surface lubricating the motion of the particles and hence lowering ablation rates or to the fact that only a small part of the blades are ablating the biomass. The interaction of the biomass and char in the ablative pyrolysis reactor may lead to mechanical comminution and the presence of char products below the rotating blade may impede ablation of the wood.

10.6 Analysis

- Liquids were analysed by a variety of methods including HPLC, GC-MS, FT-ir and SEC with the identification of chemicals such as acetic acid, hydroxyacetaldehyde, acetol, phenols and levoglucosan. These methods are suitable for low molecular weight chemicals. For larger molecules, techniques such as nuclear magnetic resonance are required and this is still an area requiring further investigation as the number and quantity of chemicals which are produced during pyrolysis vary with the process parameters and the intrinsic nature of the feedstock. The lignin derived chemicals from biomass fast pyrolysis have generally been poorly characterised and the development of other analytical techniques is required for their quantification and identification.
- Other chemicals of interest are the lignin-derived polyphenols and polynuclear aromatic rings. These may help to provide information on the possible char forming reactions which occur during pyrolysis as lignin is seen as the main source of char during pyrolysis. Analysis for higher acids would also be useful to add to the overall chemical spectra.

- The on-line gas analysers have a high span range as they were previously used for work with a gasifier, typically 30 vol.% for the CO and CO_2 analysers. The dry non-condensable gas fraction from the pyrolysis reactor is typically 95 vol.% nitrogen; therefore, the analysers have to analyse for low gas concentrations. The on-line gas analysers may therefore have high inaccuracies for the dry non-condensable gases; the GC results are more accurate as the GC was calibrated with gases of low volumetric concentrations.

10.7 Pathways

- Biomass pyrolysis pathways require further study. The possible mechanisms proposed for whole wood fast pyrolysis have reaction steps which may be difficult to measure-both the intermediate products and the reaction kinetics. For reactor design and assessment, the use of global pathways to accurately predict primary product yields and their variation with time and temperature are of the most use.
- The kinetics of biomass pyrolysis is a complex topic and the influences of feedstock, ash and moisture content, degree of polymerisation, particle size and the process [reaction] parameters are poorly understood. No suitable model has been derived to account for the wide range of products under variable conditions.
- It is also apparent that biomass kinetics cannot be obtained for temperatures above 450°C as the biomass has already begun to react substantially below this temperature. The application of kinetics above 500°C, therefore, is of limited use, in terms of the engineering design of an ablative pyrolysis reactor.
- Biomass pyrolysis kinetics are very dependent on the conditions under which the measurements were made. Global kinetic expressions lump together mass transport, heat transfer and reaction effects which cannot necessarily be applied to another set of experimental conditions beyond those originally used. Kinetics of biomass pyrolysis must therefore be of limited use in initial reactor design but should be applied to secondary gas phase processes in reactor design and optimisation.
- Secondary biomass pyrolysis kinetics do not allow for the prediction of water formation in the vapour phase from the interaction and reaction of the low molecular weight species. This is an area requiring further exploration.

The overall conclusions from the work are that the rotating blade approach can be used to effect ablative pyrolysis. The reactor has a compact design and high heat fluxes and the yields obtained were comparable to those obtained from other fast pyrolysis processes under similar conditions.

Chapter 11. Recommendations

The following recommendations are made:

11.1 Design

- The feeder tube requires modification to allow the reactor to be operated slightly above atmospheric pressure to overcome the pressure drop in the liquids collection system.
- The nitrogen which dilutes the gas/vapour products should be preheated to a higher temperature, approximately 350-400°C, depending upon the reactor temperature.
- One of the key recommendations for further work is to investigate the effects of blade number and blade angle on the reactor throughput. Although four blades as used in this work increased the available contact area, one blade may more effectively pyrolyse the feedstock by allowing the products to vaporise from the heated base and increase the contact pressure on the particles.
- The rotating blade concept requires further testing to evaluate the influence of reactor temperature, blade angle size and number on the reactor throughput.
- The removal of char was the most significant problem and alternative methods of removing the char are required.

11.2 Construction and operability

- Further experiments are required to reduce the non-ablated char fraction in the char products and the residence time of the gas/vapour products needs to be controlled between 400-500°C.
- Preheat the nitrogen used for purging and gas/vapour product dilution more accurately and improve the control of the gas/vapour product temperature and residence time.
- Investigate the influence of blade angle and configuration on the reactor throughput and consequently the applied pressure generated.
- It is recommended for small laboratory scale processes that any inert filter media is cooled to less than 20°C to minimise the loss of water vapour in the exit gases. For a commercial process, the removal of stabilised aerosols should be performed by using either electrostatic precipitation after a liquids quench system or filtration of the gases using a suitable filter material. The design of liquids recovery processes is still largely empirical based upon operational experience and is an area for further study.
- By lowering the gas temperature from the cotton wool to less than 0°C by cooling the cotton wool filter, the drying column can be removed. It is recommended that the

cotton wool filter is cooled using a salt/ice mixture to achieve this and that a maximum filter diameter be 50 mm.

- The gas analysers should be recalibrated to analyse gas concentrations of up to 10 vol.%. This would improve the on-line gas analysis and allow changes in the gas composition with time to be monitored more accurately.
- To reduce the amount of liquids passing through the product collection system, some form of liquids contact should be used to scrub out the aerosols and reduce the loading on final gas filtration/cleaning systems.
- Further optimisation of char removal from the reactor is required, although his problem has largely been reduced.
- The use of gas/vapour product residence times of less than 2 s are recommended to reduce secondary gas phase reactions and gas phase temperatures of 400-500°C.
- Measurement of the temperatures of all the main reactor system surfaces will enable a better estimate of heat losses to be made resulting in a more accurate energy balance over a small scale experimental reactor.
- Recommend better heating of the nitrogen purge to the reactor with temperature measurement in the heated gas stream into the reactor.
- It is proposed to trace heat the glass inlet line to the condenser to 400°C.
- Further experiments are required to assess:
  - the effects of blade angle and blade number on reactor throughput,
  - carry out further experiments at reduced residence times,
  - test retreated feedstocks in the reactor to confirm that similar mechanisms occur as in other reactors.
- Test scale up concepts of the rotating blade design once further evaluation of the proto-type reactor has been carried out.

11.3 Reactor design and modelling

- Modelling of ablative pyrolysis can be improved by relating the results to more detailed analytical models which, in theory, can predict the temperature distribution more accurately than simple heat transfer alone.
- The model can be further improved by using empirical data obtained at other temperatures [450-600°C] to be added to the correlations for the prediction of the ablation rate V. It can also be simplified to allow the rapid evaluation of a design for the specification of the reactor dimensions.
- Modelling could also be improved by relating the overall reactor dimensions to product yield distributions and their variation with temperature and residence time. This would give the reactor dimensions, operational volume and the possible variation in product yields with changes in the process parameters. This more integrated

modelling approach should also be related to more detailed analytical models which could predict exact product distributions if reliable kinetic data were used in the model.

- At present there is no model for the mechanical abrasion of the product char from the surface of the biomass. This would aid in the specification of power requirements for the drive system used in a reactor utilising a mechanical approach to achieve ablation. It would also help in the estimation of frictional resistances and the estimation of the contact pressure generated in rotating blade systems.
- Carry out wood rod ablation experiments to measure ablation rates with changes in reactor temperature, relative velocity and applied pressure. This would require the construction of a new experimental rig similar to that of Lédé et al. [see Section 4.2]. These experiments would include measurement of the temperature profile inside the pyrolysing solid. The results from the experiments should then be used in the development of analytical models which would solve the heat flux, chemical reactions and mass transfer equations simultaneously.
- Develop analytical models of the mechanical removal of products from the reaction interface and improve overall reactor design methods.
- Develop the reactor models for secondary gas phase kinetics which allow the prediction of product yields with variation in reactor temperature, gas/vapour product residence time and temperature.
- Further work is recommended on the determination of a range of ablation rates with reactor temperature, relative velocity and contact pressure at temperatures from 450-650°C.

11.4 Results

- The results are comparable with those from other fast pyrolysis processes under similar conditions. It is recommended that mas balance data and analyses are obtained at shorter residence times for moderate gas/vapour phase product temperatures of 400-500°C.

11.5 Analysis

- Work is required on the further development of analytical methods for fast pyrolysis liquids. Although this has been gradually developing for over 30 years, only a small percentage of the chemicals have been identified by techniques such as GC, GC-MS and quantified by GC-MS and HPLC. The area of liquids analysis requires further development.

Nomenclature

Symbol	Description/Definition	Units
A	pre-exponential factor	$[s^{-1}]$
$\hat{A}$	function of the reactor heated surface temperature	[m/sPaF]
A_c	particle contact area	$[m^2]$
A_{pa}	individual particle contact area	$[m^2]$
B_r	required dry biomass throughput	[kg/s]
C_p	heat capacity	[J/kgK]
C_{PC}:	mass of dry material from the product collection system greater than 1.4 mm	[kg]
E	activation energy	[J/mole]
$\hat{e}$	preheating zone	[m]
E_{fl}	enginnering heat flux to the reactor heated surface	$[W/m^2]$
F	constant dependent upon the solid [≈1 for wood]	
F_f	frictional force	[N/m]
F_r	radial force on the particle	[N]
h	heat transfer coefficient	$[W/m^2K]$
L	heat of fusion	[J/kg]
L_p	particle height	[m]
M_n	molecular weight of the species	[kg/mole]
m_p	dry particle mass	[kg]
p	applied [contact] pressure	[Pa]
P_c	centrifugal pressusre	[Pa]
Q_{pyr}	heat requirement to pyrolyse the biomass throughput	[W]
R	gas constant	[J/molK]
r	reactor radius	[m]
T	temperature	
T_d	wood decomposition temperature	
T_e	effective reaction temperature	
t_f	pyrolysis liquid film thickness	[m]
T_o	datum temperature	
t_p	pyrolysis time	[s]
t_{par}	particle thickness to the heat transfer surface	[m]
t_r	characteristic reaction time	[s]
t_t	characteristic heat penetration time	[s]
T_w	wall temperature	[K]
u	particle velocity	[m/s]

V	ablation rate	[m/s]
V_b	biomass volume throughput	[m^3/s]
W_F	total dry wood fed to reactor	[kg]
W_{r1}	dry reacted wood [method 1]	[kg]
W_{RC}:	mass of dry material from the reactor greater than 1.4 mm	[kg]
W_{UPC}	dry unreacted wood from product collection system	[kg]
z	distance into solid	[m]

Symbols

α	thermal diffusivity	[m^2/s]
ρ	density	[kg/m^3]
μ	viscosity	[Ns/m^2]
$\emptyset$	heat flux density	[W/m^2]
λ	thermal conductivity	[W/mK]
ΔH	enthalpy	[J/kg]
Ψ	heat transfer variable	[W/m^2KPa]
$\Re$	heat transfer coefficient constant	[W/m^2KPa]

Subscripts

b	biomass
c	contact area
char	char
ce	centrifugal
f	liquid film
l	liquid
m	mechanical
p	particle
pyr	pyrolysis
r	relative
t	tangential
w	wood
z	temperaature at distance z into solid

Abbreviations

tr.	trace amount	
abs.	absolute pressure	[Pa]
ND	not detected	
NK	not known	

References

1. Wrixon, G.T., Rooney, A.-M.E. and Palz, W., "Renewable energy-2000", Springer-Verlag, Berlin, 1993, p 69.
2. "New and Renewable Energy: future prospects for the UK", Department of Trade and Industry, Energy paper no. 62, March 1994.
3. Deglise, X. and Magne, P., "Pyrolysis and Industrial Charcoal", Biomass Regenerable Energy, Hall, D.O. and Overend, R.P. (eds.), John Wiley & Sons, Chichester, 1987, p 221-235.
4. White, L.P. and Plaskett, L.G., "Biomass as Fuel", Academic Press, London, 1981.
5. Bridgwater, A.V. and Grassi, G., "The European Community R&D programme on biomass pyrolysis, upgrading, utilisation, liquefaction and assessment", Energy from Biomass: Progress in Thermochemical conversion, Proceedings of the EC Contractors' Meeting, 7 October 1992.Grassi, G. and Bridgwater, A.V. (eds.), EUR 15389 EN, CEC DG XIII, Brussels, 1994, p 11-20.
6 Beenackers, A.A.C.M. and Bridgwater, A.V., "Gasification and Pyrolysis of Biomass in Europe", in Pyrolysis and Gasification, Luxembourg, May 1989, Ferrero, G.L, Manitis, K., Buekens, A. and Bridgwater, A.V. (eds.), Elsevier Applied Science Publishers, London and New York, 1989, p 141.
7. Hillis, W.E., "Wood and Biomass Ultrastructure", Fundamentals of Thermochemical Biomass Conversion, Overend R.P., Milne, T.A. and Mudge, L.K. (eds.), Elsevier Applied Science Publishers, New York, 1985, p 1-34.
8. Rossi, A., "Fuel Characteristics of Wood and Nonwood Biomass Fuels", Progress in Biomass Conversion, Vol. 5., Tillman, D.A. and Jahn, E.C., (eds.), Academic Press, New York, 1984, p 69-99.
9. Ray, A.K., Garceau, J.J., Kokta, B.V. and Carrasco, F., "Upgrading nonwood fibres by chemical impregnation and high pressure pulping", Advances in Thermochemical Biomass Conversion, Bridgwater, A.V. (ed.), Blackie Academic and Professional, Glasgow, 1994, p 1598-1624.
10. Bain R., Grabowski, M., "Properties of Biomass Relevant to Gasification", "A Survey of Biomass Gasification", Reed, T.B., (ed.), Solar Energy Research Institute, Colorado, USA, 1979, p 133-175.
11. Ensyn Technologies Inc. Greely, Ontario, Canada, "Rapid Thermal Processing (RTP) of Straw", Phase 1 final report, December 1992, prepared for ETSU, UK.
12. Huffman, D.R., Vogiatziz, A.J. and Freel, B.A., "Production of Fast Pyrolysis Liquids from sorghum bagasse by rapid thermal processing", final report to Aston University, July 1992, prepared by Ensyn Technologies Inc., Greely, Ontario, Canada.
13 Porteous, A., "Refuse Derived Fuels", Applied Science, London, 1981, p 62.
14. Bone, W.A., "Coal, Its Constitution and Uses", Longmans Green and Co., London, 1936, p 139.
15. Odgers, J. and Kretschmer, D., Gas Turbine Fuels and their influence on Combustion, Vol. 5 , Energy and Engineering Science Series, Abacus Press, Tunbridge Wells, 1986.
16. Hayn, M., Steiner, W., Klinger, R., Steinmüller, H., Sinner, M. and Esterbauer, H., "Basic Research and Pilot Studies on the Enzymatic Conversion of lignocellulosics", Bioconversion of Forest and Agricultural Plant Residues, Saddler, J.N., (ed.), CAB International, Wallingford, U.K., 1993, p 33-72.
17. Probstein, R.F. and Hicks, R.E., "Synthetic Fuels", McGraw-Hill, London, 1982, p 14.
18. Theander, O., "Cellulose, Hemicellulose and Extractives", Fundamentals of Thermochemical Biomass Conversion, Overend R.P., Milne, T.A. and Mudge, L.K. (eds.), Elsevier Applied Science Publishers, New York, 1985, p 35-60.
19. Beaumont, O. and Schwob, Y., "Influence of Physical and Chemical parameters on Wood Pyrolysis", Ind. Eng. Chem. Process Des. Dev., 1984, 23, p 637-641.
20. Antal Jr, M.J., "Biomass Pyrolysis: A Review of the Literature Part I - Carbohydrate Pyrolysis", Advances in Solar Energy, Boër, K.W. and Duffie, J.A., Vol. 1, Plenum Press, 1983, p 61-111.

21. Glaser, W.G., "Lignin", Fundamentals of Thermochemical Biomass Conversion, Overend R.P., Milne, T.A. and Mudge, L.K. (eds), Elsevier Applied Science Publishers, New York, 1985, p 61-76.
22. Maa, P.S. and Bailie, R.C., "Influence of particle sizes and environmental conditions on high temperature pyrolysis of cellulosic material-1 (Theoretical)", Combustion Science and Technology, 7, p 257-269.
23. Shafizadeh, F., "Pyrolytic Reactions and Products of Biomass", Fundamentals of Thermochemical Biomass Conversion, Overend R.P., Milne, T.A. and Mudge, L.K. (eds.), Elsevier Applied Science Publishers, New York, 1985, p 183-217.
24. Graboski M. and Bain R., "Properties of Biomass Relevant to Gasification", A Survey of Biomass Gasification, Reed, T.B., (ed.), Solar Energy Research Institute, Colorado, USA, July 1979, p II:21-66.
25. Goldstein, I.S., "Composition of Biomass", Organic Chemicals from Biomass, Goldstein I.S., (ed.), CRC Press, Boca Raton, Florida, 1981, p 9-18.
26. Wright, J.D., "Ethanol from Biomass by Enzymatic Hydrolysis", Chemical Engineering Progress, August 1988, p 62-74.
27. Evans, R.J. Soltys, M.N. and Milne, T.A., "Fundamental Pyrolysis Studies: Quarterly Report 1 October 1983-31 December 1983", March 1984, SERI, Golden Colorado, prepared under task no. 7505.10 for the US DoE.
28. Wenzl, H.F.Y., The Chemical Technology of Wood, Academic Press, 1970, p 131-132.
29. Shafizadeh, F., "Basic Principles of Direct Combustion", Biomass Conversion Process for Energy and Fuels, Sofer, S.S. and Zaborsky, O.R. (eds.), Plenum Press, New York, 1981, p 103-124.
30. Zaror, C.A. and Pyle, D.L., "The Pyrolysis of Biomass; A General Review", Proc. Ind. Ac. Sci., Section C, (Chem. Eng. Sci.), 1982.
31. Tillman, D.A., "Energy from Wastes: An Overview of Present Technologies and Programs", Fuels from Wastes, Anderson, L.L. and Tillman, D.A. (eds.), Academic Press, Inc. (London) Ltd, 1977, p 17-40.
32. Bio-Alternative SA, "Technique de carbonisation et dee pyrolyse", Pyrolysis as a Basic Technology for Large Agro-Energy Projects, Mattucci, E., Grassi, G. and Palz, W. (eds.), 1989, p 205.
33. Luengo, C.A. and Cencig, M.O., "Biomass Pyrolysis in Brazil: Status Report", Biomass Pyrolysis Liquids Upgrading and utilisation, Bridgwater, A.V. and Grassi, G. (eds.), Elsevier Applied Science, London, 1991, p 299-309.
34. Milne, T.A., "Pyrolysis - The Thermal Behavior of Biomass Below 600°C", A Survey of Biomass Gasification, Reed, T.B., (ed.), Solar Energy Research Institute, Colorado, USA, July 1979, p II:95-132.
35. Graham, R.G., Bergougnou, M.A., Mok, L.K.S. and de Lasa, H.I., "Fast Pyrolysis (Ultrapyrolysis) of Biomass Using Solid Heat Carriers", Fundamentals of Thermochemical Biomass Conversion, Milne, T.A. and Mudge, L.K. (eds.), Elsevier Applied Science Publishers, London and New York, 1985, p 397-410.
36. Besler, S., Kockar, O.M., Putun, A.E. , Ekinci, E. and Putun, E., "Pyrolysis of Euphorbia Rigida from central Anatolia", Advances in thermochemical biomass conversion, Bridgwater, A.V. (ed.), Blackie Academic and Professional, Glasgow 1994, p 1103-1109.
37. Graham, R.G. and Bergougnou, M.A. and Overend, R.P., "Fast Pyrolysis of Biomass", Journal of Analytical and Applied Pyrolysis, 6, 1984, p 95-135.
38 Graham, R.G., Freel, B.A., Bergougnou, M A, Overend, R.P. and Mok, L.K., "Fast Pyrolysis of Cellulose", Energy From Biomass, 3rd E C Conference, Venice, Italy, March 1985, Palz, W., Coombs, J. and Hall, D.O. (eds.), Elsevier Applied Science Publishers, London, 1985, p 860.
39. Graham, R.G., "A characterization of the Fast Pyrolysis of Cellulose and Wood Biomass", Ph.D. thesis, February 1993, University of Western Ontario, London, Ontario, Canada.
40. Berg, D.A., Briens, C.L. and Bergougnou, M.A., "Reactor Development for the Ultrapyrolysis Process", Can J. Chem. Eng. Vol. 67, February 1989, p 96-101.

41. Berg, D.A., Sumner, R.J., Meunier, M., Briens, C.L. and Bergougnou, M.A., "The Ultra-Rapid Fluidized (URF) reactor, a major new reactor system", Circulating Fluidized Bed Technology, Basu, P. (ed.), Elmsford, New York, Pergamon Books Inc., 1986, p 377-384.
42. Graham, R.G., Bergougnou, M.A., Mok, L.K., de Lasa, H.I. and Freel, B.A., "Ultrapyrolysis of Cellulose and Wood Components", 5th Canadian Bioenergy R & D Seminar, Hasnain, S. (ed.), 1984, p 386.
43. Soltes, E.J. and Lin, S-C. K., "Hydroprocessing of biomass tars for liquid engine fuels", Progress in Biomass Conversion, Vol. 5, Tillman, D.A and Jahn, E.C. (eds.), Academic press, 1984, p 1-68.
44. Baker, G.B. and Elliot, D.C., "Catalytic Hydrotreating of Biomass-Derived Oils", in Pyrolysis Oils From Biomass Producing, Analysing and Upgrading, Soltes, E.J. and Milne, T.A. (eds.), p 228-240.
45. Rupp, M., "Utilisation of Pyrolysis Liquids in Refineries", Biomass Pyrolysis Liquids Upgrading and utiliation, Bridgwater, A.V. and Grassi, G. (eds.), Elsevier Applied Science, 1991, p 217-225.
46. Diebold, J.P. and Scahill, J., "Conversion of wood to aromatic gasoline with zeolite catalysts", Energy Progress, 8, 1, March 1988, p 59-65.
47. Diebold, J.P., Evans, R.J., Levie, B.E., Milne, T.A., and Scahill, J.W., "Low Pressure Upgrading of Primary Oils from Biomass", annual report 1 January-31 December 1986, August 1987, SERI/PR-234-3169.
48. Horne, P.A. and Williams, P.T., "Catalysis of model biomass compounds over zeolite ZSM-5 catalyst", Biomass for Energy and Industry 7th EC conference, Hall, D.O., Grassi, G. and Scheer, H. (eds.), Ponte Press, Bochum, Germany, 1994, p 901-907.
49. Reed, T.B., Diebold J.P. and Désrosiers, R., "Perspectives in Heat Transfer Requirements and Mechanisms for Fast Pyrolysis", Proceedings of the Specialists' Workshop on Fast Pyrolyis of Biomass, Copper Mountain, Colorado, 20-22 October 1980, SERI/CP-622-1096, Solar Energy Research Institute, USA, p 7-20.
50. Lédé, J., Verzaro, F., Antoine, B. and Villermaux, J., "Flash Pyrolysis of Wood in a Cyclone Reactor", Chemical Engineering and Processing, 20 No. 6, 1986, p 309-317.
51. Lédé, J., Panagopoulos, J., Li, H.Z. and Villermaux, J., "Fast Pyrolysis of Wood: direct measurement and study of ablation rate", Fuel, 64, 1985, p 1514-1520.
52. di Blasi, C., "Analysis of Convection and Secondary Reaction Effects within Porous Solid Fuels Undergoing Pyrolysis", Combustion Science and Technology, 90, 1993, p 315-340.
53. Alves, S.S. and Figueiredo, J.L., "A model for pyrolysis of wet wood", Chem. Eng. Sci. Vol. 44, 12, 1989, p 2861-2869.
54. Gray, M.R., Corcoran, W.H. and Gavalas, G.R., "Pyrolysis of a wood derived material. Effects of Moisture and ash content", Ind. Eng. Chem. Process Des. Dev. 1985, 24, p 646-651.
55. Gray, M.R., "The effects of moisture and ash content on the pyrolysis of a wood derived material", Ph.D. thesis, California Institute of Technology, Pasadena, USA, 1984.
56. Shafizadeh, F., Furneaux, R.H., Cochran T.G., Scholl, J.P. and Sakai, Y., "Production of Levoglucosan and Glucose from Pyrolysis of Cellulosic Materials", J. Appl. Polym. Sci., John Wiley and Sons, Inc., 23, 1979, p 3525-3539.
57. Scott, D.S., Piskorz, J. and Radlein, D., "Liquid Products from the Continuous Flash Pyrolysis of Biomass", Ind. Eng. Chem. Process Des. Dev., 24, 3, 1985, p 581-588.
58. Scott, D.S., Piskorz, J. and Radlein, D., "Sugars from Cellulosics by the Waterloo Fast Pyrolysis Process", Pyrolysis and Gasification, Ferrero, G.L., Maniatis, K., Buekens, A. and Bridgwater, A.V. (eds.), Luxembourg, May 1989, Elsevier Applied Science Publishers, 1989, London, p 201-208.
59. Piskorz, J., Radlein, D., Scott, D.S. and Czernik, S., "Liquid Products from the Fast Pyrolysis of Wood and Cellulose", Research in Thermochemical Biomass Conversion, Phoenix, Arizona, USA, Bridgwater, A.V. and Kuester, J.L. (eds.), Elsevier Applied Science Publishers, London and New York, 1988, p 557-571.
60. Shafizadeh, F., "Pyrolysis and Combustion of Cellulosic Materials", Advan. Carbohydr. Chem., 23, 1968, p 419-474.

61. Scott, D.S., Piskorz, J., Radlein, D. and Czernik, S., "Conversion of Lignocellulosics to Sugars by Thermal Fast Pyrolysis", Proceedings of the 7th Canadian Bioenergy Research and Development Seminar, 1989, Ottawa, Canada, p 713-718.
62. Scott, D.S., Piskorz, J. and Radlein, D., "Thermal Conversion of Biomass to Liquids by the Waterloo fast Pyrolysis Process", Pyrolysis as a basic technology for large agro-energy projects, Matucci, E., Grassi, G. and Palz, W. (eds.), Commission of the European Communities, EUR 11382 EN, 1989, p 115-124.
63. Piskorz, J., Radlein, D. and Scott, D.S., "Thermal Conversion of Cellulose and Hemicellulose in wood to sugars", Advances in thermochemical Biomass Conversion, Bridgwater, A.V., (ed.), Blackie, Glasgow, 1994, p 1432-1440.
64. Radlein, D, Piskorz, J. and Scott, D.S., "Control of Selectivity in the Fast Pyrolysis of Cellulose", 6th European Conference on Biomass for Energy, Industry and the Environment, Grassi, G., Collina, A. and Zibetta, H. (eds.), Elsevier Appled Science Publishers, p 643-649.
65. Richards, G.N., "Chemistry of Pyrolysis of Polysaccharides and Lignocellulosics", Advances in Thermochemical Biomass Conversion, Bridgwater, A.V. (ed.), Blackie, Glasgow, 1994.p 727-745.
66. Bain, R., "Beneficiation of Biomass for Gasification and Combustion", A Survey of Biomass Gasification, Vol II, SERI TR-33-239, July 1979, p II:67-94.
67. Miles, T.R., "Biomass Preparation for Thermochemical Conversion (Keynote Paper)", Thermochemical Processing of Biomass, Bridgwater A.V. (ed.), Butterworths, London, 1984, p 69-90.
68. Kelbon, M., Bousman, S. and Krieger-Brockett, B., "Conditions that Favor Tar Production from Pyrolysis of Large Moist Wood Particles", Pyrolysis Oils from Biomass, Producing, Analyzing and Upgrading, Soltes, E.J. and Milne, T.A. (eds.), ACS Symposium Series 376, ACS, Washington DC, 1988, p 41-54.
69. Evans, R.J. and Milne, T.A., " Molecular Characterization of the Pyrolysis of Biomass I: Applications", Energy and Fuels, 1987, Vol 1, 1987, p 311.
70. Maniatis, K. and Buekens, A., "Fast Pyrolysis of Biomass", Research in Thermochemical Biomass Conversion, Bridgwater, A.V. and Kuester, J.L., (eds.), Elsevier Applied Science, p 179-191.
71. Mr. J. Piskorz, University of Waterloo, Canada, private communication, Oct. 1993.
72. Scott, D.S. and Piskorz, J. "The Flash Pyrolysis of Aspen-Poplar Wood" Can. J. Chem. Eng. 1982, 60, p 666-674.
73. Saastamoinen, J.J. and Aho, M., "The Simultaneous Drying and Pyrolysis of Single Wood Particles and Pellets of Peat", 1984 International Symposium on Alternative Fuels and Hazardous Wastes, Tulsa, Oklahoma, October 1984.
74. Roy, C., de Caumia, B. Brouillard, D. and Ménard, H., "The pyrolysis under vacuum of Aspen Poplar", Fundamentals of Thermochemical Biomass Conversion, Overend R P, Milne T A and Mudge, L K, (eds.), Elsevier Applied Science Publishers, New York, 1985, p 237-256.
75. Gulyurtlu, I., Cabrita, C., Franci, F., Mascarenhas and Jogo, M., "Pyrolysis of Forestry Wastes in a Fluidized bed Reactor produce medium calorific gaseous fuel", Research in Thermochemical Biomass Conversion, 1988, Bridgwater A.V. and Kuester J.L. (eds.), Elsevier Applied Science Publishers, London and New York, 1988, p 597-608.
76. Roberts, A.F., "A Review of Kinetic Data for the Pyrolysis of Wood and Related Substances", Combustion and Flame, 14, 1970, p 261-272.
77. Roberts, A.F., "Problems Associated with the Theoretical Analysis of the Burning of Wood", 13th Symposium (International) on Combustion, Combustion Institute, 1971, p 893-903.
78. Lee C., Chaiken, R.F. and Singer, J.M., "Charring Pyrolysis of Wood in Fires by Laser Simulation" 16th Symposium (International) on Combustion, Combustion Institute, 1976, p 1459.
79. Chan, W.C.R., "Analysis of Physical and Chemical Processes in the Pyrolysis of a single Large Pellet of Biomass", PhD Thesis, University of Washington, 1982.
80. Chan, W-C.R., Kelbon, M. and Krieger, B.B., "Product Formation in the Pyrolysis of Large Wood Particles", Fundamentals of Thermochemical Biomass Conversion,

Overend R.P., Milne, T.A. and Mudge, L.K. (eds.), Elsevier Applied Science Publishers, New York, 1985, 219-236.
81. Piskorz, J., Scott, D.S,. and Radlein, D., "Composition of Oils Obtained by the Fast Pyrolysis of Different Woods", Pyrolysis Oils from Biomass, Producing, Analyzing and Upgrading, Soltes, E.J. and Milne, T.A. (eds.), ACS Symposium Series 376, American Chemical Society, Washington DC, 1988, p 167-178.
82. Elliott, D.C., "Comparative Analysis of Gasification/Pyrolysis Condensates", Proceedings of the 1985 Biomass Thermochemical Conversion Contractors, Meeting, Minneapolis, Minnesota, Oct 15-16, 1985, p 361-381.
83. Lidén, A.G., Berruti, F. and Scott, D.S., "A kinetic model for the production of liquids from the flash pyrolysis of biomass", Chem. Eng. Comm., 1988, 65, p 207-221.
84. Scott, D.S., Piskorz, J., Bergougnou, M.A., Graham, R.G. and Overend, R.P, "The Role of Temperature in the Fast Pyrolysis Of Cellulose and Wood", Ind. Eng. Chem. Res., 27, 1, 1988, p 8-15.
85. Nunn, T.R, Howard, J.B., Longwell, J.P. and Peters, W.A., "Product Composition and Kinetics in the Rapid Pyrolysis of Sweet Gum Hardwood", Ind. Eng. Chem. Prod. Res. Dev., 24, 1985, p 836-844.
86. Kovac, R.J., Gorton, C.W., O'Neil, D.J. and Newman, C.J., "Low Pressure Entrained Flow Pyrolysis of Biomass to Produce Liquid Fuels", Proceedings of the 1987 Biomass Thermochemical Conversion Contractors' Review Meeting, Atlanta, USA, May 20-21, 1987, p 23.
87. Samolada, M.C. and Vasalos I.A., "A kinetic approach to the flash pyrolysis of biomass in a fluidized bed reactor", Fuel, 1991, 70, p 883-889.
88. Samolada, M.C. and Vasalos, I.C., "Effect of Experimental Conditions on the Composition of gases and liquids from biomass pyrolysis", Advances in Thermochemical Biomass Conversion, Blackie, Glasgow, 1994, p 859-873.
89. Thurner, F. and Mann, U., "Kinetic investigation of Wood Pyrolysis", Ind. Eng. Chem. Process Des. Dev. 1981, 20, 3, 482-488.
90. Scott, D.S. and Piskorz, J. "Continuous flash pyrolysis of wood for production of liquid fuels", Energy from Biomass and Wastes VII, IGT, Chicago, 1983, p 1123-1146.
91. Elliot, D.C., "Analysis and Comparison of Biomass Pyrolysis/Gasification Condensates-Final Report", prepared for the US Department of Energy under contract De-AC06-76RLO 1830, June 1986, PNL-5943 UC-61D.
92. Elliott, D.C., "Relation of Reaction Time and Temperature to Chemical Composition of Pyrolysis Oils", Pyrolysis Oils from Biomass, Producing, Analyzing and Upgrading, Soltes, E.J. and Milne, T.A. (eds), ACS Symposium Series 376, American Chemical Society, Washington DC, 1988, p 55-65.
93. Evans, R.J. and Milne, T.A., "Fundamental Pyrolysis Studies: Final Report 1 October 1980-30 December 1985", SERI/PR-234-3026, Solar Energy Research Institute, Golden Colorado, USA, 1986.
94. Vassilatos, V., "Thermal and Catalytic Cracking of tar in biomass pyrolysis gas", M.Sc. thesis, Dept. of Chemical Technology, Royal Institute of Technology, Stockholm, Sweden, 1990.
95. Scott, D.S., Piskorz, J., Grinshpun, A. and Graham, R.G., "The Effect of Temperature on Liquid Product Composition from the Fast Pyrolysis of Cellulose", Production, Analysis and Upgrading of Oils from Biomass, Rafcliffe, C.T., Suuberg, E.M. and Vorres, K.S. (eds.), ACS, Division of Fuel Chemistry, Vol. 32, No.2, p 1-11.
96. Halling, J. N., "Modelling the Liquid Product Distribution from the Waterloo Fast Pyrolysis Process", M.Sc. thesis, University of Waterloo, Canada, 1987.
97. Bilbao R, Murillo, M.B., Millera A. and Garcia-Bacaicoa, P., "Modelling of the Thermal decomposition of large pine wood particles", Biomass for Energy and Industry 7th EC conference, Hall, D.O., Grassi, G. and Scheer, H. (eds.), Ponte Press, Bochum, Germany, 1994, p 1013-1018.
98. Dérosiers, R.E. and Lin, R.J., "A phase change approach to macro-particle pyrolysis of cellulosic materials", preprints of ACS Symposium series, 1983, 28, No. 5, p338-382.
99. Havens, J.A., "Thermal Decomposition of Wood", Ph.D. thesis, University of Oklahoma, USA, 1970.

100. Ahmed, S. and Clements, L.D., "Kinetics of Biomass Pyrolysis with Radiant Heating", Research in Thermochemical Biomass Conversion, Bridgwater, A.V. and Kuester, J.L., (eds.), 1988, Elsevier Applied Science Publishers, New York, p 294-309.
101. Capart. R, Fagbemi, L. and Gelus, M., "Wood Pyrolysis: A Model Including Thermal Effect of the Reaction", Energy from Biomass, 3rd E.C. Conference, Venice, Italy, March 1985, Palz W, Coombs J and Hall D O (eds), Elsevier Applied Science Publishers, London, 1985, p 842-846.
102. Antal Jr, M.J., "Biomass Pyrolysis: A Review of the Literature Part II - Lignocellulose Pyrolysis", Advances in Solar Energy, Boër K.W. and Duffie J.A., Vol 2, Plenum Press, 1985, p 175-255.
103. Lédé, J., "Reaction temperature of solid particles undergoing an endothermal volatilization. Application to the Fast Pyrolysis of Biomass", Symposium on Fast Pyrolysis, ACS Annual Meeting, Denver, Colorado, USA, 29 March-2 April 1993, proceeding to be published in Biomass and Bioenergy, 1994.
104. Kothari, V. and Antal, Jr M.J., "Numerical studies of the flash pyrolysis of cellulose", Fuel, 64, 1985, p 1483-1494.
105. Diebold, J.P. and Scahill J.W., "Ablative Pyrolyis of Biomass in Solid-Convective Heat Transfer Environments", Fundamentals of Thermochemical Biomass Conversion, Overend R.P., Milne T.A. and Mudge L.K., (eds.), Elsevier Applied Science Publishers, New York, 1985, p 539-555.
106. Scott, D.S. and Piskorz, J., "The Continuous Flash Pyrolysis of Biomass", Can. J. Chem. Eng. 1984, 62, p 404-412.
107. Reed, T.B., "Contact Pyrolysis in a "Pyrolysis Mill"", Research in Thermochemical Biomass Conversion, Bridgwater, A.V. and Kuester, J.L. (eds.), Elsevier Applied Science Publishers, New York, 1988, p 192-202.
108. Graham, R.G., Freel, B.A. and Bergougnou, M.A., "The Production of Pyrolytic Liquids, Gas and Char from Wood and Cellulose by Fast Pyrolysis" Research in Thermochemical Biomass Conversion, Phoenix, USA, April 1988, Bridgwater A.V. and Kuester J.L. (eds), (Elsevier Applied Science Publishers, London and New York, 1988), p 629-641.
109. Czernik, S., Scahill, J. and Diebold, J.P., "The production of liquid fuel by Fast Pyrolysis of Biomass", Proceedings of the 28th Intersociety Energy Conversion Engineering Conference, Vol. 2, American Chemical Society, 1993, p 429-436.
110. van den Aarsen, F.G., Beenackers, A.A.C.M. and van Swaaij, W.P.M., "Wood Pyrolysis and Carbon Dioxide Char Gasification Kinetics in a Fluidized Bed" Fundamentals of Thermochemical Biomass Conversion, Milne, T.A. and Mudge, L.K. (eds.), Elsevier Applied Science Publishers, London and New York,1985, p 691-715.
111. Mok., S.L.K., Briens, C.L. and Bergogougnou, M.A., "Fast Pyrolysis of Wood, Part II: Theoretical heat transfer study to determine the largest pyrolyzable particle size", final report for Ensyn Technologies, University of Western Ontario contract, March 1988.
112. Simmons, G.M. and Gentry, M., "Particle size limitations due to heat transfer in determining pyrolysis kinetics of biomass", J. Anal. and Appl. Pyr., 10, 1986, p 117-127.
113. Prins, W. "Fluidised bed combustion of a single coal particle", Ph.D. thesis, Department of Chemical Engineering, University of Twente, 1987.
114. Maschio, G., Lucchesi, A. and Koufopanos, C., "Study of Kinetic and Transfer Phenomena in the Pyrolysis of Biomass Particles", Advances in Thermochemical Biomass Conversion, Bridgwater, A.V. (ed.), Blackie, Academic and Professional, Glasgow, 1994, p 746-759.
115. Lédé, J., Li, H.Z. and Villermaux, J., "Fusion-like Behaviour of Biomass Pyrolysis", ACS, Vol. 32, 2, Production, Analysis and Upgrading of Oils from Biomass, Ratcliffe, C.T., Suuberg, E.M. and Vorres, K.S. (eds.), 1987.
116. Diebold, J.P. and Power, A.J., "Engineering Aspects of the Vortex Pyrolysis Reactor to Produce Primary Pyrolysis Oil Vapours for Use in Resins and Adhesives", Research in Thermochemical Biomass Conversion, Bridgwater, A.V. and Kuester, J.L. (eds.), Elsevier Applied Science Publishers, London and New York, 1988, p 609-628.
117. Bergougnou, M.A., de Lasa, H.I., Mok, L.K., Graham, R.G. and Hazlett, J., "High Intensity Flash Pyrolysis of Wood using solid heat carriers (Ultrapyrolysis)", 3rd

Bioenergy R and D Seminar, Summers, B., (ed.), National Research Council of Canada, Ottawa, Canada, 1981, p 277-282.
118. Ekstrom, C. and Rensfelt, E., "Flash pyrolysis of Biomass in Sweden" Proceedings of the Specialists' Workshop on Fast Pyrolyis of Biomass, Copper Mountain, Colorado, 20-22nd October 1980, SERI/CP-622-1096, Solar Energy Research Institute, Golden, Colorado, p 257-267.
119. Hajaligol, M.R., Peters, W.A., Howard, J.B. and Longwell, J.P., "Product Compositions and Kinetics for rapid pyrolysis of Cellulose", Proceedings of the Specialists' Workshop on Fast Pyrolyis of Biomass, Copper Mountain, 1980, SERI/CP-622-1096, Solar Energy Research Institute, Golden, USA, p 215-236.
120. Steinberg M., Fallon P.T. and Sundaram M.S., "Flash Pyrolysis of Biomass with Reactive and Non-Reactive Gases", Biomass, 9, 1986, p 293-315.
121. Diebold, J.P., "Ablative pyrolysis of macroparticles of biomass", Proceedings of the Specialists' Workshop on Fast Pyrolyis of Biomass, Copper Mountain, 1980, SERI/CP-622-1096, Solar Energy Research Institute, Golden, Colorado, p 237-251.
122. Roy, C., Lemeuix, R., de Caumia, B. and Blanchette, D., "Processing of Wood Chips in a Semicontinuous Multiple Hearth Reactor", Pyrolysis Oils from Biomass Producing, Analyzing and Upgrading, Soltes, E.J. and Milne, T.A., (eds)., American Chemical Society, WashingtonD.C., 1988, p 16-30.
123. Agrawal, R.K. and McCluskey, R.J., "The effects of pressure on the pyrolysis of newsprint", ACS preprints, 1983, 28, 5, p 310-306.
124. Mok, W.S-L. and Antal, Jr. M.J., "Effects of Pressure on Biomass Pyrolysis. II. Heats of Reaction of Cellulose products", Thermochimica Acta, 68, 1983, p 165-186.
125. Richard, J.R., Antal, Jr. M.J., "Thermogravimetric studies of charcoal formation from cellulose at elevated pressures", Advances in thermochemical biomass conversion, 1994, Bridgwater, A.V., Blackie Academic and Professional, p 784-792.
126. Güell, A.J., Li, C-Z., Herod, A.A., Stokes, B.J., Hancock P. and Kandiyoti, R., "Mild hydropyrolysis of biomass materials: effect of pressure on product tar structures", Advances in thermochemical biomass conversion, Bridgwater, A.V., (ed.), Blackie Acacemic and Professional, 1994, p 1053-1067.
127. Hajaligol, M.R., Peters, W.A. Howard, J.B. and Longwell, J.P., "Product Compositions and Kinetics for Rapid Pyrolysis of Cellulose", Ind. Eng. Chem. Proc. Des. Dev., 1982, 21, 457- 465.
128. Steinberg, M., Fallon, P.T. and Sundaram, M.S., "Flash Methanolysis - The Flash Pyrolysis of Biomass with Methane Gas" Proceedings of the 1985 Biomass Thermochemical Conversion Contractors' Meeting, Minneapolis, USA, 1985, p 15.
129. Sundaram, M.S., Steinberg, M. and Fallon, P.T., "Flash Pyrolysis of Biomass with Reactive and Non-Reactive Gases", Fundamentals of Thermochemical Biomass Conversion, Overend, R.P., Milne, T.A. and Mudge, L.K. (eds.), Elsevier Applied Science Publishers, New York, 1985, p 167.
130. Steinberg, M., Fallon, P.T. and Sundaram, M.S., "Flash Pyrolysis of Biomass with Reactive and Non-Reactive Gases", Proceedings of the 15th Biomass Thermochemical Conversion Contractors' Meeting, Atlanta, USA, 1983, p 421.
131. Guanxing, C., Qizhuang, Y., Sjostrom, K., Bjornbom, E., "Pyrolysis/gasification of biomass in presence of dolomite in a pressurised fluidised bed", Advances in Thermochemical Biomass Conversion, Bridgwater, A.V., (ed.), Blackie Acacemic and Professional, Glasgow, 1994, p 1197-1204.
132. Eklund, H. and Wanzl, W., "Pyrolysis and Hydropyrolysis of Peat at high heating rates", Fundamentals of Thermochemical Biomass Conversion, Overend, R.P., Milne, T.A. and Mudge, L.K. (eds.), Elsevier Applied Science Publishers, New York, 1985, p 315-327.
133. Snape, C.E., Putun, E., Lafferty, C.J., Donald, F.J. and Ekinci, E., "High oil yields from Euphorbia rigida via hydropyrolysis" Advances in Thermochemical Biomass Conversion, Bridgwater, A.V. (ed.), Blackie Academic and Professional, Glasgow, 1994, p 1053-1067.
134. Trebbi, G. and Rossi, C., "Integrated Leben Project Umbria", ENEL-SpA, Progress Report, May 1993, JOUB-0059-I(A), submitted to CEC, DG XII, Brussels.

135. Maniatis, K., Baeyens, J. , Peeters, H. and Roggeman, G., "The Egemin flash pyrolysis process: commissioning and initial results", Advances in Thermochemical Biomass Conversion, 1994, Bridgwater, A.V., (ed.), Blackie Academic and Professional, Glasgow, p 1257-1264.
136. Shankaranarayanan, G.V., Bakhshi, N.N., MacDonald, D.G., "Pyrolysis of waste coffee under different gaseous environments", Energy from Biomass and Wastes XI, Klass, D.L., (ed.), IGT, Chicago, 1988, p 381-409.
137. Radlein, D., Piskorz, J. and Scott, D.S., "Fast Pyrolysis of Natural Polysaccharides as a potential industrial process", J. Anal. Appl. Pyr., 19, 1991, p 41-63.
138. Shafizadeh F., "Production of Sugar and Sugar derivatives by Pyrolysis of Biomass", J.Appl. Polymer Sci., Symposium 37, Sarko, A. (ed.), 1983, Wiley and Sons, New York, p 723-750.
139. Piskorz, J., Radlein, D., and Scott, D.S., "On the Mechanism of the Rapid Pyrolysis of Biomass", J. Anal. Appl. Pyr., 9, 1986, p 121-137.
140. Richards, G. N., "Glycoaldehyde from Pyrolysis of Cellulose", J. Anal. Appl. Pyr., 1987, 10, p 251-255.
141. Essig, M., Lowary, T., Richards, G.N. and Schenck, E., "Influences of 'Neutral' Salts on Thermochemical Conversion of Cellulose and of Sucrose", Research in Thermochemical Biomass Conversion, Bridgwater A.V. and Kuester J.L. (eds.), Elsevier Applied Science Publishers, London and New York, 1988, p 143-154.
142. Pavlath, A.E. and Gregorski, K.S., "Carbohydrate Pyrolysis.II. Formation of Furfural and Furfuryl alcohol during the pyrolysis of selected carbohydrates with acidic and basic catalysts", Research in Thermochemical Biomass Conversion, Bridgwater A.V. and Kuester J.L. (eds.), Elsevier Applied Science Publishers, London and New York, 1988, p 155-163.
143. Fung, D.P.C., "Furthr Investigation on the Effect of H_3PO_4 on the Pyrolysis of Cellulose", Wood Science, 9, 1, p 55-57.
144. Palm, M., Piskorz, J., Peacocke, G.V.C. and Scott, D.S., "Pyrolysis of Sweet Sorghum Bagasse in the Waterloo Fast Pyrolysis Process", First Biomass Conference of the Americas: Energy, Environment, Agriculture and Industry, Vol. II, US DoE. 1993, p 947-963.
145. Vasalos, I.A., Samolada, M.C., and Achladas, G.E., "Biomass pyrolysis for maximizing phenolic liquids", Research in Thermochemical Biomass Conversion, Bridgwater, A.V. and Kuester, J.L., (eds.), Elseveir Applied Science Publishers, London and New York, 1988, p 251-263.
146. Vasalos, I.A., Samolada, M.C., and Achladas, G.E., "Biomass pyrolysis for maximizing phenolic liquids", Research in Thermochemical Biomass Conversion, Bridgwater, A.V. and Kuester, J.L., (eds.), Elseveir Applied Science Publishers, London and New York, 1988, p 251-263.
147. Shafizadeh, F. and Chin, P.S., Carbohydrate Research, 46, 1976, p 149.
148. Bilbao, R., Arauzo, J. and Millera, A., "Kinetics of thermal decomposition of Cellulose. Part I. Influence of Experimental Conditions", Thermochimica Acta., 1987, 120, 121-131.
149. Bilbao, R., Arauzo, J., and Millera, A., "Kinetics of thermal decomposition of Cellulose. Part II. Temperature difference between gas and solid at high heating rates", Thermochimica Acta., 1987, 120, 133-141.
150. Bilbao, R., Millera, A. and Arauzo, J., "Thermal decomposition of lignocellulosic materials: influence of the chemical composition", Thermochimica Acta., 1989, 143, 149-159.
151. Bilbao, R., Millera, A. and Arauzo, J., "Kinetics of weight loss by thermal decomposition of different lignocellulosic materials. Relation between the results obtained from isothermal and dynamic experiments", Thermochimica Acta., 1990, 165, 103-112.
152. Shafizadeh, F. and DeGroot, W.F., "Combustion Characteristics of Cellulosic Fuels", Thermal Uses of Carbohydrates and Lignins, Shafizadeh, F., Sarkanen, K.V. and Tillman, D.A., Academic Press, New York, 1976, p 1.
153. Kilzer, F.J. and Broido, A., "Speculations on the Nature of Cellulose Pyrolysis, Pyrodynamics, Vol 2, 1965, p 151.

154. Shafizadeh, F., "Introduction to Pyrolysis of Biomass", J. Anal. Appl. Pyrol., 3, 1982, p 283.
155. Tang, W.K., "Effect of Inorganic Salts on Pyrolysis of Wood, Alpha Cellulose and Lignin", US Forest Service Research Paper, FPL71, January 1967.
156. Golova, O.P., "Chemical Effects of Heat on Cellulose", Russian Chem. Reviews, 44, No 8, 1975, p 687.
157. Shafizadeh, F., Bradbury, A.G.W., DeGroot, W.F. and Aanerud, T.W., "Role of Inorganic Additives in the Smoldering Combustion of Cotton Cellulose", Ind. Engng. Chem. Prod. Res. & Dev., 21, 1982, p 27.
158. Evans, R.J. and Milne, T.A,. "Applied Mechanistic Studies of Biomass Pyrolysis" in Proceedings of the 1985 Biomass Thermochemical Conversion Contractors' Meeting, Minneapolis, Minnesota, Oct 15-16, 1985, p 57.
159. Byrne, G.A., Gardner, D. and Holmes, F.H., "The Pyrolysis of Cellulose and the action of flame retardents II: further analysis and identification of products", J. Applied Chemistry, 16, 1966, p 81-88.
160. Madorsky, S.L., Hart, V.E. and Straus S.J., Journal of Research of the Natural Bureau of Standards, 56, 6, 1956, p 343-354.
161. Bradbury, A.G.W., Sakai Y. and Shafizadeh, F., Journal of Applied Polymer Science 23, 1979, p 3271-3280.
162. Shafizadeh, F., "Pyrolytic Reactions and Products of Biomass", Fundamentals of Thermochemical Biomass Conversion, Overend, R.P., Milne, T.A. and Mudge, L.K. (eds.), Elsevier Applied Science Publishers, New York, 1985, p 183-218.
163. Scott, D.S., Piskorz, J. and Radlein, D., "The yields of chemicals from biomass based fast pyrolysis oils", Energy from Biomass and Wastes XVI, 1992, Klass, D.L. (ed.), IGT, paper no. 18.
164. Piskorz, J., Scott, D.S., Radlein, D. and Czernik, S., "New Applications of the Waterloo Fast Pyrolysis Process", Biomass Thermal Processing, proceedings of the first Canada/European Community R&D Contractors' Meeting, 23-25 October 1990, Ottawa, Canada, Hogan, H, Bridgwater, A V, Grassi, G., and Robert, J. (eds.), CPL Press Ltd., London, 1992, p 64-73.
165. Basch, A. and Lewin, M., "The influence of fine structure on the pyrolysis of cellulose I: vacuum pyrolysis", J. Polymer Sci., 1973, 11, p 3071-3093.
166. Halpern, Y. and Patai, S. Israel J. Chem., 1969, p 673-683.
167. Essig, M., Richards, G.N. and Schenck, E., "Mechanisms of formation of the major volatile products from the pyrolysis of cellulose", Biomass Handbook, Kitani, O. and Hall, C.W., (eds.) p 841-862.
168. Arseneau, D.F. and Stanwick, J.J., "A Study of Reaction mechanisms by DSC and TG", Thermal Analysis, 1951, p 319-326.
169. Evans, R.J. and Milne, T A, " Molecular Characterization of the Pyrolysis of Biomass 2: Fundamentals", Energy and Fuels,1987, Vol 1, 4, 1987, p 311-319.
170. Soltes E.J. and Elder, T.J., "Pyrolysis", in Organic Chemicals from Biomass, Goldstein I.S. (ed.), CRC Press, Boca Raton, Florida, 1981, p 63-100.
171. Ramiah, M.V., "Thermogravimetric and Differential Thermal Analysis of Cellulose, Hemicellulose and Lignin", J. Appl. Polym. Sci., 1970, 14, p 1323-1337.
172. Williams, P.T. and Besler, S., "Thermogravimetric Analysis of the Components of Biomass" Advances in Thermochemical Biomass Conversion, 1994, Bridgwater, A.V., (ed.), Blackie Academic and Professional, Glasgow, p 771-783.
173. Varhegyi, G., Antal Jr., M.J., Szekely, T. and Szabo, P., "Kinetics of the Thermal decomposition of cellulose, hemicellulose, and sugar cane bagasse", Energy and Fuels, 3, 1989, p 329-335.
174. Varhegyi, G., Szabo, P., "Reaction kinetics of the thermal decomposition of cellulose and hemicellulose in biomass materials", Advances in Thermochemical Biomass Conversion, 1994, Bridgwater, A.V., (ed.), Blackie Academic and Professional, Glasgow, p 760-770.
175. Simkovic, I., Varhegyi, G., Antal Jr., M.J., Ebringerova, A. Szekely, T. and Szabo, P. "Thermogravimetric/Mass Spectrometric Characterization of the thermal decomposition of (4-O-methyl-D-Glucurono)-D-xylan", J. Appl. Polym. Sci., 1988, 36, p 721-728.

176. Avni, E., Davoudzadeh, F. and Coughlin, R.W., "Flash Pyrolysis of Lignin", in Fundamentals of Thermochemical Biomass Conversion, Overend, R.P., Milne, T.A. and Mudge, L.K. (eds.), Elsevier Applied Science Publishers, New York, 1985, p 329.
177. Avni, E., Coughlin, R.W., Solomon, P.R. and King, H.H., "Mathematical Modelling of Lignin Pyrolysis, Fuel, 64, 1985, p 1495.
178. Goos, A.W., "The Thermal Decomposition of Wood", Wood Chemistry, Wise, L.E. and Jahn, E.C. (eds.), Reinhold, New York, 1952, Chapter 20.
179. Allan G.G. and Matilla T, in Lignins: Occurrence, Formation, Structure and Reactions, Sarkanen, K.V. and Ludwig C.H. (eds.), Wiley-Interscience, New York, 1971.
180. Sekiguchi, Y., Frye, J.S. and Shafizadeh, F., "Structure and Formation of Cellulosic Chars", J. Appl. Polym. Sci., Vol 28, 1983, p 3515-3525.
181. Klein, M.T. and Virk, P.S., "Primary and Secondary Lignin Pyrolysis Reaction Pathways", Ind. Eng. Chem. Fundam., 22, 1983, p 35.
182. Petrocelli, F.P. and Klein, M.T., "Simulation of Kraft Lignin Pyrolysis", Fundamentals of Thermochemical Biomass Conversion, Overend R.P., Milne T.A. and Mudge, L.K. (eds.), Elsevier Applied Science Publishers, New York, 1985, p 257.
183. Iatridis, B. and Gavalas, G.R., "Pyrolysis of a Precipitated Kraft Lignin", Ind. Eng. Chem. Prod. Res. Dev., 18, Vol 2, 1979, p 127.
184. McKinley J,"Biomass Liquefaction Centralized Analysis", July 1989, Project No 4-03-837, Final Report for EMR Canada, Ottawa, Canada.
185. Jegers, H.E. and Klein, M.T., "Primary and Secondary Lignin Pyrolysis reaction pathways", Ind. Eng. Chem. Process Des. Dev., 1985, 24, p 173-183.
186. Train, P.M. and Klein, M.T., "Chemical Modeling of Lignin. A Monte Carlo Simulation of Its Structure and Catalytic liquefaction", Pyrolysis Oils from Biomass, Producing Analyzing and Upgrading, ACS Symposium Series, 376, Soltes, E.J. and Milne T.A. (eds.), ACS Washington DC, 1988, p 240-263.
187. Landau, R.N., Libanati, C. and Klein, M.T., "Monte Carlo Simulation of Lignin Pyrolysis: Sensitivity to Kinetic Parameters", Research in Thermochemical Biomass Conversion, Phoenix, Arizona, USA, April 1988, Bridgwater, A.V. and Kuester, J.L. (eds.), Elsevier Applied Science Publishers, London and New York, 1988, p 452.
188. King, H.H., Solomon, P.R, Avni, E. and Coughlin, R.W., "Modeling Tar Composition in Lignin Pyrolysis", ACS Series, Vol 28, No 5, Washington DC, August 1983, p 319.
190. Avni, E. and Coughlin R.W., "Lignin Pyrolysis in Heated Grid Apparatus: Experiment and Theory", ACS Series, Vol 28, No 5, Washington DC, August 1983, p 307.
191. Connor, M.A. and Salazar C.M., "Factors Influencing The Decomposition Processes in Wood Particles During Low Temperature Pyrolysis", Research in Thermochemical Biomass Conversion, Phoenix, Arizona, USA, April 1988, Bridgwater, A.V. and Kuester, J.L. (eds.), Elsevier Applied Science Publishers, London, 1988, p 164.
192. Koufopanos, C., Maschio, G., Paci, M. and Lucchesi, A., "Some Kinetic Aspects on the Pyrolysis of Biomass and Biomass Components", Energy from Biomass, 3rd E.C. Conference, Venice, Italy, March 1985, Palz, W., Coombs, J. and Hall, D.O. (eds.), Elsevier Applied Science Publishers, London, 1985, p 837-841.
193. Maschio, G., Koufopanos, C. and Lucchesi A., "Thermochemical Conversion of Biomass : Mathematical Models on the Lignocellulosic Materials Pyrolysis", Biomass for Energy and Industry, 4th E.C. Conference, Orléans, France, May 1987, Grassi G, Delmon, B., Molle, J-F. and Zibetta, H. (eds.), Elsevier Applied Science Publishers, London, 1987, p 1007-1012.
194. Tran D.Q. and Rai, C., "A Kinetic Model for Pyrolysis of Douglas Fir Bark", Fuel 57, 1978, p 293-298.
195. Antal Jr, M.J., "Effects of Reactor Severity on the Gas-Phase Pyrolysis of Cellulose- and Kraft Lignin-Derived Volatile Matter", Ind. Eng. Prod. Res. Dev. 22, 1983, p 366-375.
196. Antal Jr, M.J., "A Review of the Vapor Phase Pyrolysis of Biomass Derived Volatile Matter", Fundamentals of Thermochemical Biomass Conversion, Overend, R.P., Milne, T.A. and Mudge, L.K. (eds.), Elsevier Applied Science Publishers, New York, 1985, p 511-538.

197. Diebold J.P. (Workshop Chairman) in Proceedings of the Specialists' Workshop on the Fast Pyrolysis of Biomass, Copper Mountain, USA, SERI/CP-622-1096, Solar Energy Research Institute, Golden, USA, October 1980.
198. Diebold, J.P. and Scahill J., "Production of Primary Pyrolysis Oils in a Vortex Reactor", in Pyrolysis Oils from Biomass, Producing Analyzing and Upgrading, Soltes, Ed. J., and Milne, T.A., (eds.), ACS Symposium series 376, 1988, p 31-40.
199. Lédé, J., Panagopoulos J. and Villermaux, J. "Experimental Measurement of ablation rate of wood pieces, undergoing fast pyrolysis by contact with a heated wall" preprints of ACS Symposium series, 1983, 28, No. 5, p 383-389.
200. Zaror, C.A., Hutchings, I.S., Pyle, D.L., Stiles, H.N. and Kandiyoti, R., "Secondary char formation in the catalytic pyrolysis of biomass", Fuel, 64, 1985, p 990-994.
201. Denn, M.D,. "Process Modeling", Longman Scientific & Technical, London, 1987.
202. Bridge, S.A., "Flash Pyrolysis of Biomass for Liquid Fuels" M.Phil. thesis, Aston University, England, November 1990.
203. di Blasi, C., "Modeling and Simulation of Combustion Processes of Charring and Non-charring Solid Fuels", Prog. Energy Combust. Sci., 19, 1993, p 71-104.
204. di Blasi, C., "Numerical Modeling of Wood Pyrolysis-Effects of Pressure Boundary Conditions", La Rivista dei Combustibili, 46, 9, September 1992, p 265-279.
205. Diebold, J.P., "The Cracking Kinetics of Depolymerized Biomass Vapors in a Continuous Tubular Reactor", MSc Thesis, Colorado School of Mines, Golden, USA, 1985.
206. Vovelle, C., Mellottee, H. and Delfau, J.L., "Kinetics of thermal Degradation of Wood and Cellulose by TGA Comparison of the Calculation Techniques" CNRS, France, internal report, 1987.
207. Akita K. and Kase M., J. Polym. Sci., 5, A-1, 1967, p 833.
208. Broido A, "Kinetics of Solid-phase Cellolose Pyrolysis", Thermal uses and Properties of Carbohydrates and Lignins, Shafizadeh ,F., Sarkanen, K .V. and Tillman, D.A., (eds.), Academic Press, 1976, 19-36.
209. Browne, F.L. and Tang W.K., Fire Research Abs. & Rev. Nat. Acad. Sci. Nat. Res. Council, 4, No 142, (Jan and May) 1962.
210. Chätterjee, P.K. and Conrad C.M., Textile Res. J., 36, No 6, 1966, p 487.
211. Kanury, A.M, "Thermal Decomposition Kinetics of Wood Pyrolysis", Combustion and Flame, 1972, 18, 75-83.
212. Lewellen, P.C., Peters, W.A. and Howard, J.B., "Cellulose Pyrolysis Kinetics and Char Formation Mechanism", 16th Symposium (International) on Combustion, Combustion Institute, 1976, p 1471.
213. Simmons, G.M. and Lee W.H., "Kinetics of gas Formation from Cellulose and Wood Pyrolysis", Fundamentals of Thermochemical Biomass Conversion, Overend, R.P., Milne, T.A. and Mudge, L.K., (eds.), Elsevier Applied Science Publishers, London 1985, 385-395.
214. Stamm, A.J., Ind. Engng. Chem. 48, 1956, p 413.
215. Salazar, C.M. and Connor, M.A., "Kinetic studies of the Pyrolysis of wood, with particular reference to eucalyptus regnans" Chemeca 83, 4-7 September 1983, p 753-761.
216. Lipska, A.E. and Parker, W.J., Journal of Applied Polymer Science, 10, 1966, p 1439.
217. Shivadev, U.K. and Emmons, H.W., Combustion and Flame, 22, 1974, p 223-236.
218. Barooah J.N. and Long, V.D, "Rates of thermal decomposition of some carbonaceous materials in a fluidised bed", Fuel, 1976, 55, p 116-120.
219. Nunn, T.R., Howard, J.B., Longwell, J.P. and Peters, W.A., "Studies of the Rapid Pyrolysis of Sweet Gum Hardwood", Fundamentals of Thermochemical Biomass Conversion, Overend R.P., Milne, T.A. and Mudge L.K. (eds.), Elsevier Applied Science Publishers, New York, 1985, p 293-314.
220. Nunn, T.R, Howard J.B., Longwell, J.P. and Peters W.A., "Product Composition and Kinetics in the Rapid Pyrolysis of Sweet Gum Hardwood", Ind. Eng. Chem. Prod. Res. Dev., 24, 1985, p 836-844.
221. Kothari, V. and Antal Jr, M.J., "Numerical Studies of the Radiant Flash Pyrolysis of Cellulose" preprints of ACS Symposium series, Vol. 28, No. 5, 1983, p 383-389.

222. Lidén, A G, "A Kinetic and Heat Transfer Modelling Study of Wood Pyrolysis in a Fluidized Bed", MASc Thesis, University of Waterloo, Canada, 1985.
223. Gorton, C.W. and Knight, J.A., "Oil From Biomass by Entrained-Flow Pyrolysis", Biotech. and Bioeng. Symp., No 14, 1984, p 14-20.
224. Vasalos, I., Stoikos, T., Samolada, M., Achladas, G. and Papamargaritis, C., "Production and utilistion of synthetic liquid fuels", Energy from Biomass 4, 3rd Contractors' meeting, Paestum, 25-27 May, 1988, CEC DG XII, Brussels, p 510-515.
225. Bohn, M.S. and Benham, C.B., "Biomass Pyrolysis with an Entrained Flow Reactor", Ind. Eng. Chem. Process Des. Dev., 1984, 23, p 355-363.
226. Diebold, J.P. and Benham, C.B., "Pyrolysis Experiments at China Lake using a tubular entrained flow reactor", Proceedings of the Specialists' Workshop on Fast Pyrolyis of Biomass, Copper Mountain, Colorado, 20-22nd October 1980, SERI/CP-622-1096, Solar Energy Research Institute, Golden, Colorado, p 271-286.
227. Boroson, M.L., Howard, J.B., Longwell, J.P. and Peters, W.A., "Product Yields and Kinetics from the Vapor Phase Cracking of Wood Pyrolysis Tars", AIChE Journal, January 1989, 35, 1, p 120-128.
228. Nunn, T.R., Howard, J.B., Longwell, J.P. and Peters ,W.A,. "Product Composition and Kinetics in the Rapid Pyrolysis of Milled Wood Lignin", Ind. Eng. Chem. Prod. Res. Dev., 24, 1985, p 844.
229. Stiles, H.N. and Kandiyoti, R., "Secondary Reactions of Flash Pyrolysis tars measured in a fluidized bed pyrolysis reactor with some novel design features", Fuel, 1989, 68, p 275-282.
230. Chang, L. and Kyihan, F., "Kinetics of biomas pyrolysis processes with fast heating rates", Alternative Energy Sources VII, Veziroglu, T.N., (ed.) New York, Hemisphere Publishing, 1985, Volume 4: Bioconversion/Hydrogen, p 257-268.
231. Figueiredo, J.L., Valenzuela, C., Bernalte, A. and Encinar, J.M., "Pyrolysis of Holm-oak and olive wood", Biomass for Energy and Industry, 5 th EC Conference, Grassi, G., Gosse, G. and dos Santos, G. (eds.), Vol. 2, Elseveir Applied Science Publishers, 1990, p 585-589.
232. Bamford, C H., Crank, J, and Malan, D.H., Proc. Cam. Phil. Soc. 42, 1946, 166-182.
233. Lédé, J., Li, H.Z. and Villermaux, J., Martin, H., "Fusion-like Behaviour of Wood Pyrolysis", J. Anal. Appl. Pyr., 10, 1987, p 291-308.
234. Lédé, J., Li, H.Z. and Villermaux, J., "Pyrolysis of Biomass: Evidence for a Fusion-like Phenomenon" ACS Symposium series 376, Pyrolysis Oils from Biomass: Producing Analyzing and Upgrading, Soltes, E.J. and Milne, T.A. (eds.), 1988, p 66-78.
235. Martin, H., Lédé, J., Li, H.Z., Villermaux, J., Moyne, C. and Dégiovanni, A.m "Ablative melting of a solid cylinder perpendicularly pressed against a heated wall", Int. J. Heat Mass Transfer, Vol. 29, 9, 1986, p 1407-1415.
236. Reed, T.B. and Cowdrey, C.D., "Heat Flux Requirements for Fast Pyrolysis and a New Method for Generating Biomass Vapour", in Production, Analysis and Upgrading of Oils from Biomass, ACS Annual Meeting, Denver, Colorado, April 5th, 1987, p 59.
237. Reed, T.B., "Principles and Operation of a novel "Pyrolysis Mill"", in Thermochemical Conversion Programme Annual Meeting, June 1988 SERI/CP-231-3355, DE 88001187, prepared under task no. BF832010 for the US Dept. of Energy, p 247-258.
238. Cowdrey, C., "Measurement of the Mass and Energy Balance in Contact Fast Pyrolysis of Wood", MASc thesis 1987, Colorado School of Mines, Boulder, USA, T-3459.
239. Dr. T.B. Reed, Colorado School of Mines, Golden, USA, personal communication, 13 May 1992.
240. Wagenaar, B.M., Kuipers, J.A.M, Prins, W, and van Swaaij, W.P.M., "Hydrodynamics of the rotating cone pyrolysis reactor", Biomass for Energy, Industry and the Environment, Athens, 22-26 April 1991, Grassi, G., Collina, A and Zibetta, H. (eds.), Elsevier Applied Science Publishers, p 732-736.
241. van Swaaij, W.P.M., B.M., Kuipers, J.A.M, Prins and Wagenaar, B.M., ", Energy from Biomass Thermochemical Conversion, proceedings of the EC Contractors'

Meeting, 29-31 October 1991, Gent, Belgium, Grassi, G. and Bridgwater, (eds.), 1992, p 115-123.
242. Wagenaar, B.M., Kuipers, J.A.M, Prins, W, and van Swaaij, W.P.M., "The Rotating Cone Flash Pyrolysis Reactor", Advances in Thermochemical Biomass Conversion, Interlaken, Switzerland, 11-15 May 1992, Blackie, Glasgow, 1994, p 1122-1133.
243. van Swaaij, W.P.M., B.M., Kuipers, J.A.M, Prins and Wagenaar, B.M., "The Rotating Cone Flash Pyrolysis Reactor", , Energy from Biomass: Progress in Thermochemical conversion, Proceedings of the EC Contractors' Meeting, 7 October 1992.Grassi, G. and Bridgwater, A.V. (eds.), EUR 15389 EN, CEC DG XIII, Brussels, 1994, p 43-50
244. Wagenaar, B.M., "The Rotating Cone Reactor for rapid thermal solids processing", Ph.D. thesis, University of Twente, Enschede, the Netherlands, 1994.
245. Black, J.W. and Brown, D.B., "Preliminary Mass Balance Testing of the Continuous Ablation Reactor", in Biomass Thermal Processing, 23-25 October 1990, Ottawa, Canada, CPL Press, Newbury, 1992, p 123-125.
246. Roy, C. and Unsworth, J., "Pilot Plant Demonstration of Used Tyres Vacuum Pyrolysis" in Pyrolysis and Gasification, Ferrero, G.L., Maniatis, K., Buekens, A. and Bridgwater, A.V. (eds.), Luxembourg, May 1989, (Elsevier Applied Science Publishers, 1989), p 180-189.
247. Black, J.W. and Brown, D.B., "Rapid Pyrolysis of Shredded rubber tires" report of DSS Contract file No. 23440-9-9513/01-SZ. Alternate Energy Division: Energy, Mines and Resources Canada, Ottawa, Ontario, Canada, March 1993.
248. Diebold, J.P. and Smith, G.D., "Noncatalytic Conversion of Biomass to Gasoline", Gas Turbine Conference and Exhibit and Solar Energy Conference, San Diego, USA, March 12-15, 1979.
249. Diebold, J.P. and Smith, G., "Commercialization potential of the China Lake Trash-to-Gasoline Process", Design and Manegement for Resource Recovery, Vol. 1, Energy form Waste, Frankiewicz, T.C. (ed.), Ann Arbor Science Publishers inc., Michigan, USA, p 113-139.
250. Diebold, J.P. and Scahill, J.W., "Ablative Entrained-Flow Fast Pyrolysis of Biomass", proceedings of the 16th Biomass Thermochemical Conversion Contractors' Meeting, Portland, Oregon, USA, 1984, p 319-347.
251. Diebold, J.P. and Scahill, J.W., "Progress in the Entrained Flow, Fast Ablative Pyrolysis of Biomass" proceedings of the 12th Biomass Thermochemical Conversion Contractors' Meeting, Washington, USA, 18-19 March, 1981.
252. Diebold, J.P. and Scahill, J.W., "October 1981 Update on the Progress in the Entrained Flow, Fast Ablative Pyrolysis of Biomass", 13th Biomass Thermochemical Conversion Contractors' Meeting, Arlington, USA, 27-29 October, 1981, p 332-365.
253. Diebold, J.P. and Scahill, J.W., "Ablative Fast Pyrolysis of Biomass in the Entrained-Flow Cyclonic Reactor at SERI", ,14th Biomass Thermochemical Conversion Contractors' Meeting, Arlington, USA, 23-24 June, 1982, p 272-311.
254. Diebold, J.P. and Scahill, J.W., "Ablative Fast Pyrolysis of Biomass in the Entrained Flow Cyclonic Reactor at SERI", 15th Biomass Thermochemical Conversion Contractors' Meeting, Atlanta, USA, 16-17 March, 1983, p 300-357.
255. Mr. J.P. Diebold, NREL, Colorado, USA, personal communication, March 1993.
256. Mr. J.P. Diebold, NREL, Colorado, USA, personal communication 1991.
257. Diebold, J.P. Evans, R. and Scahill J.W., "Fast Pyrolysis of RDF to Produce Fuel Oils, Char and a metal rich by-product", Energy from Biomass and Wastes XIII, Klass, D. (ed.), IGT Conference, New Orleans, Louisiana, USA, 13-17 February 1989, p 851-878.
258. Roy, C., de Caumia, B. and Plante, P., "Performance Study of a 30 kg/h vacuum pyrolysis process development unit" 5th European Conference on Biomass for Energy and Industry, Grassi, G., Gosse, G. and dos Santos, G., Elsevier Applied Science London, 1990, Vol 2, p 2.595.
259. Huffman, D.R. and Vogiatzis, A.J., Ensyn Technologies Inc., "Research into the Utilization of Biomass Pyrolyssi Oils in Power Production", report for Efficiency and Alternative Energy Technology Branch, Energy, Mines and Resources Canada, Ottawa, Canada, 1993.

260. Knight, J.A., Gorton, C.W., Kovac, R.J., Elston ,L.W. and Hurst D.R., "Oil Production Via Entrained Flow Pyrolysis of Biomass", Proceedings of the 13th Biomass Thermochemical Conversion Contractors' Meeting, Arlington, Virginia, Oct 27-29, 1981, p 475-492.
261. Levie, B. Diebold, J.P. and West, R., "Pyrolysis and Combustion of Refuse Derived Fuel", in Thermochemical Conversion Program Annual Meeting, June 21-22, 1988, SERI/CP-231-3355 DE88001187, prepared under task no. BF831010, p 259-268.
262. Levie, B., Diebold, J.P. and West, R., "Pyrolysis of Single Particles of Refuse Derived Fuel", Research in Thermochemical Biomass Conversion, Phoenix, Arizona, USA, April 1988, Bridgwater, A.V. and Kuester, J.L. (eds.), Elsevier Applied Science Publishers, London, New York, 1988, p 312-326.
263. Scahill, J. and Diebold, J.P., "Adaptation of the SERI Vortex Reactor for RDF Pyrolysis", in Thermochemical Conversion Program Annual Meeting, June 21-22, 1988, SERI/CP-231-3355 DE88001187, prepared under task no. BF831010, p 237-246.
264. Rejal, B., Evans, R.J., Milne, T.A., Diebold, J.P. and Scahill, J., "The Conversion of Biobased Feedstocks to Liquid Fuels through Pyrolysis", Energy from Biomass and Wastes XV, 25-29 March 1991, Washington, D.C., IGT, Chicago, p 855-876.
265. Diebold, J.P., Overend, R., Rejai, B. and Power, A.J., "Reformulated Gasoline Components Production from Renewable Feeds", Liquid fuels from Renewable Resources, Cundiff, J.S. (ed.), American Society of Agricultural Engineers, Michigan, 1992, p 154-161.
266. Bain, R., Diebold, J.P., Overend, R., Power, A.J. and Rejai, B., "The production of reformulated gasoline components from biomass and RDF", Energy from Biomass and Wastes XVI, Klass, D.L. (ed.), IGT, Orlando, USA, 1992, Paper 18.
267. Ayres, W.A., "Commercial Application of Wood Derived Oil", Energy Progress, Vol. 7, No. 2, June 1987, p 77-79.
268. Ayres, W.A., "Commercial Application of Oxygenated Oil derived from an Entrained flow Ablative Fast Pyrolysis System", Energy from Biomass and Wastes XII, 1988, Klass, D.L., (ed.), IGT, Chicago, p 1141-1151.
269. Kansas City Star, 11 August 1989, p 5C.
270. Johnson, D.A., Ayres, W. A. and Tomberlin, G., "Scale-up of the Ablative fast Pyrolysis Process", in Biomass Thermal Processing, 23-25 October 1990, Ottawa, Canada, CPL Press, Newbury 1992, p 236-240.
271. Johnson, D.A., Tomberlin, G., and Ayres, W.A., "Conversion of Wood Waste to Fuel Oil and Charcoal", Energy from Biomass and Wastes XV, 25-29 March 1991, Washington, D.C.,IGT Chicago, 1991, p 915-925.
272. Johnson, D.A., Maclean, Feller, J., Diebold, J.P. and Chum, H., "Ablative Fast Pyrolysis: Prototype plant", American Chemical Society Annual Meeting, 28 March - 2 April 1993, Denver, Colorado, USA, proceedings to be published in Biomass and Bioenergy, 1994.
273. US patent, 3001879 "Treating of Food Products with Smoke", 26 September 1961, H.R. Rasmussen, H.J. Rasmussen, filed 9 June 1958.
274. US patent, 30090373 "Smoke Generator", 19 September 1961, R.A. Hawley, filed 26 January 1959.
275. US patent, 3009457 "Method and apparatus for the production of smoke for Food Treating purposes", 21 November 1961, H.R. Rasmussen, H.J. Rasmussen, filed 9 June 1958.
276. Freel, B.A. and Graham, R.G., "Method and Appararus for a Circulating Bed Transport Fast Pyrolysis Reactor", Ensyn Engineering Associates, Markham, Greely, Ontario, Canada, Canadian patent application no. 2009021, filed 31 January 1990.
277. Professor D. S. Scott, University of Waterloo, personal communication, August 1993.
278. Chang, L., "Secondary Tar Cracking in the Pyrolysis of Biomass", in Strategies for Energy Efficicnet Plants and Intelligent Buildings, 1987, Fairmont Press Inc., p 433-438.
279. le Lan, A., "Fast Pyrolysis of Wood wastes to Medium Energy Gas", Thermochemical Processing of Biomass, Bridgwater, A.V. (ed.), Butterworths and Co Ltd., 1984, p 159-163.

280. Solantausta, Y., VTT, Finland, private communication, November 1993.
281. Antonelli, L., "Improvement of Pyrolysis Products: Bio-oil and Bio-carbon/emulsion and Slurries", Energy from Biomass 4, Proceedings of the Third Contractors' Meeting, Paestum, 25-27 May 1988, Grassi, G., Pirrwitz, D. and Zibetta, H. (eds), Elsevier Applied Science, London, 1989, p 531.
282. Boukis, Y., CRES, Pikermi, Greece, private communication, November 1993.
283. Maniatis, K., Baeyens, J., Roggeman, G., Peeters ,H., "Flash Pyrolysis of Biomass in an Entrained Bed Reactor", Final report of EEC Contract JOUB 0025, submitted to the CEC DG XII, 1993.
284. Fransham, P.B. and Lynch, D., "Development of a Mobile Fluid-Bed Pyrolysis Unit for Waste Disposal-Energy Recovery", Energy from Biomass and Wastes XV, IGT, Chicago, 1991, p 895-906.
285. Johnson, D.A., Maclean, D., Chum, H. and Overend, R.P., "Ablative Fast Pyrolysis: converting wood, agricultural wastes and crops into energy and chemicals" First Biomass Conference of the Americas: Energy, Environment, Agriculture and Industry, Vol. II, p 1367-1384.
286. Union Electrica Fenosa, plant visit, Raiano, Spain, June 1993.
287. Perry, R.H. and Chilton, C.H., "Chemical Engineers' Handbook" 5th edition, 1973, McGraw-Hill Kogakusha Ltd., Tokyo, 1973, p 20.81-20.85.
288. Scott, D.S., Piskorz, J. and Radlein, D., "Chemicals from Biomass Pyrolysis", internal report, July 1991, University of Waterloo, Canada.
289. Scott, D.S. and Piskorz, J., "Flash Pyrolysis of Biomass" Fuels from Biomass and Wastes, Klass, D.L. and Emert, G.H., (eds.), Ann Arbor Science Publishers Inc., 1981, p 421-434.
290. Freel, B.A. and Graham, R.G., "Rapid Pyrolysis of Wood and Wood-derived Liquids to Produce Olefins and High quality Fuels", Report of Contract File No 51SZ 23216-6-6656, Renewable Energy Branch, Energy, Mines and Resources, Canada, 1988.
291. Knight, J.A., Gorton, C.W., Kovac, R.J. and Newman, C.W., "Entrained Flow Pyrolysis of Biomass", in Proceedings of the 1985 Biomass Thermochemical Conversion Contractors' Meeting, Minneapolis, USA, Oct 15-16, 1985, p 99.
292. Williams, P.T. and Horne, P.A., "Characterisation of Oils from the fluidised bed pyrolysis of biomass with zeolite catalyst upgrading" presented at the ACS annual meeting, March 1993, Denver, USA, to be published in Biomass and Bioenergy, 1994.
293. Gregoire, C.E. and Bain, R.L., "Technoeconomic Analysis of the production of BioCrude from Wood", presented at the ACS Annual meeting, March 1993, Denver, Colorado, , to be published in Biomass and Bioenergy, 1994.
294. Baker, E.G. and Elliot, D.C., "Catalytic upgrading of Biomass Pyrolysis Oils", Research in Thermochemical Biomass Conversion, Phoenix, Arizona, USA, April 1988, Bridgwater, A.V. and Kuester, J.L. (eds.), Elsevier Applied Science Publishers, London and New York, 1988, p 883-895.
295. Elliot, D.C. and Baker, B.S., "Hydrotreating biomass liquids to produce hydrocarbon fuels" Energy from Biomass and Wastes X, Klass, D.L. (ed.), Elsevier Applied Science Publishers, 1987, p 765-782.
296. Scott, D.S. and Piskorz, J., "Production of Liquids from Biomass by Continuous Flash Pyrolysis" BioEnergy 84, Egneus, H. and Ellegard, A. (eds.), Vol.3, Elsevier Applied Science Publishers, London , 1985, p 15-23.
297. Faix, O., Fortmann, I., Bremer, J. and Meier, D., "Thermal Degradation Products of Wood - Gas chromatographic separation and mass spectrometric charactersiation of polysaccharide derived products", Holz als Roh- und Werkstoff, vol. 49, Springer-Verlag, 1991, p. 213-219.
298. Pyle, D.L. and Zaror, C.A., "Heat transfer and Kinetics in the low Temperature Pyrolysis of Solids", Chem. Eng. Sci. Vol 39, 1984, p 147-158.
299. Villermaux, J., Antoine, B., Lédé, J. and Soulignac, F., "A new model for thermal volatilization of solid particles undergoing flash pyrolysis" Chem. Eng. Sci., Vol 41, no. 1, 1986, p 151-157.

Appendix I. Publications

I.1 Publications carried out during the course of this thesis work

A list of publications which were completed during the course of the thesis are given below. Most of the publications have been incorporated into the thesis as chapters or parts of chapters, however two publications which not integrated in the main part of the thesis are:

- G.V.C. Peacocke, P.A. Russell, J.D. Jenkins and A.V. Bridgwater, "Physical Properties of Flash Pyrolysis Liquids", to be published in Biomass and Bioenergy, 1994. [Appendix IA].
- G.V.C. Peacocke, E.S. Madrali, A.J. Güell, C-Z Li, W. Fan, A.V. Bridgwater and R. Kandiyoti, "Effect of Reactor Configuration on Yields and Structures of Wood Derived Pyrolysis Liquids: A Comparison between Ablative and Wire Mesh Pyrolysis", to be published in Biomass and Bioenergy, 1994. [Appendix IB].

I.2 Other publications

Fully refereed

- G.V.C. Peacocke and A.V. Bridgwater, "Ablative Plate Pyrolysis of Biomass for Liquids" to be published in Biomass and Bioenergy, 1994.
- G.V.C. Peacocke and A.V. Bridgwater, "Design of a novel ablative pyrolysis reactor", Advances in Thermochemical Biomass Conversion, Bridgwater, A.V., (ed.), Blackie Academic and Professional, Glasgow, 1994, p 1134-1150.

Non-refereed

- G.V.C. Peacocke and A.V. Bridgwater, "Ablative Biomass of Pyrolysis for Liquid Fuels", Energy from Biomass Thermochemical Conversion: Proceedings of EC Thermochemical Contractors' Meeting, 29-31 October 1991, Gent, Belgium, Grassi, G. and Bridgwater, A.V. (eds.), CEC DG XII, 1992, p 103-111.
- G.V.C. Peacocke and A.V Bridgwater, "Ablative Pyrolysis of Biomass for the production of liquid fuels", Biomass for Energy and Industry 7th EC conference, Hall, D.O., Grassi, G. and Scheer, H. (eds.), Ponte Press, Bochum, Germany, 1994, p 931-937.
- G.V.C. Peacocke and A.V Bridgwater, "Ablative Pyrolysis of biomass for the production of liquids in high yields", The 1994 I.Chem.E. Research Event, I.Chem.E., Rugby, England, 1994, p 556-558.
- G.V.C. Peacocke and A.V Bridgwater, "Ablative Pyrolysis of Biomass", 6th European Conference on Biomass for Energy, Industry and the Environment, Athens, 22-26 April 1991, Grassi, G., Collina, A and Zibetta, H. (eds.), Elsevier Applied Science Publishers, 1992, p 721-727.
- M. Palm, J. Piskorz, G.V.C. Peacocke, D.S. Scott and A.V. Bridgwater, "Pyrolysis of Sweet Sorghum Bagasse in the Waterloo Fast Pyrolysis Process", First Biomass Conference of the Americas: Energy, Environment, Agriculture and Industry, Vol. II, National Renewable Energy Laboratory, 1993, NREL/CP-200-5768 DE 93010050, p 947-963.
- G.V.C. Peacocke and A.V. Bridgwater, "Advanced Flash (Ablative) Biomass of Pyrolysis for Liquid Fuels", Proceedings of Energy from Biomass Contractors' Meeting, Grassi, G. Moncada, P. and Zibetta, H., CEC DG XII/77/91, Biomass Unit (F/4), 1991, p 294-306.
- G.V.C. Peacocke and A.V. Bridgwater, "Advanced Flash (Ablative) Biomass of Pyrolysis for Liquid Fuels: Progress of JOUB-0032-C", Energy from Biomass: Progress in Thermochemical conversion, Proceedings of the EC Contractors' Meeting, 7 October 1992, Grassi, G. and Bridgwater, A.V. (eds.), EUR 15389 EN, CEC DG XIII, Brussels, 1994, p 31-41.

Table 1
Reported Values for Pyrolysis Liquid Density (6,7,8,9)

ρ_L, g/cm^3	H_2O content (wt%)	Temp. (°C)	Source	Reference
1.22	17	20	NREL	7
1.28	16.1	24	NREL	6
1.22	22.4	55	U.Waterloo	8, 9
1.20	18.7	20	U.Waterloo	9
1.23	18.6	20	U.Waterloo	9
1.27	16.6	23	GTRI	6

Table 2
Dynamic Viscosity values for Batch 1 Samples 1 and 5 and Batch 2 (mPa s)

Temperature (°C)	Batch 1 Sample 1	Batch 1 Sample 5	Batch 2
25	95	97	124
35	50	52	70
45	29	28	39
50	24	23	31
60	15	15	20
70	11	11	

Table 3
Reported Dynamic Viscosity values for Pyrolysis Liquids

Viscosity	Units	H_2O content (wt%)	Reported char content (wt%) *	Reference and source
1300 @ 30°C	mPa s	17.0	NK	6, NREL
10 @ 60°C	mPa s	29.0	27-31	8, GTRI
Comparable Fuel oils				
2-3.6 (No.2 oil)	cSt	0.05 vol%	0.35#	ASTM D396-69
5.8-26.4§ (No.4)	cSt	0.5 vol%	No value	ASTM D396-69

\# carbon residue on 10% bottoms
§ information values only: not necessarily limiting
* details not supplied by any author on measurement method

Table 4
Refractive index values for Batch 1 Samples 1 and 5 and Batch 2

	Batch 1 Sample 1	Batch 1 Sample 1 Control	Batch 1 Sample 5 Control	Batch 2
Index, η				
22°C	1.4778	1.4623	1.4659	1.4781

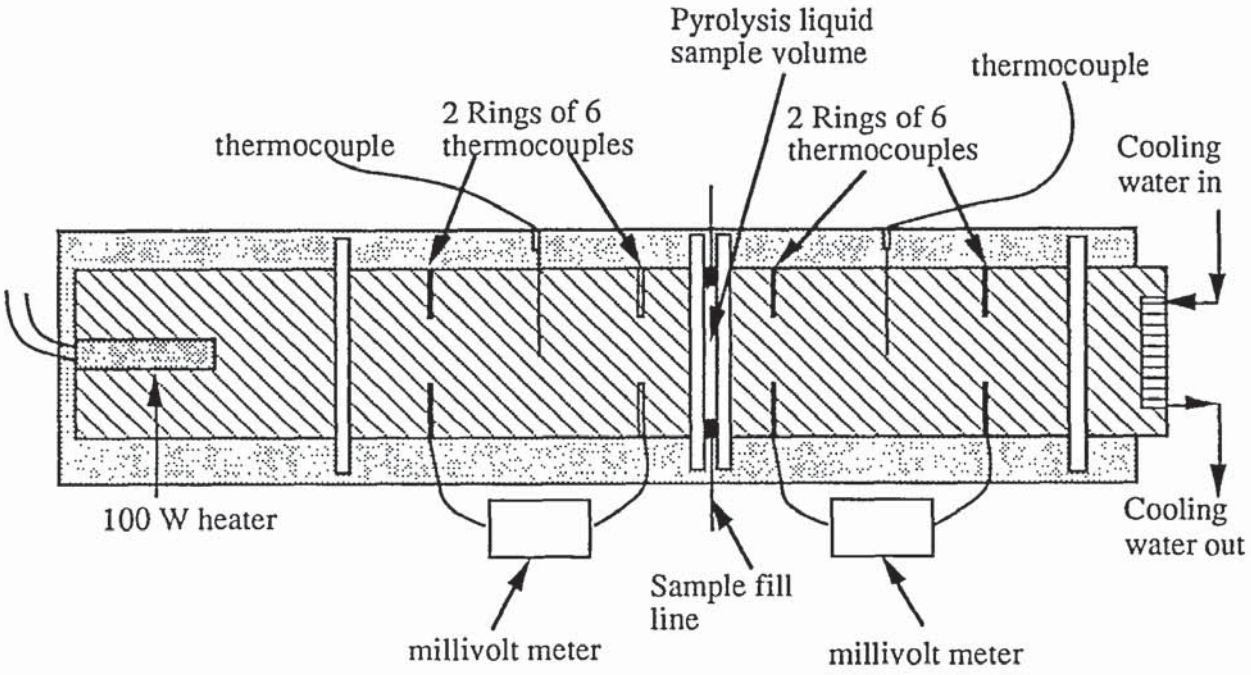

Figure 1. Thermal Conductivity Rig and Ancillary Equipment

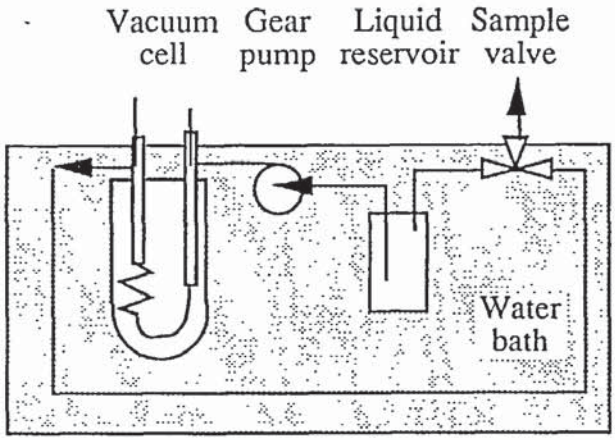

Figure 2. Specific Heat Capacity Rig

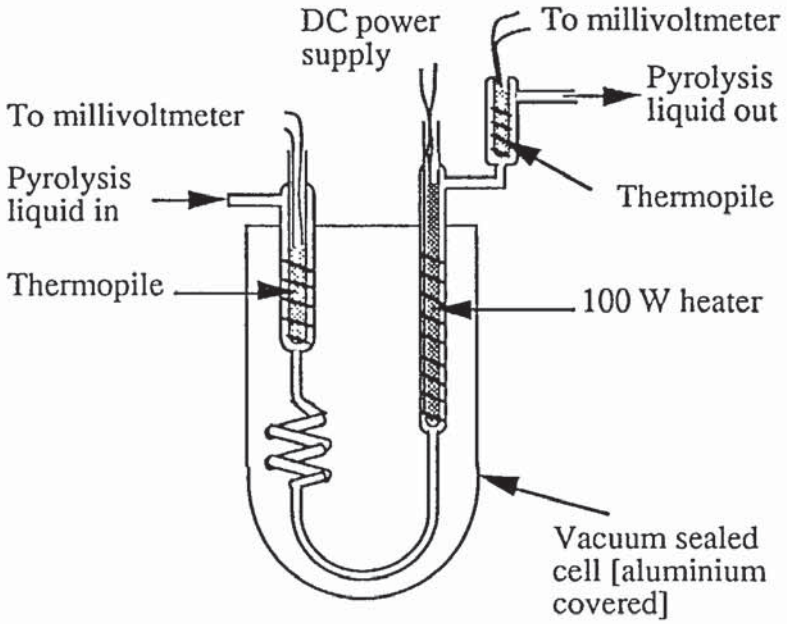

Figure 3. Detailed Drawing of the Specific Heat Capacity Rig

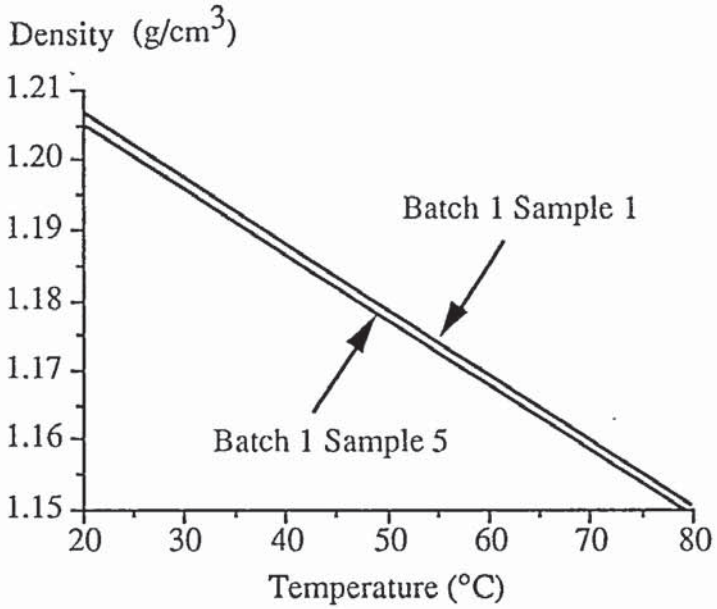

Figure 4. Variation in Pyrolysis Liquid density in samples taken from different heights, 280 mm (sample 1) and 560 mm (sample 5) from the barrel top

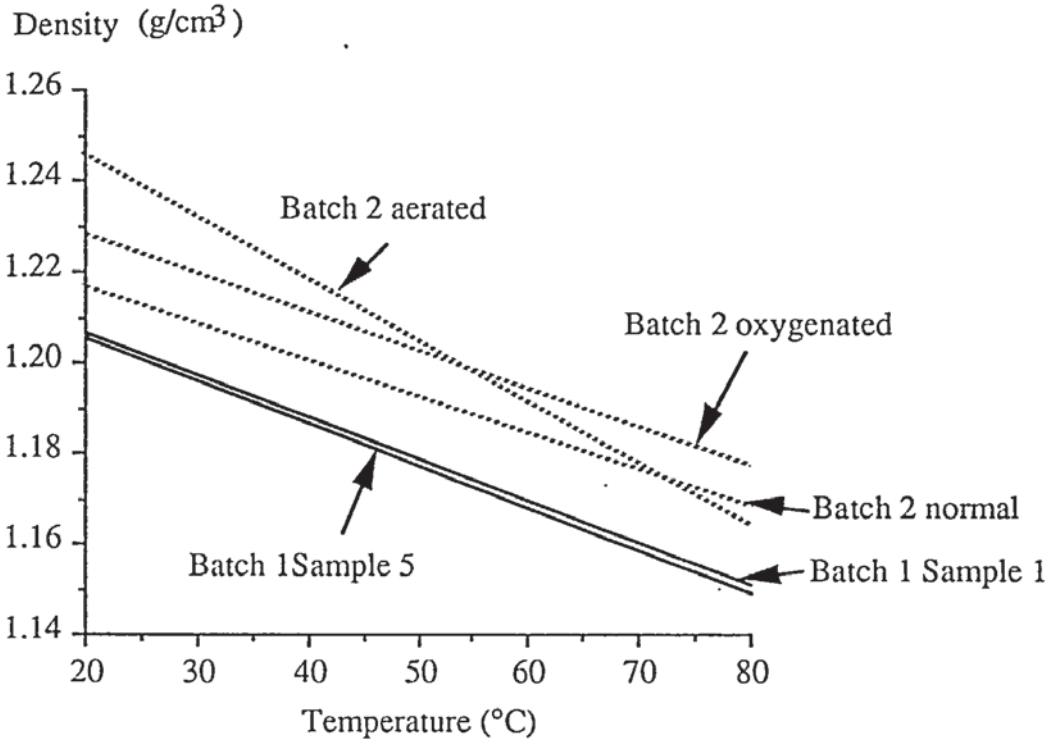

Figure 5. Variation of liquid density for raw liquid, aerated and oxygenated pyrolysis liquid Batch 2 and Batch 1

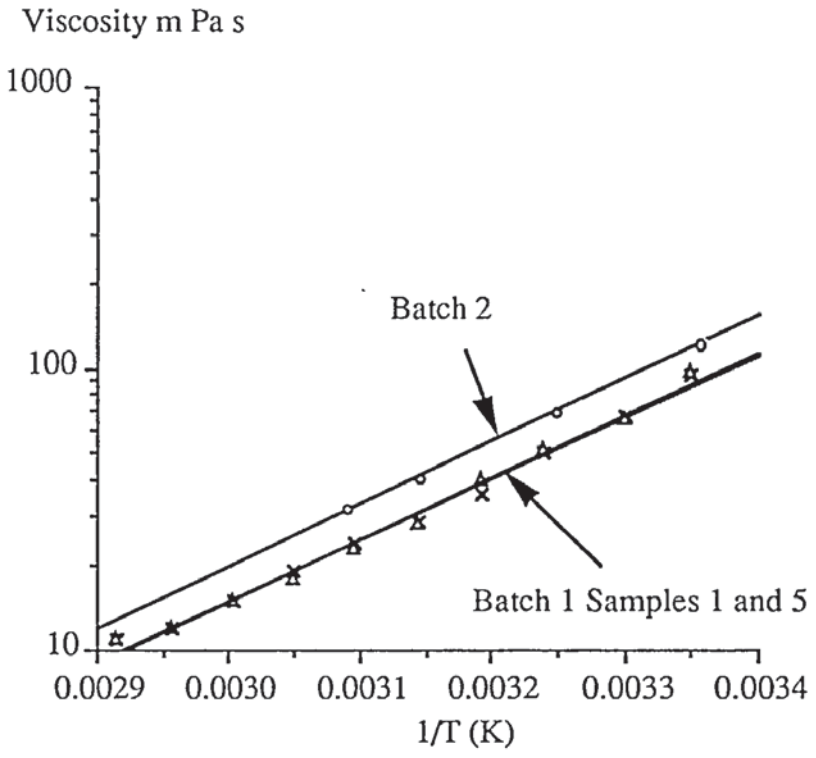

Figure 6. Dynamic Viscosity μ, ν's absolute Temperature for Batch 1, Sample 1,5 and Batch 2

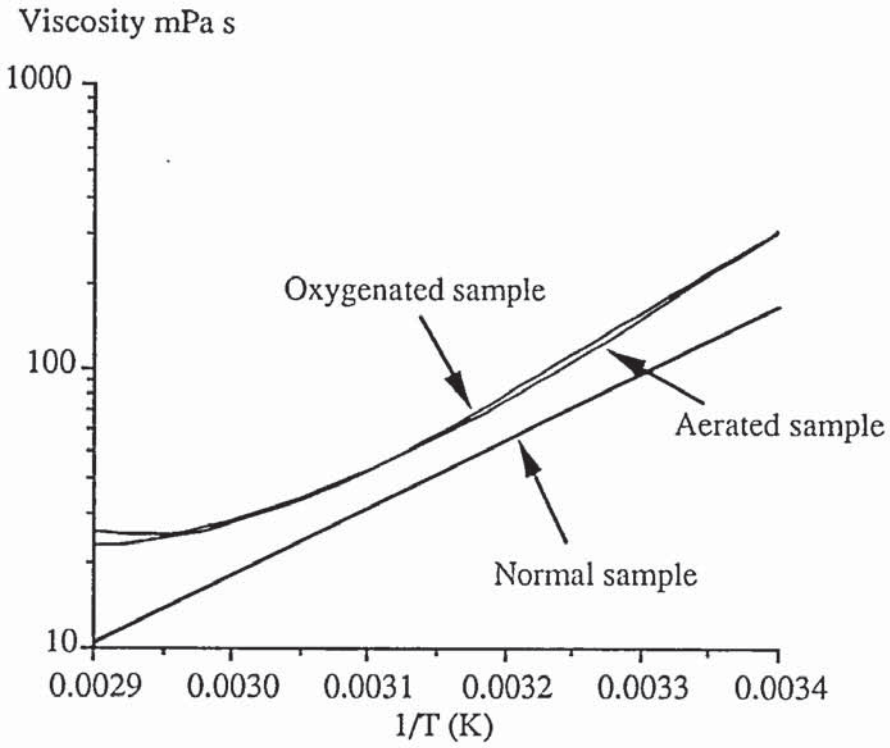

Figure 7. Comparison of aerated, oxygenated and normal Batch 2 samples

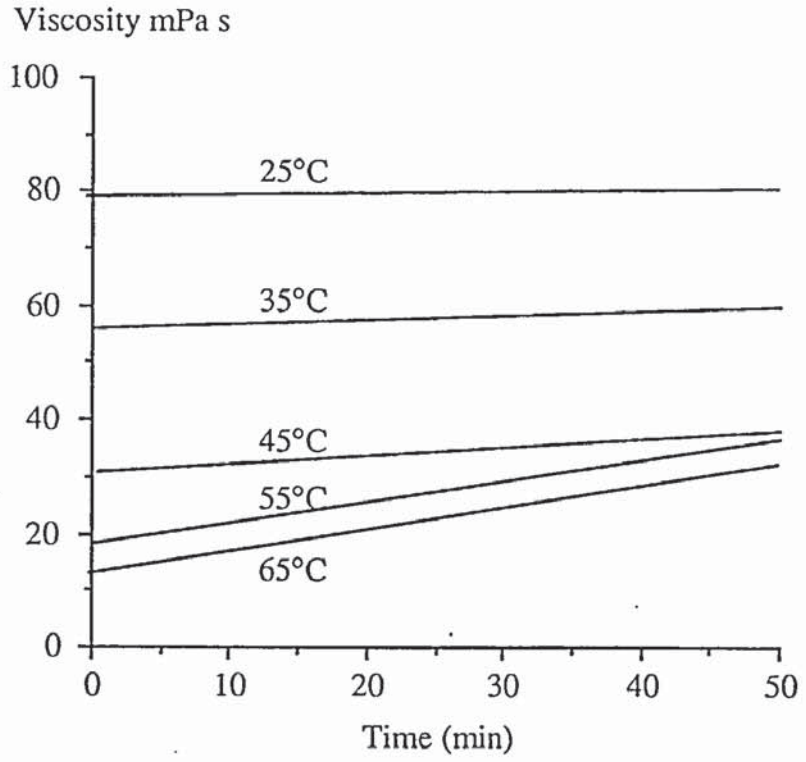

Figure 8. Thixotropic effects on Batch 1 Sample 5

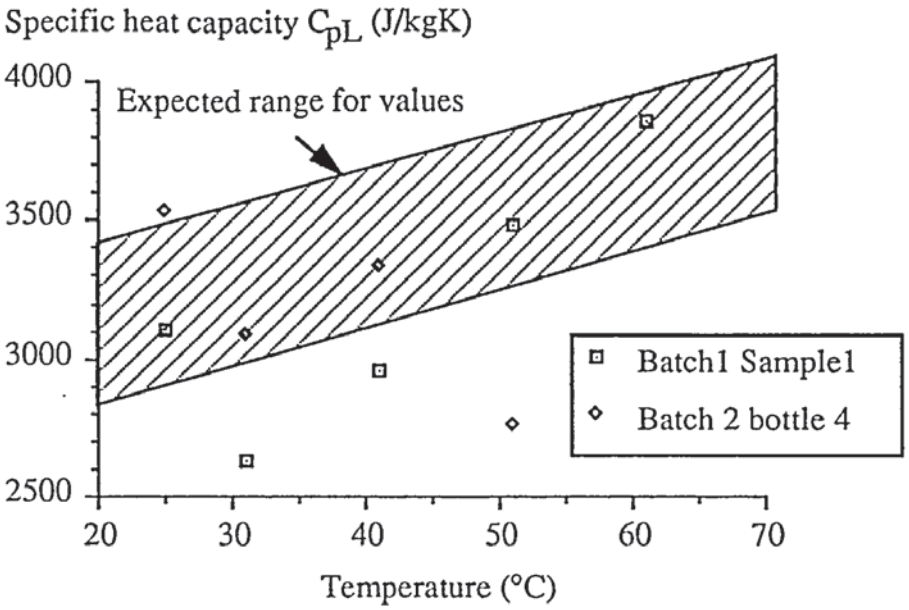

Figure 9. Specific Heat Capacity for Batch 1 Sample 1 and Batch 2

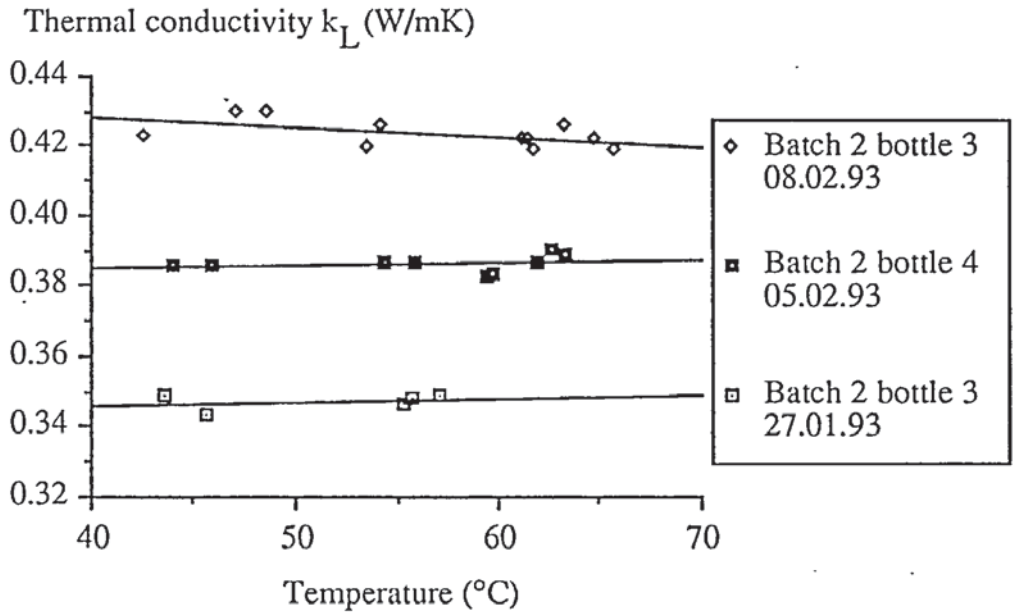

Figure 10. Thermal Conductivity values for Batch 2, bottles 3 and 4

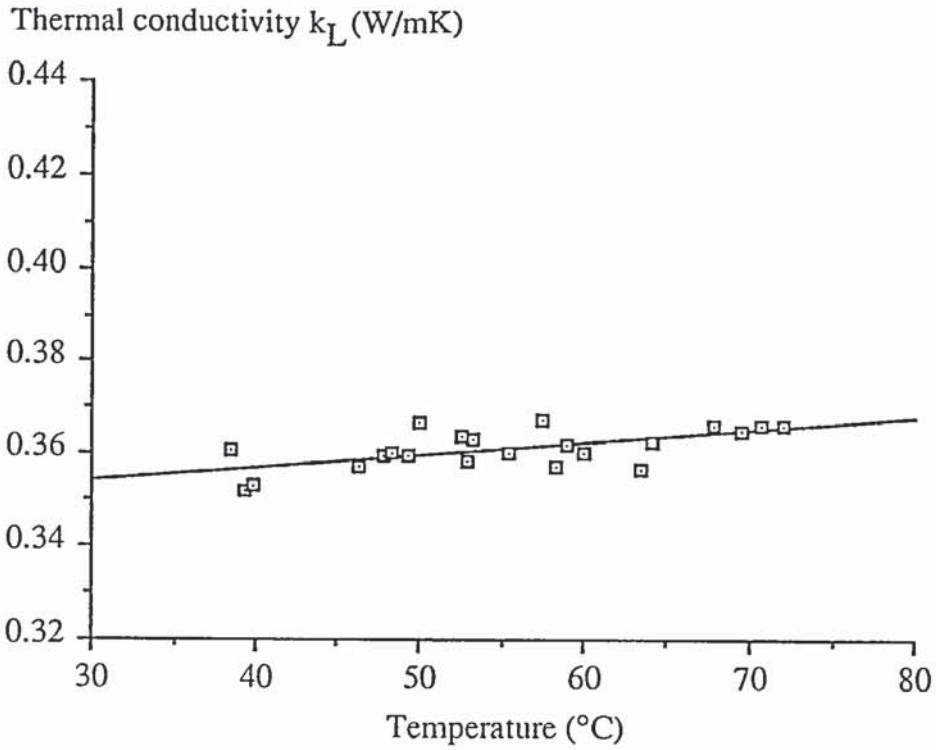

Figure 11. Thermal Conductivity plot for Batch 1 both samples

Table 1.
Comparison of pine-wood pyrolysis yields obtained from wire-mesh pyrolysis reactor

	Organic Liquids Yield, d.b.%	Total Volatile Yield, d.b.%
Atmospheric Wire-Mesh Reactor		
400°C, 1000 Ks^{-1}, 10 s	34.0	54.2
	32.2	
450°C, 1000 Ks^{-1}, 10 s	56.9	82.1
	56.2	
500°C, 1000 Ks^{-1}, 10 s	61.5	90.7
550°C, 1000 Ks^{-1}, 10 s	62.1	92.1
	57.6	
550°C, 1 Ks^{-1}, 10 s	51.2	85.5
	45.1	
600°C, 1000 Ks^{-1}, 10s	60.7	92.9
High Pressure Wire-Mesh Reactor		
550°C, 1000 Ks^{-1}, 10 s, 5 bar	57.3	93.9
550°C, 1000 Ks^{-1}, 10 s, 10 bar	48.6	92.9
	47.7	*93.6*
550°C, 1 Ks^{-1}, 10 s, 10 bar	39.3	85.6

Oil yields in italic were determined by the indirect method described for the high pressure oil yield determination.

Table 2.
Average molecular masses [MM] of pyrolysis liquids as a function temperature and comparison of MM's of liquids obtained from different reactors

Heating Rate, Ks-1	Holding Temp. °C	Holding time, s	Pressure [bar]	Number Average MM, Da	Weight Average MM, Da
Atmospheric wire-mesh reactor					
1000	400	10	1	310	400
1000	450	10	1	320	420
1000	550	10	1	340	480
High Pressure wire-mesh reactor					
1000	550	10	5	290	410
1000	550	10	10	280	380
Ablative reactor [Run no.CR07]					
	550	up to 10*	1	240	360

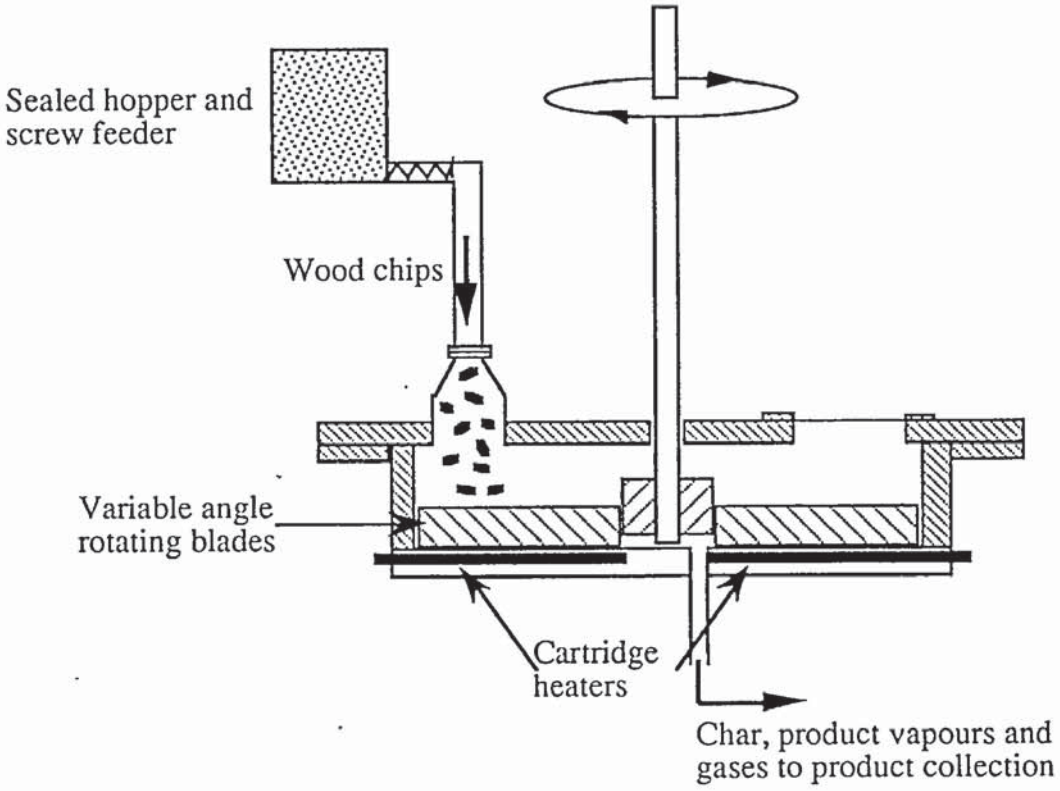

Figure 1. Ablative Pyrolysis Reactor

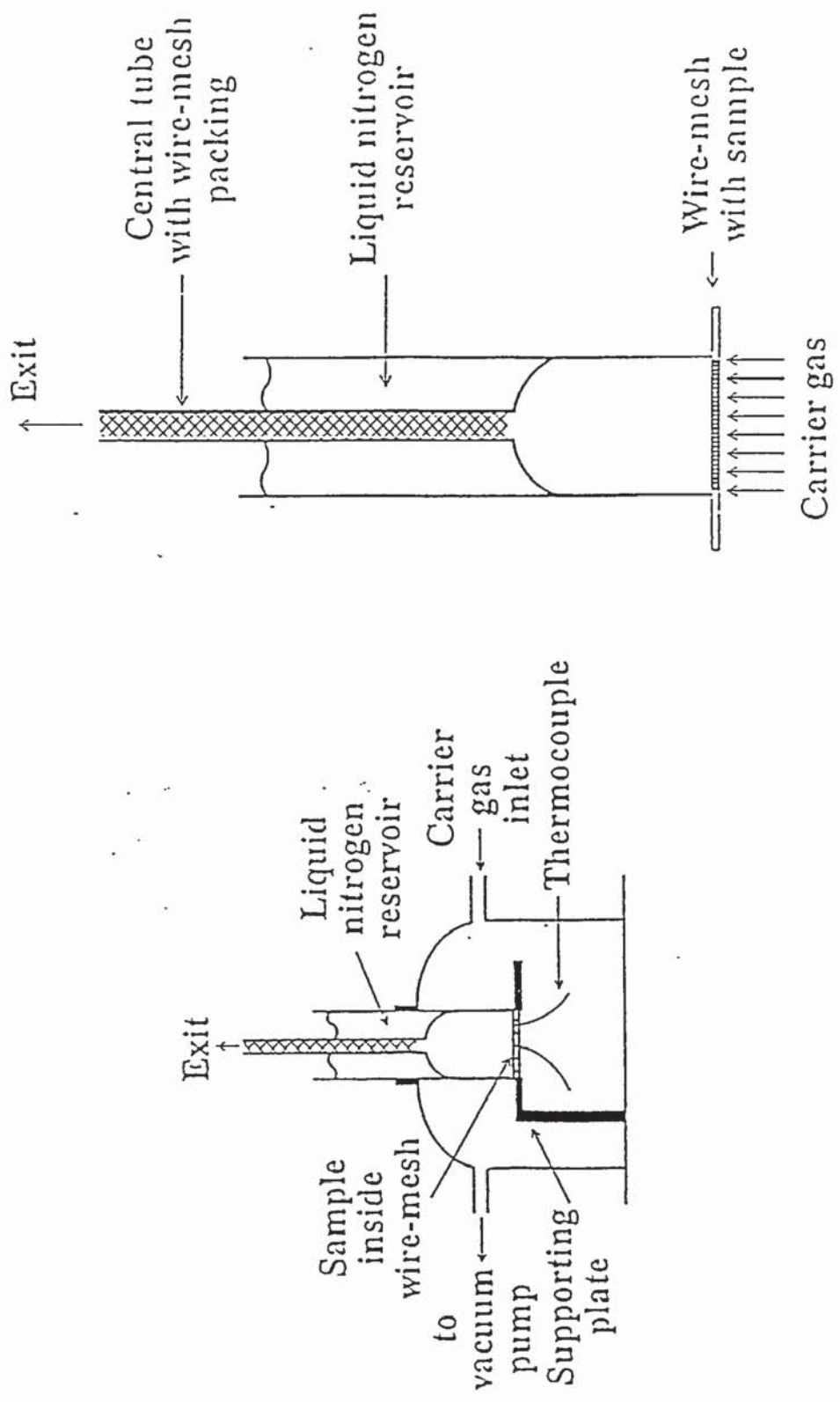

Figure 2. Wire-mesh pyrolysis reactor and liquid trap assembly

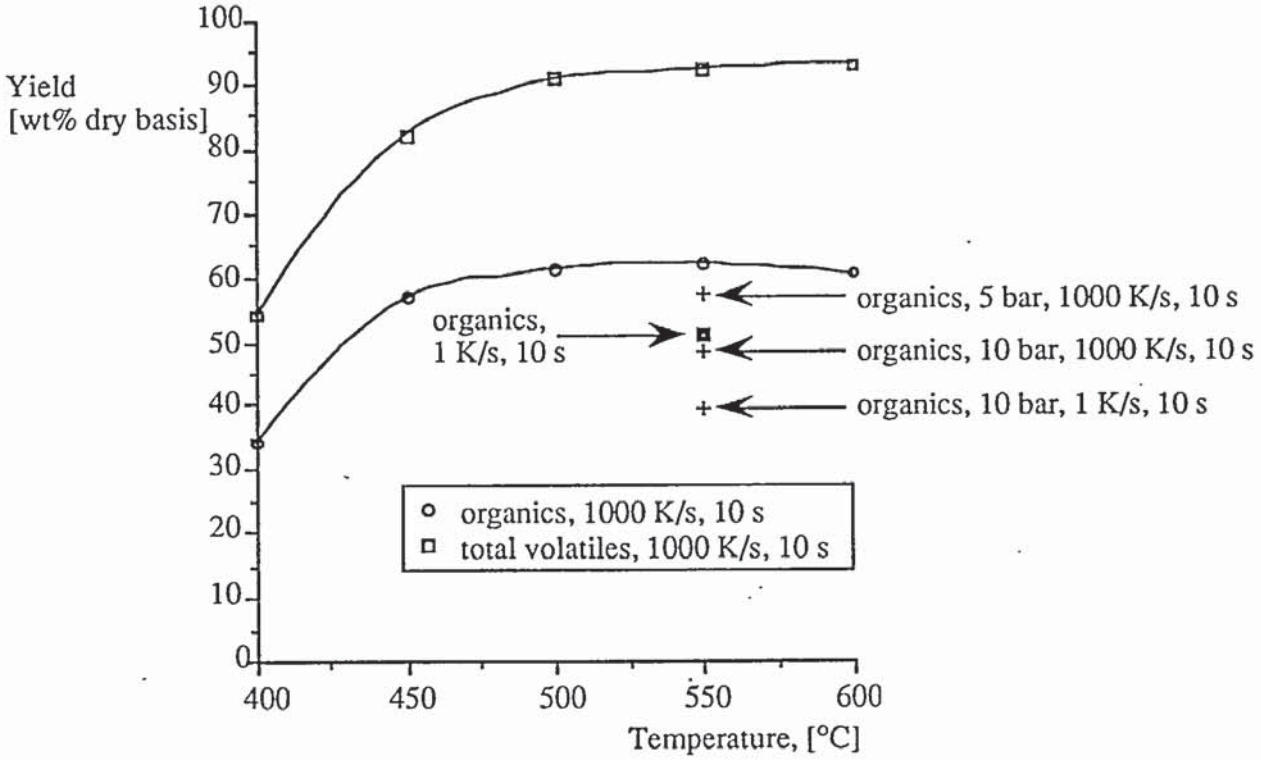

Figure 3. Wire-mesh reactor temperature v's total volatile yield, atmospheric pressure

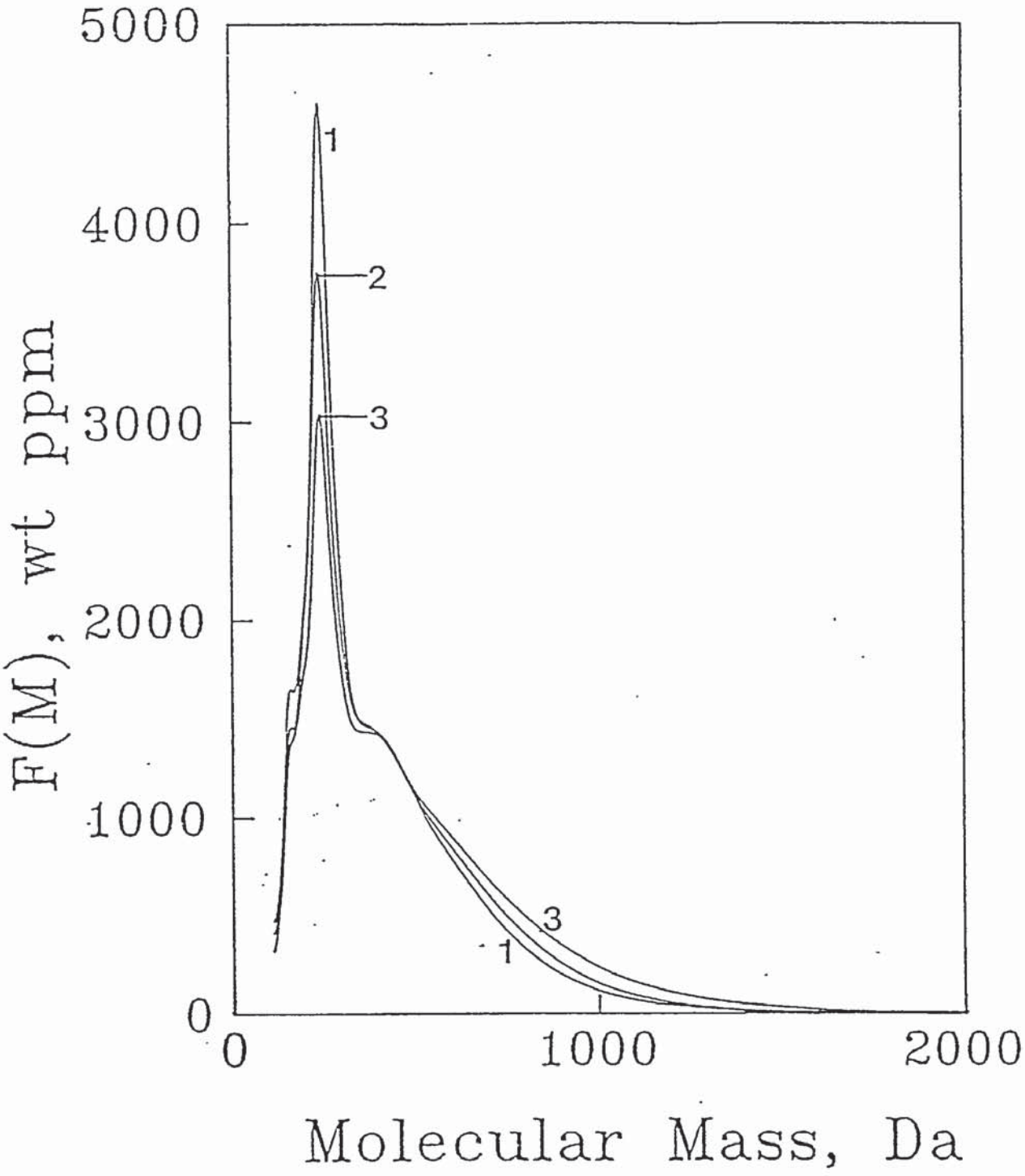

Figure 4. Molecular Mass distributions of pine wood derived pyrolysis liquids from the wire-mesh reactor, 1000 Ks^{-1}, curves 1-3, 400, 450 and 550°C respectively

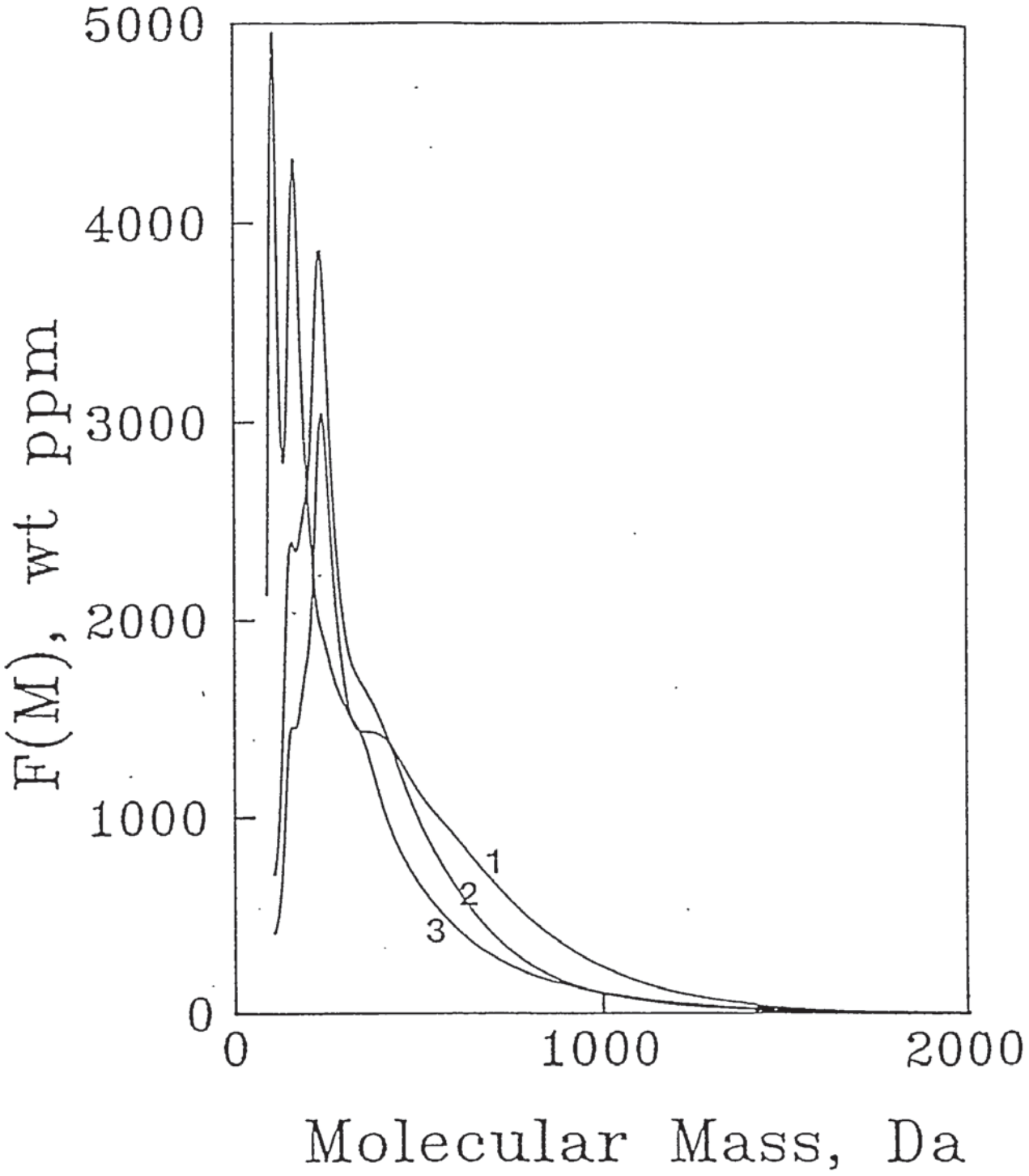

Figure 5. Molecular Mass distributions of pine wood derived pyrolysis liquids from both reactors:

curve 1: wire-mesh, 1000Ks^{-1}, 550°C, atmospheric pressure,
curve 2: wire-mesh, 1000Ks^{-1}, 550°C, 10 bar pressure,
curve 3: ablative pyrolysis reactor, 550°C, 2.8s gas/vapour residence time.

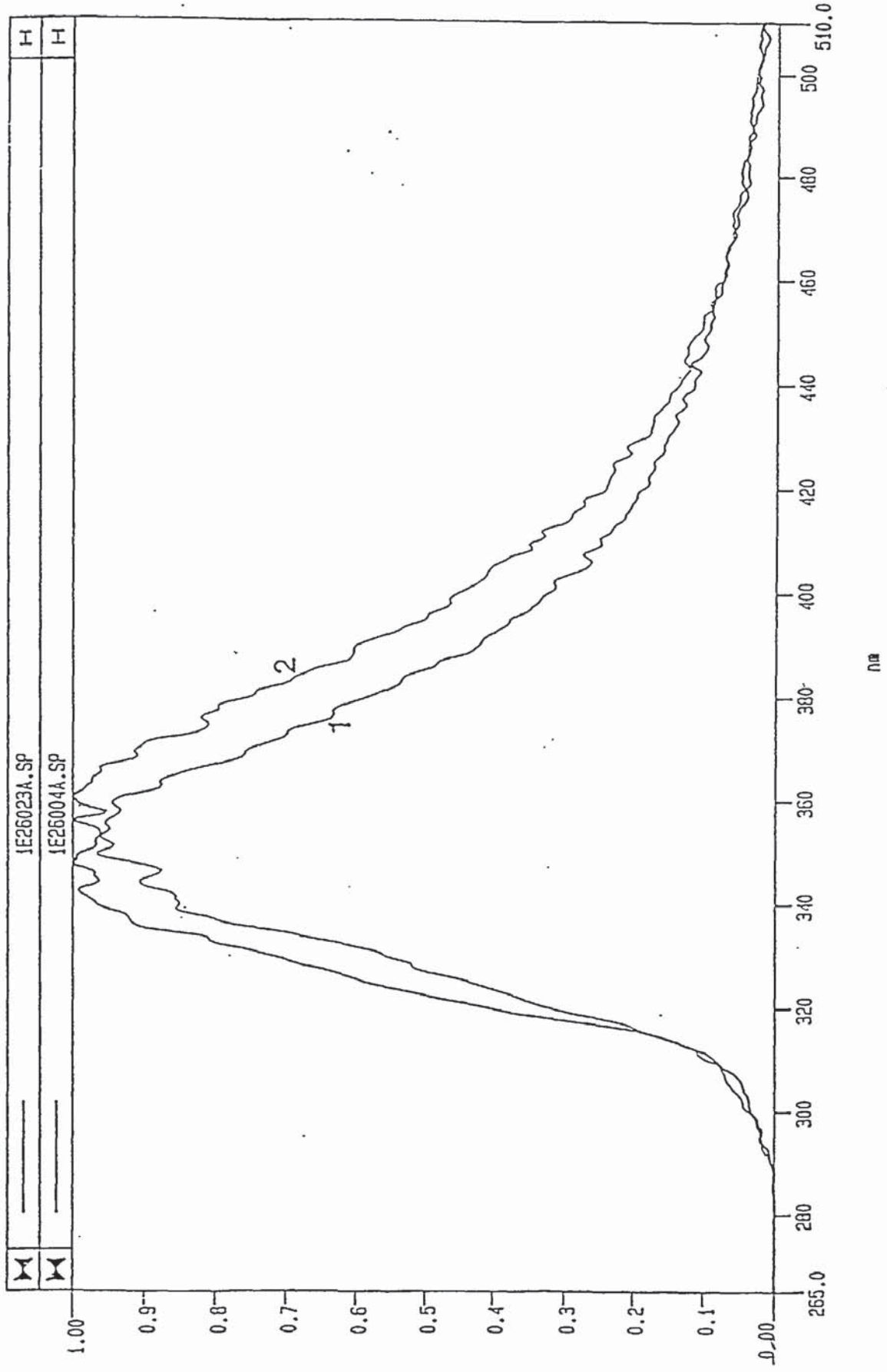

Figure 6a. UV-fluoresence spectra of SEC fractions of pyrolysis liquid, retention time 16.5-17.28 min:

curve 1: wire-mesh liquid, 550°C, 1000Ks^{-1};
curve 2: ablative pyrolysis reactor, 550°C, 2.0 s gas/vapour residence time.

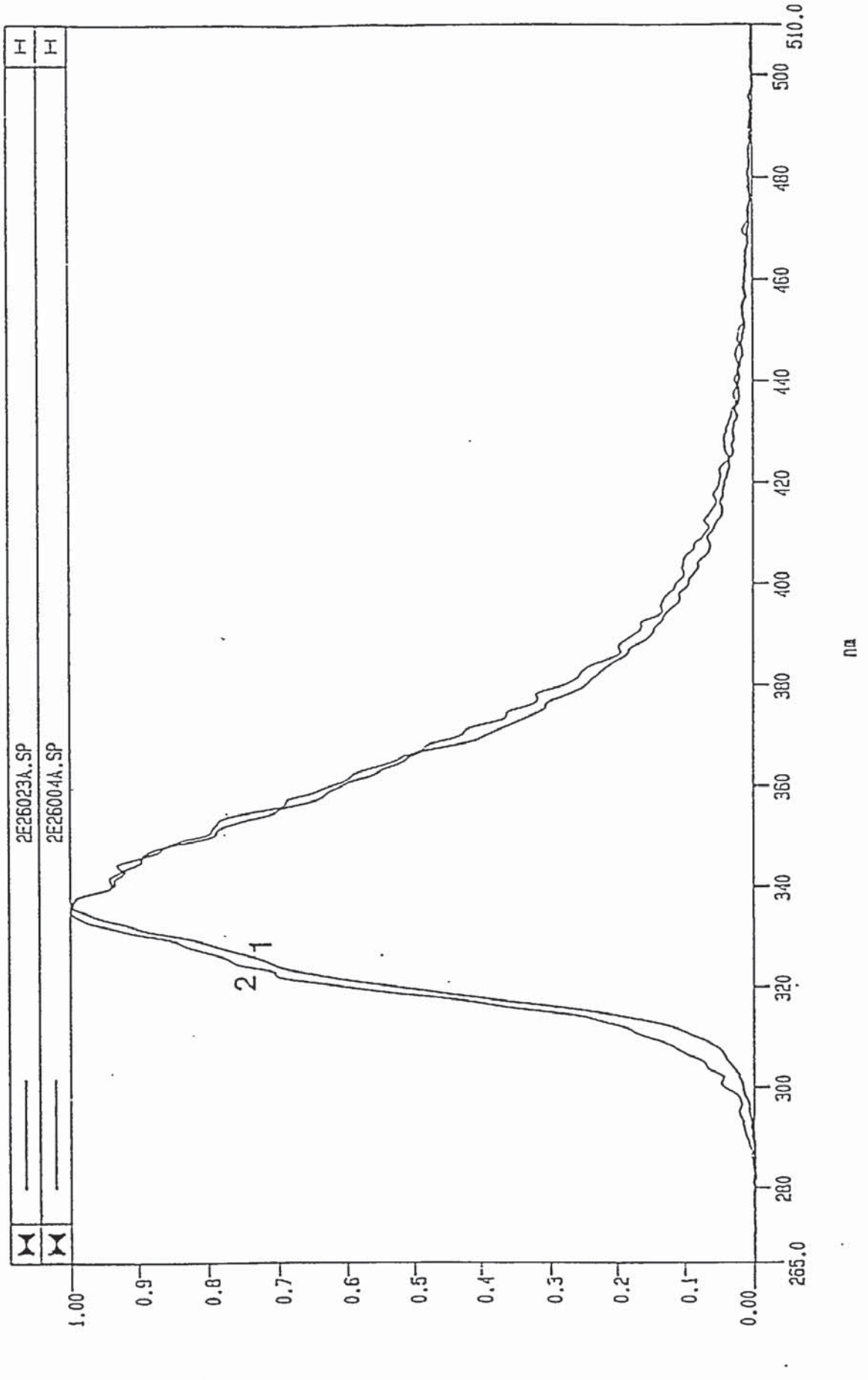

Figure 6b. UV-fluoresence spectra of SEC fractions of pyrolysis liquid, retention time 16.5-17.28 min, curves as in Figure 6a.

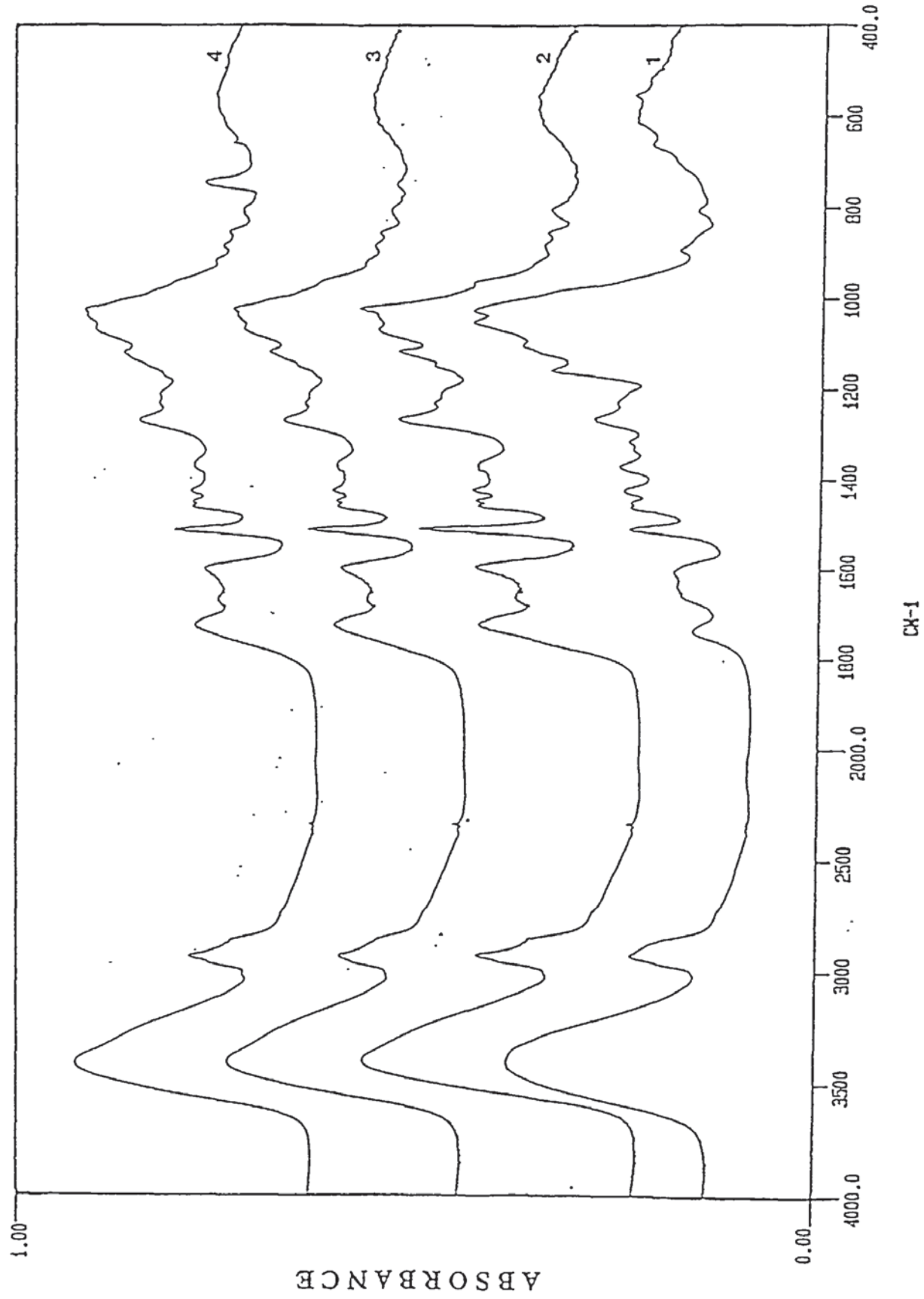

Figure 7. FT-ir spectra for liquids from the wire-mesh reactor
spectrum 1: unpyrolysed pine wood,
spectrums 2,3 and 4: 400, 450 and 550°C liquid respectively.

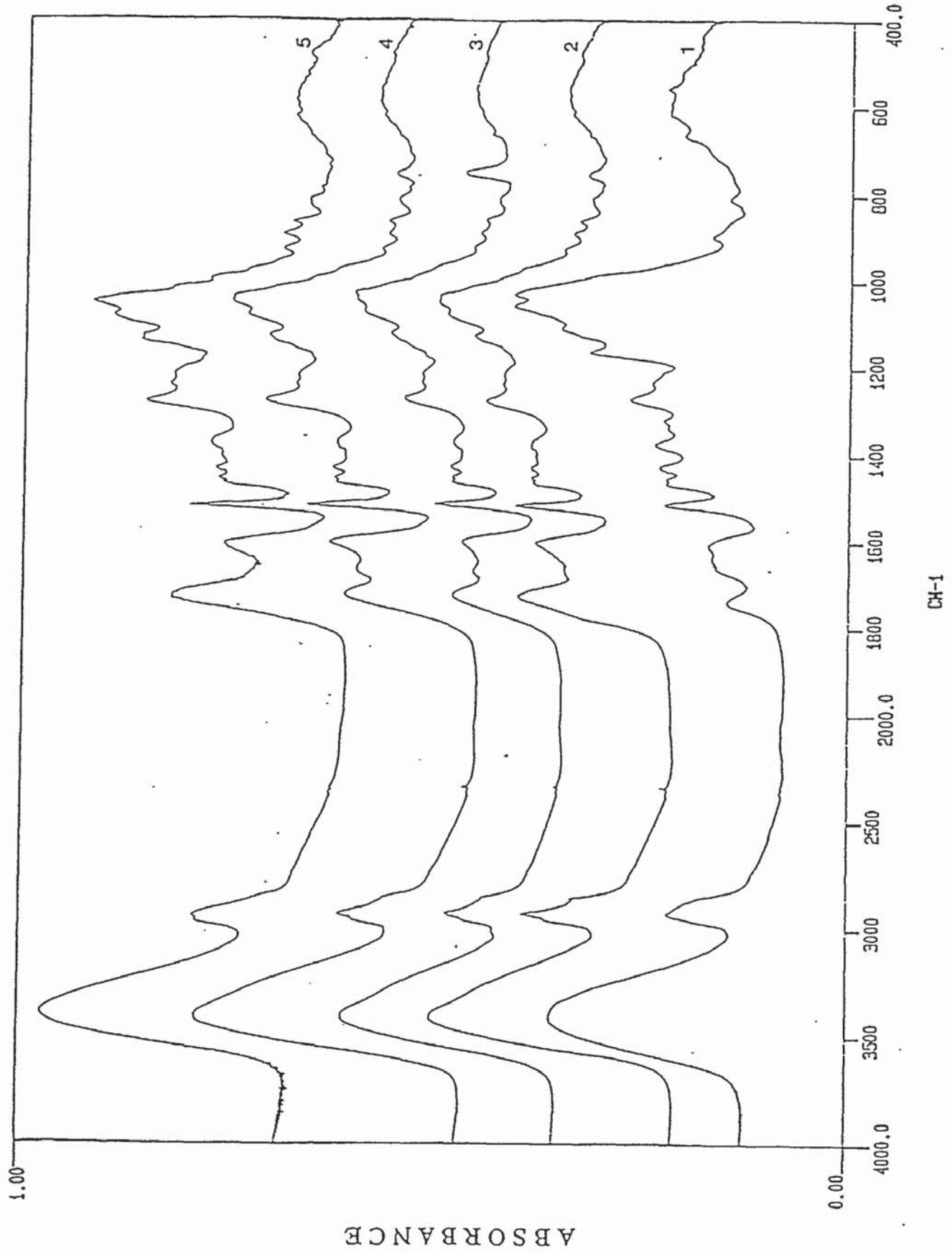

Figure 8. FT-ir spectra for liquids from both reactors
spectrum 1: unpyrolysed pine wood,
spectrums 2 and 3: wire-mesh reactor, 550°C, atmospheric pressure,1 Ks^{-1} and 1000 Ks^{-1} respectively
spectrum 4: wire-mesh reactor, 550°C, 10 bar pressure, 1000 Ks^{-1}
spectrum 5: ablative pyrolysis reactor, 550°C, 2.8 s gas/vapour product residence time.

Appendix II. Data management and equipment calibration

II.1 Datalogging hardware

Data is recorded directly to the computer during an experimental run using Microlink hardware and Windmill™ datalogging and management software. This is depicted in Figure II.01 below. The system consists of a Microlink 3040 A-D converter card which receives signals from the 3903 thermocouple box, containing a cold junction Pt RTD. The 3054 interface card conditions the signals and then the 3040 card converts the analogue signals to digital [A-D converter]. The digital signals are passed to the 3301 serial interface card and then via an RS232 interface lead to the datalogging software on the computer.

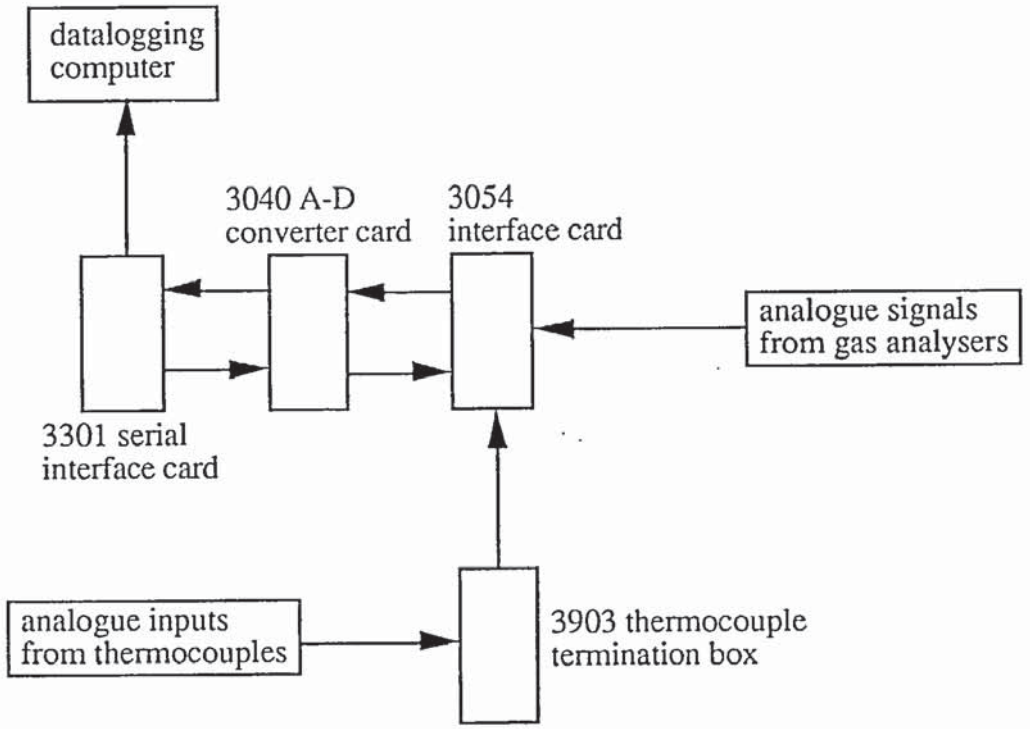

Figure II.01. Data management system

The 3054 module provides multi-channel inputs with facilities for voltage inputs with resistance, bridge, and RMS options. An auxiliary channel is provided which is reserved for special inputs such as cold junction measurement. The analogue signals are first conditioned and then passed to a 3040 analogue to digital converter [A-D] module. The module provides 32 differential analogue inputs or 15 thermocouple inputs since there is one auxiliary channel for cold junction measurement. The right hand side of the 3040 module accepts other differential analogue inputs.

The 3040 module is a 12-bit A-D converter which converts the conditioned analogue inputs from the 3054 module to digital signals for the 3301 serial interface card which links with the datalogging software run by the computer.

The 3301 serial interface card communicates between the Microlink hardware and the software programs running on the computer. The 3301 card should have the following communications settings; baud rate 9600, 8 data bits, 2 stop bits and no parity. The 3301 will also recognise the Xon/Xoff flow control protocol if enabled. If the data is being sent to the computer faster than it can deal with it, then the computer can send the Xoff character to the 3301, suspending data transfer, until it is able to deal with the data. It will send an Xon

character to the 3301 card to re-establish data transfer. This protocol is known as "software handshaking".

The 3903 module is the thermocouple input isothermal box. The module is fitted with a cold junction reference platinum RTD. The platinum reference junction receives a constant 1 mA giving a resistance of 1 ohm per measured millivolt.

II.2 Software and data management

There are four programs run within the Windows™ environment under the Windmill™ directory:

1	ConfigIML:	allows the hardware connections to the computer to be specified, i.e. which port the RS 232 lead from the Microlink 3301 serial interface card is connected to. It also registers which cards are present in the Microlink frame. There is at present one additional card: the 3040 A-D converter card. This receives the voltage inputs from the four gas analysers and the thermocouple isothermal box 3093.
2	SetupIML:	allows a file called an IMS file [Intelligent Microlink Software] to be defined. This contains the channel numbers and settings for the digital inputs from the 3040 A-D converter and converts the signals back to their original value, i.e. voltage readings from the gas analysers and other equipment such as pressure transducers and voltage readings to temperatures from the 3093 thermocouple termination box. This file also allows unused channels to be disabled, except for the Platinum RTD in the 3093 box. Scan rates, low pass filters, conversion factors and voltage ranges can be defined using this program.
3	AnalogIn:	this allows the outputs from the 3301 card to be visually displayed in the Windows environment based upon the settings of the SetupIML file. The signal scan speed can be varied during display. The Pt RTD is always displayed in the AnalogIn file.
4	Logger	This file has 16 input channels which are specified for each experimental run as the settings are held in the RAM when Windows is open. On screen, the data is displayed in columns with the recording time of each sample. This data is continuously logged to an Excel™ compatible file on disk. The logging frequency can be varied and the real start and stop times are recorded.

The AnalogIn file with the appropriate settings for the experimental run is loaded and run. The Logger program is then run and the channels configured which are to be recorded. The other equipment calibrations are then carried out as described below. Further details on the functions of the software and hardware may be found in the Microlink user manuals.

During an experimental run, the analogue inputs from up to 16 thermocouples are transmitted from the 3903 thermocouple box to the 3040 analogue to digital converter [A-D] card and as four channels from the gas analysers. The digital signal is then scanned by the 3301 serial interface card, depending upon the pre-set sampling rate, and the signal transferred to the Windows™ driven software. A pre-configured IMS file receives the signal and gives a visual display using the "Analogin" software program. Data values are then recorded using the "Logger" software program as an Excel™ compatible file. If there is a power failure during the experiment, data is not lost as it is continuously being written to the hard disk.

II.3 Gas analyser calibration

During an experimental run gas analysis is performed by two methods; direct on-line gas analysis for CO, CO_2, CH_4 and H_2 and batch sample analysis by gas chromatography for higher hydrocarbons [C_2-C_4's] and water vapour.

For the on-line gas analysis, the analysers are calibrated before each experimental run using a zero gas, [nitrogen, oxygen free] and with a standard span gas with known proportions of the four gases noted.

II.3.1 CO, CO_2 and CH_4 analysis

The three on line infrared gas analysers [model Lira 3000] are used to determine the volume % of CO, CO_2 and CH_4 in the non-condensable gases from the pyrolysis system after drying. The gas composition is related to the analyser display and hence the output voltage by the curve shown in Figure II.02. The analogue signal produced by the gas analysers is converted into a digital signal which is recorded by the datalogging software. The gas composition and the digital signal to the computer are related by:

$$C_X = C_{calib}\left(\frac{X'}{\alpha-(\alpha-1)X'}\right) \qquad \{II.01\}$$

where:

Ccalib: calibration limit of the gas analyser [vol%],
α: variable determined from the gas analyser calibration curve
X': actual gas analyser output [V], where:

$$X' = \left(\frac{X_X - X_O}{Xc_{alib}}\right) \qquad \{II.02\}$$

where:

X_X: actual instrument reading [V],
X_O: zero offset of the instrument [V],
X_{calib}: calibration voltage of the gas analyser [0.1 V].

Calculated values are given in Table II.01 below.

Table II.01
Calibration values for the LIRA 3000 on-line gas analysers

CO_2 Calibration [1985] C_{calib} =35 volume %			CO_2 Calibration [1994] C_{calib} = 35 volume %		
X	C_x	α	X	C_x	α
0.1	2.765	1.2954	0.1	1.96	1.8730
0.2	5.635	1.3028	0.2	4.235	1.8161
0.3	8.575	1.3207	0.3	6.93	1.7359
0.4	11.655	1.3353	0.4	9.8	1.7143
0.5	15.05	1.3256	0.5	12.95	1.7027
0.6	18.725	1.3037	0.6	16.534	1.6753
0.7	22.575	1.2842	0.7	20.51	1.6485
0.8	26.81	1.2219	0.8	24.78	1.6497
0.9	30.849	1.2110	0.9	29.4	1.7143

CO Calibration [1985]
C_{calib} = 30 volume %

X	C_x	α
0.1	2.34	1.3134
0.2	4.794	1.3145
0.3	7.29	1.3351
0.4	9.93	1.3474
0.5	12.9	1.3256
0.6	16.02	1.3090
0.7	19.236	1.3057
0.8	22.68	1.2910
0.9	26.22	1.2975

CH_4 Calibration [1985]
C_{calib} =10 volume %

X	C_x	α
0.1	0.7	1.4762
0.2	1.46	1.4623
0.3	2.28	1.4511
0.4	3.175	1.4331
0.5	4.033	1.4795
0.6	5.01	1.4940
0.7	6.08	1.5044
0.8	7.3	1.4795
0.9	8.6	1.4651

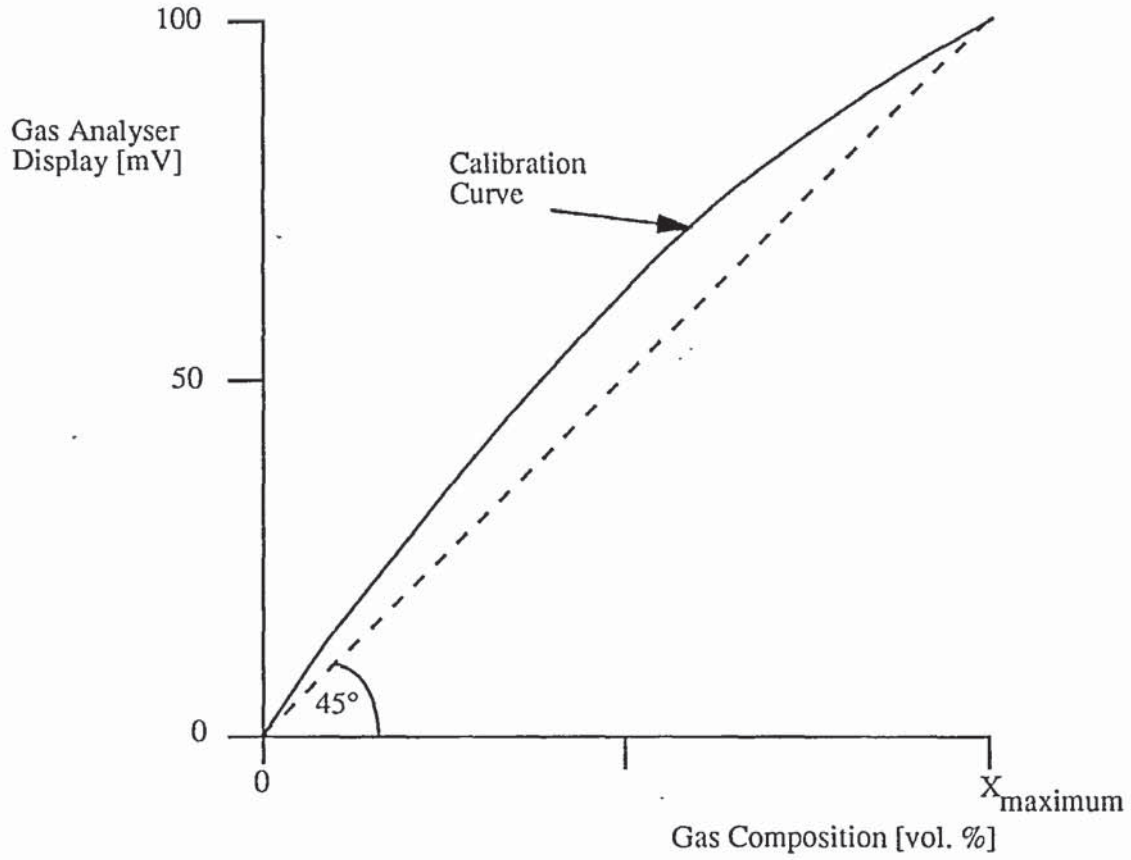

Figure II.02. Gas analyser calibration curve

II.3.2 Hydrogen analyser calibration

The gas composition is directly proportional to the analogue signal output from the analyser [Leybold Hereaus Hydros]. This is read directly by the Microlink datalogger as a voltage input via the 3040 A-D converter. The voltage is then calibrated to the volume % hydrogen [C_{H2}] by:

$$C_{H2} = C_{calib}\left(\frac{X_X - X_O}{X_{calibH2} - X_O}\right) \qquad \{II.03\}$$

where $X_{calibH2}$ is the voltage measured for the span gas [V] and C_{calib} is the span gas volume for hydrogen [vol%].

II.4 Biomass Feeder Calibration

The biomass feeder was calibrated using air dried wood, particle size 4.75-6.35 mm, with a moisture content of 9 wt% [dry basis]. The feeder calibration curve is shown in Figure II.03 below.

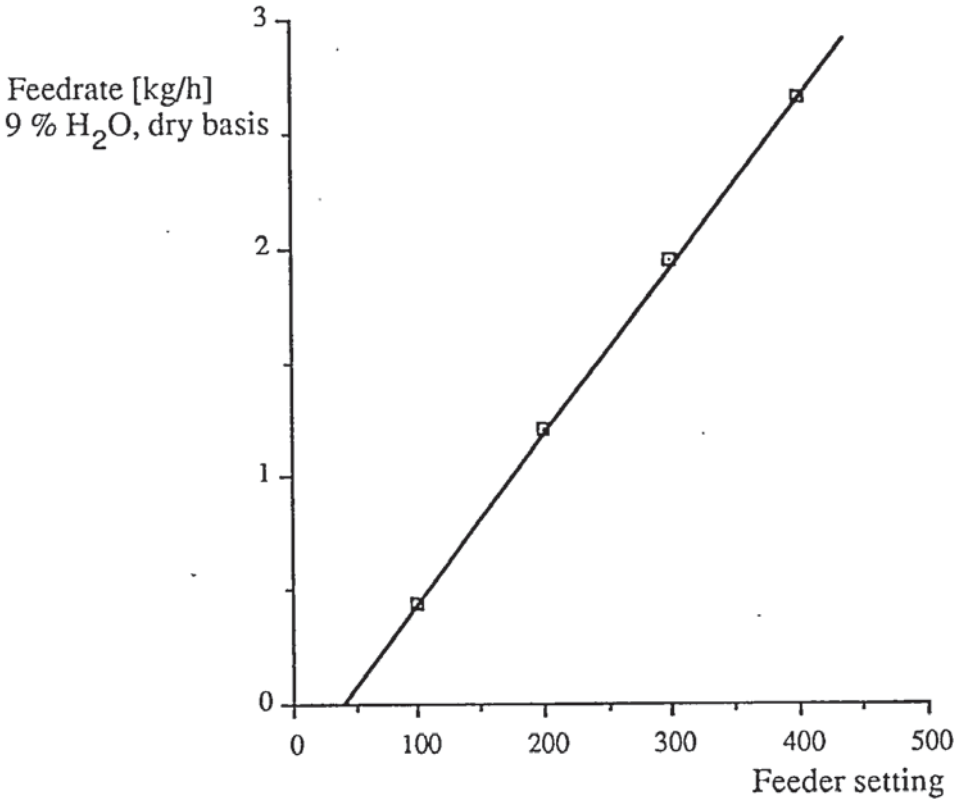

Figure II.03. Biomass feeder calibration graph

The calibration curve is given by:

Biomass feedrate [kg/h at 9 wt% H_2O] = - 0.28260 + 7.3974e-3 [FS] $R^2 = 1$ {II.04}

where [FS] is the biomass feeder setting.

II.5 Rotameter calibrations

The nitrogen rotameters were calibrated using a certified nitrogen rotameter [GEC Process Instruments Ltd.] for gas flows up to 25 l/min at atmospheric temperature and pressure. The calibration curve for the rotameter is shown below in Figure II.04, tube number 7, float type K. The calibration curve for the rotameters is given in equation {II.05} below as:

Nitrogen flow = - 2.7656e-3 + 0.35560[RR] + 6.7148e-4$[RR]^2$ $R^2 = 1.000$ {II.05}
[l/min, 101325 Pa, 298 K]

where [RR] is the rotameter reading.

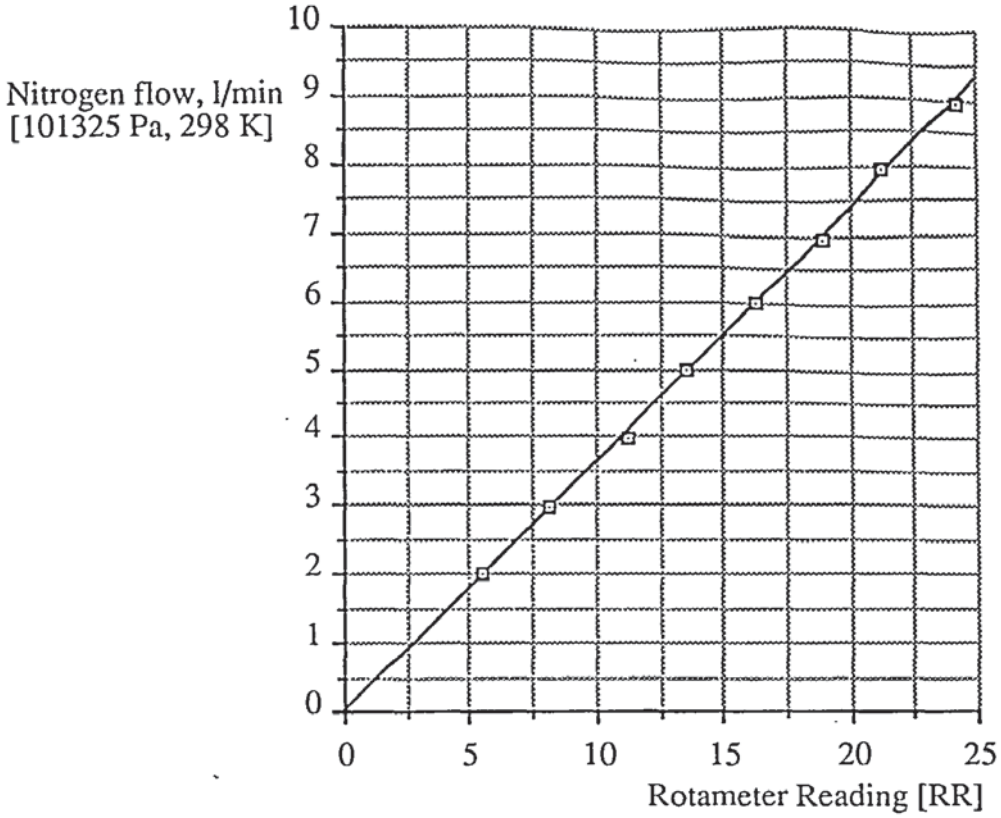

Figure II.04. Nitrogen rotameters calibration curve

II.6 Thermocouple calibration

The RTD has an accuracy of ± 0.25°C at room temperatures. The temperature readings from the type K thermocouples calculated used in this work are accurate to ± 3°C using the 3054 A-D converter for temperatures up to 510°C. For temperatures up to 1290°C, the permitted maximum error is quite poor at 9°C. This high error is due to many factors including sensor tolerance, thermal contact to sensor, non-uniformity of the thermocouple wire, electrical noise, amplifier offset and gain errors.

II.7 Pressure measurement

Pressure measurement is performed with barometric pressure gauges which measure the reactor pressure above atmospheric pressure [101325 Pa]. The pressure gauge was calibrated against a mercury manometer and found to have a slight constant offset of 3013 Pa. The results for the calibration are shown in Figure II.05 below.

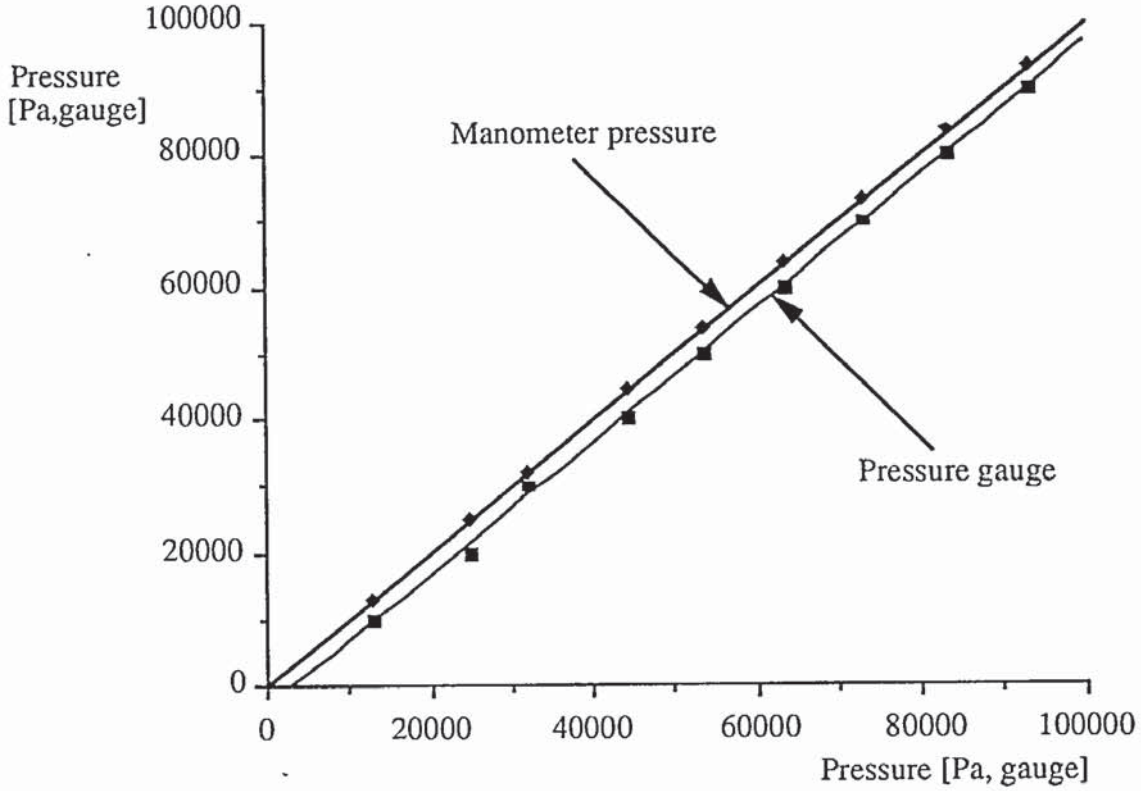

Figure II.05. Calibration of the pressure gauge above 101325 Pa absolute

To convert the actual pressure gauge readings to the correct pressure, equation {II.06} is used.

reactor pressure [Pa, gauge] = - 3013 + 0.9763*[PG] + 2.361e-7*[PG]^2 $R^2 = 1$ {II.06}

where [PG] is the pressure gauge reading.

II.8 Gas meter calibration

The gas meter used a ft^3 scale which was calibrated against the nitrogen rotameter for a range of flowrates from 5-20 l/min. The gas meter reading in ft^3 was 1.74 times the actual gas flow at atmospheric temperature and pressure and this was taken into account during calculation of the gas volumetric flowrate and total gas volume measured for an experiment.

Appendix III. Experimental run preparation

This appendix detailed the necessary equipment checks and procedures to ensure safe operation of the reactor and product collection system.

III.1 Gas analyser calibration

The gas analysers are usually left on 24 hours a day. If the gas analysers have been turned off for more than 24 hours they require at 24 hours to warm up and stabilise. Once the analysers have stabilised, the following calibrations may be carried out. The gases flowing to the gas analyser must be dry to prevent damage to the analysers. The nitrogen purge lines are shown in Figure III.01.

Calibrate the gas analyser on zero gas [oxygen free nitrogen] and using the BOC span gas [CO, CO_2, CH_4 and H_2, balance N_2] by opening each cylinder and starting the gas pump in the gas analyser cabinet. When using the zero gas, the instruments should be set to give a zero visual output and 0 mV reading in the AnalogIn program [see Appendix II]. Ensure that the instrument readings [mV] match the manufacturers' specification for CO, CH_4, CO_2 and H_2 in conjunction with the instrument calibration charts supplied by MSA Appliances, Glasgow. Repeat three times or until the readings are consistent to give accurate calibration of the gas analysers. The span gas composition should be checked periodically [every 3 months] by gas chromatography.

III.2 Carbon monoxide alarm test

Use the 200ppm Crowcon gas bottle to test the alarm. The CO alarm will emit a high pitch whine and the small red light on top of the unit will flash until the CO concentration begins to drop below 200 ppm. If the alarm activates during an experiment, shut down the reactor, close the doors on the fume hood and leave [see Section III.3 for emergency shutdown procedure].

III.3 Reactor Preparation

3.3.1 Shut off the fume hood, the gasification rig hood by 90% and open the butterfly valve on the extraction hood for the ablative pyrolysis reactor. Check that the extraction fan is running when turned ON at the fume hood. Check the electrical trip on the main switching unit.

DO NOT CARRY OUT ANY EXPERIMENTS WITHOUT FUME EXTRACTION.

III.3.2 Check that the reactor interior plate on the inside of the lid is secure and that the feed tube, drive shaft seal holder and the sightglass covers are firmly screwed in place and that all are free of carbon deposits. Check the type K thermocouple which protrudes from the inside of the lid for measurement of the gas/vapour phase temperature is not damaged. Check that the composite drive shaft seal is not mis-aligned or worn. Place the drive shaft through the drive shaft seal with the lid above the reactor base. Check that the reactor gasket is not broken or damaged and place on the lower reactor base.

III.3.3 Check that the 14 cartridge heaters are firmly located in the reactor base and that the power leads are not worn. Replace any heater which has signs of worn leads or scorching. Check the band heater around the outer reactor wall and ensure that the electrical terminals are not exposed. Ensure that the control type K thermocouple from the temperature controller is located securely between the band heater and the outer reactor wall. If the thermocouple is not there to control the temperature, the band heater may short out. The

thermocouple can be checked during start up as the controller has a direct thermocouple reading scale in conjunction with the set point. This will rise when the band heater is turned on, the set point being 400°C to reduce the collection of char on the reactor wall. Check the electrics to the drive motor and the heaters are not worn.

III.3.4. Check that the blades are firmly mounted at the required angle and that the holder with the four blades is attached to the bottom of the drive shaft which was inserted through the drive shaft seal with the locking nut. Tighten the small grub screw in the nut into the small machined recess to prevent the locking nut from unscrewing itself during the experiment. Ensure adequate clearance of the blades from the heated surface, i.e. 1.5 mm using the feeler gauges and lock the drive shaft in its vertical position with the two locking collars on the drive shaft bearings. Lower the reactor lid onto the reactor base. Check that the drive shaft is free running and that it is not scraping the reactor wall. Bolt down the lid with the twelve M10 mild steel bolts, ensuring that the reactor is earthed. Lubricate the bolts, if necessary, with the high temperature lubricant, i.e., MoS_2 spray. Connect the cooling water supply to the drive shaft seal holder and the outlet pipe to the drain.

III.3.5. Fit the biomass feed tube and pressure sensor line with the nitrogen purge. Attach the biomass feeder outlet to the top of the sightglass which fits between the feeder tube and the feeder outlet. This allows observation of the particles falling into the reactor.

III.3.6 Check the drive belt is not worn and is correctly tensioned to the drive wheel on the reactor drive shaft. If the drive belt is loose, the motor and 5:1 speed reducer can be moved to tighten the belt by means of a threaded bar located at the front of the drive motor. Fit the belt guard in place at the drive shaft and at the top of the reactor. Fit the drive shaft guard on top of the drive shaft.

III.3.7 Fill the biomass feeder with sufficient dried biomass to last one hour, depending upon the reactor heated surface temperature. This should be a maximum of 5 kg of dried biomass of size no greater than 6.35 mm across their major axis. Place the lid on top of the hopper. Check the nitrogen line is connected to the hopper and the valve NL 01 is closed as shown in Figure IV.01 below. Check there is enough nitrogen in the cylinder to complete an experimental run, i.e. > 100 psi. Check that the backup nitrogen cylinder is connected and turned on with a similar quantity to the main cylinder. Close the valve from the gasifier sample line at the gas meter and open the gas sample valve MV 05 at the filter box at the gas analyser.

III.3.8 Fit insulation around the band heater, the reactor base, lid and feeder tube to a depth of 30 mm. Fit insulation around the gas/vapour outlet on the base of the reactor.

III.4 Product collection system preparation [see Figure 7.01]

III.4.1 Ensure that all the glassware and fittings are clean before use and that all joints are lubricated with silicon grease.

III.4.2 Weigh the following equipment :

- the reactor base outlet pipe to the cyclone,
- the char cyclone and its inlet and outlet fittings
- the cyclone outlet pipe to the brass cupped connector,
- the condensers, connecting fittings and the liquids collection flasks.

III.4.3 Fill the second liquids collector with 7-8 g of pre-weighed oven dried [105°C for 24 hours] non-adsorbent cotton wool. Fill the cotton wool filter on the outlet of the second liquids condenser with 12-14 g of similar cotton wool. Do not overpack this filter or the system pressure drop will results in an increase in the reactor pressure above atmospheric. Attach the liquids collection flasks to the liquids outlet lines from the liquids collectors.

III.4.4 Fit the type K thermocouples to:

- the inlet to the first liquids collector,
- the outlet of the second liquids collector,
- the inlet to the molecular sieve adsorbent,

ensuring that they are located in the middle of the gas stream.

III.4.5 Add a pre weighed amount of activated molecular sieve 3A° [~125 g after drying for 24 hours at 200-260°C in the muffle furnace] to the fixed bed. Connect the gas outlet from the fixed bed to the gas meter.

III.4.6 After checking for gas leaks by adding nitrogen to the reactor and purging through the product collection system, fit the trace heating tapes around the reactor base outlet pipe, the char cyclone and the cyclone outlet pipe to the liquids collectors. Ensure that the trace heating tapes do not overlap. Fit the control thermocouple from the trace heating tape temperature controller below a heating tape and insulate the pipes and char cyclone to a 25-30 mm thickness with high temperature insulation. The setpoint for the trace heating tapes [Cole-Parmer Ltd.] is 400°C. The maximum operating temperature for the trace heating tapes is 486°C.

III.4.7 The system is now ready for operation once the liquids collection system from the inlet to the first liquids collection flask to the inlet to the cotton wool filter have been immersed in ice which has had salt added to it. During nitrogen purging of the equipment, as described below, the gas temperature into the packed cotton wool filter should be less than 10°C.

AIII.4.8 Check that the non-condensable gas outlet from the gas meter is connected to the gas sampling line for the gas analysers and also that the side leg for batch gas samples is connected. Purge the gas sample bottles twice with nitrogen. Gas sample bottles used in previous experiments should be used with the gas sample pump after purging with nitrogen.

III.5 Reactor start up procedure

Once the reactor and the product collection system have been set as described in Sections AIII.1 to III.5, the start up procedure can be initiated as detailed below.

III.5.1 Turn on the electrical supply to the:

- band heater temperature controller [set point 400°C],
- reactor heated base temperature controller [Eurotherm controller] and heaters switch box,
- variable speed motor controller for the drive shaft,
- trace heating tapes temperature controller [set point 400°C],
- biomass feeder and controller [set point dependent on reactor temperature].

The red light on the heaters switch box will be on and the red lights on the trace heating tapes controller and the band heater controller will be

illuminated. The emergency stop switch on the drive motor should be at the "RUN" position. Check that the datalogger is configured correctly and reading the inputs from the heater thermocouples, the product collection system thermocouples and the calibrated gas analysers. Record the atmospheric temperature and pressure.

III.5.2 Set the temperature controller for the heaters to 100°C initially and increase in 50°C increments until the desired setpoint has been reached. Set the overload dial to 20C° above the setpoint using the manual controller on the left of the control panel. Check that the thermocouples in the reactor base are reading the same temperature to ±5C°. The minimum heated surface reactor temperature must be 450°C to ensure ablative pyrolysis occurs. The upper limit on the compact cartridge heaters fitted inside the base of the reactor is 625°C. Do not exceed this limit as there is a risk the heaters will short out and lead to the solid state switch in the heaters switching box becoming fried. The band heater and the trace heating tapes temperature controllers should be set to 400°C.

III.5.3 During the warm up of the reactor and the ancillary equipment, open the nitrogen cylinder isolating valve which supplies the diluting nitrogen to the reactor and the biomass feeder [see Figure III.01]. Purge the reactor and the product collection system. The gasmeter should be rotating. If not, check for blockages. After purging the biomass feeder [NL 02] and the reactor, with a total equipment volume [35 l] x 3, in order to displace all air, set the flows on the various rotameters [NR1, NR2 and NR3] at atmospheric pressure as:

		Typical reading
NR1	biomass feeder tube flow	20-25 l/min
NR2	biomass feeder flow	10-15 units
NR3	surface blow line	8 units

Set the gas analyser valve to SAMPLE and start the gas analyser sampling pump. The purging nitrogen will act also as a zero gas to check the gas analyser calibrations.

III.5.4 Start the blades rotating at 160 rpm [80% of the maximum rotational speed]. Allow the motor to run for 10 minutes to allow the rotational speed to stabilise and for the blades to heat up in the reactor. Once the reactor temperature has stabilised and the nitrogen flows are set, start the datalogging program and start the biomass feeder. Note at which time biomass begins to enter the reactor and note the gas meter reading. Continue to log values for the reactor heated base temperature controller, gas meter and the nitrogen rotameters during the experiment.

III.6 Standard shutdown

III.6.1 Turn off the biomass feeder. Check no more particles are being fed by checking the sightglass on the feeder tube to the reactor. Continue to run the blades for 3 minutes to ensure that any residual particle in the reactor have been ablatively pyrolysed and entrained out of the reactor. Turn off the heaters switch box and the band heaters and trace heating tapes controllers. Reduce the nitrogen flows to zero and note the final gas meter reading.

III.6.2 After a few minutes when there is no sign of any more pyrolysis vapours entering the liquids collection system, disconnect the liquids collection system from the brass domed connector and plug the pipe from the cyclone. Remove the liquids collection system after sealing it off from the air and weigh all parts.

III.6.3 Remove the insulation from the reactor top and allow to cool down to below 100°C before removing the cyclone and char collector from the base of the reactor. Remove the feeder from the top of the reactor feed tube and weight he amount of biomass remaining. Re-determine the moisture content of the remaining feed. Remove the reactor lid and remove any product char which may be in the reactor and retain for analysis. Weight the char separation system and recover the product char from the cyclone, pipes and char pot.

III.6.4 Filter the liquid products to determine the quantity of char in the methanol recovered liquids and the raw condensed liquids. Carry out water analysis on the liquid and carry out the mass balance using the measured gas volume and compositions, the recovered char and liquid fractions.

III.7 Emergency stop procedures

Problem diagnosis

- gas analyser readings begin to decrease/increase [Section III.7.1]
- reactor pressure begins to increase [Section III.7.2]
- no liquids flowing into collection receivers [Section III.7.3]
- drive shaft stops rotating [Section III.7.4]

III.7.1

- If the gas analyser readings begin to drop, it is possible that the biomass feeder tube may have become blocked and that material is rapidly building up in the feeder tube. If particles become visible in the sightglass turn the biomass feeder off immediately. Turn NR2 to zero and continue to purge with nitrogen for three minutes. Carry out the shut down procedure as normal.
- if the gas analysers readings begin to increase, the nitrogen supply has stopped. Check the first nitrogen cylinder is not empty. If it is empty, switch to the second cylinder and continue the experiment. If this is no the case, check for leaks around the reactor and in particular from the feeder. If the nitrogen leak cannot be found, shut down the reactor and product collection system.
- The gas analyser pump may be sucking in air, possibly if a sample valve is open. Check that the valve is closed and that the gas sample pump is not leaking. Check that the hand pump for the batch gas sample has not been left open.

III.7.2

- If the reactor outlet is blocked, the system pressure will rapidly increase. There is now a risk of overpressure in the reactor which will cause the feeder lid to rise. Turn off the biomass feeder and turn off the nitrogen to the reactor and feeder to prevent over pressurisation of the reactor. Turn off the drive shaft and all the electrical supplies to the band heater, the reactor heaters and the trace heating tapes. Remove the insulation off the lid and from the walls and maintain a flow of cooling water to the drive shaft seal.
- check that the inlet pipes to the liquids collector is not blocked by the presence of white smoke swirling around the top of the first liquids collector. This may occur when the experiment is over 40 minutes. Shut down the biomass feed to the reactor and turn of the nitrogen flows to the biomass feed tube and reduce the nitrogen flow to the feeder to less than 1/min. Turn off the surface blow line NR3 after one minute.

III.7.3

- the inlet pipe from the condenser to the collector may have become blocked. The experiment can continue, but liquids may increase in the first condenser until they

flow into the second condenser. This is usually not a problem and the experiment can be completed as normal.

III.7.4

- If the drive belt breaks, stop the motor with the Emergency Stop button. The motor will stop immediately. Switch off the electrical supply to the drive motor.
- the rotating blades in the reactor may have become distorted and have contacted either the heated reactor base or the reactor wall. Turn off the power to the drive motor and stop the biomass feeder and turn of the reactor heaters, the band heater and the trace heating tapes. Continue to purge with nitrogen for 3 minutes and increase NR3 to 20 units to blow char and unreacted wood out of the reactor and to remove residual vapour and gaseous products from the reactor. Turn off the biomass feeder and complete the pyrolysis of the remaining material in the reactor. Rapidly blow the remaining material out of the reactor with NR3 by increasing the flow to 20 units. Turn off the heaters and continue to flow nitrogen through the reactor from the biomass feeder to cool the reactor. Remove the insulation from the reactor.

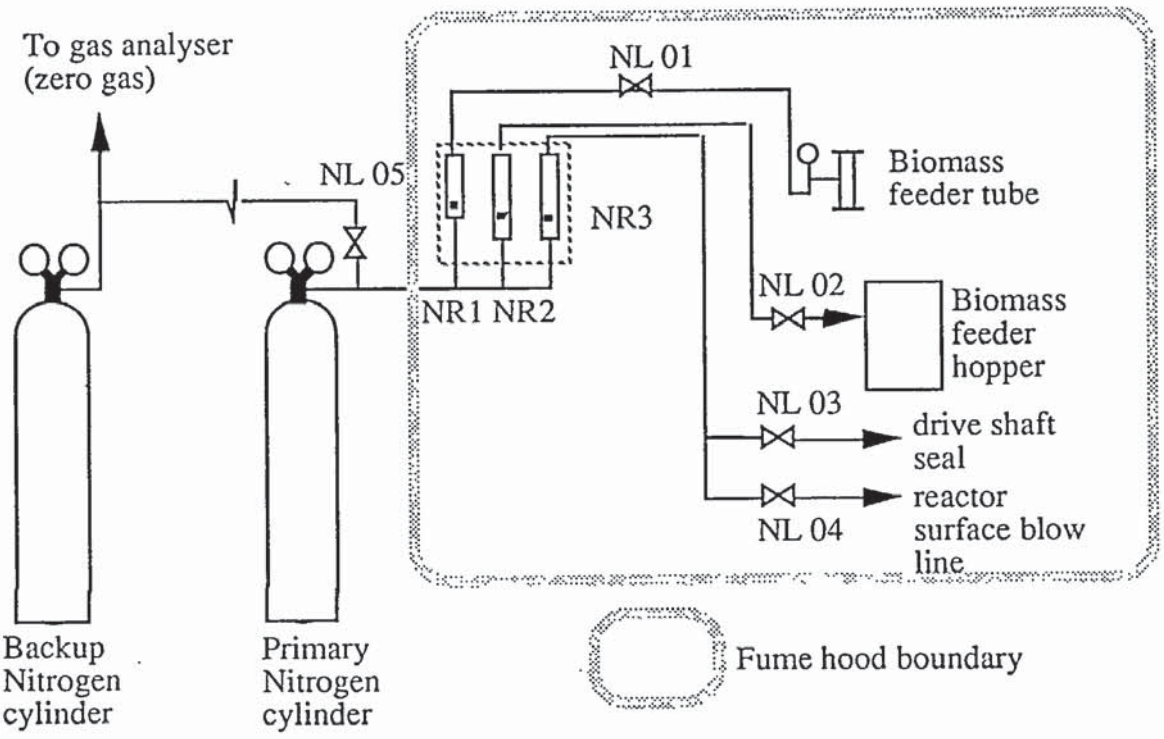

Figure III.01. Reactor system nitrogen lines

Appendix IV. Basis for the Product Yields

IV.1 Basis for the mass balances

There are two char fractions which may be recovered from the ablative pyrolysis system after the completion of an experimental run: reactor char and non reactor char [product collection and separation system char]. These two fractions may also be sub-divided into ablatively produced char and unreacted [un-ablated, slowly carbonised wood and secondary char] wood.

During the experimental programme the blade clearance was set at 1.5 mm from the clean reactor surface. Due to slight carbon build up on the reactor surface, the clearance from the blade edge to the surface after a run was reduced slightly to 1.4 mm. This was used as the cut-off point for the assessment of ablated and non-ablated char.

Therefore, there are two types of char which care are distinguished from each other by particle size. To confirm this hypothesis, several char sizes were examined: visually and by elemental analysis for the determination of ablatively produced char and non-ablated material. From Table 8.03, the elemental analysis did not allow a clear difference to be made between one char fraction and another. The other approach which was also used was visual inspection of the char. It was possible that the char produced by ablation would not retain the original wood structure. Microscopic examination of all char down to 100 μm showed that the original wood structure remained. It was also noted that for large char particle, i.e. those greater than 1.4 mm, some did not have a reacted core, however char particles below 1.4 mm were clearly reacted to form a char. The different char products are classified as:

Fast pyrolysis char [produced by ablation]

- char particles less than 1.4 mm. It is assumed that char less than the blade clearance from the final deposited layer on the reactor heated surface is ablatively produced. This is recovered from the reactor and product collection system.

Slow pyrolysis char [formed by lower heating carbonisation and secondary reaction]:

- particles greater than 1.4 mm which have then carbonised after shut down and are found in the reactor,
- particles greater than 1.4 mm which have not been ablated but may have partially carbonised in the product collection system and suffered a small loss of volatiles [for runs CR06-CR12, approximately 18 wt% dry basis was lost].

The recovered fractions are therefore diverse in their degree of conversion during pyrolysis and this is taken into account during the assessment of ablatively pyrolysed wood and that wood which has not been ablated.

IV.2 Calculation of dry ablatively pyrolysed wood only

The density of the bone dry wood dried is 396 kg/m^3 with a 1% increase in water content increasing the density by 4 kg/m^3 on a dry basis, assuming negligible increase in wood volume at low moisture concentrations less than 10 wt%. This can be used to calculate the quantity of wood which is slowly pyrolysed, based upon the dry density of the reactor char and product collection char. Char particles greater than 1.4 mm recovered from the reactor have a dry density of 290 kg/m^3 [independent of the reactor temperature] and similar particles recovered from the product collection system have a dry density of 328 kg/m^3. Therefore, using the ratios of the density, the amount of dry wood as fed to the reactor which was not ablatively pyrolysed can be calculated by equation {IV.01}:

$$W_{r2} = W_F - W_{upc} - W_{ur} \qquad \{IV.01\}$$

ablated wood = dry wood fed - carbonised wood [reactor]-unreacted wood

where:

W_{r2}: dry ablatively pyrolysed wood [method 2]
W_{ur}: dry slowly carbonised wood which is calculated by equation {IV.02}:

$$W_{ur} = W_{rc} \times \left(\frac{396}{290}\right) + C_{pc} \times \left(\frac{396}{328}\right) \qquad \{IV.02\}$$

where:

W_{rc}: mass of dry material from the reactor greater than 1.4 mm
C_{pc}: mass of dry material from the product collection system greater than 1.4 mm

The product yields are then calculated on a weight % basis on the ablated wood only. The results based on the total ablated and carbonised wood may be found in Table IV.01.

The average product distribution is shown in Figure IV.01 for runs CR06-CR16. The yields of organics, water and gas have been normalised to account for losses during the experiments with known leaks

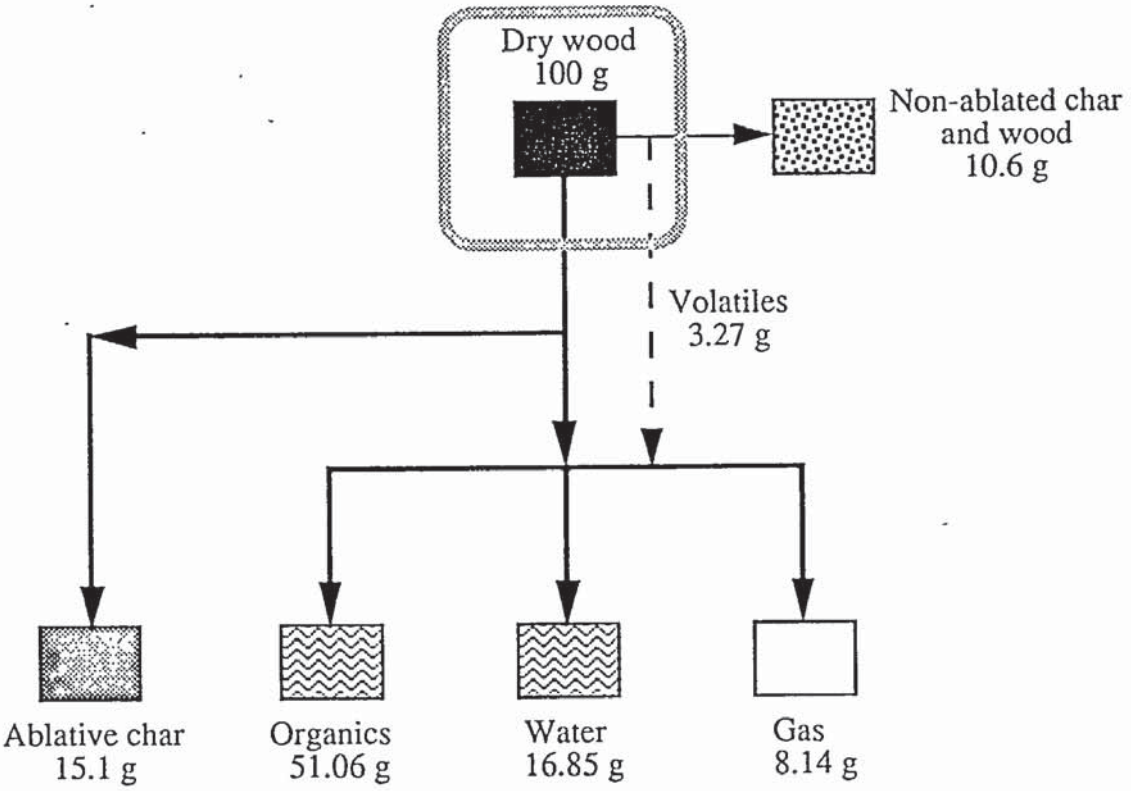

Figure IV.01. Averaged normalised product distribution for runs CR06-CR16

Table IV.01
Results for the ablative pyrolysis reactor, yields on dry wood as fed basis [wt%]

Run number	CR09	CR14	CR15	CR13	CR07	CR08
Reactor surface temp. [°C]	456	458	501	505	550	550
Wood H_2O [wt %, d.b.]	2.86	1.37	1.2	1.21	2.44	2.08
Gas/vapour temp. [°C]	318	323	350.3	278	389	366
Reactor pres. [kPa, abs.]	101.9	101.3	100.4	100.4	91.0	101.9
Run time	45	27	35	18	15	33
Wood fed [wet]	352.8	124.0	318.2	326.0	493.5	1106.6
Residence time of gas/vapour products (s)	2.45	5.83	6.57	2.73	2.83	2.02
Total char yield	29.0	21.8	26.3	25.7	24.5	26.5
{Ablative char yield}	{9.7}	{18.0}	{21.2}	{10.0}	{11.8}	{19.5}
Organic liquids yield	46.8	48.2	39.8	46.6	48.7	45.0
H_2O yield	13.7	19.4	16.7	20.2	19.0	9.6
Gas (N_2 free)	7.8	5.6	5.7	10.6	7.6	6.1
Closure	97.2	95.0	88.5 *	103.0	99.8	87.1 *

Run number	CR11	CR16	CR12	CR10	CR06
Reactor surface temp. [°C]	550	551	554	602	597
Wood H_2O [wt %, d.b.]	1.86	0.36	3.21	1.99	9.25
Gas/vapour temp. [°C]	294	289	418	368	415
Reactor pres. [kPa, abs.]	101.6	100.5	100.9	102.7	76.0
Run time	15	41	21	14	12
Wood fed [wet]	466.0	288.5	679.2	454.3	464.0
Residence time of gas/vapour products (s)	1.97	NK	0.76	1.75	5.85
Total char yield	24.8	18.7	28.1	24.9	17.5
{Ablative char yield}	{11.1}	{15.8}	{10.9}	{10.7}	{11.3}
Organic liquids yield	44.9	46.6	48.0	56.8	49.2
H_2O yield	14.6	13.6	8.7	9.9	26.8
Gas (N_2 free)	6.9	2.2	7.7	7.9	9.7
Closure	91.2	81.1 *	92.5	99.6	103.2

IV.2 Contribution of non reacted particles to overall volatiles yield

From Figure IV.01, there is a small contribution of volatiles from the wood which is slowly carbonised and dried in the reactor and in the product collection system during the experiment. To estimate the contribution of volatiles to the overall product yields from the slowly carbonised wood and dried unreacted wood, it was assumed that the wood reacts by slow pyrolysis in the reactor during the experiment to lose 18 wt% of its dry mass, i.e. the mass loss of particles recovered from the product collection system for runs CR06-CR12. This was equivalent to a change in particle density from 396 to 328 kg/m^3 as discussed above.

This has been averaged over the 11 experiments to be a maximum of 3.27 % of the original dry wood fed to the reactor. Since this contribution of volatiles is due to drying and slower

pyrolysis reactions due to radiation from the reactor base, walls and gases, this is most likely to be water due to dehydration reactions and possibly some carbon dioxide [recognised as being a primary pyrolysis product]. The average contribution to the overall volatile yields is a maximum of 4.3 wt%. Since the exact contribution to each product is unknown, using the ablatively pyrolysed wood only, although giving slightly higher yields and hence slightly higher closures, is justified as the quantity of non-ablated wood and char would be minimised on a larger scaled up reactor by improved operability and optimisation.

Table IV.02
Analysis of the char fractions for runs CR10 and CR16

Analysis	C	H	N	O by diff.	Ash
Original Wood	49.84	6.09	0.05	43.54	0.48
CR10 Reactor char					
> 3.35 mm	80.26	3.27	0.09		
< 1.7 mm > 1.4 mm	80.93	3.19	0.09		
< 1.4 mm > 1.18 mm	81.03	3.13	0.07		
< 1.18>600µm	82.36	3.15	0.09		
< 600 µm	82.53	3.10	0.09		
CR10 Product collection system char					
> 3.35 mm	63.75	5.07	0.05		
> 3.35 mm [interior]	51.04	5.54	0.15		
< 3.35 mm > 1.7 mm	69.15	4.56	0.05		
< 1.7 mm > 1.4 mm	73.25	4.16	0.06		
< 1.4 mm > 1.18 mm	74.18	3.98	0.06		
< 1.18>600µm	73.87	4.10	0.07		
< 600 > 355 µm	73.62	4.09	0.07		
< 250 >106 µm	75.35	3.84	0.06		
< 75 µm	75.94	3.69	0.09		
CR16 Product Collection System Char					
<3.35 > 1.7 mm	77.02	3.42	0.09		
<1.7 mm > 1.4 mm	80.18	3.12	0.06		
< 1.4 mm > 1.18 mm	80.17	3.08	0.10		
< 1.18 mm > 1.0 mm	73.84	3.25	0.07		
< 1.0 mm > 0.710 mm	75.61	3.29	0.07		
< 0.71 > 0.6 mm	75.94	3.26	0.07		
< 0.6 mm > 0.355 mm	75.27	3.33	0.10		
< 0.355 > 0.25 mm	75.99	3.26	0.09		
< 0.25 mm > 0.106 mm	76.53	3.19	0.08		
< 0.106 > 0.075 mm	77.47	3.13	0.10		
< 0.075 mm	78.5	3.10	0.07		
CR10 reactor surface char	85.04	2.95	0.10		
CR08 reactor surface char	81.55	2.68	0.11		

Table IV.03
Gas analysis for runs CR06-CR16 [wt% dry feed basis]

Run number	CR09	CR14	CR15	CR13	CR07	CR08	CR11
H_2	0.000	0.000	0.000	0.000	0.000	0.003	0.046
CO	3.351	2.298	2.334	4.499	3.407	2.531	3.262
CO_2	6.649	3.339	3.367	7.738	5.319	3.918	4.913
CH_4	0.000	0.128	0.199	0.342	0.274	0.148	0.279
C_2H_4	0.000	0.035	0.000	0.002	0.000	0.000	0.000
C_2H_6	0.000	0.000	0.053	0.060	0.000	0.000	0.000
C_3H_6	0.000	0.000	0.049	0.260	0.000	0.000	0.000
C_3H_8	0.000	0.003	0.000	0.078	0.000	0.000	0.000
ln CO/CH_4		2.885	2.462	2.578	2.519	2.839	2.458
ln CO/CO_2	-0.685	-0.374	-0.367	-0.542	-0.445	-0.437	-0.410
ln $CO/(C_2H_4+C_2H_6)$		4.182	3.794	4.289			

Run number	CR16	CR12	CR06	CR10
H_2	0.007	0.029	0.001	0.021
CO	1.251	4.765	2.856	4.178
CO_2	0.866	4.997	5.560	4.558
CH_4	0.116	0.409	0.360	0.262
C_2H_4	0.000	0.000	0.114	0.096
C_2H_6	0.000	0.000	0.064	0.086
C_3H_6	0.000	0.000	0.345	0.000
C_3H_8	0.000	0.000	0.000	0.050
ln CO/CH_4	2.376	2.455	2.070	2.770
ln CO/CO_2	0.368	-0.047	-0.666	-0.087
ln $CO/(C_2H_4+C_2H_6)$			2.776	3.131

Appendix V. Modelling of wood rod heat transfer

V.1.1 Estimation of the temperature profile in the ablating solid

In order to evaluate energy balances and predict temperature profiles in the remaining solid, heat transfer model for the case of wood ablation was derived based upon basic assumptions and fundamental heat transfer. This was then subsequently applied to the empirical data from the single particle experiments to estimate the temperature profiles in the particles during pyrolysis.

The simplest case is for an ablating wood rod of known dimensions and thermal properties as shown in Figure V.01.

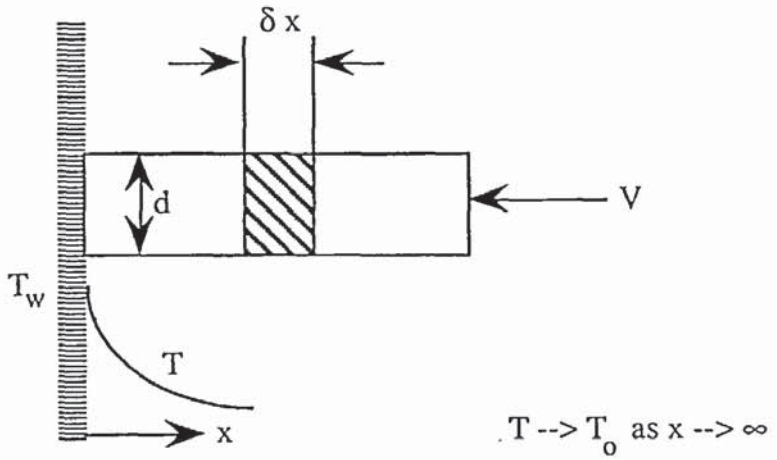

Figure V.01. Wood rod temperature profile during ablation

Basic assumptions:

- minimal thermal resistance in the hot surface,
- char layer in contact with the heat transfer surface is at the same temperature,
- products are rapidly removed from the reaction interface and impose no restrictions to heat transfer,
- the kinetics are assumed to be described by a global reaction model which will lump the heat transfer, mass transfer and reaction kinetics into one expression,
- the physical and thermal properties are assumed to remain constant during decomposition and there is no shrinkage of the reaction interface during decomposition,
- radial variations are minimal and a 1 dimensional approach can be used.
- the pyrolysis reactions are assumed to be negligible compared to the specific heat requirements.

V.1.2 Energy balance for a fixed step change

conduction: $$\varnothing_{c,x}\left(\frac{\pi d^2}{4}\right) = \varnothing_{c,x+dx}\left(\frac{\pi d^2}{4}\right) \quad \{V.01\}$$

flow: $$H_{,x}\left(\frac{\pi d^2}{4}\right) = H_{,x+\delta x}\left(\frac{\pi d^2}{4}\right) \quad \{V.02\}$$

Therefore:

$$\frac{(H_{x+\delta x} - H_x)}{\delta x} = \frac{(\varnothing_{c,x+\delta x} - \varnothing_{c,x})}{\delta x} \quad \{V.03\}$$

where:

$$H = V\rho_w C_p(T-T_o) \qquad \{V.04\}$$

$$\emptyset = -\lambda \frac{dT}{dx} \qquad \{V.05\}$$

As δx tends to zero, equation {V.04}becomes:

$$V\rho_w C_p \frac{d}{dx}\left(\frac{T-T_o}{T_w-T_o}\right) = -k \frac{d}{dx}\left(\frac{d}{dx}\left(\frac{T-T_o}{T_w-T_o}\right)\right) \qquad \{V.06\}$$

Let $\theta = \left(\frac{T-T_o}{T_w-T_o}\right)$ and $\alpha = \frac{\lambda}{\rho_w C_p}$, therefore:

$$\frac{d\theta}{dx} = -\frac{\alpha}{V}\frac{d}{dx}\left(\frac{d\theta}{dx}\right) \qquad \{V.07\}$$

The boundary conditions for the problem:

$x = 0, \theta = 1$

$x = \infty, \theta \rightarrow 0$ and $\frac{d\theta}{dx} \rightarrow 0$

Integrating equation {V.07} with respect to x:

$$\int_{\theta_\infty}^{\theta_x} d\theta = -\frac{\alpha}{V}\int_{\left(\frac{d\theta}{dx}\right)_\infty}^{\left(\frac{d\theta}{dx}\right)_x} \frac{d}{dx}\left(\frac{d\theta}{dx}\right)dx \qquad \{V.08\}$$

gives the first integrated form:

$$\theta_x = \frac{\alpha}{V}\left(\frac{d\theta}{dx}\right) \qquad \{V.09\}$$

Integrating equation {V.09}a second time gives:

$$-\frac{\alpha}{V}\int_0^x dx = -\frac{\alpha}{V}\int_{\theta_{0=1}}^{\theta} \frac{d\theta}{\theta} \qquad \{V.10\}$$

which gives the solution:

$$-\frac{V}{\alpha}x = (\log_e\theta_x - 0) \qquad \{V.11\}$$

Taking antilog of both sides gives the final solution:

$$\theta_x = \exp\left(\frac{-Vx}{\alpha}\right) \qquad \{V.12\}$$

This is a standard heat transfer solution for heat conduction into a solid of low thermal conductivity at high heat transfer rates. Equation {V.12} allows the prediction of temperature profiles in the solid. From the estimate for heat flow into the rod:

$$\emptyset = \frac{\pi d^2}{4} \lambda \frac{dT}{dx}\Big|_{x=0} \qquad \{V.13\}$$

which yields equation {V.14}:

$$\frac{d\theta_x}{dx} = \frac{-V}{\alpha} \exp\left(\frac{-Vx}{\alpha}\right) \qquad \{V.14\}$$

which leads to the overall heat flux into the solid, assuming that the heat of pyrolysis is constant over the temperature range 450-600°C:

$$\emptyset = \rho_w C_p V(T_w - T_o) + \rho_w V \Delta H_{pyr} \qquad \{V.15\}$$

To estimate the thickness of the reaction zone in the biomass during ablation, a minimum temperature is required at which reaction begins. For a temperature T_z at a distance z into the ablating solid, equation {V.16} allows z to be calculated:

$$z = \frac{\alpha}{V} \ln \frac{T_w - T_o}{T_z - T_o} \qquad \{V.16\}$$

or:

$$zV = \alpha \ln \frac{T_w - T_o}{T_d - T_o} \qquad \{V.17\}$$

From the single particle experiments, described in Chapter 9; the temperature profiles in the ablating biomass can be estimated if the reactor temperature, ablation rate and and the biomass physical and thermal propeties are known. These results are described in Chapter 9.

The ratio of (Vz/α) is analogous to the approach used by Pyle and Zaror who derived the Pyrolysis number as in equation {V.18} (298):

$$\frac{\lambda}{\kappa \rho_w C_p L_p^2} \qquad \{V.18\}$$

where: L_p is the particle radius [m]. Their pyrolysis number is the inverse of the Thermal modulus, M, defined by Villermaux et al. (299), based upon a ratio of a charactersitic heat reaction time tr [s] and a characteristic heat penetration time t_t [s] given by equations {V.19 and V.20}:

$$t_r = \frac{L_p^2}{\alpha} \qquad \{V.19\}$$

$$t_t = \frac{\rho_w}{\kappa} \qquad \{V.20\}$$

where κ is the reaction rate constant at the reaction temperature:

$$\kappa = A \exp\frac{-E}{RT_d} \qquad \{V.21\}$$

The thermal modulus M was defined as the ratio of the heat penetration time and the characteristic reaction time as given by equation {V.22}:

$$M = \frac{t_t}{t_r} \qquad \{V.22\}$$

For cases where M is less than 1 the thermal front has time to penetrate the biomass before reaction occurs, i.e. the chemical regime. For cases where M is greater than 1, the particle does not have time to heat up and reaction occurs in a thin layer close to the particle surface, i.e. the ablation regime.

For the single particle experiments, assuming that the calculated biomass decomposition temperatures of Table 9.04 are the reaction temperature, the thermal Thiele modulus can be calculated. The kinetic data of Thurner and Mann were used [used in the estimation of T_d]. These results are shown in Table V.01 below for a cube of uniform dimensions: 5.55 mm by 5.55 mm by 5.55 mm- the average particle dimensions used in the experimental work.

Table V.01
Variation of the thermal Thiele modulus with reactor temperature

Reactor temperature, T_w [°C]	450	500	550	600
biomass decomposition temperature, T_d [°C]	317	328	334	342
κ [s^{-1}]	1.56	2.37	2.97	3.97
t_t [s]	341.54	341.54	341.54	341.54
t_r [s]	254.10	166.87	133.53	99.86
M	1.34	2.05	2.56	3.42

For all temperatures, the value of M is greater than 1, indicating that the rate of ablation of the biomass is controlled by the rate of heat supply to the biomass, i.e. the ablation regime.